Investigational peptide-based therapeutics: antibacterial agents, adjuvants and combinations thereof against Gram-negative bacteria

by

Ronald John Domalaon

A Thesis submitted to the Faculty of Graduate Studies of

The University of Manitoba

in partial fulfilment of the requirements of the degree of

DOCTOR OF PHILOSOPHY

Department of Chemistry

University of Manitoba

Winnipeg, Manitoba, Canada

Abstract

Antimicrobial peptides represent a vast pool of biomolecules that may serve as the next generation of therapeutic agents. The alarming surge of multidrug-resistant bacterial pathogens able to repel and deactivate almost all clinically-used antibiotics drives our necessity to develop novel therapeutics, such as peptide-based agents. Arguably, the problem of antimicrobial resistance is more serious in Gram-negative bacteria (GNB), relative to Gram-positive bacteria, as they typically carry multiple chromosomal-mediated resistance mechanisms and possess an intrinsic mechanism that restricts the entry of most antibiotics. This intrinsic resistance mechanism in GNB consists of the outer (OM) and inner membranes (IM), and overexpressed multidrug efflux systems. The OM and IM impose an orthogonal constraint on the type of molecules able to traverse to the cytosol. The OM prevents the entry of large hydrophobic molecules while the IM prevents the diffusion of large hydrophilic molecules. Once the antibiotic enters the periplasm or the cytosol, it can then be efficiently expelled by a multitude of efflux pumps.

Peptide-based agents, including naturally-occurring antimicrobial peptides and their mimics, usually target bacterial membranes. These membranotropic actions include perturbation of both the OM and IM (that can lead to lysis and intracellular component leakage), and sequestering of lipid components that may inactivate transmembrane proteins such as efflux pumps. The degree of membrane perturbation varies from each peptide, as some peptides result in overall membrane dissolution (lysis) while some induce only localized membrane disruption. My doctoral research work capitalized on this membranotropic mechanism to develop investigative peptide-based agents against GNB that act as stand-alone antibiotics or as helper molecules, called adjuvants, in combination with other established antibiotics. In this context, peptide-based adjuvants work in

synergy through the enhancement of antibiotic cellular entry by either inducing localized imperfections (pores) in membranes, that allow diffusion of molecules, or sequestering lipid components surrounding efflux pumps, that prevent the debilitating action of efflux.

My work took inspiration from amphiphilic membrane-acting antimicrobial peptides to develop potent short synthetic lead adjuvants that in combination with clinically-used antibiotics can effectively eradicate GNB. Peptide-based adjuvants in this thesis comprised of short proline-rich lipopeptides, dilipid ultrashort cationic lipopeptides and polymyxins derivatives. Specifically, polymyxin analogs in this thesis included dilipid polymyxins and polymyxin B_3-tobramycin hybrid. The work described herein utilized these membranotropic adjuvants to revitalize the activity of antibiotics from intrinsic resistance of GNB. My doctoral research work presented herein follow a 'sandwich thesis' format.

Acknowledgements

If there is a moment where I could be granted the option to stop time, I wish it to be in this moment as I write my gratitude and reminisce about the good old times; for a man who do not look at his past is nothing but a fool who's bound to nothingness.

I would not be able to accomplish all this work without any support system, and I am very grateful for them.

I am forever in debt to my supervisor, Dr Frank. Schweizer, for guiding me on this intellectual journey. He's always there to advice when I'm in doubt, there to support when I needed help and there to steer my efforts towards excellence. A great mentor is someone who gives you freedom to learn from your mistakes and to celebrate glory from your initiative, but with an unwavering guidance whichever path you take. I could not ask for a better mentor!

I am thankful to my advisory committee members Dr. George G. Zhanel, Dr. Joe O'Neil and Dr. Ayush Kumar for supporting my inquisitions in the multidisciplinary field of research. I value each member's expertise and guidance towards my growth as an organic chemist learning biochemistry, microbiology, pharmaceutical and medical/life science.

My journey will never be the same without the energetic and dynamic team of personnel in the Schweizer Research Group. I, without a doubt, believe that our group have been the most enthusiastic and liveliest group in our floor, if not our building. I thank all my research peers Xuan Yang, Temilolu Idowu, Nicole Nolasco, Dr. Yinfeng Lyu, Marie Haufroid, Camilo Fabra Prieto,

More importantly, I give thanks to my immediate and extended family whom always proactively supported my study. Nothing compares to the extensive support system a Filipino family have for each other, especially my 50+-member family that reside in Winnipeg, MB, Canada. Many thanks to all my friends and peers, in the Philippines and in Canada. Lastly, I would like to thank my significant other for providing emotional support and understanding throughout my study.

Table of Contents

List of Tables

List of Figures

List of Schemes

List of Abbreviations

ADEP	acyl depsipeptide
AMA	aspergillomarasmine A
AMP	antimicrobial peptide
ANOVA	analysis of variance
ATCC	American Type Cell Culture
Boc	*tert*-butyloxycarbonyl
CAN-ICU	Canadian National Intensive Care Unit surveillance study
CANWARD	Canadian Ward Surveillance study
Cbz	carboxybenzyl
CLSI	the Clinical and Laboratory Standards Institute
cIAI	complicated intra-abdominal infection
COL	colistin
cUTI	complicated urinary tract infection
DCM	dichloromethane
DIPEA	diisopropylethylamine
DMF	*N*,*N*-dimethylformamide
DMSO	dimethyl sulfoxide
DNA	deoxyribonucleic acid
dUSCL	dilipid ultrashort cationic lipopeptide
ESBL	extended-spectrum β-lactamase
ESI-MS	electrospray ionization mass spectrometer
EUCAST	the European Committee on Antimicrobial Susceptibility Testing
FDA	the United States Food and Drug Administration
FIC	fractional inhibitory concentration
Fmoc	fluorenylmethyloxycarbonyl
GNB	Gram-negative bacteria
HABP	hospital-acquired bacterial pneumonia
HDP	host-defense peptide
HOBt	hydroxybenzotriazole
HPLC	high-performance liquid chromatography
IDSA	the Infectious Diseases Society of America
IC$_{50}$	concentration to inhibit the proliferation of 50% cell population
IM	inner membrane
LC-MS	liquid chromatography tandem to mass spectrometer
LPS	lipopolysaccharide
MALDI-MS	matrix-assisted laser desorption ionization mass spectrometry
MDR	multidrug-resistant
MIC	minimum inhibitory concentration
MHB	Mueller-Hintron broth
MHC	minimum concentration that resulted in 5% red blood cell hemolysis
MS	mass spectrometry
NME	new molecular entity
NMR	nuclear magnetic resonance

OM	outer membrane
OprH	outer membrane protein H
PBS	phosphate-buffered saline
PDR	pandrug-resistant
PMBN	polymyxin B nonapeptide
PMB3	polymyxin B_3
PMF	proton motive force
PRAMP	proline-rich antimicrobial peptide
PyBOP	benzotriazole-1-yl-oxy-trispyrrolidino-phosphonium hexafluorophosphate coupling reagent
RNA	ribonucleic acid
SAMP	synthetic antimicrobial peptide
SAR	structure-activity relationship
SMAPM	small molecular antibacterial peptoid mimics
SPRLP	short proline-rich lipopeptide
TARAMP	tryptophan- and arginine-rich antimicrobial peptide
TBAHS	tetrabutylammonium hydrogen sulfate
TBDMS	*tert*-butyldimethylsilyl ether
TBTU	O-(benzotriazol-1-yl)-*N*,*N*,*N′*,*N′*-tetramethyluronium tetrafluoroborate coupling reagent
TOB	tobramycin
TFA	trifluoroacetic acid
USCL	ultrashort cationic lipopeptide
VABP	ventilator-associated bacterial pneumonia
WHO	the World Health Organization
XDR	extensively drug-resistant

Chapter 1: Antimicrobial peptides as promising therapeutic agents

This chapter is based on my publication:

Ronald Domalaon, George G. Zhanel, Frank Schweizer. **2016**. Short antimicrobial peptides and peptide scaffolds as promising antibacterial agents. Curr Top Med Chem 16:1217-1230. doi: 10.2174/1568026615666150915112459.

Reproduced with permission.

1.1. Introductory remarks

In this chapter, antimicrobial peptides will be discussed as a vast reservoir of potential therapeutic agents that may mitigate the problem of antimicrobial resistance. Most of these peptides act on bacterial membranes and therefore are perceived to by-pass most of the resistance mechanisms in Gram-negative and Gram-positive bacteria, including the sieving properties of the outer and inner membranes, and the intracellular concentration-limiting efflux. Large (≥20 amino acids) antimicrobial peptides require significant cost in production and development, and therefore their shorter counterparts are more *via*ble options as clinical candidates. Hence, the peptides that will be elaborated in this chapter are specifically those with shorter lengths of ≤10 amino acids.

1.2. Contributions of authors

Ronald Domalaon did an extensive literature survey on the topics: antimicrobial peptides and peptide-based mimetics. This review article is fully written by Ronald Domalaon with guidance from George G. Zhanel and Frank Schweizer. All authors were responsible for the final form of this review paper.

1.3. Abstract

Antimicrobial peptides have recently garnered significant attention as an emerging source of potential antibiotics, due to the swift emergence of multidrug-resistant bacteria and a dwindling antibiotic pipeline. The vast majority of antimicrobial peptides are long, comprised of more than 10 amino acids, resulting in significant production costs for their synthesis while simultaneously displaying metabolic instability and relatively poor pharmacological profiles. To counter these problems, efforts have been shifted to shorter molecules and the development of new peptidomimetic approaches. In this paper, we review promising short, naturally-isolated or synthetic, antimicrobial peptides, along with their mimics, and discuss their merits as potential antibacterial agents.

1.4. Antimicrobial peptides as an emerging class of antibacterials

Emergence of resistant microorganisms to conventional antibiotics, especially multidrug-resistant (MDR) strains to which the pathogen is resistant to more than three antibiotic classes, imposes a severe health threat worldwide (1–3). A recent update by the World Health Organization (WHO) indicates that antimicrobial resistance is rising rapidly whereas effective antibacterial agents are dwindling to a few, causing much burden physically, economically and socially to governments across the globe (4). Thus, development of new antibiotics able to combat resistant bacterial strains is crucial.

Antimicrobial peptides (AMPs) are promising antibiotic candidates as they usually possess multiple modes of action in which the bacterial cell membrane is the main target, rendering less

likely for the pathogen to overcome; although distinct resistance mechanisms have been described (5). AMPs can be of natural origin or synthetically made. The former may be classified as host-defense peptides (HDPs) as higher organisms (plants and animals) produce these molecules as a part of their innate immunity. The first reported HDPs are cecropins (isolated from pupae of the moth *Hyalophora cecropia* in 1981 (6)), defensins (obtained from mammalian neutrophils in 1985 (7)) and magainins (isolated from the skin of the African clawed frog *Xenopus laevis* in 1987 (8)). HDPs are genetically-encoded conserved natural immunity components that may modulate cellular functions such as chemoattraction, gene transcription and cytokine production and/or release, while simultaneously possessing direct antimicrobial activity (9–12). HDPs may also take part in wound healing and angiogenesis processes (13). For example, the cathelicidin LL-37 is expressed in immune cells (such as neutrophils, monocytes, dendritic cells, and macrophage subsets), mast cells and epithelial cells (14, 15). LL-37 is an amphipathic α-helical 37 amino acid-containing peptide that exhibits broad-spectrum direct antimicrobial activity, as well as various indirect beneficial immunomodulatory properties for rapid bacterial clearance. Induction of endogenous LL-37 has been an attractive concept in anti-infective therapy (14) as certain inducer molecules such as butyrate (16), vitamin D_3 (17), litocholic acid (18), bacterial products (19) are found to induce their expression in cells, strengthening the immune system to abate bacterial invasion. However, the increased expression of LL-37 may also have adverse consequences such as altered inflammatory responses in the body. Polymyxins make up another class of important AMPs. Polymyxins were first isolated from the bacterial culture of the Gram-positive *Bacillus polymyxa* in 1947 (20), in which polymyxin B and E (also known as colistin) are the most well-known as they are both FDA-approved antibiotics used as last resort agents against multidrug-resistant (MDR) Gram-negative bacterial infection (21–23). Polymyxins are non-ribosomal cyclic

decalipopeptides that possess narrow spectrum antibacterial activity with multiple modes of action. It is widely accepted that polymyxin's main mode of action involves enhanced permeability of the bacterial cell membrane, resulting from an initial lipopolysaccharide-specific interaction (24, 25). Polymyxin has also been reported to inhibit the bacterial respiratory pathway (26), to bind to ribosomal RNA (27) and induce hydroxyl radical production (28). Moreover recent research suggests that polymyxins may also possess immunoprotective properties (29).

The search for a common motif or scaffolds amongst AMPs/HDPs and the advancement of the understanding on how they act upon their target drives the development of synthetic AMPs (SAMPs). Some SAMPs are developed by truncating existing HDPs to the minimum residues needed for their biological activity. Others are designed with the knowledge that most HDPs rely solely on their physicochemical properties for their antimicrobial activity (30). The latter approach takes into account that most AMPs are amphiphilic, possessing a spatially separated hydrophobic and hydrophilic (usually cationic) domain. Their amphiphilic nature has proven to be crucial for antimicrobial activity, independent of the amino acids present in the peptide (30, 31) Thus, engineering small peptides that have a distinct portion consisting of hydrophobic amino acids and another portion consisting of hydrophilic (usually cationic) amino acids has yielded biologically active compounds against microorganisms (32). Another successful approach is the conjugation of hydrophilic (usually cationic) amino acid residues to hydrophobic fatty acids, hence, the production of synthetic lipopeptides (33). One of the most successful antimicrobial agents produced by this approach is the semi-synthetic tridecalipopeptide surotomycin (CB-183, 315) (34) by Cubist Pharmaceuticals, which has potent activity against *Clostridium difficile*, *Enterococcus faecalis* and other Gram-positive pathogens (35, 36). Surotomycin is a derivative of

the naturally-occurring FDA-approved antibacterial lipopeptide daptomycin (Cubicin®) (37, 38). Currently[1], surotomycin is undergoing two phase-III clinical trials for the treatment of *C. difficile*-associated diarrhea (39). It is noteworthy that some AMPs also possess antitumor and antiproliferative activity (40, 41).

Concerns about AMPs as possible antibiotics are their metabolic instability and relatively poor pharmacological profile. Some AMPs also exhibit hemolytic activity against erythrocytes and toxicity against eukaryotic cells. In order to circumvent these problems, peptidomimetic approaches or the removal of the "peptide-like" character are performed on AMP lead structures resulting in an increase in promising antibiotic candidates in clinical trials. These include the introduction of D-amino acids, cyclization, and/or different molecular scaffolds.

How do AMPs exert their biological function? Amphiphilicity, achieved by peptide organization into certain secondary structures or aggregates, is arguably the most important physicochemical property of AMPs. Secondary structures such as α-helices, β-sheets (β-hairpins), and extended structures are commonly seen in longer AMPs with more than 10 amino acid residues but are usually absent in short AMPs (42). AMPs are usually cationic, which confers selectivity for the anionic bacterial cell membrane when compared to the zwitterionic eukaryotic cell membrane. While still unclear due to the complexity of experimental designs, the presence of sterols (such as cholesterol and phytosterol) in eukaryotic cell membranes may also impart protection from AMPs *via* alteration in membrane fluidity, which in turn may disrupt the membrane insertion of AMPs

---

[1] The term current in the context of surotomycin refers to data up to 2014. Unfortunately. surotomycin failed to demonstrate superiority to vancomycin against *C. difficile* in the two phase 3 clinical trials referred in the text (Boix V, Fedorak RN, Mullane KM, Pesant Y, *et al.* 2017. Open Forum Infect Dis. doi: 10.1093/ofid/ofw275.).

(43, 44). Electrostatic interaction of the positively charged AMP with either lipopolysaccharide (LPS) in Gram-negative or lipoteichoic acid in Gram-positive bacteria (both negatively charged) is believed to be the first step in AMP's mode of action. Subsequently, AMPs exhibit their antibacterial activity through different reported mechanisms: (1) by changing membrane potential (45), (2) by producing transmembrane pore formation or defects resulting in cell leakage (46), (3) by modifying the native distribution of membrane lipids resulting in destabilization of structure (47), (4) by triggering lethal processes such as the induction of autolytic enzymes (48) and (5) by interacting and/or interfering with intracellular targets (49). Notably, most AMPs exhibit multiple modes of action (50, 51), rendering the pathogen less likely to develop resistance.

1.5. Short AMPs of ten or fewer amino acids as lead antibacterial molecules

The development of new anti-infective agents requires a repetitive cycle of lead optimization where the desired biological activity is maximized and the toxicity to mammalian cells reduced. The vast majority of AMPs are comprised of 10 or more amino acids. However, shorter AMPs are especially attractive as lead compounds as production costs are lower. In addition, many short AMPs are of equal antibacterial potency against clinical isolates when compared to longer AMPs.

As of November 2014, the "Antimicrobial Peptide Database" (APD) recorded 52 antibacterial peptides of 10 amino acids or less out of 2008 reported AMPs of natural origin (although the database only records AMPs less than or equal to 100 residues) (52). Note that the reported figures only take into account isolated AMPs and adding unnatural (synthetic) ones would greatly increase the count. In order for our survey to be feasible, we will highlight the merits of two promising classes of short AMPs containing five to ten amino acid residues: the tryptophan- & arginine- rich

short AMPs and the proline-rich short AMPs. We will also briefly discuss ultrashort AMPs, which contain four amino acids or fewer, and their benefits for further shortening the peptide length.

Tryptophan- and arginine-rich short antimicrobial peptides (TARAMPs). Perhaps the two most common amino acids present in AMPs are tryptophan (W) and arginine (R) as both are found in many antimicrobial peptides, such as the cathelicidins indolicidin and tritrpticin, at an unusually high proportion. Both, tryptophan and arginine play important roles for the function of AMPs. It is known that tryptophan residues have a strong preference for the interfacial regions of lipid bilayers, as observed in experimental and theoretical studies (53, 54). For example, a molecular dynamics (MD) simulation of the AMP dermaseptin S3 demonstrated that the tryptophan residue is involved in peptide-lipid interactions (55). Another study showed that tryptophan associates with the polar choline head group in bilayers *via* a cation-π interaction, resulting in favorable intermolecular interactions (56). This cation-π interaction comes from the quadrupole moment of tryptophan's indole ring donating electron density to a positively charged atom (usually an amino/ammonium group but also guanidinium groups) (57, 58). Therefore, an indole ring is more optimal for interacting with positively charged groups in phospholipids than with hydrophobic fatty acyl chains, rendering the tryptophan-rich AMP with excellent membrane inserting capabilities. Intramolecular cation-π interactions are observed in most AMPs rich in tryptophan and arginine residues, preferring a parallel (stacked) intramolecular arrangement of the two residues as the AMP inserts itself into the membrane (59, 60). This interaction makes the entry of the peptide into the lipid bilayer more energetically favorable as the positively charged guanidinium group of arginine is effectively shielded from the hydrophobic environment (57, 61).

There have been several comprehensive review articles focused on TARAMPs longer than ten amino acids in the literature (54, 62).

So far, all reported short TARAMPs with ten or fewer amino acids are synthetically made by either modifying HDPs or were discovered by screening combinatorial peptide libraries. Most HDP-based TARAMPs are obtained from truncating lactoferrin, an 80 kDa antimicrobial protein that also acts as an iron-binding protein found in milk. The idea of truncation stemmed from the discovery of a 25-residue peptide called lactoferricin, released from the N-terminal region of bovine lactoferrin by pepsin that exhibited potent bactericidal activity (63). Further truncation and sequence modification led to the discovery of short lactoferrin-derived TARAMPs LF11-324, M6 and Octa 1 (Table 1-1). LF11-324 is a decapeptide with an amidated C-terminus that exhibited good bactericidal activity against *E. coli* and showed low hemolysis (<10%) at 500 µg/mL (64). LF11-324's mode of action is most likely cell membrane perturbation due to its ability to induce membrane curvature strain and bilayer thinning in *E. coli* lipid model membranes (65). Both peptides M6 and Octa 1 exhibit better antimicrobial activity than LF11-324. Furthermore, M6 scored an EC_{50} of 765 µg/mL against red blood cell (RBC) while no hemolytic activity was reported for Octa 1 up to a concentration of 1000 µg/mL (66, 67). Unfortunately, no mode of action studies have been published for either compound. As seen in Table 1-1, both M6 and Octa 1 contain significantly more tryptophan residues (at least three) in comparison to LF11-324 (which only has one) while all three peptides contain a significant number of arginines. One may argue that the better biological activity of M6 and Octa 1 in comparison to LF11-324 may derive from the increased number of cation-π interactions.

Table 1-1 Minimum inhibitory concentration (MIC) of selected short tryptophan- and arginine-rich antimicrobial peptides (TARAMPs)

Compound / Sequence	MIC (µM unless otherwise specified) [Organism tested]		Ref
LF11-324 / PFFWRIRIRR-NH$_2$	8 µg/mL [*E. coli*]		(64)
M6 / WRFRWRW-NH$_2$	<2.1 [*S. aureus*]	4.2 [*E. coli*]	(66)
Octa 1 / RRWYRWWR-NH$_2$	1.8 [*S. aureus*]	3.7 [*E. coli*]	(67)
Ac-RRWWCR-NH$_2$	11-12 µg/mL [*S. aureus*]	12-18 µg/mL [*E. coli*]	(68)
Pac-525 / Ac-KWRRWVRWI-NH$_2$	4 [*S. aureus*]	2 [*E. coli*]	(70)
Pac-525$_{rev}$ / Ac-IWRVWRRWK-NH$_2$	4 [*S. aureus*]	4 [*E. coli*]	(70)
MP196 / RWRWRW-NH$_2$	5 µg/mL [*S. aureus*]	5 µg/mL [*E. coli*]	(72)
	5.3 [MRSA]	1.3 [*B. subtilis*]	(74)
FcCO-WRWRW-NH$_2$	48 [MRSA]	12 [*B. subtilis*]	(74)
MP276 / RcCO-WRWRW-NH$_2$	5.8 [MRSA]	2.9 [*B. subtilis*]	(74)
N-C$_8$ / K(C$_8$)RWRWRW-NH$_2$	1 [*S. aureus*]	5 [*E. coli*]	(75)
C-C$_8$ / RWRWRWK(C$_8$)-NH$_2$	2 [*S. aureus*]	2-5 [*E. coli*]	(75)
D5-NH$_2$ / RWKRWWRRKK-NH$_2$	3 [*S. aureus*]	3 [*E. coli*]	(77)
D5-COOH / RWKRWWRRKK	6 [*S. aureus*]	3 [*E. coli*]	(77)
AMP-C10-3 / C$_{10}$-RKWWK-NH$_2$	3.9 µg/mL [*S. aureus*]	3.9-7.8 µg/mL [*E. coli*]	(79)
RW3 / Ac-RRWFWR-NH$_2$	31.3 [*B. subtilis*]	125 [*E. coli*]	(80)
cRW3 / cyclo(RRWFWR)	3.9 [*B. subtilis*]	2 [*E. coli*]	(80)

E. coli = *Escherichia coli*; *S. aureus* = *Staphylococcus aureus*; MRSA = methicillin-resistant *S. aureus*; *B. subtilis* = *Bacillus subtilis*

Arguably the earliest non-hemolytic short TARAMP, Ac-RRWWCR-NH$_2$ was described in 1991 by Houghten and coworkers using combinatorial strategies (68). This hexapeptide displayed modest antibacterial activity against Gram-negative and Gram-positive bacteria (Table 1-1) (68, 69). Another TARAMP, Pac-525, exhibited good antibacterial activity and was found to bind strongly to negatively charged phospholipid vesicles, resulting in an efficient calcein dye leakage (even at a very low peptide concentration of 1 µM) (70). This, along with the fact that its all-D analog possesses similar activity (70), suggested that Pac-525 does not require chiral recognition by a receptor and targets the cell membrane resulting in permeation and cell death. Interestingly,

the amino acid sequence does not seem to be of importance as its reverse sequence Pac-525$_{rev}$ exhibits similar antibacterial activities (Table 1-1). Most likely, these synthetically developed TARAMPs rely on their overall amphiphilicity, in addition to the before-mentioned tryptophan-arginine interactions, for their biological activity.

A library of tri-, tetra-, penta- and hexa-peptide AMPs consisting of only R and W residues were reported by Strøm and coworkers who found that the hexapeptide MP196 (RWRWRW-NH$_2$) as the most active (Table 1-1) (71). Additional studies on MP196 was described by Liu and coworkers in which they found that a decrease of RW repeats results in a loss of antibacterial activity while addition of RW repeats leads to an increase in hemolytic activity (72). MP196's mode of action against pathogens was found to be membrane depolarization (not membrane permeabilization or pore formation) since no ion leakage was observed in model membranes or *in vivo* experiments; although bacterial cell morphology was found to be disturbed (73). Further studies confirmed that MP196 inhibited the bacterial respiratory chain by interacting with cytochrome c, resulting in its detachment from the membrane (73). Also, MP196 induces delocalization of the lipid II biosynthesis protein MurG from the intracellular membrane surface. Both actions of MP196 explain the observed disturbance in the bacterial cell morphology, which is indicative of cell stress.

Modifications on both terminal ends of MP196, as a scaffold, have been reported by Metzler-Nolte and coworkers in hopes of achieving a better pharmacological profile (Fig. 1-1 & Table 1-1). First, they explored the effects of metallocenoyl groups incorporated into MP196's N-terminus (*via* an amide linkage) by replacing arginine with an organometallic moiety resulting into the sequence M(CO)WRWRW-NH$_2$ (74). The presence of a metallocenoyl fragment may contribute lipophilic

bulk and/or intricate redox-activity to MP196. They found that the ruthenocene Rc(CO)WRWRW-NH_2 analog, also known as MP276, showed similar activity as MP196 while the ferrocene Fc(CO)WRWRW-NH_2 exhibits inferior activity (74). Unfortunately, MP276 also showed higher hemolytic activity against RBC (64% hemolysis at 192 µM) and toxicity against several mammalian cell lines (74). Another approach reported was the introduction of an unnatural lysine residue, where either a ferrocenoyl or acyl group (from 2 to 14 carbons-long) is attached to the amino-side chain of lysine, to either the N- or C- terminal region of MP196 in hopes of optimizing its amphiphilic characteristic (Fig. 1-1). The most active derivative contains octanoic acid (C_8) within the design, having both N- and C- terminus incorporation (*N*-C_8 and *C*-C_8, respectively) exhibit similar antimicrobial activity (Table 1-1) (75). Interestingly, the *C*-C_8 analog displayed significantly lower hemolytic activity of 10-20% at 250 µg/mL in comparison to *N*-C_8, having >50% hemolysis at similar concentration. Combinatorial efforts *via* L- to D-amino acid replacement of *C*-C_8 yielded several derivatives that exhibited similar antibacterial activity but much lower hemolytic activity (76).
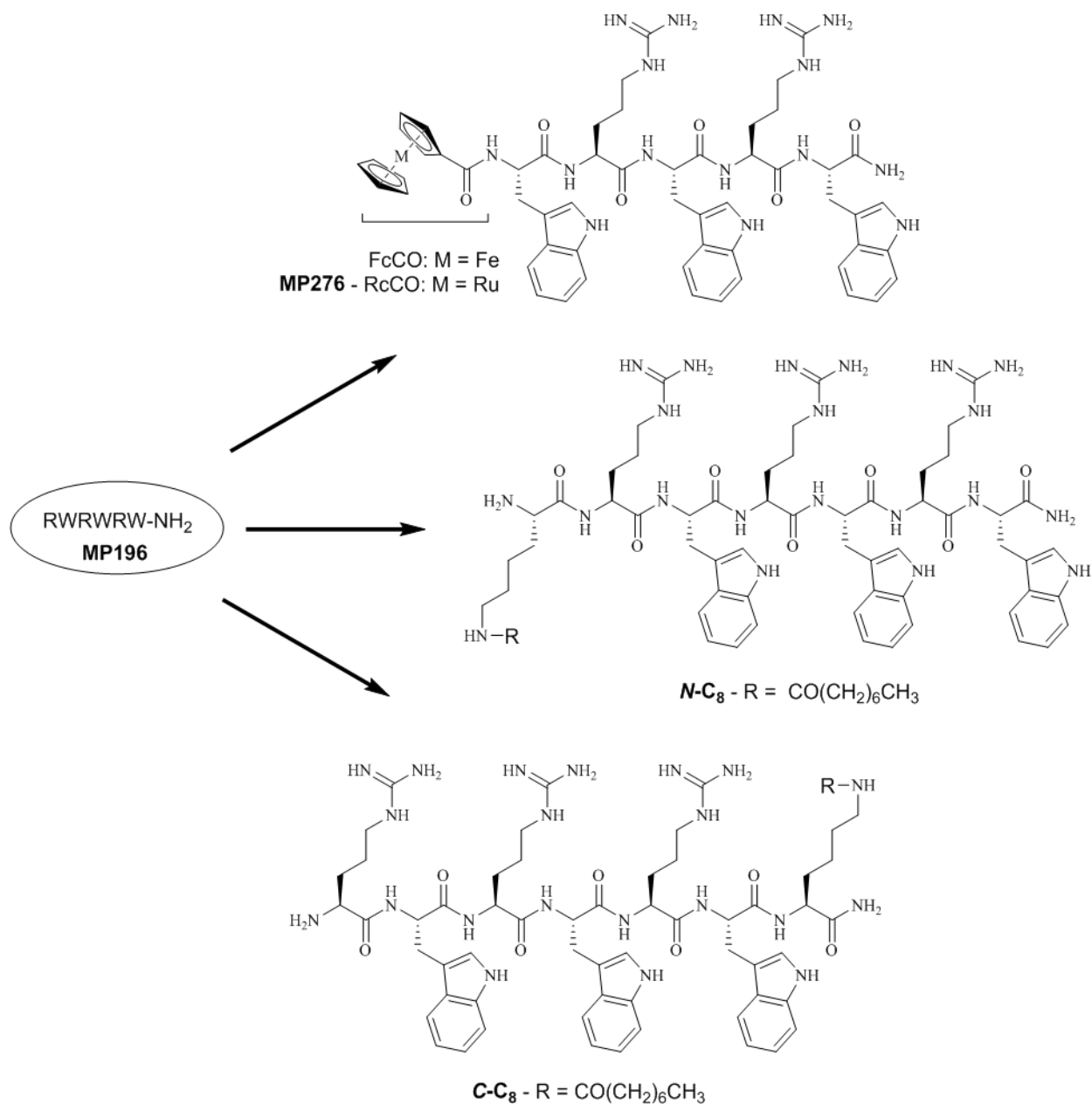
Figure 1-1 Modifications of the lead sequence MP196 by the attachment of a metallocenoyl group or an N-ε-anchored fatty acid lysine residue at either the C- or N- terminus.

Attempts to optimize the activity of TARAMPs have also been reported on different lead peptide sequences. The antibacterial effect of C-terminal amidation was explored on the membrane-

targeting decapeptide D5 (Table 1-1). It was found that the amidated counterpart D5-NH$_2$ was slightly more active than the free carboxylic acid D5-COOH against *S. aureus* although its % hemolysis at 100 µM increased by a factor of two (from 3% to 6.5%) (77). The subtle biological activity differences between the amidated and non-amidated counterparts may not significantly impact the design but the fact that an amidated C-terminus renders possible exopeptidase resistance is an advantage to keep in mind (78). Fatty acyl addition, from hexanoic to octadecanoic acid, on the N-terminus of the peptide sequence RKWWK-NH$_2$ resulted in a library of lipopeptides that clearly exhibits a hydrophobic threshold (79). AMP-C10-3 containing decanoic acid (C10) was found to be the optimal acyl length as an increase or a decrease in the length resulted in a loss of activity. The effects of cyclization have also been reported. Wessolowski and coworkers found that cyclization increases both antibacterial and hemolytic activity for a series of hexapeptides (80). For example, the peptide sequence Ac-RRWFWR-NH$_2$ is 62-fold less active against *E. coli* in its linear form than its cyclized form (Table 1-1). Similarly, its hemolytic activity is lower by a factor of three when it is linear (6.1% hemolysis in comparison to 18.5% at 100 µM peptide concentration) (80). A merit of their design is that peptide cyclization confers much better peptidase resistance in comparison to either amidation of the C-terminus, acylation of the N-terminus or both peptide terminal modifications (78).

Proline-rich short antimicrobial peptides (PRAMPs). Proline-rich antimicrobial peptides (PRAMPs) are bacterial-targeting molecules that contain an unusually high amount of proline (typically from 25 to 50%) (81). Commonly, PRAMPs have a PXP or PXYP sequence-motif, where X and Y can be any of the common 20 amino acids but usually is L-arginine and P is L-proline (81). The mode of action of PRAMPs differs from other AMPs as they do not kill the

pathogen *via* lysis, rather, they translocate inside the cell membrane to affect intracellular machineries (82). In fact, several studies have shown that their all-D enantiomers are much less active (if not completely inactive) (82, 83), indicating that PRAMPs interact with chiral intracellular targets. Interestingly, many PRAMPs show antibacterial selectivity against Gram-negative bacteria and are less active against Gram-positive microorganisms. There have been several comprehensive review articles focused on PRAMPs longer than ten amino acids in the literature (81, 84, 85).

A paradox is observed with shorter PRAMPs, containing ten or fewer amino acids, with respect to their longer counterparts. Almost all (with the exception of stylisin) reported short PRAMPs exhibit good antimicrobial activity against Gram-positive but little activity against Gram-negative microorganisms (see Table 1-2). Moreover, in contrast to larger acyclic PRAMPs, all reported short PRAMPs are cyclic and do not possess PXP or PXYP motifs (except stylisin).

Table 1-2 Minimum inhibitory concentration (MIC) of selected short proline-rich antimicrobial peptides (PRAMPs)

Compound / Sequence	MIC (µg/mL) [Organism tested]		Ref
empedopeptin	1.6 [*S. aureus*]	>100 [*E. coli*]	(86)
tripropeptin A	6.25 [MRSA]	50 [*E. faecium* VCM res]	(89)
tripropeptin B	0.78 [MRSA]	25 [*E. faecium* VCM res]	(89)
tripropeptin C	0.78 [MRSA]	6.25 [*E. faecium* VCM res]	(89)
tripropeptin D	0.78 [MRSA]	3.13 [*E. faecium* VCM res]	(89)
tripropeptin E	0.78 [MRSA]	3.13 [*E. faecium* VCM res]	(89)
tripropeptin Z	25 [MRSA]	>100 [*E. faecium* VCM res]	(89)
plusbacin A1	1.6 [MRSA]	6.3 [*E. faecium*]	(91)
plusbacin A2	0.8 [MRSA]	3.1 [*E. faecium*]	(91)
plusbacin A3	0.4 [MRSA]	1.6 [*E. faecium*]	(91)
plusbacin A4	0.4 [MRSA]	1.6 [*E. faecium*]	(91)
plusbacin B1	1.6 [MRSA]	12.5 [*E. faecium*]	(91)
plusbacin B2	0.8 [MRSA]	3.1 [*E. faecium*]	(91)
plusbacin B3	0.8 [MRSA]	3.1 [*E. faecium*]	(91)
plusbacin B4	0.8 [MRSA]	6.3 [*E. faecium*]	(91)
ADEP-4	0.05 [*S. aureus*]	≤0.01 [*E. faecalis*]	(100)
ADEP-4-analog1	0.6 [MRSA]	0.04 [*E. faecalis* VCM res]	(101)
ADEP-4-analog2	0.024 [*S. aureus*]	<0.00002 [*E. faecalis*]	(102)
stylisin 1 cyc[YPLPFIP]	12.5 [*S. aureus*] 25 [*B. subtilis*]	6 [*K. pneumoniae*] 6 [*P. aeruginosa*]	(104)
linear stylisin 1 Boc-YPLPFIP-OMe	12.5 [*S. aureus*] 25 [*B. subtilis*]	6 [*K. pneumoniae*] 6 [*P. aeruginosa*]	(104)
stylisin 2 cyc[PIPFPPY]	12.5 [*S. aureus*] 25 [*B. subtilis*]	6 [*K. pneumoniae*] 6 [*P. aeruginosa*]	(105)
linear stylisin 2 Boc-PIPFPPY-OMe	12.5 [*S. aureus*] 25 [*B. subtilis*]	6 [*K. pneumoniae*] 6 [*P. aeruginosa*]	(105)

E. coli = *Escherichia coli*; *S. aureus* = *Staphylococcus aureus*; MRSA = methicillin-resistant *S. aureus*; *B. subtilis* = *Bacillus subtilis*; *E. faecium* = *Enterococcus faecium*; *E. faecalis* = *Enterococcus faecalis*; VCM res = vancomycin resistant; *K. pneumoniae* = *Klebsiella pneumoniae*; *P. aeruginosa* = *Pseudomonas aeruginosa*

The naturally-occuring empedopeptin, tripropeptin and plusbacin are lipodepsioctapeptide PRAMP families which differ only in the composition of three amino acids (Fig. 1-2). Empedopeptin shows good activity against Gram-positive bacteria (Table 1-2) and low inherent toxicity, with an intravenous LD_{50} of 560 mg/kg in mouse models (86). Empedopeptin is found to selectively interfere with late stages of cell wall biosynthesis *via* calcium ion-dependent complex formation with peptidoglycan precursors (lipid II and other bactoprenol-containing molecules) (87). Studies on the nature of the hydrophobic acyl chain in tripropeptins indicate that a certain hydrophobic threshold is needed for antibacterial activity (88). Indeed, tripropeptins C, D and E containing 14-, 15- and 16-carbon acyl chains, respectively, are most active against Gram-positive bacteria in comparison to shorter acyl chain counterparts (Fig 1-2 & Table 1-2) (89). Interestingly, variant branched acyl chains do not confer any differences as the iso-branched tripropeptin C and the anteiso-branched tripropeptin aiC have similar antibacterial activity (90). Isolated from *Pseudomonas* spp. PB-6250, the plusbacin family exhibit excellent activity against Gram-positive bacteria *in vitro* and *in vivo* (Fig. 1-2 & Table 1-2) (91). It has been suggested on the basis of their structural similarity that the tripropeptin and plusbacin families display the same mode(s) of action (87, 92).
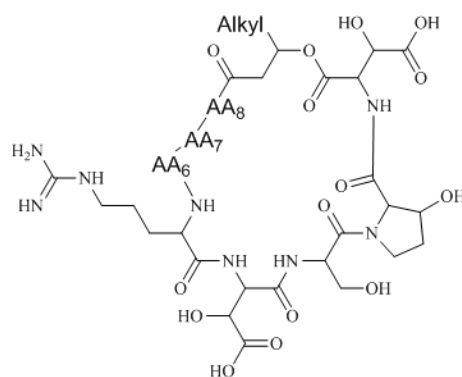
Compound	AA$_6$	AA$_7$	AA$_8$	Alkyl	Ref
empedopeptin	Pro	Ser	Pro	-(CH$_2$)$_{10}$-CH$_3$	(93)
tripropeptin A	Thr	Pro	Pro	-(CH$_2$)$_7$-CH(CH$_3$)CH$_3$	(94)
tripropeptin B	Thr	Pro	Pro	-(CH$_2$)$_8$-CH(CH$_3$)CH$_3$	(94)
tripropeptin C	Thr	Pro	Pro	-(CH$_2$)$_9$-CH(CH$_3$)CH$_3$	(94)
tripropeptin aiC	Thr	Pro	Pro	-(CH$_2$)$_8$-CH(CH$_3$)CH$_2$CH$_3$	(90)
tripropeptin D	Thr	Pro	Pro	-(CH$_2$)$_{10}$-CH(CH$_3$)CH$_3$	(94)
tripropeptin E	Thr	Pro	Pro	-(CH$_2$)$_{11}$-CH(CH$_3$)CH$_3$	(89)
tripropeptin Z	Thr	Pro	Pro	-(CH$_2$)$_6$-CH(CH$_3$)CH$_3$	(94)
plusbacin A1	Thr	Ala	Hyp	-(CH$_2$)$_{10}$-CH$_3$	(95)
plusbacin A2	Thr	Ala	Hyp	-(CH$_2$)$_9$-CH(CH$_3$)CH$_3$	(95)
plusbacin A3	Thr	Ala	Hyp	-(CH$_2$)$_{10}$-CH(CH$_3$)CH$_3$	(95)
plusbacin A4	Thr	Ala	Hyp	-(CH$_2$)$_{12}$-CH$_3$	(95)
plusbacin B1	Thr	Ala	Pro	-(CH$_2$)$_{10}$-CH$_3$	(95)
plusbacin B2	Thr	Ala	Pro	-(CH$_2$)$_9$-CH(CH$_3$)CH$_3$	(95)
plusbacin B3	Thr	Ala	Pro	-(CH$_2$)$_{10}$-CH(CH$_3$)CH$_3$	(95)
plusbacin B4	Thr	Ala	Pro	-(CH$_2$)$_{12}$-CH$_3$	(95)

Figure 1-2 Structure of empedopeptin, tripropeptins and plusbacins.

Residues consist of a mixture of L- and D- amino acids. Stereochemistry of each component removed for simplicity but can be found in their corresponding references.

One of the best studied natural product-inspired short PRAMPs are the cyclic acyldepsipeptides (ADEPs). ADEPs kill Gram-positive pathogens *via* a unique mechanism that involves dysregulation of caseinolytic peptidase (ClpP) activity (96, 97), which is crucial for cellular protein

turnover. Progress in ADEP development is due to consecutive pharmacological improvements, at Bayer Healthcare AG and other research groups, of the lead natural products A54556 A & B (98) and enopeptins A & B (99) (Fig. 1-3). The synthetic ADEP-4 was first reported as an optimized molecule in 2006 (100), followed by ADEP-4-analog1 in 2010 (101) and ADEP-4-analog2 in 2014 (102). All three ADEPs have excellent antibacterial activity against Gram-positive bacteria with MICs in the low µg/mL to ng/mL range (100–102) (Table 1-2) while no activity has been reported against Gram-negative bacteria.

The cyclic stylisins 1 and 2, naturally-isolated from the Jamaican sponge *Stylissa caribica* (103), were synthesized in the laboratory and found to exhibit good antimicrobial activity (Table 1-2) against Gram-negative and Gram-positive (to a lesser extent) bacteria (104, 105). Furthermore, both their linear counterparts (although acylated on the N-terminus and methyl esterified on the C-terminus) yielded similar MIC values. Interestingly, both stylisins 1 and 2 are the only reported short PRAMPs to demonstrate a similar antimicrobial activity profile (higher activity against Gram-negative bacteria than Gram-positive) when compared to their longer counterparts, although no mechanistic studies are yet reported. This similarity in antibacterial activity may be due to the presence of the PXP motif within the stylisin sequence.
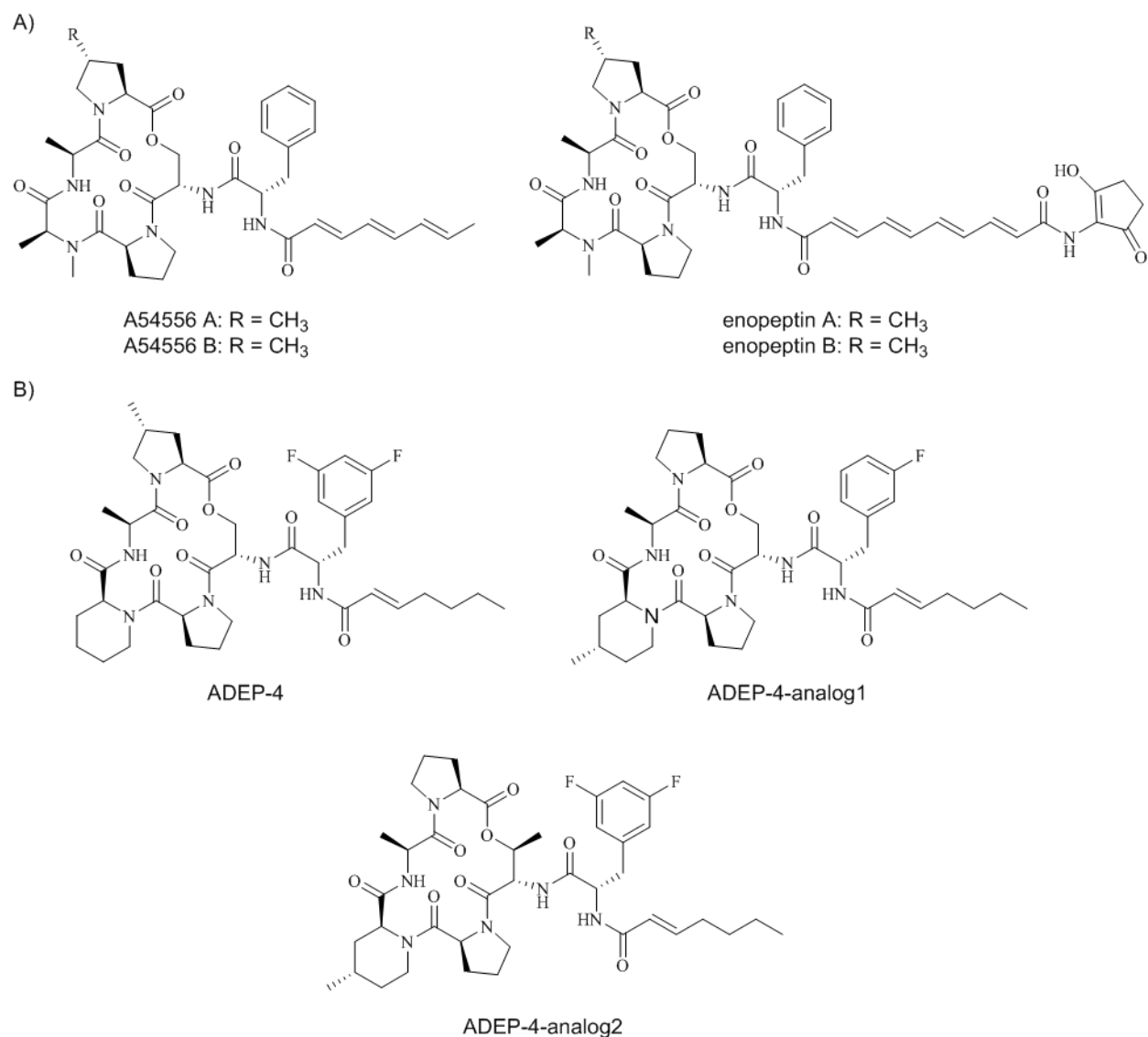
Figure 1-3 Structure of A) natural product and B) synthetic ADEPs.

Synthetic ADEPs are obtained by successive structure optimizations and modifications of natural product ADEPs.

Ultrashort antimicrobial peptides. Antimicrobial peptides consisting of four or fewer amino acids form the subcategory of ultrashort peptides. The term "ultrashort" was coined in order to further classify AMPs by their sequence length and examples which fit into this subcategory include

antibacterial diketopiperazines (106) and N-terminally quaternized dipeptide amphiphiles (107, 108). Our research group has been interested in the development of ultrashort cationic lipopeptides (USCLs) which were initially reported by Shai and coworkers (109) in 2006. These amphiphilic USCLs consist of four or fewer amino acids (which are usually hydrophilic) conjugated to a fatty acid. They exhibit broad-spectrum antibacterial activity against Gram-positive and Gram-negative bacteria *via* cell membrane disruption and permeabilization. We have found that some USCLs may also display beneficial immunomodulatory properties and do not stimulate the production of pro-inflammatory cytokines such as TNF-α and IL-1β (110). There are recent publications involving the optimization of the USCL-template (111, 112). For instance, we described the importance of amino acid-side chain flexibility in USCLs as incorporation of ring-constrained amino acids resulted in loss of antibacterial activity. MIC comparison of the side chain-flexible USCL-Dab1 to its ring-constrained USCL-P_{Cat}1 counterpart (Fig. 1-4) showed up to a 32-fold decrease in activity (8 µg/mL versus 32 µg/mL against MRSA and 8 µg/mL versus 256 µg/mL against *P. aeruginosa*, respectively) (113). Interestingly, we found that USCL-P_{Cat}1 that only contain four L-4-aminoprolines conjugated to palmitic acid populate a left-handed polyproline II helical secondary structure in water (113), possibly the first smallest ultrashort antimicrobial peptide reported to have a high secondary structural propensity as they are thought not to favor any secondary structure in solution.
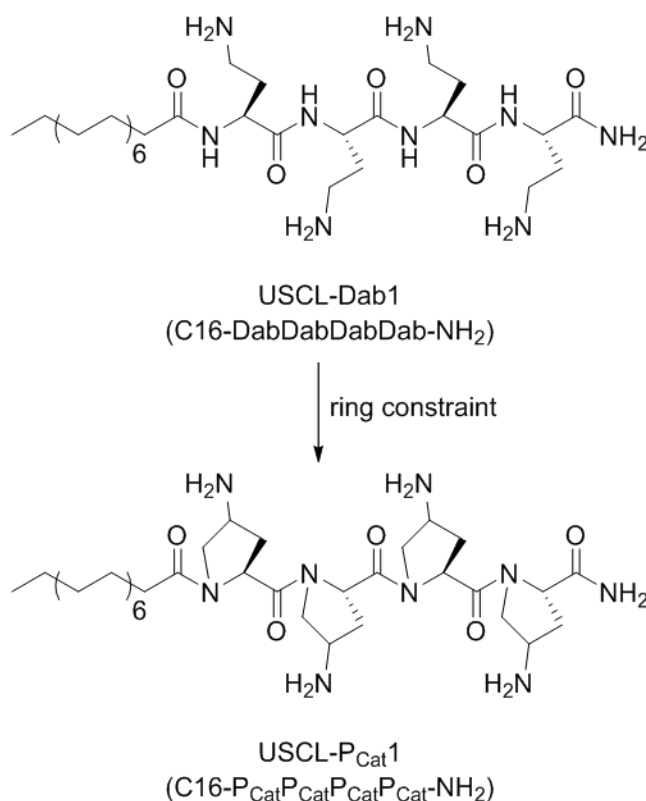
Figure 1-4 Ultrashort cationic lipopeptide structure comparison of the side-chain flexible L-diaminobutyric acid (Dab) and its ring-constrained counterpart L-4-aminoproline (P_{Cat}).

Both compounds have their N-terminus ligated to palmitic acid (C16) and their C-terminus amidated.

1.6. Peptidomimetic approaches

Major drawbacks of AMPs and short AMPs are their limited stability toward proteolysis resulting in short half-lives, inherent toxicity, poor bioavailability and rapid excretion. In order to circumvent these problems, peptide mimics coined "peptidomimetics" have been designed. Peptidomimetics encompasses all performed modifications on a lead peptide structure in order to remove their "peptide-like" characteristics in hopes for increased stability against proteases and improved pharmacological profile while retaining their biological activity. It includes strategies employing β-peptides (114), peptoids (114), arylamide and phenylene ethynylene oligomers (115),

ceragenin-based mimetics (116), α-helical mimetics (115, 117, 118), β-turn mimetics (117), N-acylated-N-aminoethyl peptides (AA peptides) (119, 120), oligoacyllysines (OAKs) (115, 121) and peptide dendrimers (115, 117). Extensive reviews have been published for peptidomimetics, thus, we will only highlight some of the new approaches reported in the past two years.

Table 1-3 Minimum inhibitory concentration (MIC) of selected peptidomimetic compounds

Compound	MIC (µg/mL unless otherwise specified) [Organism tested]		Ref
HDM-4	8 µM [*E. coli*[a]]	2 µM [*E. coli*[b]]	(122)
	10 µM [*A. baumannii*]	10 µM [*P. aeruginosa*]	(123)
SMAPM 3	2.8 [MRSA]	5.2 [VRE]	(124)
	3.5 [*E. coli*]	1.6 [*P. aeruginosa*]	
GS-Sw(LF) open	8 [*S. aureus*]	16 [*S. epidermidis*]	(125)
GS-Sw(LF) closed	128 [*S. aureus*]	128 [*S. epidermidis*]	(125)

[a] = CTX-M-15 extended-spectrum β-lactamase (ESBL)-producer; [b] = New Delhi metallo-β-lactamase-1 (NDM-1)-producer; *E. coli* = *Escherichia coli*; *S. aureus* = *Staphylococcus aureus*; MRSA = methicillin-resistant *S. aureus*; *S. epidermidis* = *Staphylococcus epidermidis*; *P. aeruginosa* = *Pseudomonas aeruginosa*; *A. baumannii* = *Acinetobacter baumannii*; VRE = vancomycin-resistant *Enterococci;*

HDM-4 (Fig. 1-5A) consists of an alternating L-lysine and phenylalanine peptoid mimic, NPhe, with its N-terminus acetylated and C-terminus amidated. HDM-4 has been reported to possess excellent antibacterial activity (Table 1-3) against a wide array of clinically-relevant multi-drug resistant *E. coli* strains (including extended-spectrum β-lactamase- and New Delhi metallo-β-lactamase-1- producing strains) (122). Also, HDM-4 exhibits low toxicity against red blood cells and HeLa cells. A follow-up report shows that it is also active against other Gram-negative bacteria and possesses multispecies anti-biofilm activity at sub-MIC levels (123). As a mode of action against pathogens, strong evidence suggests a multiple non-specific targeting mechanism similar to most AMPs (123). As expected, HDM-4 does not confer resistance development of *E. coli* as shown after 20 cycles of repetitive sub-MIC treatment. More interesting is that HDM-4 exhibits

beneficial immunomodulatory properties as it induces the production of the chemoattractants interleukin-8 (IL-8), monocyte chemotactic protein-1 (MCP-1) and MCP-3 from human peripheral blood mononuclear cells (123). Furthermore, it has been shown to suppress LPS-mediated release of the pro-inflammatory cytokines IL-6 and tumor necrosis factor-α (TNF-α).
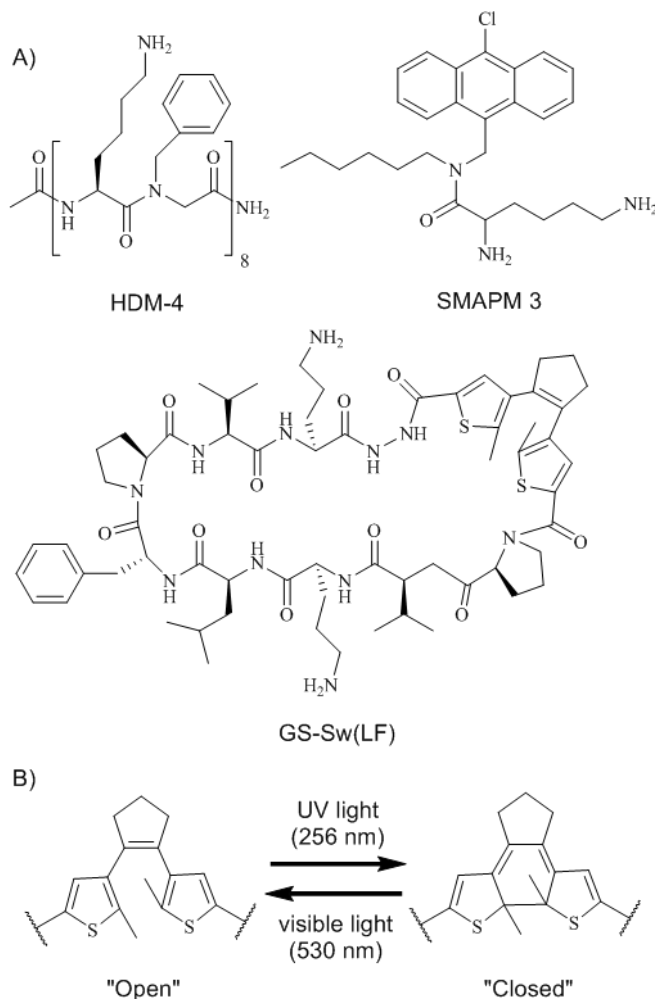
Figure 1-5 A) Structures of highlighted peptidomimetics and B) the photoreversible nature of the diarylethene-based amino acid analog incorporated to gramicidin S.

Another interesting class of peptidomimetics published in 2014 are the small molecular antibacterial peptoid mimics (SMAPM) by Haldar and coworkers in which aliphatic, aromatic and

lysine residues are covalently fused *via* a tertiary amide linkage (124). Both the aliphatic and aromatic portions confer hydrophobicity while the lysine residue confers hydrophilicity (*via* its N-terminal and amino side-chain). SMAPM possess good *in vitro* activity against both Gram-positive and Gram-negative bacteria. As an example, SMAPM 3 (Fig. 1-5A & Table 1-3) exhibits broad-spectrum activity and shows bactericidal activity within an hour (at 3x and 6x MIC). Furthermore, the antibacterial activity of SMAPM in the presence of plasma does not change, suggesting good proteolytic stability and bioavailability (as the compound's antibacterial activity seems to be unaffected by the presence of plasma proteins) (124).

Very unconventional to anti-infective agent development, peptidomimetics of the AMP gramicidin S that possess antibacterial activity tunable by light have been recently reported (Fig. 1-5A & Table 1-3) (125). This was achieved by incorporating a reversibly photoisomerizable diarylethene-based amino acid analog into the peptide sequence. The resulting photochromic compounds possess two different molecular isomers, open and closed forms that are tunable by irradiation with ultraviolet/visible light (Fig. 1-5B). The compounds' open form possesses stronger antibacterial activity than their closed form (up to 16-fold difference) (125). Similarly, their hemolytic activity against erythrocytes is also different for each isomer (125). As an example, GS-Sw(LF) loses antibacterial activity by 16-fold against *S. aureus* and decreases hemolytic activity by a factor of three (from 47μg/mL to >128μg/mL concentration to reach 50% RBC hemolysis) in its closed form. MD simulations provided a possible rationale for the differences: photoswitching leads to changes in amphiphilicty and that the open form closely resembles the spatial arrangement of unmodified gramicidin S (125).

1.7. Short AMP-based peptidomimetics in clinical trials

As proof that the peptidomimetic approach can yield promising anti-infective agents, we will highlight several of these AMP-mimics currently in clinical trials (see Fig. 1-6). Lytixar (LTX-109) owned by Lytix Biopharma AS was developed by continuous structural modifications of short TARAMP lead molecules undertaken by Svendsen and coworkers (126–128). To impart bulk hydrophobicity, they incorporated a synthetically-modified tryptophan analog they called "supertryptophan" also known as β-(2,5,7-tri-tert-butylindol-3-yl)alanine (Tbt). Moreover, they attached 2-phenylethylamine on the C-terminus *via* an amide linkage to further impart hydrophobicity and proteolytic resistance. Lytixar exhibits potent *in vitro* bactericidal activity against multidrug-resistant *S. aureus* strains (MRSA, vancomycin-intermediate, vancomycin-resistant, daptomycin-nonsusceptible and linezolid-nonsusceptible strains) (129). Interestingly, they found that Lytixar's activity against the Gram-negative bacteria *E. coli* and *P. aeruginosa* is sensitive to its stereochemical composition (L- or D-amino acids) while its activity is devoid of stereochemical bias against the Gram-positive *S. aureus* (130). Changes in the compound's stereochemistry results in different degrees of spatial amphipathicity, as observed by MD simulations and NMR studies. Analogs that possess a lower amphipathic nature exhibit lower antimicrobial activity against the two Gram-negative bacteria (130). Indeed, the drug's amphipathic nature certainly plays a big role in effective insertion into the pathogen's cell membrane that leads to cell death. Lytixar[2] successfully completed two Phase I/IIa clinical studies for (1) nasal decolonization of MRSA/MSSA (methicillin-resistant and methicillin-sensitive *S. aureus*) bacteria and (2) treatment of uncomplicated Gram-positive skin infections in 2011.

---

[2] As of 2018, lytixar also known as LTX 109 had been discontinued and removed in the drug pipeline of Lytix Biopharma (https://adisinsight.springer.com/drugs/800032182).
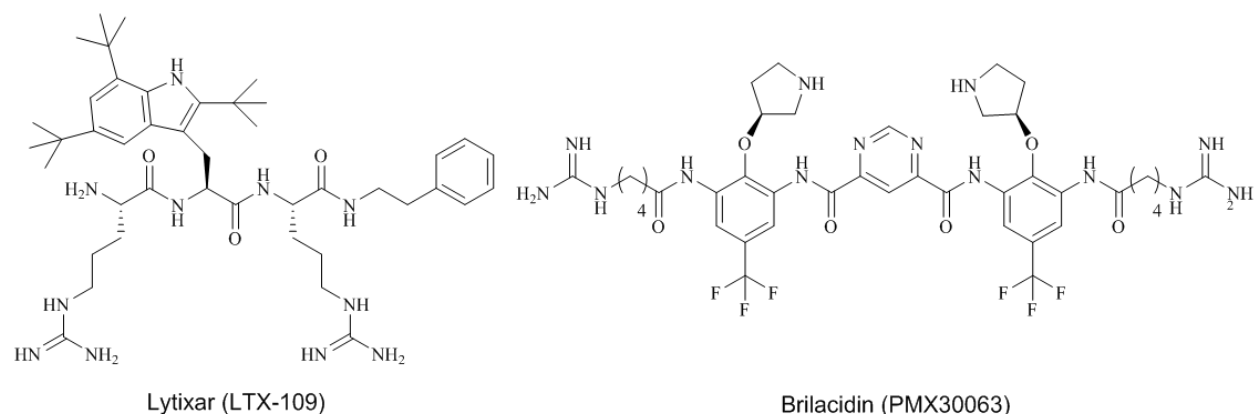
Figure 1-6 Structures of the highlighted peptidomimetics currently in clinical trials.

The arylamide foldamer peptidomimetic brilacidin (PMX30063), previously owned by PolyMedix but was then acquired by Cellceutix in September 2013[3], was initially engineered by DeGrado and coworkers (131–133). Successive modification of lead compounds were performed by decorating the arylamide scaffold with different functional groups in efforts to refine the overall amphiphilic nature, which resulted in an increase in potency and decrease in toxicity. Brilacidin possesses a planar, conformationally-restrained, scaffold with four positive guanadinyl and pyridinyl moieties as well as two hydrophobic trifluoromethane groups (Fig. 1-6). It exhibits potent and broad spectrum *in vitro* bactericidal activity against Gram-positive and Gram-negative pathogens, including several multidrug-resistant strains. Brilacidin has been demonstrated to cause membrane depolarization in *S. aureus* (134). Cellceutix disclosed that the compound also has anti-inflammatory and anti-biofilm properties. A completed multinational double-blind Phase 2a clinical trial with Brilacidin for the treatment of Acute Bacterial Skin and Skin Structure Infections (ABSSSI) revealed the compound's safe and generally well-tolerated profile. In October 2014,

---

[3] Brilacidin is currently being developed by Innovation Pharmaceuticals Inc.

Cellceutix completed a Phase 2b clinical trial with Brilacidin for ABSSSI, focusing on different dosing regimens and its comparison to a standard 7-day regimen of the FDA-approved daptomycin. They found that a single-dose of Brilacidin administered intravenously is well tolerated and has a comparable efficacy to a standard 7-day intravenous treatment with daptomycin. According to the company, this dosing regimen will be used in an upcoming Phase 3 program[4].

The *Pseudomonas*-specific antibacterial POL7080, based on the AMP protegrin I, was developed by researchers at the University of Zurich and Polyphor Ltd by employing a Protein Epitope Mimetics (PEM) approach. This peptidomimetic approach undertakes the design of molecules that mimic the functionally important epitopes of biologically relevant peptides and proteins, such as those based on β-hairpin and α-helix secondary structures (117). POL7080 contains the loop sequence found in protegrin I which is linked to a D-proline-L-proline template, previously reported to stabilize β-hairpin conformations within the macrocycle (135). Unfortunately, the structure of POL7080 has yet to be disclosed in the literature. POL7080 possesses a nanomolar range antibacterial activity against *Pseudomonas* spp. and kills the pathogen *via* a non-membranolytic mode of action, in contrast to most AMPs (136). It was found that POL7080 targets a homolog of the β-barrel protein LptD (Omp/OstA), which is a widely distributed outer membrane protein in Gram-negative bacteria that functions in the assembly of LPS. Furthermore, the drug candidate showed potent *in vivo* antimicrobial activity in a mouse septicemia infection model

---

[4] Brilacidin has completed another Phase 2 clinical trial for the prevention of oral mucositis in head and neck cancer patients, to which positive clinical outcome was met (http://www.ipharminc.com/press-release/2017/12/11/innovation-pharmaceuticals-reports-positive-topline-results-from-phase-2-placebo-controlled-trial-of-brilacidin-for-the-prevention-of-oral-mucositis-in-head-and-neck-cancer-patients). However, Phase 3 clinical trial has yet to commence as of November 2018.

(136). Currently[5], POL7080 is in a Phase 1 clinical trial to evaluate the pharmacokinetics and safety of the drug administered in a single intravenous infusion to subjects with renal impairment. Also, POL7080 is undergoing two Phase 2 clinical trials for lower respiratory tract infections caused by *P. aeruginosa*, specifically for patients suffering exacerbation of non-cystic fibrosis bronchiectasis and for patients with ventilator-associated *P. aeruginosa* pneumonia.

1.8. Conclusion

AMPs are emerging as a new source of antibacterials with impressive activity against drug-resistant bacterial strains. While initial work has concentrated on AMP sequences with more than ten amino acids, recent research indicates that many of the relevant biological properties of AMPs are retained in shorter sequences and small peptide scaffolds. This may facilitate easier drug development and optimization due to their short nature. Furthermore, new peptidomimetic approaches have been developed to circumvent drawbacks of peptide-based drugs, resulting in an increased number of AMP-based drug candidates currently in clinical trials. As such, AMPs are considered as frontrunners for future antibiotics.

1.9. References

1.   Balsalobre LC, Dropa M, Matte MH. 2014. An overview of antimicrobial resistance and its public health significance. Braz J Microbiol 45:1–5.

---

[5] POL 7080, now called murepavadin, have completed the referred Phase 1 and Phase 2 clinical trials in this text, to which the peptidomimetic antibiotic have met targetted outcomes. Polyphor has now commenced two Phase 3 clinical study of murepavadin in treatment of ventilator-associated bacterial pneumonia (VABP) (https://clinicaltrials.gov/ct2/show/NCT03409679) and nosocomial pneumonia (https://clinicaltrials.gov/ct2/show/NCT03582007) that is suspected or confirmed due to *Pseudomonas*.

2.   Stanton TB. 2013. A call for antibiotic alternatives research. Trends Microbiol 21:111–113.

3.   Boucher HW, Talbot GH, Bradley JS, Edwards JE, Gilbert D, Rice LB, Scheld M, Spellberg B, Bartlett J. 2009. Bad bugs, no drugs: no ESKAPE! An update from the Infectious Diseases Society of America. Clin Infect Dis 48:1–12.

4.   World Health Organization. 2014. Antimicrobial resistance: global report on surveillance.

5.   Guilhelmelli F, Vilela N, Albuquerque P, Derengowski LDS, Silva-Pereira I, Kyaw CM. 2013. Antibiotic development challenges: the various mechanisms of action of antimicrobial peptides and of bacterial resistance. Front Microbiol 4:1–12.

6.   Steiner H, Hultmark D, Engstrom A, Bennich H, Boman HG. 1981. Sequence and specificity of two antibacterial proteins involved in insect immunity. Nature 292:246–248.

7.   Ganz T, Selsted ME, Szklarek D, Harwig SS, Daher K, Bainton DF, Lehrer RI. 1985. Defensins. Natural peptide antibiotics of human neutrophils. J Clin Invest 76:1427–1435.

8.   Zasloff M. 1987. Magainins, a class of antimicrobial peptides from Xenopus skin: isolation, characterization of two active forms, and partial cDNA sequence of a precursor. Proc Natl Acad Sci U S A 84:5449–5453.

9.   Mangoni ML. 2011. Host-defense peptides: from biology to therapeutic strategies. Cell Mol Life Sci 68:2157–2159.

10.   Alba A, Lopez-Abarrategui C, Otero-Gonzalez AJ. 2012. Host defense peptides: an alternative as antiinfective and immunomodulatory therapeutics. Biopolymers 98:251–267.

11.   Mookherjee N, Hancock REW. 2007. Cationic host defence peptides: innate immune regulatory peptides as a novel approach for treating infections. Cell Mol Life Sci 64:922–933.

12.   Hilchie AL, Wuerth K, Hancock REW. 2013. Immune modulation by multifaceted cationic host defense (antimicrobial) peptides. Nat Chem Biol 9:761–768.

13.   Lai Y, Gallo RL. 2009. AMPed up immunity: how antimicrobial peptides have multiple roles in immune defense. Trends Immunol 30:131–141.

14.   van der Does AM, Bergman P, Agerberth B, Lindbom L. 2012. Induction of the human cathelicidin LL-37 as a novel treatment against bacterial infections. J Leukoc Biol 92:735–742.

15.   Vandamme D, Landuyt B, Luyten W, Schoofs L. 2012. A comprehensive summary of LL-37, the factotum human cathelicidin peptide. Cell Immunol 280:22–35.

16.   Schauber J, Iffland K, Frisch S, Kudlich T, Schmausser B, Eck M, Menzel T, Gostner A, Luhrs H, Scheppach W. 2004. Histone-deacetylase inhibitors induce the cathelicidin LL-37 in gastrointestinal cells. Mol Immunol 41:847–854.

17.   Wang T-T, Nestel FP, Bourdeau V, Nagai Y, Wang Q, Liao J, Tavera-Mendoza L, Lin R, Hanrahan JW, Mader S, White JH. 2004. Cutting edge: 1,25-dihydroxyvitamin D3 is a direct inducer of antimicrobial peptide gene expression. J Immunol 173:2909–2912.

18.   Termen S, Tollin M, Rodriguez E, Sveinsdottir SH, Johannesson B, Cederlund A, Sjovall J, Agerberth B, Gudmundsson GH. 2008. PU.1 and bacterial metabolites regulate the human gene CAMP encoding antimicrobial peptide LL-37 in colon epithelial cells. Mol

Immunol 45:3947–3955.

19. Nell MJ, Tjabringa GS, Vonk MJ, Hiemstra PS, Grote JJ. 2004. Bacterial products increase expression of the human cathelicidin hCAP-18/LL-37 in cultured human sinus epithelial cells. FEMS Immunol Med Microbiol 42:225–231.

20. Ainsworth GC, Brown AM, Brownlee G. 1947. Aerosporin, an antibiotic produced by Bacillus aerosporus Greer. Nature 159:263.

21. Sarkar S, Hermes DeSantis ER, Kuper J. 2007. Resurgence of colistin use. Am J Heal Pharm 64:2462–2466.

22. Mostardeiro MM, Pereira CAP, Marra AR, Pestana JOM, Camargo LFA. 2013. Nephrotoxicity and efficacy assessment of polymyxin use in 92 transplant patients. Antimicrob Agents Chemother 57:1442–1446.

23. Averbuch D, Horwitz E, Strahilevitz J, Stepensky P, Goldschmidt N, Gatt ME, Shapira MY, Resnick IB, Engelhard D. 2013. Colistin is relatively safe in hematological malignancies and hematopoietic stem cell transplantation patients. Infection 41:991–997.

24. Velkov T, Thompson PE, Nation RL, Li J. 2010. Structure-activity relationships of polymyxin antibiotics. J Med Chem 53:1898–1916.

25. Velkov T, Roberts KD, Nation RL, Thompson PE, Li J. 2013. Pharmacology of polymyxins: new insights into an "old" class of antibiotics. Future Microbiol 8:711–724.

26. Deris ZZ, Akter J, Sivanesan S, Roberts KD, Thompson PE, Nation RL, Li J, Velkov T. 2014. A secondary mode of action of polymyxins against Gram-negative bacteria involves the inhibition of NADH-quinone oxidoreductase activity. J Antibiot (Tokyo) 67:147–151.

27. Mccoy LS, Roberts KD, Nation RL, Thompson PE, Velkov T, Li J, Tor Y. 2013. Polymyxins and analogues bind to ribosomal RNA and interfere with eukaryotic translation in vitro. ChemBioChem 14:2083–2086.

28. Sampson TR, Liu X, Schroeder MR, Kraft CS, Burd EM, Weiss DS. 2012. Rapid killing of Acinetobacter baumannii by polymyxins is mediated by a hydroxyl radical death pathway. Antimicrob Agents Chemother 56:5642–5649.

29. Cai Y, Cao X, Aballay A. 2014. Whole-animal chemical screen identifies colistin as a new immunomodulator that targets conserved pathways. MBio 5:e01235-14.

30. Takahashi D, Shukla SK, Prakash O, Zhang G. 2010. Structural determinants of host defense peptides for antimicrobial activity and target cell selectivity. Biochimie 92:1236–1241.

31. Haney EF, Hunter HN, Matsuzaki K, Vogel HJ. 2009. Solution NMR studies of amphibian antimicrobial peptides: linking structure to function? Biochim Biophys Acta 1788:1639–1655.

32. Wiradharma N, Khoe U, Hauser CAE, Seow SV, Zhang S, Yang Y-Y. 2011. Synthetic cationic amphiphilic alpha-helical peptides as antimicrobial agents. Biomaterials 32:2204–2212.

33. Jerala R. 2007. Synthetic lipopeptides: a novel class of anti-infectives. Expert Opin Investig Drugs 16:1159–1169.

34. Pearson AL, Metcalf CAI, Li J, Cubist Pharmaceuticals Inc. 2010. Novel lipopeptide antibacterial agents for the treatment of Gram positive infections US Patent 20100184649.

35.   Mascio CTM, Chesnel L, Thorne G, Silverman JA. 2014. Surotomycin demonstrates low in vitro frequency of resistance and rapid bactericidal activity in Clostridium difficile, Enterococcus faecalis, and Enterococcus faecium. Antimicrob Agents Chemother 58:3976–3982.

36.   Snydman DR, Jacobus N V, McDermott LA. 2012. Activity of a novel cyclic lipopeptide, CB-183,315, against resistant Clostridium difficile and other Gram-positive aerobic and anaerobic intestinal pathogens. Antimicrob Agents Chemother 56:3448–3452.

37.   Humphries RM, Pollett S, Sakoulas G. 2013. A current perspective on daptomycin for the clinical microbiologist. Clin Microbiol Rev 26:759–780.

38.   Beiras-Fernandez A, Vogt F, Sodian R, Weis F. 2010. Daptomycin: a novel lipopeptide antibiotic against Gram-positive pathogens. Infect Drug Resist 3:95–101.

39.   Butler MS, Blaskovich MA, Cooper MA. 2013. Antibiotics in the clinical pipeline in 2013. J Antibiot (Tokyo) 66:571–591.

40.   Schweizer F. 2009. Cationic amphiphilic peptides with cancer-selective toxicity. Eur J Pharmacol 625:190–194.

41.   Gaspar D, Veiga AS, Castanho MARB. 2013. From antimicrobial to anticancer peptides. A review. Front Microbiol 4:294.

42.   Nguyen LT, Haney EF, Vogel HJ. 2011. The expanding scope of antimicrobial peptide structures and their modes of action. Trends Biotechnol 29:464–472.

43.   McHenry AJ, Sciacca MFM, Brender JR, Ramamoorthy A. 2012. Does cholesterol suppress the antimicrobial peptide induced disruption of lipid raft containing membranes?

Biochim Biophys Acta 1818:3019–3024.

44.   Dennison SR, Phoenix DA. 2011. Effect of cholesterol on the membrane interaction of Modelin-5 isoforms. Biochemistry 50:10898–10909.

45.   Han FF, Gao YH, Luan C, Xie YG, Liu YF, Wang YZ. 2013. Comparing bacterial membrane interactions and antimicrobial activity of porcine lactoferricin-derived peptides. J Dairy Sci 96:3471–3487.

46.   Gee ML, Burton M, Grevis-James A, Hossain MA, McArthur S, Palombo EA, Wade JD, Clayton AHA. 2013. Imaging the action of antimicrobial peptides on living bacterial cells. Sci Rep 3:1557.

47.   Matsuzaki K, Murase O, Fujii N, Miyajima K. 1996. An antimicrobial peptide, magainin 2, induced rapid flip-flop of phospholipids coupled with pore formation and peptide translocation. Biochemistry 35:11361–11368.

48.   Bierbaum G, Sahl HG. 1985. Induction of autolysis of staphylococci by the basic peptide antibiotics Pep 5 and nisin and their influence on the activity of autolytic enzymes. Arch Microbiol 141:249–254.

49.   Haney EF, Petersen AP, Lau CK, Jing W, Storey DG, Vogel HJ. 2013. Mechanism of action of puroindoline derived tryptophan-rich antimicrobial peptides. Biochim Biophys Acta 1828:1802–1813.

50.   Yeung ATY, Gellatly SL, Hancock REW. 2011. Multifunctional cationic host defence peptides and their clinical applications. Cell Mol Life Sci 68:2161–2176.

51.   Friedrich CL, Rozek A, Patrzykat A, Hancock RE. 2001. Structure and mechanism of

action of an indolicidin peptide derivative with improved activity against gram-positive bacteria. J Biol Chem 276:24015–24022.

52. Wang LK, Shuman S. 2010. Mutational analysis of the 5'-OH oligonucleotide phosphate acceptor site of T4 polynucleotide kinase. Nucleic Acids Res 38:1304–1311.

53. Yau WM, Wimley WC, Gawrisch K, White SH. 1998. The preference of tryptophan for membrane interfaces. Biochemistry 37:14713–14718.

54. Chan DI, Prenner EJ, Vogel HJ. 2006. Tryptophan- and arginine-rich antimicrobial peptides: structures and mechanisms of action. Biochim Biophys Acta 1758:1184–1202.

55. Shepherd CM, Vogel HJ, Tieleman DP. 2003. Interactions of the designed antimicrobial peptide MB21 and truncated dermaseptin S3 with lipid bilayers: molecular-dynamics simulations. Biochem J 370:233–243.

56. Aliste MP, MacCallum JL, Tieleman DP. 2003. Molecular dynamics simulations of pentapeptides at interfaces: salt bridge and cation-pi interactions. Biochemistry 42:8976–8987.

57. Dougherty DA. 1996. Cation-pi interactions in chemistry and biology: a new view of benzene, Phe, Tyr, and Trp. Science 271:163–168.

58. Kachel K, Asuncion-Punzalan E, London E. 1995. Anchoring of tryptophan and tyrosine analogs at the hydrocarbon-polar boundary in model membrane vesicles: parallax analysis of fluorescence quenching induced by nitroxide-labeled phospholipids. Biochemistry 34:15475–15479.

59. Mitchell JB, Nandi CL, McDonald IK, Thornton JM, Price SL. 1994. Amino/aromatic

interactions in proteins: is the evidence stacked against hydrogen bonding? J Mol Biol 239:315–331.

60. Minoux H, Chipot C. 1999. Cation−π interactions in proteins: can simple models provide an accurate description? J Am Chem Soc 121:10366–10372.

61. Jing W, Demcoe AR, Vogel HJ. 2003. Conformation of a bactericidal domain of puroindoline a: structure and mechanism of action of a 13-residue antimicrobial peptide. J Bacteriol 185:4938–4947.

62. Vogel HJ, Schibli DJ, Jing W, Lohmeier-Vogel EM, Epand RF, Epand RM. 2002. Towards a structure-function analysis of bovine lactoferricin and related tryptophan- and arginine-containing peptides. Biochem Cell Biol 80:49–63.

63. Bellamy W, Takase M, Yamauchi K, Wakabayashi H, Kawase K, Tomita M. 1992. Identification of the bactericidal domain of lactoferrin. Biochim Biophys Acta 1121:130–136.

64. Zweytick D, Deutsch G, Andra J, Blondelle SE, Vollmer E, Jerala R, Lohner K. 2011. Studies on lactoferricin-derived Escherichia coli membrane-active peptides reveal differences in the mechanism of N-acylated versus nonacylated peptides. J Biol Chem 286:21266–21276.

65. Zweytick D, Tumer S, Blondelle SE, Lohner K. 2008. Membrane curvature stress and antibacterial activity of lactoferricin derivatives. Biochem Biophys Res Commun 369:395–400.

66. Yang N, Strom MB, Mekonnen SM, Svendsen JS, Rekdal O. 2004. The effects of

shortening lactoferrin derived peptides against tumour cells, bacteria and normal human cells. J Pept Sci 10:37–46.

67.   Strom MB, Rekdal O, Svendsen JS. 2002. Antimicrobial activity of short arginine- and tryptophan-rich peptides. J Pept Sci 8:431–437.

68.   Blondelle SE, Perez-Paya E, Houghten RA. 1996. Synthetic combinatorial libraries: novel discovery strategy for identification of antimicrobial agents. Antimicrob Agents Chemother 40:1067–1071.

69.   Houghten RA, Pinilla C, Blondelle SE, Appel JR, Dooley CT, Cuervo JH. 1991. Generation and use of synthetic peptide combinatorial libraries for basic research and drug discovery. Nature 354:84–86.

70.   Wei S-Y, Wu J-M, Kuo Y-Y, Chen H-L, Yip B-S, Tzeng S-R, Cheng J-W. 2006. Solution structure of a novel tryptophan-rich peptide with bidirectional antimicrobial activity. J Bacteriol 188:328–334.

71.   Strom MB, Haug BE, Skar ML, Stensen W, Stiberg T, Svendsen JS. 2003. The pharmacophore of short cationic antibacterial peptides. J Med Chem 46:1567–1570.

72.   Liu Z, Brady A, Young A, Rasimick B, Chen K, Zhou C, Kallenbach NR. 2007. Length effects in antimicrobial peptides of the (RW)n series. Antimicrob Agents Chemother 51:597–603.

73.   Wenzel M, Chiriac AI, Otto A, Zweytick D, May C, Schumacher C, Gust R, Albada HB, Penkova M, Kramer U, Erdmann R, Metzler-Nolte N, Straus SK, Bremer E, Becher D, Brotz-Oesterhelt H, Sahl H-G, Bandow JE. 2014. Small cationic antimicrobial peptides

delocalize peripheral membrane proteins. Proc Natl Acad Sci U S A 111:E1409-18.

74.   Albada HB, Chiriac A-I, Wenzel M, Penkova M, Bandow JE, Sahl H-G, Metzler-Nolte N. 2012. Modulating the activity of short arginine-tryptophan containing antibacterial peptides with N-terminal metallocenoyl groups. Beilstein J Org Chem 8:1753–1764.

75.   Albada HB, Prochnow P, Bobersky S, Langklotz S, Schriek P, Bandow JE, Metzler-Nolte N. 2012. Tuning the activity of a short arg-trp antimicrobial Peptide by lipidation of a C- or N-terminal lysine side-chain. ACS Med Chem Lett 3:980–984.

76.   Albada HB, Prochnow P, Bobersky S, Langklotz S, Bandow JE, Metzler-Nolte N. 2013. Short antibacterial peptides with significantly reduced hemolytic activity can be identified by a systematic L-to-D exchange scan of their amino acid residues. ACS Comb Sci 15:585–592.

77.   Saravanan R, Li X, Lim K, Mohanram H, Peng L, Mishra B, Basu A, Lee J-M, Bhattacharjya S, Leong SSJ. 2014. Design of short membrane selective antimicrobial peptides containing tryptophan and arginine residues for improved activity, salt-resistance, and biocompatibility. Biotechnol Bioeng 111:37–49.

78.   Rink R, Arkema-Meter A, Baudoin I, Post E, Kuipers A, Nelemans SA, Akanbi MHJ, Moll GN. 2010. To protect peptide pharmaceuticals against peptidases. J Pharmacol Toxicol Methods 61:210–218.

79.   Fang Y, Zhong W, Wang Y, Xun T, Lin D, Liu W, Wang J, Lv L, Liu S, He J. 2014. Tuning the antimicrobial pharmacophore to enable discovery of short lipopeptides with multiple modes of action. Eur J Med Chem 83:36–44.

80. Wessolowski A, Bienert M, Dathe M. 2004. Antimicrobial activity of arginine- and tryptophan-rich hexapeptides: the effects of aromatic clusters, D-amino acid substitution and cyclization. J Pept Res 64:159–169.

81. Scocchi M, Tossi A, Gennaro R. 2011. Proline-rich antimicrobial peptides: converging to a non-lytic mechanism of action. Cell Mol Life Sci 68:2317–2330.

82. Podda E, Benincasa M, Pacor S, Micali F, Mattiuzzo M, Gennaro R, Scocchi M. 2006. Dual mode of action of Bac7, a proline-rich antibacterial peptide. Biochim Biophys Acta 1760:1732–1740.

83. Casteels P, Tempst P. 1994. Apidaecin-type peptide antibiotics function through a non-poreforming mechanism involving stereospecificity. Biochem Biophys Res Commun 199:339–345.

84. Markossian KA, Zamyatnin AA, Kurganov BI. 2004. Antibacterial proline-rich oligopeptides and their target proteins. Biochemistry (Mosc) 69:1082–1091.

85. Otvos LJ. 2002. The short proline-rich antibacterial peptide family. Cell Mol Life Sci 59:1138–1150.

86. Konishi M, Sugawara K, Hanada M, Tomita K, Tomatsu K, Miyaki T, Kawaguchi H, Buck RE, More C, Rossomano VZ. 1984. Empedopeptin (BMY-28117), a new depsipeptide antibiotic. I. Production, isolation and properties. J Antibiot (Tokyo) 37:949–957.

87. Muller A, Munch D, Schmidt Y, Reder-Christ K, Schiffer G, Bendas G, Gross H, Sahl H-G, Schneider T, Brotz-Oesterhelt H. 2012. Lipodepsipeptide empedopeptin inhibits cell

wall biosynthesis through Ca2+-dependent complex formation with peptidoglycan precursors. J Biol Chem 287:20270–20280.

88.   Hashizume H, Igarashi M, Hattori S, Hori M, Hamada M, Takeuchi T. 2001. Tripropeptins, novel antimicrobial agents produced by Lysobacter sp. I. Taxonomy, isolation and biological activities. J Antibiot (Tokyo) 54:1054–1059.

89.   Hashizume H, Hattori S, Igarashi M, Akamatsu Y. 2004. Tripropeptin E, a new tripropeptin group antibiotic produced by Lysobacter sp. BMK333-48F3. J Antibiot (Tokyo) 57:394–399.

90.   Hashizume H, Igarashi M, Sawa R, Adachi H, Nishimura Y, Akamatsu Y. 2008. A new type of tripropeptin with anteiso-branched chain fatty acid from Lysobacter sp. BMK333-48F3. J Antibiot (Tokyo) 61:577–582.

91.   Shoji J, Hinoo H, Katayama T, Matsumoto K, Tanimoto T, Hattori T, Higashiyama I, Miwa H, Motokawa K, Yoshida T. 1992. Isolation and characterization of new peptide antibiotics, plusbacins A1-A4 and B1-B4. J Antibiot (Tokyo) 45:817–823.

92.   Maki H, Miura K, Yamano Y. 2001. Katanosin B and plusbacin A(3), inhibitors of peptidoglycan synthesis in methicillin-resistant Staphylococcus aureus. Antimicrob Agents Chemother 45:1823–1827.

93.   Sugawara K, Numata K, Konishi M, Kawaguchi H. 1984. Empedopeptin (BMY-28117), a new depsipeptide antibiotic. II. Structure determination. J Antibiot (Tokyo) 37:958–964.

94.   Hashizume H, Hirosawa S, Sawa R, Muraoka Y, Ikeda D, Naganawa H, Igarashi M. 2004. Tripropeptins, novel antimicrobial agents produced by Lysobacter sp. J Antibiot (Tokyo)

57:52–58.

95.   Shoji J, Hinoo H, Katayama T, Nakagawa Y, Ikenishi Y, Iwatani K, Yoshida T. 1992. Structures of new peptide antibiotics, plusbacins A1-A4 and B1-B4. J Antibiot (Tokyo) 45:824–831.

96.   Li DHS, Chung YS, Gloyd M, Joseph E, Ghirlando R, Wright GD, Cheng Y-Q, Maurizi MR, Guarne A, Ortega J. 2010. Acyldepsipeptide antibiotics induce the formation of a structured axial channel in ClpP: A model for the ClpX/ClpA-bound state of ClpP. Chem Biol 17:959–969.

97.   Conlon BP, Nakayasu ES, Fleck LE, LaFleur MD, Isabella VM, Coleman K, Leonard SN, Smith RD, Adkins JN, Lewis K. 2013. Activated ClpP kills persisters and eradicates a chronic biofilm infection. Nature 503:365–370.

98.   Michel K., Kastner R. 1985. A54556 antibiotics and process for production thereof. US Patent 4492650.

99.   Osada H, Yano T, Koshino H, Isono K. 1991. Enopeptin A, a novel depsipeptide antibiotic with anti-bacteriophage activity. J Antibiot (Tokyo). Japan.

100.   Hinzen B, Raddatz S, Paulsen H, Lampe T, Schumacher A, Habich D, Hellwig V, Benet-Buchholz J, Endermann R, Labischinski H, Brotz-Oesterhelt H. 2006. Medicinal chemistry optimization of acyldepsipeptides of the enopeptin class antibiotics. ChemMedChem 1:689–693.

101.   Socha AM, Tan NY, LaPlante KL, Sello JK. 2010. Diversity-oriented synthesis of cyclic acyldepsipeptides leads to the discovery of a potent antibacterial agent. Bioorg Med Chem

18:7193–7202.

102. Carney DW, Schmitz KR, Truong J V, Sauer RT, Sello JK. 2014. Restriction of the conformational dynamics of the cyclic acyldepsipeptide antibiotics improves their antibacterial activity. J Am Chem Soc 136:1922–1929.

103. Mohammed R, Peng J, Kelly M, Hamann MT. 2006. Cyclic heptapeptides from the Jamaican sponge Stylissa caribica. J Nat Prod 69:1739–1744.

104. Dahiya R, Kumar A, Gupta R. 2009. Synthesis, cytotoxic and antimicrobial screening of a proline-rich cyclopolypeptide. Chem Pharm Bull (Tokyo) 57:214–217.

105. Dahiya R, Gautam H. 2010. Total synthesis and antimicrobial activity of a natural cycloheptapeptide of marine origin. Mar Drugs 8:2384–2394.

106. Kumar SN, Mohandas C, Nambisan B. 2014. Purification, structural elucidation and bioactivity of tryptophan containing diketopiperazines, from Comamonas testosteroni associated with a rhabditid entomopathogenic nematode against major human-pathogenic bacteria. Peptides 53:48–58.

107. Roy S, Das PK. 2008. Antibacterial hydrogels of amino acid-based cationic amphiphiles. Biotechnol Bioeng 100:756–764.

108. Mitra RN, Shome A, Paul P, Das PK. 2009. Antimicrobial activity, biocompatibility and hydrogelation ability of dipeptide-based amphiphiles. Org Biomol Chem 7:94–102.

109. Makovitzki A, Avrahami D, Shai Y. 2006. Ultrashort antibacterial and antifungal lipopeptides. Proc Natl Acad Sci U S A 103:15997–16002.

110. Findlay B, Mookherjee N, Schweizer F. 2013. Ultrashort cationic lipopeptides and

lipopeptoids selectively induce cytokine production in macrophages. PLoS One 8:e54280.

111.   Serrano GN, Zhanel GG, Schweizer F. 2009. Antibacterial activity of ultrashort cationic

lipo-beta-peptides. Antimicrob Agents Chemother 53:2215–2217.

112.   Findlay B, Zhanel GG, Schweizer F. 2012. Investigating the antimicrobial peptide

"window of activity" using cationic lipopeptides with hydrocarbon and fluorinated tails.

Int J Antimicrob Agents 40:36–42.

113.   Domalaon R, Yang X, O'Neil J, Zhanel GG, Mookherjee N, Schweizer F. 2014.

Structure-activity relationships in ultrashort cationic lipopeptides: the effects of amino

acid ring constraint on antibacterial activity. Amino Acids 46:2517–2530.

114.   Godballe T, Nilsson LL, Petersen PD, Jenssen H. 2011. Antimicrobial beta-peptides and

alpha-peptoids. Chem Biol Drug Des 77:107–116.

115.   Giuliani A, Rinaldi AC. 2011. Beyond natural antimicrobial peptides: multimeric peptides

and other peptidomimetic approaches. Cell Mol Life Sci 68:2255–2266.

116.   Herzog IM, Fridman M. 2014. Design and synthesis of membrane-targeting antibiotics:

from peptides- to aminosugar-based antimicrobial cationic amphiphiles. Medchemcomm

5:1014–1026.

117.   Obrecht D, Robinson JA, Bernardini F, Bisang C, DeMarco SJ, Moehle K, Gombert FO.

2009. Recent progress in the discovery of macrocyclic compounds as potential anti-

infective therapeutics. Curr Med Chem 16:42–65.

118.   Jamieson AG, Boutard N, Sabatino D, Lubell WD. 2013. Peptide scanning for studying

structure-activity relationships in drug discovery. Chem Biol Drug Des 81:148–165.

119. Niu Y, Wu H, Li Y, Hu Y, Padhee S, Li Q, Cao C, Cai J. 2013. AApeptides as a new class of antimicrobial agents. Org Biomol Chem 11:4283–4290.

120. Mendez-Samperio P. 2014. Peptidomimetics as a new generation of antimicrobial agents: current progress. Infect Drug Resist 7:229–237.

121. Findlay B, Zhanel GG, Schweizer F. 2010. Cationic amphiphiles, a new generation of antimicrobials inspired by the natural antimicrobial peptide scaffold. Antimicrob Agents Chemother 54:4049–4058.

122. Jahnsen RD, Frimodt-Moller N, Franzyk H. 2012. Antimicrobial activity of peptidomimetics against multidrug-resistant Escherichia coli: a comparative study of different backbones. J Med Chem 55:7253–7261.

123. Jahnsen RD, Haney EF, Franzyk H, Hancock REW. 2013. Characterization of a proteolytically stable multifunctional host defense peptidomimetic. Chem Biol 20:1286–1295.

124. Ghosh C, Manjunath GB, Akkapeddi P, Yarlagadda V, Hoque J, Uppu DSSM, Konai MM, Haldar J. 2014. Small molecular antibacterial peptoid mimics: the simpler the better! J Med Chem 57:1428–1436.

125. Babii O, Afonin S, Berditsch M, Reibetaer S, Mykhailiuk PK, Kubyshkin VS, Steinbrecher T, Ulrich AS, Komarov I V. 2014. Controlling biological activity with light: diarylethene-containing cyclic peptidomimetics. Angew Chem Int Ed Engl 53:3392–3395.

126. Haug BE, Stensen W, Stiberg T, Svendsen JS. 2004. Bulky nonproteinogenic amino acids permit the design of very small and effective cationic antibacterial peptides. J Med Chem

47:4159–4162.

127. Haug BE, Stensen W, Svendsen JS. 2007. Application of the Suzuki-Miyaura cross-coupling to increase antimicrobial potency generates promising novel antibacterials. Bioorg Med Chem Lett 17:2361–2364.

128. Haug BE, Stensen W, Kalaaji M, Rekdal O, Svendsen JS. 2008. Synthetic antimicrobial peptidomimetics with therapeutic potential. J Med Chem 51:4306–4314.

129. Saravolatz LD, Pawlak J, Johnson L, Bonilla H, Saravolatz LD 2nd, Fakih MG, Fugelli A, Olsen WM. 2012. In vitro activities of LTX-109, a synthetic antimicrobial peptide, against methicillin-resistant, vancomycin-intermediate, vancomycin-resistant, daptomycin-nonsusceptible, and linezolid-nonsusceptible Staphylococcus aureus. Antimicrob Agents Chemother 56:4478–4482.

130. Isaksson J, Brandsdal BO, Engqvist M, Flaten GE, Svendsen JSM, Stensen W. 2011. A synthetic antimicrobial peptidomimetic (LTX 109): stereochemical impact on membrane disruption. J Med Chem 54:5786–5795.

131. Tew GN, Liu D, Chen B, Doerksen RJ, Kaplan J, Carroll PJ, Klein ML, DeGrado WF. 2002. De novo design of biomimetic antimicrobial polymers. Proc Natl Acad Sci U S A 99:5110–5114.

132. Liu D, Choi S, Chen B, Doerksen RJ, Clements DJ, Winkler JD, Klein ML, DeGrado WF. 2004. Nontoxic membrane-active antimicrobial arylamide oligomers. Angew Chem Int Ed Engl 43:1158–1162.

133. Choi S, Isaacs A, Clements D, Liu D, Kim H, Scott RW, Winkler JD, DeGrado WF. 2009.

De novo design and in vivo activity of conformationally restrained antimicrobial arylamide foldamers. Proc Natl Acad Sci U S A 106:6968–6973.

134. Mensa B, Howell GL, Scott R, DeGrado WF. 2014. Comparative mechanistic studies of brilacidin, daptomycin, and the antimicrobial peptide LL16. Antimicrob Agents Chemother 58:5136–5145.

135. Robinson JA, Demarco S, Gombert F, Moehle K, Obrecht D. 2008. The design, structures and therapeutic potential of protein epitope mimetics. Drug Discov Today 13:944–951.

136. Srinivas N, Jetter P, Ueberbacher BJ, Werneburg M, Zerbe K, Steinmann J, Van der Meijden B, Bernardini F, Lederer A, Dias RLA, Misson PE, Henze H, Zumbrunn J, Gombert FO, Obrecht D, Hunziker P, Schauer S, Ziegler U, Kach A, Eberl L, Riedel K, DeMarco SJ, Robinson JA. 2010. Peptidomimetic antibiotics target outer-membrane biogenesis in *Pseudomonas aeruginosa*. Science 327:1010–1013.

1.10. Concluding remarks

This chapter highlighted antimicrobial peptides as potential source of therapeutic agents. The advantages and disadvantages of this class of biomolecules were discussed, including chemical techniques in the form of peptidomimetics to alle*via*te the issue peptide lability in biological systems. Several subclasses of antimicrobial peptides were also elaborated that would be the background of upcoming chapters. For instance, the proline-rich antimicrobial peptides (PRAMPs) will be the main peptide scaffold used on Chapter 4. Ultrashort cationic lipopetides will then be designed and elaborated on Chapter 5. Furthermore, the development of new polymyxin derivatives will be discussed on Chapter 6.

Chapter 2: Challenges in developing therapeutic agents targeting Gram-negative bacteria

This chapter is based on my publication:

Ronald Domalaon, Temilolu Idowu, George G. Zhanel, Frank Schweizer. **2018**. Antibiotic Hybrids: the Next Generation of Agents and Adjuvants against Gram-Negative Pathogens?. Clin Microbiol Rev 31:e00077-17. doi: 10.1128/CMR.00077-17.

Reproduced with permission.

2.1. Introductory remarks

The previous chapter emphasized the potential of antimicrobial peptides as therapeutic agents. However, it is not easy to develop therapeutic agents, more so if these agents are meant to eradicate antibiotic-resistant Gram-negative pathogens. My doctoral research involved the chemical preparation and microbiological evaluation of agents aimed against Gram-negative bacteria. For one to fully realize the importance of this research, one must understand the difficulties and intricacies in the development of these agents. In this chapter, the problem in developing therapeutic agents to combat antibiotic-resistant Gram-negative bacteria will be extensively discussed. Moreover, several innovative strategies will be introduced that may address the issue of antimicrobial resistance.

2.2. Contributions of authors

Ronald Domalaon did an extensive literature survey on the topics: developmental challenges in designing antibiotics aimed to treat Gram-negative bacterial infections and antibiotic hybrids with

a focus on those active against Gram-negative bacteria. Consequently, sections pertaining to these topics were fully written by Ronald Domalaon. Temilolu Idowu focused on sections pertaining to tobramycin-based hybrids and adjuvants, including examples and mechanistic interpretation of relevant data (sections not included in this chapter). Guidance and helpful feedback were provided by George G. Zhanel and Frank Schweizer. All authors were responsible for the final form of this review paper.

2.3. Drug resistance drives the development of new antibiotics

The rapid global dissemination of Gram-positive and Gram-negative bacterial pathogens that are resistant to currently available antimicrobial therapies, in both hospital and community settings, marks the onset of a possible severe worldwide health crisis (1–3). Out of all these pathogens, the ESKAPE (*Enterococcus faecium*, *Staphylococcus aureus*, *Klebsiella pneumoniae*, *Acinetobacter baumannii*, *Pseudomonas aeruginosa* and *Enterobacter* species) bacteria (4), account for the majority of nosocomial infections worldwide with increasing incidence of drug resistance every year (2, 5). Incidence of clinical isolates belonging to the ESKAPE group that exhibit either multidrug-resistance (MDR), extensively drug-resistance (XDR) or pandrug-resistance (PDR) is quite alarming (6–8). MDR is defined as non-susceptibility to at least one agent in ≥3 chemically dissimilar antibiotic classes, XDR as non-susceptibility to at least one agent in all but ≤2 chemically dissimilar antibiotic classes, and PDR as non-susceptibility to all agents in all antibiotic classes (9). However, the problem is arguably more serious for Gram-negative organisms which are more frequently MDR and for which no novel antibacterial drug entities with novel modes of action (only new drug combinations) have been approved for clinical use in five decades (2, 10,

11). Indeed, four out of the six ESKAPE pathogens (*K. pneumoniae*, *A. baumannii*, *P. aeruginosa* and *Enterobacter* spp.) are Gram-negative bacilli.

Various health organizations have been vocal about the urgent need to develop new antibiotics, especially against drug-resistant Gram-negative ESKAPE bacilli. For instance, the World Health Organization (WHO) has raised its utmost concern about the possibility of a post-antibiotic era where common infections and minor injuries may result in significant morbidity and mortality (12). World leaders convened in September 2016 during the 71st United Nations General Assembly (UNGA) to discuss the issue of antimicrobial resistance, an event that resulted in each governing body taking a unified stance towards preventing a post-antibiotic era (13–15). The increasing frequency of bacterial infections caused by MDR pathogens and the lack of effective therapeutic options for treatment is apparent worldwide. In response to the dwindling antibiotic pipeline, the Infectious Diseases Society of America (IDSA) in 2010 launched the "10 × '20 Initiative" that challenged stakeholders to advance ten new US Food and Drug Administration (FDA)-approved systemic agents to treat bacterial infections by 2020 (16). In a follow-up report three years later (2013), IDSA noted the definite but slow progress towards achieving the goal of 10 × '20 Initiative, to which only one systemic agent (ceftaroline fosamil) has materialized (17). As of November 2017, nine new FDA-approved systemic new molecular entities (NME) antibiotics have been developed (Table 2-1), with a projection that the goal of IDSA will most likely come to fruition[6]. However, only six (ceftaroline fosamil, ceftolozane-tazobactam, ceftazidime-avibactam, delafloxacin, meropenem-vaborbactam, and secnidazole) out of the nine

---

[6] Three more systemic NME have been approved as of November 2018, including the tetracyclines eravacycline and omadacycline, and the aminoglycoside plazomicin (https://www.fda.gov/Drugs/DevelopmentApprovalProcess/DrugInnovation/ucm537040.htm). Therefore, the IDSA goal had been successfully met. Notably, all three agents possessed activity against MDR Gram-negative bacteria.

systemic agents are used for the treatment of drug-resistant Gram-negative bacterial infections. Two (fidaxomicin and finafloxacin otic suspension) are approved as non-systemic antibacterial agents.

Table 2-1 FDA-approved New Molecular Entities (NME) antibiotics from 2010 – November 2017

Year	Name	Class	Able to treat antibiotic-resistant Gram-negative ESKAPE bacterial infection?	Route of drug administration
2010	ceftaroline fosamil	cephalosporin	Yes	Systemic
2011	fidaxomicin	macrolide	No	Non-systemic
2014	dalbavancin	lipoglycopeptide	No	Systemic
2014	oritavancin	lipoglycopeptide	No	Systemic
2014	tedizolid phosphate	oxazolidinone	No	Systemic
2014	ceftolozane-tazobactam	cephalosporin + β-lactamase inhibitor	Yes	Systemic
2014	finafloxacin otic suspension	fluoroquinolone	Yes	Non-systemic
2015	ceftazidime-avibactam	cephalosporin + β-lactamase inhibitor	Yes	Systemic
2017	delafloxacin	fluoroquinolone	Yes	Systemic
2017	meropenem - vaborbactam	carbapenem + β-lactamase inhibitor	Yes	Systemic
2017	secnidazole	nitroimidazole	Yes	Systemic

The limited availability of antibiotics to treat MDR Gram-negative bacterial infections remains a serious problem. It is therefore imperative to develop new agents or new therapeutic strategies able to overcome drug resistance in these organisms.

2.4. Permeability is an important consideration in developing antibiotics for Gram-negative bacteria

Bacteria are classified as Gram-positive and Gram-negative (with some exceptions such as mycobacteria) based on their prokaryotic cell membrane structure. Gram-positive bacteria possess a thick cell wall that consists of peptidoglycan and teichoic acid layers anchored on the cytoplasmic membrane. On the other hand, Gram-negative bacteria have a thin peptidoglycan layer that is surrounded by an inner (IM) and outer membrane (OM), thus forming the periplasmic space (Fig. 2-1). The double layer of protection in Gram-negative bacteria, in addition to an abundance of efflux pumps and highly-selective porins, makes it more difficult for an intracellularly targeting agent to elicit its antibacterial function (18).

The outer membrane is efficient in restricting molecular passage. The OM is an asymmetric bilayer (Fig. 2-1) with an inner leaflet solely consisting of phospholipids and an outer leaflet that contains an abundance of lipopolysaccharides (LPS). The polymeric LPS is composed of three domains: the hydrophobic lipid A, the hydrophilic core oligosaccharides and the hydrophilic O-antigen. Lipid A is responsible for forming a lipid bilayer with the inner leaflet. Core oligosaccharides and O-antigen, which extend outwards to the extracellular environment, are responsible for cellular recognition and virulence (amongst other functions). The presence of the OM makes Gram-negative bacteria intrinsically resistant to many antibiotics, especially those with high molecular

weight and hydrophobicity. For instance, the LPS structure renders the bacterial OM more restrictive to hydrophobic antibiotics in comparison to the IM (19). It has been argued that the hydrophilic carbohydrate component of LPS creates a hydration sphere that restricts the movement and passage of hydrophobic molecules across the membrane (20). The efficient packing of lipid A, due to its molecular organization and lower unsaturated fatty acid content in comparison to a normal phospholipid bilayer, results in lower OM fluidity (21–23), thus limiting membrane permeation of hydrophobic agents. Integral membrane proteins that interact directly with LPS, such as the outer membrane protein H (OprH) in *P. aeruginosa* (24) and the Tol-Pal complex in *Escherichia coli* (25), further augment the stability and therefore the impermeability of the membrane. Experimental evidence shows 50-100 times slower hydrophobic probe permeation rates in lipid bilayers that contain lipopolysaccharide (reflective of the OM) in comparison to bilayers that only consist of phospholipids (reflective of the IM) (26). Structural variabilities and modifications in the LPS, especially the lipid A portion, result in significant differences in drug permeation rates among Gram-negative organisms (27). It is therefore clear that the OM constitutes a major hurdle for drug uptake in Gram-negative bacteria, especially for *P. aeruginosa* that has a 12-100 times reduced outer membrane permeability relative to *E. coli* (28).
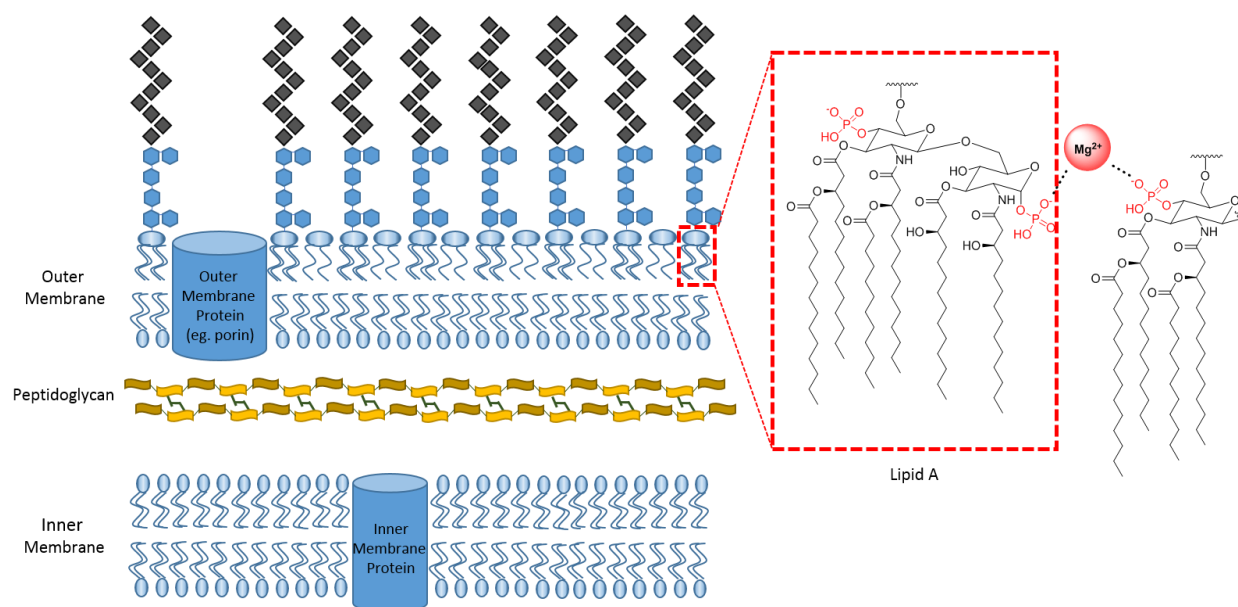
Figure 2-1 Dual-membrane of Gram-negative bacteria.

The periplasmic space that contains a thin peptidoglycan layer is enclosed by the outer (OM) and the inner membrane (IM). The asymmetric OM has an inner leaflet composed of phospholipids and an outer leaflet abundant with lipopolysaccharide (LPS). The LPS is mainly sectioned into the hydrophobic lipid A (structure expanded in dashed red box), the hydrophilic core oligosaccharides (blue hexagons) and the hydrophilic O-antigen (black diamonds). Some degree of variation, however, exist between Gram-negative bacteria. The lipid A structure typically has two negatively-charged phosphate groups stabilized by divalent cation (such as Mg^{2+}) bridge between adjacent lipid A phosphate groups that imparts structural stability to the OM. Both inner and outer leaflet of the IM consists mainly of hydrophobic phospholipids. The difference in molecular composition between the OM and IM results in their orthogonal sieving properties.

Membrane permeation is a limitation to most but not all agents with high molecular weight. The glycopeptide antibiotic vancomycin, with a molecular weight of 1449.3 g/mol, lacks antibacterial activity against most clinically-relevant Gram-negative bacteria. Vancomycin inhibits peptidoglycan synthesis by sequestering peptidoglycan precursors that ultimately prevent glycan cross-linking. In Gram-positive organisms, vancomycin exerts its antibacterial activity uninhibited as its target is located at the cell membrane. However, it must traverse the OM and reach the periplasmic space to elicit its function in Gram-negative organisms, a feat which vancomycin is incapable of achieving due to the protective membrane barrier. The loss of antibacterial activity

due to membrane impermeability is true for almost all clinically-used glycopeptide antibiotics (29, 30). Most antibiotics and biomolecules with molecular weights higher than 600 g/mol are incapable of traversing the OM (31), with few exceptions including polybasic amphiphiles, such as polymyxins and antimicrobial peptides, and nonbasic energy-sources, such as maltohexaoses (32, 33).

Charged (cationic or zwitterionic) or non-charged small hydrophilic molecules are typically able to enter the periplasmic space *via* non-specific protein channels called porins. Examples of such antibiotics with porin-dependent uptake include β-lactams, fluoroquinolones, and sulfonamides. These β-barrel-structured integral protein channels allow water-soluble molecules to traverse the restrictive hydrophobic membrane through their water-filled cavity (34–36). However, porins impose molecular sieving properties as only small molecules, typically ≤ 600 g/mol, are believed to pass through its narrow channel (37–39). Drug permeation through porins may also vary among Gram-negative bacteria. For instance, *P. aeruginosa* possesses a lower outer membrane permeability in comparison to *E. coli* as they express a more selective outer membrane protein F (OprF) porin (28, 39). The OprF porin constitutes a majority of the porins present in *P. aeruginosa* (40). Porins that are present in relatively lower amounts in *P. aeruginosa* include OprB, OprC, OprD, OprE, OprF, OprG, OprH, and others (41, 42). OprF porin has been shown to also allow solute diffusion much more slowly than classical porins as a consequence of their structural conformation (39, 43). For example, the monosaccharide L-arabinose was found to diffuse 50-times slower in OprF porin in *P. aeruginosa* relative to the OmpF porin channel of *E. coli* (44). Low intracellular drug concentration due to slow porin-mediated influx in *P. aeruginosa* is

exacerbated by the abundance of multidrug efflux pumps and resistance-encoding genes (28, 43, 45)(28, 43, 45).

However, several antibiotics with high molecular weight (> 600 g/mol) are able to pass through the OM in a mode of uptake independent of porins or passive diffusion. These compounds are mostly cationic and are hydrophilic (such as aminoglycosides (46)) or amphiphilic (such as polymyxins) in nature (46). They are able to transit the OM *via* a 'self-promoted' uptake mechanism which is characterized by the initial displacement of divalent cations (Ca^{2+} or Mg^{2+}) that results in OM destabilization (47). Electrostatic interaction between the positively-charged divalent cations and the negatively-charged phosphate groups on lipid A stabilizes the LPS structure (48–50). It is perceived that the subsequent localized OM disruption from divalent cation displacement facilitates the penetration of the antibiotic into the periplasmic space (51, 52). It has been widely documented in early years that the antibacterial activity of aminoglycosides and polymyxins are antagonized by the exogenous addition of Mg^{2+} and Ca^{2+} cations (53–56). This observation was later attributed to be a hallmark of the self-promoted uptake mechanism; that it entails the displacement of divalent cation LPS bridges and that exogenous supplementation of the divalent cations immediately arrests the process (57). The physicochemical requirements for a molecule to display a self-promoted uptake are yet to be fully understood, although the propensity of a molecule to be protonated (to effectively carry one or more positive charges) under physiological conditions and to strongly interact with LPS may be necessary characteristics.

Inner membrane as second restrictive barrier for agents with cytosolic targets. The phospholipid bilayer that comprises the IM greatly limits the diffusion of hydrophilic molecules. Compared to

the OM, hydrophobic molecules easily traverse the IM through passive diffusion. However, charged solutes such as sodium cations and hydrophilic nutrients such as glucose enter freely into the cytosol once they traverse the OM. Their uptake is achieved through the use of solute-specific energy-dependent transporter proteins (58). Some weakly-charged or neutral amphiphilic compounds may also enter the cytosol by utilizing the proton motive force (PMF) (59, 60). Bacterial PMF is governed by proton gradient, ΔpH, and membrane potential, $\Delta\Psi$. The ΔpH is believed to facilitate the diffusion of weakly-charged molecules through charge neutralization, while the $\Delta\Psi$ is perceived to stimulate electrochemical interaction that leads to molecular uptake (61, 62). For instance, the cytoplasmic uptake of the sulfonamide (63) and tetracycline (64) classes of antibiotics is ΔpH-dependent, while the uptake of the aminoglycoside class of antibiotics appears to be $\Delta\Psi$-dependent (65).

Intracellular drug concentration is greatly affected by efflux. Once a drug makes its way intracellularly, it could be effluxed out before mediating its antibacterial effect. Efflux pumps are membrane proteins that can expel their substrates from the cytosol into the periplasm or from the periplasm into the external environment. So far, all studied Gram-negative organisms are known to express at least one multidrug efflux pump (66). Bacterial efflux systems have been extensively reviewed in the literature, and readers are encouraged to consult references (67–72). However, it should be noted that drug efflux affects the intracellular concentration of a therapeutic agent and overexpression of multidrug efflux pumps confers intrinsic antibiotic resistance on the pathogen.

There is an urgent need for guidelines to develop agents able to penetrate both outer and inner membranes. It is evident that drug permeability in Gram-negative bacteria is more challenging for

antibiotics with cytosolic targets as they must transit two protective lipid bilayers (73). One approach to overcome this involves appending or tweaking different functional groups on a lead structure, in the hope of generating more amenable derivatives with enhanced biological activity and cellular permeation. 'Rules of thumb' knowledge in structural modification are used by medicinal chemists to make rational decisions for drug optimization. The Lipinski's rule of five for favorable drug oral bioavailability (74) has become a popular *in silico* guideline for developing therapeutic agents that are able to cross the intestinal epithelial cells. To possess good pharmacokinetics in the human body, Lipinski's rule proposes that an agent may not have: (1) more than five hydrogen bond donors, (2) more than ten hydrogen bond acceptors, (3) molecular weight greater than 500 g/mol and a lipophilicity factor (log P) greater than five, as measured by the octanol-water partition coefficient (74, 75). Unfortunately, Lipinski's metrics do not hold true for antibacterial agents that require bacterial membrane penetration. Molecular passage through the OM appears to be governed by a different set of physicochemical rules that are orthogonal to the IM (18). Compounds that are solely optimized to traverse the OM most likely would not be able to cross the IM, and *vice-versa*. A widely-acceptable set of membrane permeation rules for antibacterial agents appear to be non-existent (76). An attempt had earlier been made to formulate a guideline by binning all antibiotics in the pipeline and in clinical evaluation to correlate discernable physicochemical parameters with antibacterial activity (77). Compounds were binned into three categories, namely; compounds with only anti-Gram-positive activity, compounds that have anti-Gram-negative activity, and compounds that are anti-pseudomonal. A high polarity (for porin uptake) and reasonable level of lipophilicity (to ensure lipid membrane penetration) was observed to be ideal for anti-Gram-negative agents (77). By exploiting the ideal physicochemical properties revealed from binning antibiotics, an effort to optimize the anti-Gram-negative bacteria

activity of oxazolidinones was recently described (78). Members of the oxazolidinone class of antibiotic, such as linezolid, do not have potent activity against most Gram-negative organisms, presumably due to permeation impediments across the OM and/or efflux (79). The most active prepared oxazolidinone analog demonstrated only modest enhancement against *E. coli* and that, as the authors noted, a fully-realized set of permeation guidelines are direly needed for optimizing lead compounds (78). A recent article emphasized the inherent hurdles in developing agents able to permeate the Gram-negative membranes and suggested that the binning process should be further refined to include the route(s) of cellular entry for each antibacterial agents (18). However, the development of reliable methods that allows data mining for cellular entry and accumulation of antibiotics are necessary to realize this suggestion. At this point, several experimental protocols may hold the key to tackling this proposition. For instance, the elucidation of bacterial uptake mechanisms and subsequent quantification of cytoplasmic accumulation that utilizes techniques such as tandem liquid chromatography – mass spectrometry (LC-MS) (80, 81), Raman spectroscopy (82) and microspectroscopy (83), have been reported. A proof-of-concept study that utilizes LC-MS for quantification and several correlation programs for analysis has been described for ten sulfonyladenosine-containing agents in terms of their membrane permeation in *E. coli*, *Bacillus subtilis*, and *Mycobacterium smegmatis* (84). This systematic approach successfully delineated the relationship between the physicochemical properties and the cytoplasmic accumulation of sulfonyladenosines. For instance, the cytoplasmic accumulation of the ten sulfonyladenosine-containing compounds in *E. coli* were positively correlated to hydrophobicity but negatively correlated with polarity (84). The platform is envisioned by the authors (84) to be applicable to a larger diverse panel of chemical agents and other bacterial organisms, and may therefore be utilized in formulating a set of antibacterial permeation rules in the future.

The impermeability of Gram-negative bacterial membranes greatly limits our capability to develop new antibiotics, and there is an apparent void in the fundamental understanding of physicochemical properties necessary for an agent to overcome the double barrier of protection in Gram-negative bacteria. However, recent advances have shed some light on this hurdle (84, 85). It has recently been shown that for small molecules to accumulate in the Gram-negative bacteria *E. coli*, they must contain an amine group (primary amine preferred over secondary or tertiary), be amphiphilic, be rigid, and have low globularity (defined as the spatial parameter of the molecule) (85). Applying these rules, the natural product deoxynybomycin, that targets DNA gyrase and which is only active against Gram-positive bacteria, was converted into an antibiotic with activity against a diverse panel of multidrug-resistant Gram-negative pathogens, excluding *P. aeruginosa* (85).

It may also be argued that instead of spending great efforts and resources in the development of intracellularly-targeting antibacterials, one may focus on exploring membrane targets that are easily accessible (86). For instance, the membranolytic function of antimicrobial peptides and amphiphilic agents (87–90) or the inhibition of essential outer membrane proteins (91, 92) may be exploited. Looking forward, we foresee the materialization of the essential paradigm to predict bacterial membrane penetration. But for how long? Only time will tell.

2.5. Therapeutic approaches to overcome antimicrobial resistance

Clinicians have been saddled with the onerous task of refining medical practices and procedures to combat the spread of antibiotic resistance, but only so much can be achieved if new agents are

not developed to supplement our current antibiotic arsenal. Pathogens have shown their resilience to withstand antibiotic monotherapy due to their rapid doubling times and high mutation rates. Some pathogens, such as from the mycobacterium genus or those that form persister cells, display antibiotic tolerance due to their slow growth or dormancy (93). However, the notion of antibiotic tolerance has only been observed *in vitro*, and a recent *in vivo* experiment suggests that non-replicating bacteria might not necessarily confer resistance (94). Acquired resistance is mostly due to the selective pressure an agent exerts towards a bacterial population. Mutation(s) that confer overall fitness under such antibiotic stress (causing the bacteria to survive) are propagated in surviving cells and therefore give rise to a drug-resistant population. Moreover, it has been documented that some pathogens under antibiotic monotherapy may induce resistance mechanisms that confer cross-resistance to other chemically-unrelated antibiotic classes (95). For instance, overexpression of multidrug efflux systems possessing wide ambiguity in substrates may confer resistance to several chemically-unrelated antibiotic classes. Conversely, resistance mechanisms that confer hypersusceptibility to other antibiotics, known as collateral susceptibility, have also been reported (96). Drug-resistant bacteria may overexpress genes that encode molecular defense mechanisms such as efflux pumps or drug-inactivating enzymes. These resistance genes can disseminate to a different organism *via* horizontal gene transfer of mobile genetic elements such as plasmids, transposons and integrons (97). One way to solve this problem is to continually develop new antibiotics and/or new drug classes that delay the evolution of drug resistance. Further understanding of the molecular interplay that governs pathogenic responses during antibiotic therapy is, however, essential to guide the developmental process of overcoming drug resistance. Fundamental progress in basic science is as vital as it is in clinical science. A close rapport between clinicians and scientists is indeed critical to address the problem of antibiotic resistance

development and dissemination. Herein, we discuss some therapeutic approaches that may be able to delay the development of antibiotic resistance and briefly elucidate the hypotheses behind them.

Anti-virulence therapy. The development of agents that are not bactericidal but indirectly inhibit the molecular pathway responsible for bacterial communication is a *via*ble strategy to address the problem of antibiotic resistance (98–100). This therapeutic approach is based on the purported delayed bacterial resistance development as it is perceived that such agents exert reduced evolutionary selective pressure (101). On the other hand, agents that challenge bacterial survival by directly inhibiting a molecular target may result in higher rates of resistance development. For example, blocking bacterial quorum sensing may be a feasible approach. Quorum sensing is characterized by bacterial production release and group-wide detection of auto-inducer molecules as a mode of bacterial communication with their neighbors (102). This network of communication is triggered by environmental factors within the microbial community, such as differences in bacterial density or the presence of environmental challenges (either physical or chemical) (103, 104). Once these signaling molecules are detected, cascades of physiological and metabolic changes occur by orchestrated alterations in bacterial gene expression, resulting in the secretion of biomolecules needed for biofilm formation and virulence (105). Therefore, hindering quorum sensing may result in the pathogen not being able to cause harm to the host. For extensive discussion of bacterial quorum sensing and the development of agents able to quench this bacterial process, the readers are directed to other informative review papers (103, 105–108). Several agents that block quorum sensing are in pre-clinical development. For example, the synthetic agent meta-bromothiolactone (mBTL) has been reported to curb the production of the virulence factor pyocyanin and biofilm formation in *P. aeruginosa* by affecting the regulation of Las and Rhl

quorum-sensing systems (109). Moreover, *in vitro* protection of human lung epithelial cells and *in vivo* protection of *Caenorhabditis elegans* by mBTL against *P. aeruginosa* have been described (109). A follow-up report detailed the optimization of mBTL for enhanced stability as the thiolactone ring is susceptible to chemical and enzymatic hydrolysis (110). Other anti-quorum sensing agents (111–114) have also been reported to exhibit similar promising *in vitro* and *in vivo* results. However, this paradigm has been recently challenged (115, 116) and several clinical isolates have been reported to be resistant to established anti-quorum sensing agents (117). Anti-quorum sensing agents are yet to reach clinical trials.

Combination therapy. Combination therapy has been well-received by the scientific and medical community, and has existed for more than three decades (118). Clinicians often prescribe two or more antibiotics concomitantly, during empirical treatment to ensure coverage of all possible bacterial pathogens and resistance profiles. It was later realized that the use of multiple antibiotic agents in a therapeutic cocktail may limit the development of resistance *in vitro* in comparison to drug monotherapy. The overall expected clinical outcome for this strategy is to have lower patient mortality rates. However, combination therapy is not limited to antibiotic agents but includes therapeutic interventions that may use bio-active helper molecules, also known as adjuvants, to enhance the efficacy of a primary antibiotic. In fact, it has been argued that the adjuvant-antibiotic combination approach offers a more attractive option in the treatment of drug resistant bacterial infection than using multiple antibiotics (119). Here we discuss combination therapy as: (i) an antibiotic-adjuvant approach and (ii) antibiotic-antibiotic approach.

(i) Antibiotic-adjuvant combination approach. Arguably the most successful therapeutic strategy of the 21st century, the antibiotic-adjuvant approach has resulted in several drug entities on the market. The paradigm entails the use of bio-active adjuvants that augment the antibiotic efficacy of a primary antibiotic against drug-resistant pathogens. The adjuvant may possess weak to no antibacterial activity on its own but is able to either impede antibiotic resistance mechanisms or potentiate antibiotic action. An adjuvant may be an efflux pump inhibitor (to prevent extrusion of drugs), a membrane permeabilizer (to increase the number of molecules that penetrate the membrane) or an enzyme inhibitor (to prevent degradation of drugs before reaching their targets) (119).

(a) β-lactam and β-lactamase inhibitor combination. Augmentin® is a clinically-used broad-spectrum antibiotic combination of amoxicillin and clavulanic acid (120). Clavulanic acid is a β-lactamase inhibitor that acts in synchrony with the β-lactam amoxicillin to prevent bacterial growth. These β-lactamase inhibitors, such as clavulanic acid, block the function of β-lactamases or β-lactam-hydrolyzing enzymes by forming an irreversible bond with the enzyme's functional/active site. Clavulanic acid by itself possesses poor intrinsic activity against pathogens but it efficiently inhibits wide-spread β-lactamases such as many types of the extended-spectrum β-lactamase (ESBL) family (121). Inhibition of ESBLs is especially important as this group of β-lactamases are promiscuous and are able to hydrolyze penicillins, cephalosporins (first-, second- and third- generations) and monobactams (such as aztreonam) (122, 123). Augmentin® was first introduced in 1981 by GlaxoSmithKline and continues its clinical usefulness even today (124, 125). It is not surprising for a β-lactam to be a cornerstone antibiotic in an antibiotic-adjuvant approach as they are considered to be an ideal drug in terms of their efficacy and tolerability.

Unfortunately, their "idealness" has been significantly threatened by the global spread of bacterial β-lactamase-encoding genes. The pursuit of adjuvants that inhibit β-lactamases is therefore crucial to retain clinical effectiveness of the β-lactam class of antibiotics. The recent approvals of ceftolozane-tazobactam in 2014, ceftazidime-avibactam in 2015, and meropenem-vaborbactam by the FDA in 2017 (Table 2-1), for the treatment of drug-resistant Gram-positive and Gram-negative bacterial infections, are indicative of the continued interest in the development of combination therapies that includes a β-lactam and a β-lactamase inhibitor. At least four more β-lactam-based antibiotic-adjuvant combinations are currently in clinical trials (126, 127). The popularity of the antibiotic-adjuvant strategy is apparent in the amount of drug combinations under pre-clinical evaluation. We will briefly highlight three examples, although readers are encouraged to further read extensive reviews elsewhere (119, 128–130).

(b) Imipenem-cilastatin-relebactam triple combination. In 1985, the combination of the carbapenem, imipenem, and the adjuvant cilastatin was approved for use in the United States under the trade name Primaxin® (131). Imipenem is a broad spectrum antibiotic that is rapidly degraded by the human renal enzyme dehydropeptidase-1, and the resulting metabolite poses potential for nephrotoxicity (132). Thus, addition of the dehydropeptidase-1 inhibitor cilastatin to imipenem prevents imipenem's degradation and nephrotoxicity. Cilastatin also blocks megalin-mediated proximal tubule uptake of cationic antibiotics (133), further lowering the risk of kidney damage. However, the recent increase in bacterial infections caused by carbapenemase-producing organisms that inactivate imipenem calls for an improvement in this therapy. The combination of imipenem-cilastatin with the addition of the diazabicyclooctane β-lactamase inhibitor relebactam (also known as MK-7655) is currently in Phase 3 clinical trial for the treatment of Gram-negative

bacterial infections (134). The adjuvant relebactam is able to inhibit the activity of ESBL, class A (e.g. KPC) and class C (e.g. AmpC) β-lactamases against imipenem by irreversibly blocking their functional/active site (135). The triple combination was found to be generally well tolerated in patients, with commonly reported adverse effects being nausea, vomiting and diarrhea (136). Recently, a Phase 3 randomized, double-blind, non-inferiority study of imipenem-cilastatin/relebactam in comparison to imipenem-cilastatin/colistimethate sodium for the treatment of hospital-acquired bacterial pneumonia (HABP), ventilator-associated bacterial pneumonia (VABP), complicated intra-abdominal infection (cIAI) and complicated urinary tract infection (cUTI) (https://clinicaltrials.gov/ct2/show/study/NCT02452047) was completed. Results are yet to be disclosed. Another Phase 3 randomized, double-blind non-inferiority study of imipenem-cilastatin/relebactam against piperacillin/tazobactam for the treatment of HABP or VABP is currently recruiting (https://clinicaltrials.gov/ct2/show/NCT02493764). Moreover, a Phase 3 non-randomized, open label study for the efficacy and safety of imipenem-cilastatin/relebactam for the treatment of cIAI and cUTI is currently ongoing in Japan (https://clinicaltrials.gov/ct2/show/NCT03293485). The activity of the triple combination, unfortunately, is very limited against organisms that harbor metallo-β-lactamase such as New Delhi Metallo-β-lactamase-1 (NDM-1), imipenemase (IMP) and Verona integron-encoded metallo-β-lactamase (VIM) (134, 135).

(c) Aspergillomarasmine A. The adjuvant aspergillomarasmine A (AMA) was recently discovered to resuscitate the biocidal activity of the carbapenem drug, meropenem, against metallo-β-lactamase-producing organisms (137). The fungal metabolite AMA was first isolated in the 1960s (138) and was later evaluated for its anti-hypertensive properties (139, 140). In an antibiotic era

where enzymes capable of degrading even the most powerful β-lactam (eg. carbapenems) are abundant, it is promising to find AMA able to inhibit metallo-β-lactamases such as the NDM-1 enzyme. AMA was found to sequester zinc cations (137) which are essential for the hydrolytic activity of metallo-β-lactamases (141, 142). In a mouse model of NDM-1-positive *K. pneumoniae* infection, a single dose of meropenem (10 mg/kg) and AMA (30 mg/kg) combination led to > 95% survival after five days post-infection (137). Meropenem alone (10 mg/kg) or AMA alone (30 mg/kg) both resulted in 0% survival (137). These promising results stimulate the need for an optimized dosing regimen of AMA in combination with carbapenems for the treatment of metallo-β-lactamase-producing pathogens. Currently, medicinal chemists are looking into optimizing the chemical structure of this adjuvant. The total synthesis (143), structure-activity relationship studies (144), and structural reassignment (145) of AMA have all been recently reported.

(d) SPR741. A polymyxin-based antimicrobial peptide SPR741 (formerly NAB741) is currently being developed by Evotec AG and Spero Therapeutics as an adjuvant that potentiates antibiotics against Gram-negative pathogens (146). The recently completed randomized, quadruple-blind Phase 1 clinical study for safety and tolerability in healthy volunteers (https://clinicaltrials.gov/ct2/show/NCT03022175) yielded favorable results for this adjuvant. SPR741 was well tolerated by healthy adult volunteers in a single dose of up to 800 mg, and at doses of up to 600 mg every eight hours for 14 days (https://sperotherapeutics.com/). In contrast to polymyxins, SPR741 has poor activity against Gram-negative pathogens on its own but can permeabilize the outer membrane to facilitate entry of other antibiotics into the bacterial cell (147). For instance, SPR741 was reported to sensitize *Enterobacteriaceae* and *A. baumannii* but not *P. aeruginosa* to an extensive panel of antibiotics including clarithromycin, fusidic acid and

rifampicin (148–150). These three antibiotics are not classical drugs used to treat Gram-negative bacillary infections due to intrinsic resistance, notably OM impermeability. At 2 µg/mL of SPR741, the MIC_{50} and MIC_{90} of rifampicin against a panel of MDR *E. coli* were 0.016 and 0.06 µg/mL, respectively (148). Rifampicin alone has an MIC_{50} and MIC_{90} of 16 and >128 µg/mL, respectively, against the same panel of *E. coli* strains (148). At similar concentrations of SPR741, strong rifampicin potentiation was also described against a panel of MDR *A. baumannii* (148). The *in vivo* efficacy of SPR741 and rifampicin combination was shown in murine thigh and lung infection models (151, 152). Interestingly, the characteristic nephrotoxic concerns usually associated with polymyxins (153, 154) were not observed with SPR741 at a dose of 60 mg/kg/day in cynomolgus monkeys after seven days of a one-hour infusion thrice daily (155).

(ii) Antibiotic-antibiotic combination approach. The use of two or more antibiotic agents that have different targets, which may or may not be for a single biochemical process, presents another attractive strategy to overcome drug resistance. The hypotheses of the antibiotic-antibiotic combination approach are: (a) to achieve drug synergism between each drug component in a way that enhances treatment efficacy, and (b) to simultaneously impact multiple targets in pathogens, resulting in the suppression of antibiotic resistance development and complete eradication of bacterial strains with intermediate susceptibility or resistance to one of two antibiotics. The assumption is that the bacterial cell will have difficulty surviving with multiple "hits" at the same time. Clinicians sometimes employ this strategy during empirical treatment of infection, and such an approach might indeed prolong the clinical utility of antibiotics. For instance, the combination of trimethoprim-sulfamethoxazole has been in use since 1968 for the treatment of bacterial infections caused by the *Enterobacteriaceae* family and non-fermentative opportunistic pathogens

(156, 157). Both antibiotics work together to inhibit sequential steps in bacterial folic acid synthesis, which is detrimental as most bacteria are obligate folate synthesizers while humans acquire folate through diet. The sulfonamide, sulfamethoxazole, inhibits dihydropteroate synthase that converts para-aminobenzoic acid to dihydrofolate and trimethoprim inhibits dihydrofolate reductase that converts dihydrofolate to tetrahydrofolate (folic acid's bioactive form) (157). Trimethoprim-sulfamethoxazole is an efficacious antibiotic used to treat urinary tract and select gastrointestinal bacterial infections (158, 159). Sulfamethoxazole may be replaced with the sulfonamide, sulfametrole, in some European Union countries, although both, when combined with trimethoprim, exhibit the same clinical efficacy (160). However, the success of the trimethoprim-sulfamethoxazole combination has been affected by the dissemination of resistance mechanisms that prevent both antibiotics from eliciting their biological functions. Overexpression of multidrug efflux pumps able to expel both trimethoprim and sulfamethoxazole out of the cell and membrane modifications that limit their intracellular permeation are problematic (156). Many other antibiotic-antibiotic combinations are used in the clinic including those of tigecycline + gentamicin, tigecycline + colistin and carbapenem + colistin (161), to name a few.

Challenges of combination therapy. Considering the 'success' of several antibiotic-antibiotic combinations in the past few decades, the strategy remains fallible as several important pharmacological questions remain unanswered. For instance, other than in tuberculosis, there is no clinical evidence to support the notion that antibiotic resistance is suppressed by antibiotic-antibiotic combinations (162). This is a tough concept to prove as clinical studies are usually designed not to measure emergence of antibiotic resistance, but to prevent or treat it. This data may only be extrapolated from *in vitro* and in animal models, but may be different in human hosts.

The clinical translatability of drug synergy *in vitro* and in animal models to humans is also debatable (162). The limited available clinical evidence suggests a statistically-insignificant difference between antibiotic-antibiotic combination therapy and monotherapy in the treatment of Gram-negative bacterial infections in terms of mortality rates, which is the postulated clinical outcome for synergistic drug combinations (163–165). For instance, a systematic study reports no appreciable improvement for the combination of β-lactam/aminoglycoside over β-lactam monotherapy in treating endocarditis caused by a Gram-positive bacterial (e.g. *Staphylococcus aureus*) infection, even though the combination shows synergism *in vitro* (166). Another study shows that the combination of β-lactam and either aminoglycoside or fluoroquinolone in comparison to β-lactam monotherapy impose no benefit in patient mortality for treating infections caused by the Gram-negative *P. aeruginosa* (164). However, it should be noted that the supporting evidence for these studies were based on meta-analyses of a small number of available clinical data that includes those during early years where drug resistance was not as prevalent. Caution should therefore be taken in data extrapolation to fit the current landscape where incidences of MDR and XDR bacterial infections are much higher. Currently, there seems to be an apparent consensus that combination therapy is preferred for treating MDR pathogenic infections of severely ill patients and for empirical therapy (167). Lack of pharmacokinetic complementarity between different drugs might indeed contribute to the discrepancies between *in vitro* data and clinical observations (168). Each drug component may be absorbed or distributed in the human body to different degrees. Pharmacokinetic variances, but also the patient's overall condition, would certainly impose a challenge in fine-tuning dosages of administered drugs to replicate their observed *in vitro* synergy as both drugs are required to be at the site of infection at their optimal concentrations simultaneously. Non-complementary absorption and distribution rates may

therefore be circumvented by fusing both pharmacophoric molecules together to make a single hybrid antibacterial agent.

Antibiotic hybrids against antibiotic-resistant bacteria. The antibiotic hybrid strategy precipitated from the countless attempts to discover new synthetic scaffolds that may yield antibiotics capable of overcoming drug resistance. Scientific ingenuity led to the development of molecular hybrids (Fig. 2-2) by fusing different biologically-active agents into one heteromeric entity with the hope of retaining the biological action of the constituent fragments. A molecular linker/tether is often used to append the participating agents together *via* a covalent bond, although molecules could also be fused together directly. The mode of covalent attachment also could be designed as either cleavable or non-cleavable (see Fig. 2-2). A cleavable linker is expected to be enzymatically biotransformed once the hybrid reaches its site of action (the bacteria) while a non-cleavable linker remains unchanged throughout its time-course in the body. The former constitutes a hybrid prodrug approach while the latter constitutes a hybrid drug approach. The hypothesis of antibiotic hybrid integrates the working concept of suppressing drug resistance evolution in combination therapy into a monotherapy, thus presenting a molecular agent (instead of two) with single pharmacokinetic profile. It also eliminates the problem of non-complementary pharmacodynamics. Hybrid drugs are also postulated to eradicate bacterial strains with intermediate susceptibility or resistance to one of the covalently-linked drug fragments. Although unpredictable, retaining antibacterial potency against pathogens that possess intermediate susceptibility or resistance to both drug components is possible as the process of hybridization may also impart additional physicochemical properties that could alter the hybrid's

pharmacological spectrum. For instance, hybridization of two therapeutic agents may enhance the

efficacy or even impart a new mechanism of antibacterial action to the resulting hybrid agent.
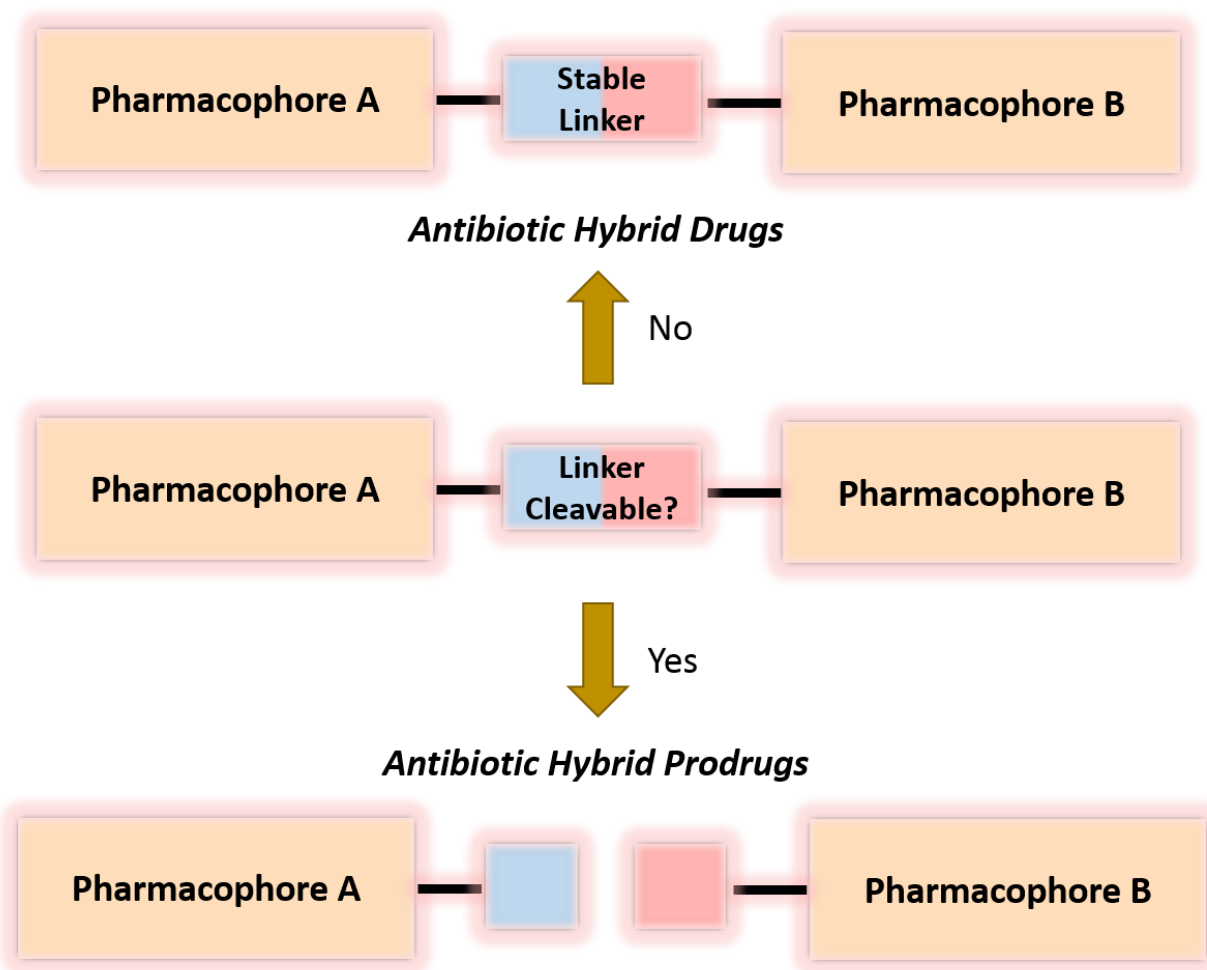
Figure 2-2 Two different pharmacophoric domains attached covalently by a linker domain.

The lability of the linker determines the type of antibiotic hybrid generated. A linker that can be enzymatically degraded (preferably by only bacterial-specific enzymes) gives rise to two functional pharmacophoric entities and thus used in the antibiotic hybrid prodrug strategy. A linker that is inert to enzymatic degradation is used to hold the two pharmacophoric domains together in the antibiotic hybrid drug strategy.

Definition of an antibiotic hybrid. What defines a hybrid agent? The literature offers various

subjective definitions of hybrid agents, depending on the context in which they are being used. In

this account however, we define a hybrid antibiotic as a synthetic construct of two or more pharmacophores belonging to an established agent known to elicit a desired antimicrobial effect. This encompasses agents described as either dual-action antibiotic hybrids (169, 170), chimeric antibiotics (171, 172), multivalent/divalent antibiotics (173–175) and antibiotic conjugates (176). Moreover, the antibiotic hybrid approach is not confined to covalent fusion of antibacterial agents and may also include beneficial adjuvants such as resistance enzyme inhibitors, membrane permeabilizers, siderophores, and efflux pumps inhibitors. The notion of bimodality (coined as "dual-action" in 1994 (169)) in prospective antibiotic hybrids suggests the need for the covalently-appended agents to retain their known biological action. However, our experience reveals that it might indeed not be necessary to retain both known activities as an unexpected third mode of action may arise from the fusion of two therapeutic agents (*vide infra*). Moreover, some antibiotic hybrids are able to "resuscitate" the antibacterial potency of legacy antibiotics against drug-resistant pathogens. Legacy antibiotics pertains to widely-used antibacterial agents that have been clinically-used for decades and that their clinical efficacy is currently being challenged by the rise of antibiotic resistance mechanisms.

2.6. Conclusion

There is an urgent need to develop new therapeutics able to treat antibiotic-resistant infections, especially those caused by MDR Gram-negative pathogens. However, coming up with a magic bullet to address this problem has over the years proven to be elusive. Several strategies were highlighted to potentially develop new efficacious antibiotics, yet, these are only a few of the possible solutions to this ever-worsening global issue. Imagination is perhaps the greatest limitation to drug discovery.

2.7. References

1.   Lowy F. 2003. Antimicrobial resistance: the example of Staphylococcus aureus. J Clin Invest 111:1265–1273.

2.   Boucher HW, Talbot GH, Bradley JS, Edwards JE, Gilbert D, Rice LB, Scheld M, Spellberg B, Bartlett J. 2009. Bad bugs, no drugs: no ESKAPE! An update from the Infectious Diseases Society of America. Clin Infect Dis 48:1–12.

3.   Yoneyama H, Katsumata R. 2006. Antibiotic resistance in bacteria and its future for novel antibiotic development. Biosci Biotechnol Biochem 70:1060–1075.

4.   Rice LB. 2008. Federal funding for the study of antimicrobial resistance in nosocomial pathogens: no ESKAPE. J Infect Dis 197:1079–1081.

5.   Rice LB. 2010. Progress and challenges in implementing the research on ESKAPE pathogens. Infect Control Hosp Epidemiol 31:S7–S10.

6.   Karlowsky JA, Hoban DJ, Hackel MA, Lob SH, Sahm DF. 2017. Antimicrobial susceptibility of Gram-negative ESKAPE pathogens isolated from hospitalized patients with intra-abdominal and urinary tract infections in Asia-Pacific countries: SMART 2013-2015. J Med Microbiol 66:61–69.

7.   Karlowsky JA, Hoban DJ, Hackel MA, Lob SH, Sahm DF. 2017. Resistance among Gram-negative ESKAPE pathogens isolated from hospitalized patients with intra-abdominal and urinary tract infections in Latin American countries: SMART 2013-2015. Braz J Infect Dis 21:343–348.

8.   Cardoso T, Ribeiro O, Aragao IC, Costa-Pereira A, Sarmento AE. 2012. Additional risk factors for infection by multidrug-resistant pathogens in healthcare-associated infection: a large cohort study. BMC Infect Dis 12:375.

9.   Magiorakos A-P, Srinivasan A, Carey RB, Carmeli Y, Falagas ME, Giske CG, Harbarth S, Hindler JF, Kahlmeter G, Olsson-Liljequist B, Paterson DL, Rice LB, Stelling J, Struelens MJ, Vatopoulos A, Weber JT, Monnet DL. 2012. Multidrug-resistant, extensively drug-resistant and pandrug-resistant bacteria: an international expert proposal for interim standard definitions for acquired resistance. Clin Microbiol Infect 18:268–281.

10.   Ho J, Tambyah P a, Paterson DL. 2010. Multiresistant Gram-negative infections: a global perspective. Curr Opin Infect Dis 23:546–553.

11.   Butler MS, Blaskovich MA, Cooper MA. 2013. Antibiotics in the clinical pipeline in 2013. J Antibiot (Tokyo) 66:571–591.

12.   World Health Organization. 2014. Antimicrobial resistance: global report on surveillance.

13.   Houghton F. 2017. Antimicrobial resistance (AMR) and the United Nations (UN). J Infect Public Health. England.

14.   Boucher HW, Bakken JS, Murray BE. 2016. The United Nations and the urgent need for coordinated global action in the fight against antimicrobial resistance. Ann Intern Med 165:812–813.

15.   Laxminarayan R, Sridhar D, Blaser M, Wang M, Woolhouse M. 2016. Achieving global targets for antimicrobial resistance. Science 353:874–875.

16.   Gilbert DN, Guidos RJ, Boucher HW, Talbot GH, Spellberg B, Edwards Jr JE, Scheld

MW, Bradley JS, Bartlett JG. 2010. The 10 x '20 Initiative: pursuing a global commitment to develop 10 new antibacterial drugs by 2020. Clin Infect Dis 50:1081–1083.

17.   Boucher HW, Talbot GH, Benjamin DKJ, Bradley J, Guidos RJ, Jones RN, Murray BE, Bonomo RA, Gilbert D. 2013. 10 x '20 Progress--development of new drugs active against gram-negative bacilli: an update from the Infectious Diseases Society of America. Clin Infect Dis 56:1685–1694.

18.   Silver LL. 2016. A Gestalt approach to Gram-negative entry. Bioorg Med Chem 24:6379–6389.

19.   Gutsmann T, Seydel U. 2010. Impact of the glycostructure of amphiphilic membrane components on the function of the outer membrane of Gram-negative bacteria as a matrix for incorporated channels and a target for antimicrobial peptides or proteins. Eur J Cell Biol 89:11–23.

20.   Wu EL, Engstrom O, Jo S, Stuhlsatz D, Yeom MS, Klauda JB, Widmalm G, Im W. 2013. Molecular dynamics and NMR spectroscopy studies of *E. coli* lipopolysaccharide structure and dynamics. Biophys J 105:1444–1455.

21.   Khalid S, Berglund NA, Holdbrook DA, Leung YM, Parkin J. 2015. The membranes of Gram-negative bacteria: progress in molecular modelling and simulation. Biochem Soc Trans 43:162–167.

22.   Piggot TJ, Holdbrook DA, Khalid S. 2011. Electroporation of the *E. coli* and S. Aureus membranes: molecular dynamics simulations of complex bacterial membranes. J Phys Chem B 115:13381–13388.

23.   Nikaido H. 1994. Prevention of drug access to bacterial targets: permeability barriers and active efflux. Science 264:382–388.

24.   Kucharska I, Liang B, Ursini N, Tamm LK. 2016. Molecular interactions of lipopolysaccharide with an outer membrane protein from *Pseudomonas aeruginosa* probed by solution NMR. Biochemistry 55:5061–5072.

25.   Kowata H, Tochigi S, Kusano T, Kojima S. 2016. Quantitative measurement of the outer membrane permeability in Escherichia coli lpp and tol-pal mutants defines the significance of Tol-Pal function for maintaining drug resistance. J Antibiot (Tokyo) 69:863–870.

26.   Vaara M, Plachy WZ, Nikaido H. 1990. Partitioning of hydrophobic probes into lipopolysaccharide bilayers. Biochim Biophys Acta 1024:152–158.

27.   Needham BD, Trent MS. 2013. Fortifying the barrier: the impact of lipid A remodelling on bacterial pathogenesis. Nat Rev Microbiol 11:467–481.

28.   Breidenstein EBM, de la Fuente-Nunez C, Hancock REW. 2011. *Pseudomonas aeruginosa*: all roads lead to resistance. Trends Microbiol 19:419–426.

29.   Butler MS, Hansford KA, Blaskovich MAT, Halai R, Cooper MA. 2014. Glycopeptide antibiotics: back to the future. J Antibiot (Tokyo) 67:631–644.

30.   Boger D. 2001. Vancomycin, teicoplanin, and ramoplanin: synthetic and mechanistic studies. Med Res Rev 21:356–381.

31.   Silver LL. 2008. Are natural products still the best source for antibacterial discovery? The bacterial entry factor. Expert Opin Drug Discov 3:487–500.

32.   Oldham ML, Chen S, Chen J. 2013. Structural basis for substrate specificity in the

Escherichia coli maltose transport system. Proc Natl Acad Sci U S A 110:18132–18137.

33.   Ning X, Lee S, Wang Z, Kim D, Stubblefield B, Gilbert E, Murthy N. 2011. Maltodextrin-based imaging probes detect bacteria in vivo with high sensitivity and specificity. Nat Mater 10:602–607.

34.   Fairman JW, Noinaj N, Buchanan SK. 2011. The structural biology of beta-barrel membrane proteins: a summary of recent reports. Curr Opin Struct Biol 21:523–531.

35.   Zeth K, Thein M. 2010. Porins in prokaryotes and eukaryotes: common themes and variations. Biochem J 431:13–22.

36.   Cowan SW, Schirmer T, Rummel G, Steiert M, Ghosh R, Pauptit RA, Jansonius JN, Rosenbusch JP. 1992. Crystal structures explain functional properties of two *E. coli* porins. Nature 358:727–733.

37.   Delcour AH. 2009. Outer membrane permeability and antibiotic resistance. Biochim Biophys Acta 1794:808–816.

38.   Nakae T. 1975. Outer membrane of Salmonella typhimurium: reconstitution of sucrose-permeable membrane vesicles. Biochem Biophys Res Commun 64:1224–1230.

39.   Nikaido H. 2003. Molecular basis of bacterial outer membrane permeability revisited. Microbiol Mol Biol Rev 67:593–656.

40.   Hancock RE, Decad GM, Nikaido H. 1979. Identification of the protein producing transmembrane diffusion pores in the outer membrane of *Pseudomonas aeruginosa* PA01. Biochim Biophys Acta 554:323–331.

41.   Chevalier S, Bouffartigues E, Bodilis J, Maillot O, Lesouhaitier O, Feuilloley MGJ,

Orange N, Dufour A, Cornelis P. 2017. Structure, function and regulation of *Pseudomonas aeruginosa* porins. FEMS Microbiol Rev 41:698–722.

42.   Nikaido H, Nikaido K, Harayama S. 1991. Identification and characterization of porins in *Pseudomonas aeruginosa*. J Biol Chem 266:770–779.

43.   Hancock RE. 1998. Resistance mechanisms in *Pseudomonas aeruginosa* and other nonfermentative gram-negative bacteria. Clin Infect Dis 27 Suppl 1:S93-9.

44.   Yoshimura F, Zalman LS, Nikaido H. 1983. Purification and properties of *Pseudomonas aeruginosa* porin. J Biol Chem 258:2308–2314.

45.   Alvarez-Ortega C, Wiegand I, Olivares J, Hancock REW, Martinez JL. 2011. The intrinsic resistome of *Pseudomonas aeruginosa* to beta-lactams. Virulence 2:144–146.

46.   Hancock RE, Farmer SW, Li ZS, Poole K. 1991. Interaction of aminoglycosides with the outer membranes and purified lipopolysaccharide and OmpF porin of Escherichia coli. Antimicrob Agents Chemother 35:1309–1314.

47.   Hancock RE. 1984. Alterations in outer membrane permeability. Annu Rev Microbiol 38:237–264.

48.   Arunmanee W, Pathania M, Solovyova AS, Le Brun AP, Ridley H, Basle A, van den Berg B, Lakey JH. 2016. Gram-negative trimeric porins have specific LPS binding sites that are essential for porin biogenesis. Proc Natl Acad Sci U S A 113:E5034-43.

49.   Clifton LA, Skoda MWA, Le Brun AP, Ciesielski F, Kuzmenko I, Holt SA, Lakey JH. 2015. Effect of divalent cation removal on the structure of gram-negative bacterial outer membrane models. Langmuir 31:404–412.

50.   Herrmann M, Schneck E, Gutsmann T, Brandenburg K, Tanaka M. 2015. Bacterial lipopolysaccharides form physically cross-linked, two-dimensional gels in the presence of divalent cations. Soft Matter 11:6037–6044.

51.   George S, Hamblin MR, Kishen A. 2009. Uptake pathways of anionic and cationic photosensitizers into bacteria. Photochem Photobiol Sci 8:788–795.

52.   Hancock RE, Bell A. 1988. Antibiotic uptake into gram-negative bacteria. Eur J Clin Microbiol Infect Dis 7:713–720.

53.   Nicas TI, Hancock RE. 1980. Outer membrane protein H1 of *Pseudomonas aeruginosa*: involvement in adaptive and mutational resistance to ethylenediaminetetraacetate, polymyxin B, and gentamicin. J Bacteriol 143:872–878.

54.   Zimelis VM, Jackson GG. 1973. Activity of aminoglycoside antibiotics aganst *Pseudomonas aeruginosa*: specificity and site of calcium and magnesium antagonism. J Infect Dis 127:663–669.

55.   Davis SD, Iannetta A, Wedgwood RJ. 1971. Activity of colistin against *Pseudomonas aeruginosa*: inhibition by calcium. J Infect Dis 124:610–612.

56.   Newton BA. 1954. Site of action of polymyxin on *Pseudomonas aeruginosa*: antagonism by cations. J Gen Microbiol 10:491–499.

57.   Hancock RE, Wong PG. 1984. Compounds which increase the permeability of the *Pseudomonas aeruginosa* outer membrane. Antimicrob Agents Chemother 26:48–52.

58.   Tamber S, Hancock REW. 2003. On the mechanism of solute uptake in Pseudomonas. Front Biosci 8:s472-83.

59.   Farha MA, Verschoor CP, Bowdish D, Brown ED. 2013. Collapsing the proton motive force to identify synergistic combinations against Staphylococcus aureus. Chem Biol 20:1168–1178.

60.   Chopra I. 1988. Molecular mechanisms involved in the transport of antibiotics into bacteria. Parasitology 96 Suppl:S25-44.

61.   Shultis DD, Purdy MD, Banchs CN, Wiener MC. 2006. Outer membrane active transport: structure of the BtuB:TonB complex. Science 312:1396–1399.

62.   Kashket ER. 1985. The proton motive force in bacteria: a critical assessment of methods. Annu Rev Microbiol 39:219–242.

63.   Zarfl C, Matthies M, Klasmeier J. 2008. A mechanistical model for the uptake of sulfonamides by bacteria. Chemosphere 70:753–760.

64.   Yamaguchi A, Ohmori H, Kaneko-Ohdera M, Nomura T, Sawai T. 1991. Delta pH-dependent accumulation of tetracycline in Escherichia coli. Antimicrob Agents Chemother 35:53–56.

65.   Taber HW, Mueller JP, Miller PF, Arrow AS. 1987. Bacterial uptake of aminoglycoside antibiotics. Microbiol Rev 51:439–457.

66.   Zgurskaya HI, Lopez CA, Gnanakaran S. 2015. Permeability barrier of Gram-negative cell envelopes and approaches to bypass it. ACS Infect Dis 1:512–522.

67.   Li X-Z, Plesiat P, Nikaido H. 2015. The challenge of efflux-mediated antibiotic resistance in Gram-negative bacteria. Clin Microbiol Rev 28:337–418.

68.   Song S, Kim J-S, Lee K, Ha N-C. 2015. Molecular architecture of the bacterial tripartite

multidrug efflux pump focusing on the adaptor bridging model. J Microbiol 53:355–364.

69.   Delmar JA, Su C-C, Yu EW. 2014. Bacterial multidrug efflux transporters. Annu Rev Biophys 43:93–117.

70.   Kumar S, Varela MF. 2012. Biochemistry of bacterial multidrug efflux pumps. Int J Mol Sci 13:4484–4495.

71.   Nikaido H. 2009. Multidrug resistance in bacteria. Annu Rev Biochem 78:119–146.

72.   Piddock LJ V. 2006. Clinically relevant chromosomally encoded multidrug resistance efflux pumps in bacteria. Clin Microbiol Rev 19:382–402.

73.   Singh SB, Young K, Silver LL. 2017. What is an "ideal" antibiotic? Discovery challenges and path forward. Biochem Pharmacol 133:63–73.

74.   Lipinski CA, Lombardo F, Dominy BW, Feeney PJ. 2001. Experimental and computational approaches to estimate solubility and permeability in drug discovery and development settings. Adv Drug Deliv Rev 46:3–26.

75.   Lipinski CA. 2016. Rule of five in 2015 and beyond: Target and ligand structural limitations, ligand chemistry structure and drug discovery project decisions. Adv Drug Deliv Rev 101:34–41.

76.   Ebejer J-P, Charlton MH, Finn PW. 2016. Are the physicochemical properties of antibacterial compounds really different from other drugs? J Cheminform 8:30.

77.   O'Shea R, Moser HE. 2008. Physicochemical properties of antibacterial compounds: implications for drug discovery. J Med Chem 51:2871–2878.

78.   Takrouri K, Cooper HD, Spaulding A, Zucchi P, Koleva B, Cleary DC, Tear W, Beuning

PJ, Hirsch EB, Aggen JB. 2016. Progress against Escherichia coli with the oxazolidinone class of antibacterials: test case for a general approach to improving whole-cell Gram-negative activity. ACS Infect Dis 2:405–426.

79.   Schumacher A, Trittler R, Bohnert JA, Kummerer K, Pages J-M, Kern W V. 2007. Intracellular accumulation of linezolid in Escherichia coli, Citrobacter freundii and Enterobacter aerogenes: role of enhanced efflux pump activity and inactivation. J Antimicrob Chemother 59:1261–1264.

80.   Zhou Y, Joubran C, Miller-Vedam L, Isabella V, Nayar A, Tentarelli S, Miller A. 2015. Thinking outside the "bug": a unique assay to measure intracellular drug penetration in gram-negative bacteria. Anal Chem 87:3579–3584.

81.   Bhat J, Narayan A, Venkatraman J, Chatterji M. 2013. LC-MS based assay to measure intracellular compound levels in Mycobacterium smegmatis: linking compound levels to cellular potency. J Microbiol Methods 94:152–158.

82.   Heidari-Torkabadi H, Che T, Lombardo MN, Wright DL, Anderson AC, Carey PR. 2015. Measuring propargyl-linked drug populations inside bacterial cells, and their interaction with a dihydrofolate reductase target, by Raman microscopy. Biochemistry 54:2719–2726.

83.   Cinquin B, Maigre L, Pinet E, Chevalier J, Stavenger RA, Mills S, Refregiers M, Pages J-M. 2015. Microspectrometric insights on the uptake of antibiotics at the single bacterial cell level. Sci Rep 5:17968.

84.   Davis TD, Gerry CJ, Tan DS. 2014. General platform for systematic quantitative evaluation of small-molecule permeability in bacteria. ACS Chem Biol 9:2535–2544.

85.   Richter MF, Drown BS, Riley AP, Garcia A, Shirai T, Svec RL, Hergenrother PJ. 2017. Predictive compound accumulation rules yield a broad-spectrum antibiotic. Nature 545:299–304.

86.   Hurdle JG, O'Neill AJ, Chopra I, Lee RE. 2011. Targeting bacterial membrane function: an underexploited mechanism for treating persistent infections. Nat Rev Microbiol 9:62–75.

87.   Ghosh C, Haldar J. 2015. Membrane-active small molecules: designs inspired by antimicrobial peptides. ChemMedChem 10:1606–1624.

88.   Herzog IM, Fridman M. 2014. Design and synthesis of membrane-targeting antibiotics: from peptides- to aminosugar-based antimicrobial cationic amphiphiles. Medchemcomm 5:1014–1026.

89.   Domalaon R, Zhanel GG, Schweizer F. 2016. Short antimicrobial peptides and peptide scaffolds as promising antibacterial agents. Curr Top Med Chem 16:1217–1230.

90.   Benhamou RI, Shaul P, Herzog IM, Fridman M. 2015. Di-N-methylation of anti-Gram-positive aminoglycoside-derived membrane disruptors improves antimicrobial potency and broadens spectrum to Gram-negative bacteria. Angew Chem Int Ed Engl 54:13617–13621.

91.   Cigana C, Bernardini F, Facchini M, Alcala-Franco B, Riva C, De Fino I, Rossi A, Ranucci S, Misson P, Chevalier E, Brodmann M, Schmitt M, Wach A, Dale GE, Obrecht D, Bragonzi A. 2016. Efficacy of the novel antibiotic POL7001 in preclinical models of *Pseudomonas aeruginosa* pneumonia. Antimicrob Agents Chemother 60:4991–5000.

92.   Srinivas N, Jetter P, Ueberbacher BJ, Werneburg M, Zerbe K, Steinmann J, Van der Meijden B, Bernardini F, Lederer A, Dias RLA, Misson PE, Henze H, Zumbrunn J, Gombert FO, Obrecht D, Hunziker P, Schauer S, Ziegler U, Kach A, Eberl L, Riedel K, DeMarco SJ,

Robinson JA. 2010. Peptidomimetic antibiotics target outer-membrane biogenesis in *Pseudomonas aeruginosa*. Science 327:1010–1013.

93.   Cohen NR, Lobritz MA, Collins JJ. 2013. Microbial persistence and the road to drug resistance. Cell Host Microbe 13:632–642.

94.   Certain LK, Way JC, Pezone MJ, Collins JJ. 2017. Using engineered bacteria to characterize infection dynamics and antibiotic effects in vivo. Cell Host Microbe 22:263–268.e4.

95.   Oz T, Guvenek A, Yildiz S, Karaboga E, Tamer YT, Mumcuyan N, Ozan VB, Senturk GH, Cokol M, Yeh P, Toprak E. 2014. Strength of selection pressure is an important parameter contributing to the complexity of antibiotic resistance evolution. Mol Biol Evol 31:2387–2401.

96.   Pál C, Papp B, Lázár V. 2015. Collateral sensitivity of antibiotic-resistant microbes. Trends Microbiol 23:401–407.

97.   Barlow M. 2009. What antimicrobial resistance has taught us about horizontal gene transfer. Methods Mol Biol 532:397–411.

98.   Williams SCP. 2014. News Feature: Next-generation antibiotics. Proc Natl Acad Sci U S A 111:11227–11229.

99.   Brannon JR, Hadjifrangiskou M. 2016. The arsenal of pathogens and antivirulence therapeutic strategies for disarming them. Drug Des Devel Ther 10:1795–1806.

100.   Dickey SW, Cheung GYC, Otto M. 2017. Different drugs for bad bugs: antivirulence strategies in the age of antibiotic resistance. Nat Rev Drug Discov.

101.   Rampioni G, Leoni L, Williams P. 2014. The art of antibacterial warfare: Deception through interference with quorum sensing-mediated communication. Bioorg Chem 55:60–68.

102.   Asfahl KL, Schuster M. 2017. Social interactions in bacterial cell-cell signaling. FEMS Microbiol Rev 41:92–107.

103.   Grandclement C, Tannieres M, Morera S, Dessaux Y, Faure D. 2016. Quorum quenching: role in nature and applied developments. FEMS Microbiol Rev 40:86–116.

104.   Lee J, Zhang L. 2015. The hierarchy quorum sensing network in *Pseudomonas aeruginosa*. Protein Cell 6:26–41.

105.   Papenfort K, Bassler BL. 2016. Quorum sensing signal-response systems in Gram-negative bacteria. Nat Rev Microbiol 14:576–588.

106.   Maura D, Ballok AE, Rahme LG. 2016. Considerations and caveats in anti-virulence drug development. Curr Opin Microbiol 33:41–46.

107.   Singh RP, Desouky SE, Nakayama J. 2016. Quorum quenching strategy targeting Gram-positive pathogenic bacteria. Adv Exp Med Biol 901:109–130.

108.   Zambelloni R, Marquez R, Roe AJ. 2015. Development of antivirulence compounds: a biochemical review. Chem Biol Drug Des 85:43–55.

109.   O'Loughlin CT, Miller LC, Siryaporn A, Drescher K, Semmelhack MF, Bassler BL. 2013. A quorum-sensing inhibitor blocks *Pseudomonas aeruginosa* virulence and biofilm formation. Proc Natl Acad Sci U S A 110:17981–17986.

110.   Miller LC, O'Loughlin CT, Zhang Z, Siryaporn A, Silpe JE, Bassler BL, Semmelhack MF. 2015. Development of potent inhibitors of pyocyanin production in *Pseudomonas aeruginosa*. J Med Chem 58:1298–1306.

111.   Simonetti O, Cirioni O, Cacciatore I, Baldassarre L, Orlando F, Pierpaoli E, Lucarini G,

Orsetti E, Provinciali M, Fornasari E, Di Stefano A, Giacometti A, Offidani A. 2016. Efficacy of the quorum sensing inhibitor FS10 alone and in combination with tigecycline in an animal model of Staphylococcal infected wound. PLoS One 11:e0151956.

112.   Alasil SM, Omar R, Ismail S, Yusof MY. 2015. Inhibition of quorum sensing-controlled virulence factors and biofilm formation in *Pseudomonas aeruginosa* by culture extract from novel bacterial species of Paenibacillus using a rat model of chronic lung infection. Int J Bacteriol 2015:671562.

113.   Oh K-B, Nam K-W, Ahn H, Shin J, Kim S, Mar W. 2010. Therapeutic effect of (Z)-3-(2,5-dimethoxyphenyl)-2-(4-methoxyphenyl) acrylonitrile (DMMA) against Staphylococcus aureus infection in a murine model. Biochem Biophys Res Commun 396:440–444.

114.   Lidor O, Al-Quntar A, Pesci EC, Steinberg D. 2015. Mechanistic analysis of a synthetic inhibitor of the *Pseudomonas aeruginosa* LasI quorum-sensing signal synthase. Sci Rep 5:16569.

115.   Kalia VC, Wood TK, Kumar P. 2014. Evolution of resistance to quorum-sensing inhibitors. Microb Ecol 68:13–23.

116.   Scutera S, Zucca M, Savoia D. 2014. Novel approaches for the design and discovery of quorum-sensing inhibitors. Expert Opin Drug Discov 9:353–366.

117.   Garcia-Contreras R, Martinez-Vazquez M, Velazquez Guadarrama N, Villegas Paneda AG, Hashimoto T, Maeda T, Quezada H, Wood TK. 2013. Resistance to the quorum-quenching compounds brominated furanone C-30 and 5-fluorouracil in *Pseudomonas aeruginosa* clinical isolates. Pathog Dis 68:8–11.

118.   Hilf M, Yu VL, Sharp J, Zuravleff JJ, Korvick JA, Muder RR. 1989. Antibiotic therapy for *Pseudomonas aeruginosa* bacteremia: outcome correlations in a prospective study of 200 patients. Am J Med 87:540–546.

119.   Wright GD. 2016. Antibiotic adjuvants: rescuing antibiotics from resistance. Trends Microbiol 24:862–871.

120.   White AR, Kaye C, Poupard J, Pypstra R, Woodnutt G, Wynne B. 2004. Augmentin (amoxicillin/clavulanate) in the treatment of community-acquired respiratory tract infection: a review of the continuing development of an innovative antimicrobial agent. J Antimicrob Chemother 53:i3–i20.

121.   Drawz SM, Bonomo RA. 2010. Three decades of beta-lactamase inhibitors. Clin Microbiol Rev 23:160–201.

122.   Gniadkowski M. 2001. Evolution and epidemiology of extended-spectrum beta-lactamases (ESBLs) and ESBL-producing microorganisms. Clin Microbiol Infect 7:597–608.

123.   Paterson DL, Bonomo RA. 2005. Extended-spectrum beta-lactamases: a clinical update. Clin Microbiol Rev 18:657–686.

124.   Ball P. 2007. Conclusions: the future of antimicrobial therapy - Augmentin and beyond. Int J Antimicrob Agents 30 Suppl 2:S139-41.

125.   Geddes AM, Klugman KP, Rolinson GN. 2007. Introduction: historical perspective and development of amoxicillin/clavulanate. Int J Antimicrob Agents 30 Suppl 2:S109-12.

126.   Taneja N, Kaur H. 2016. Insights into newer antimicrobial agents against Gram-negative bacteria. Microbiol insights 9:9–19.

127.   Butler MS, Blaskovich MA, Cooper MA. 2017. Antibiotics in the clinical pipeline at the end of 2015. J Antibiot (Tokyo) 70:3–24.

128.   Gill EE, Franco OL, Hancock REW. 2015. Antibiotic adjuvants: diverse strategies for controlling drug-resistant pathogens. Chem Biol Drug Des 85:56–78.

129.   Pieren M, Tigges M. 2012. Adjuvant strategies for potentiation of antibiotics to overcome antimicrobial resistance. Curr Opin Pharmacol 12:551–555.

130.   Kalan L, Wright GD. 2011. Antibiotic adjuvants: multicomponent anti-infective strategies. Expert Rev Mol Med 13:e5.

131.   Jacobs RF. 1986. Imipenem-cilastatin: the first thienamycin antibiotic. Pediatr Infect Dis 5:444–448.

132.   Hikida M, Kawashima K, Yoshida M, Mitsuhashi S. 1992. Inactivation of new carbapenem antibiotics by dehydropeptidase-I from porcine and human renal cortex. J Antimicrob Chemother 30:129–134.

133.   Hori Y, Aoki N, Kuwahara S, Hosojima M, Kaseda R, Goto S, Iida T, De S, Kabasawa H, Kaneko R, Aoki H, Tanabe Y, Kagamu H, Narita I, Kikuchi T, Saito A. 2017. Megalin blockade with cilastatin suppresses drug-induced nephrotoxicity. J Am Soc Nephrol 28:1783–1791.

134.   Falagas ME, Mavroudis AD, Vardakas KZ. 2016. The antibiotic pipeline for multi-drug resistant gram negative bacteria: what can we expect? Expert Rev Anti Infect Ther 14:747–763.

135.   Blizzard TA, Chen H, Kim S, Wu J, Bodner R, Gude C, Imbriglio J, Young K, Park Y-W, Ogawa A, Raghoobar S, Hairston N, Painter RE, Wisniewski D, Scapin G, Fitzgerald P,

Sharma N, Lu J, Ha S, Hermes J, Hammond ML. 2014. Discovery of MK-7655, a beta-lactamase inhibitor for combination with Primaxin(R). Bioorg Med Chem Lett 24:780–785.

136.   Lucasti C, Vasile L, Sandesc D, Venskutonis D, McLeroth P, Lala M, Rizk ML, Brown ML, Losada MC, Pedley A, Kartsonis NA, Paschke A. 2016. Phase 2, dose-ranging study of relebactam with imipenem-cilastatin in subjects with complicated intra-abdominal infection. Antimicrob Agents Chemother 60:6234–6243.

137.   King AM, Reid-Yu SA, Wang W, King DT, De Pascale G, Strynadka NC, Walsh TR, Coombes BK, Wright GD. 2014. Aspergillomarasmine A overcomes metallo-beta-lactamase antibiotic resistance. Nature 510:503–506.

138.   Haenni AL, Robert M, Vetter W, Roux L, Barbier M, Lederer E. 1965. Chemical structure of Aspergellomarasmines A and B. Helv Chim Acta 48:729–750.

139.   Arai K, Ashikawa N, Nakakita Y, Matsuura A, Ashizawa N, Munekata M. 1993. Aspergillomarasmine A and B, potent microbial inhibitors of endothelin-converting enzyme. Biosci Biotechnol Biochem 57:1944–1945.

140.   Matsuura A, Okumura H, Asakura R, Ashizawa N, Takahashi M, Kobayashi F, Ashikawa N, Arai K. 1993. Pharmacological profiles of aspergillomarasmines as endothelin converting enzyme inhibitors. Jpn J Pharmacol 63:187–193.

141.   Karsisiotis AI, Damblon CF, Roberts GCK. 2014. A variety of roles for versatile zinc in metallo-beta-lactamases. Metallomics 6:1181–1197.

142.   Meini M-R, Llarrull LI, Vila AJ. 2015. Overcoming differences: The catalytic mechanism of metallo-beta-lactamases. FEBS Lett 589:3419–3432.

143.   Koteva K, King AM, Capretta A, Wright GD. 2016. Total synthesis and activity of the metallo-beta-lactamase inhibitor Aspergillomarasmine A. Angew Chem Int Ed Engl 55:2210–2212.

144.   Albu SA, Koteva K, King AM, Al-Karmi S, Wright GD, Capretta A. 2016. Total synthesis of Aspergillomarasmine A and related compounds: a sulfamidate approach enables exploration of structure-activity relationships. Angew Chem Int Ed Engl 55:13259–13262.

145.   Liao D, Yang S, Wang J, Zhang J, Hong B, Wu F, Lei X. 2016. Total synthesis and structural reassignment of aspergillomarasmine a. Angew Chem Int Ed Engl 55:4291–4295.

146.   Zabawa TP, Pucci MJ, Parr TRJ, Lister T. 2016. Treatment of Gram-negative bacterial infections by potentiation of antibiotics. Curr Opin Microbiol 33:7–12.

147.   Pogliano J, Sharp M, Lister T, Rubio A. 2016. Bacterial cytological profiling of SPR741 mechanism of action is consistent with membrane permeabilization that allows penetration of antibiotics into Gram-negative (G-) bacteria, p. abstr P493. *In* American Society for Microbiology Microbe 2016.

148.   Corbett D, Wise A, Langley T, Skinner K, Trimby E, Birchall S, Dorali A, Sandiford S, Williams J, Warn P, Vaara M, Lister T. 2017. Potentiation of antibiotic activity by a novel cationic peptide: potency and spectrum of activity of SPR741. Antimicrob Agents Chemother 61.

149.   Corbett D, Wise A, Birchall S, Trimby E, Smith J, Lister T, Vaara M. 2016. Potentiation of antibiotic activity by a novel cationic peptide, SPR741, p. abstr P492. *In* American Society for Microbiology Microbe 2016.

150.   Vaara M, Siikanen O, Apajalahti J, Fox J, Frimodt-Moller N, He H, Poudyal A, Li J,

Nation RL, Vaara T. 2010. A novel polymyxin derivative that lacks the fatty acid tail and carries only three positive charges has strong synergism with agents excluded by the intact outer membrane. Antimicrob Agents Chemother 54:3341–3346.

151.   Warn P, Teague J, Burgess E, Payne L, Corbett D, Sharp A, Lister T, Parr Jr TR. 2016. In vivo efficacy of combinations of novel antimicrobial peptide SPR741 and rifampicin in short-duration murine lung infection models of K. pneumoniae or E. cloacae infection, p. abstr P497. *In* American Society for Microbiology Microbe 2016.

152.   Warn P, Thommes P, Vaddi S, Corbett D, Coles D, Vaccaro L, Lister T, Parr Jr TR. 2016. In vivo efficacy of combinations of novel antimicrobial peptide SPR741 and rifampicin in short-duration murine thigh infection models of Gram-negative bacterial infection, p. abstr P561. *In* American Society for Microbiology Microbe 2016.

153.   Zavascki AP, Nation RL. 2017. Nephrotoxicity of polymyxins: Is there any difference between colistimethate and polymyxin b? Antimicrob Agents Chemother 61.

154.   Pogue JM, Ortwine JK, Kaye KS. 2016. Are there any ways around the exposure-limiting nephrotoxicity of the polymyxins? Int J Antimicrob Agents 48:622–626.

155.   Coleman S, Bleavins M, Lister T, Vaara M, Parr Jr TR. 2016. The assessment of SPR741 for nephrotoxicity in cynomolgus monekys and Sprague-Dawley rats, p. abstr P523. *In* American Society for Microbiology Microbe 2016.

156.   Huovinen P. 2001. Resistance to trimethoprim-sulfamethoxazole. Clin Infect Dis 32:1608–1614.

157.   Masters PA, O'Bryan TA, Zurlo J, Miller DQ, Joshi N. 2003. Trimethoprim-

sulfamethoxazole revisited. Arch Intern Med 163:402–410.

158.   McIsaac WJ, Prakash P, Ross S. 2008. The management of acute uncomplicated cystitis in adult women by family physicians in Canada. Can J Infect Dis Med Microbiol = J Can des Mal Infect la Microbiol medicale 19:287–293.

159.   Libecco JA, Powell KR. 2004. Trimethoprim/sulfamethoxazole: clinical update. Pediatr Rev 25:375–380.

160.   Livermore DM, Mushtaq S, Warner M, Woodford N. 2014. Comparative in vitro activity of sulfametrole/trimethoprim and sulfamethoxazole/trimethoprim and other agents against multiresistant Gram-negative bacteria. J Antimicrob Chemother 69:1050–1056.

161.   Falagas ME, Lourida P, Poulikakos P, Rafailidis PI, Tansarli GS. 2014. Antibiotic treatment of infections due to carbapenem-resistant Enterobacteriaceae: systematic evaluation of the available evidence. Antimicrob Agents Chemother 58:654–663.

162.   Kmeid JG, Youssef MM, Kanafani ZA, Kanj SS. 2013. Combination therapy for Gram-negative bacteria: what is the evidence? Expert Rev Anti Infect Ther 11:1355–1362.

163.   Marcus R, Paul M, Elphick H, Leibovici L. 2011. Clinical implications of beta-lactam-aminoglycoside synergism: systematic review of randomised trials. Int J Antimicrob Agents 37:491–503.

164.   Vardakas KZ, Tansarli GS, Bliziotis IA, Falagas ME. 2013. beta-Lactam plus aminoglycoside or fluoroquinolone combination versus beta-lactam monotherapy for *Pseudomonas aeruginosa* infections: a meta-analysis. Int J Antimicrob Agents 41:301–310.

165.   Chamot E, Boffi El Amari E, Rohner P, Van Delden C. 2003. Effectiveness of

combination antimicrobial therapy for *Pseudomonas aeruginosa* bacteremia. Antimicrob Agents Chemother 47:2756–2764.

166.   Falagas ME, Matthaiou DK, Bliziotis IA. 2006. The role of aminoglycosides in combination with a beta-lactam for the treatment of bacterial endocarditis: a meta-analysis of comparative trials. J Antimicrob Chemother 57:639–647.

167.   Poulikakos P, Tansarli GS, Falagas ME. 2014. Combination antibiotic treatment versus monotherapy for multidrug-resistant, extensively drug-resistant, and pandrug-resistant Acinetobacter infections: a systematic review. Eur J Clin Microbiol Infect Dis 33:1675–1685.

168.   Tamma PD, Cosgrove SE, Maragakis LL. 2012. Combination therapy for treatment of infections with Gram-negative bacteria. Clin Microbiol Rev 25:450–470.

169.   Hamilton-Miller JM. 1994. Dual-action antibiotic hybrids. J Antimicrob Chemother 33:197–200.

170.   Bremner JB, Ambrus JI, Samosorn S. 2007. Dual action-based approaches to antibacterial agents. Curr Med Chem 14:1459–1477.

171.   Karoli T, Mamidyala SK, Zuegg J, Fry SR, Tee EHL, Bradford TA, Madala PK, Huang JX, Ramu S, Butler MS, Cooper MA. 2012. Structure aided design of chimeric antibiotics. Bioorg Med Chem Lett 22:2428–2433.

172.   Basak A, Pal R. 2005. Synthesis of beta-lactam nucleoside chimera *via* Kinugasa reaction and evaluation of their antibacterial activity. Bioorg Med Chem Lett 15:2015–2018.

173.   Blais J, Lewis SR, Krause KM, Benton BM. 2012. Antistaphylococcal activity of TD-1792, a multivalent glycopeptide-cephalosporin antibiotic. Antimicrob Agents Chemother

56:1584–1587.

174.   Long DD, Aggen JB, Christensen BG, Judice JK, Hegde SS, Kaniga K, Krause KM, Linsell MS, Moran EJ, Pace JL. 2008. A multivalent approach to drug discovery for novel antibiotics. J Antibiot (Tokyo) 61:595–602.

175.   Liang C-H, Romero A, Rabuka D, Sgarbi PWM, Marby KA, Duffield J, Yao S, Cheng ML, Ichikawa Y, Sears P, Hu C, Hwang S-B, Shue Y-K, Sucheck SJ. 2005. Structure-activity relationships of bivalent aminoglycosides and evaluation of their microbiological activities. Bioorg Med Chem Lett 15:2123–2128.

176.   Kline T, Fromhold M, McKennon TE, Cai S, Treiberg J, Ihle N, Sherman D, Schwan W, Hickey MJ, Warrener P, Witte PR, Brody LL, Goltry L, Barker LM, Anderson SU, Tanaka SK, Shawar RM, Nguyen LY, Langhorne M, Bigelow A, Embuscado L, Naeemi E. 2000. Antimicrobial effects of novel siderophores linked to beta-lactam antibiotics. Bioorg Med Chem 8:73–93.

2.8. Concluding remarks

This chapter highlighted the difficulties in developing agents and strategies able to overcome the intrinsic and genetic antibiotic resistance mechanism, with much emphasis on the former, of Gram-negative bacteria. Combination therapy of antibiotics and adjuvants was emphasized as a possible way to overcome resistance, to which strategy will be employed in the upcoming chapters (4, 5, 6 and 7). The concept of antibiotic hybrids was also defined, to which will be the main concept in Chapter 7. The following chapter will outline this thesis objectives.

Chapter 3: Thesis objectives

In line with the necessity to address the problem of antimicrobial resistance, my thesis seeks to explore new investigational agents based on antimicrobial peptides to serve as lead structures for the development of future therapeutic agents. While the antibacterial activity of each developed agent in the upcoming chapters were evaluated, the main strategy for these projects followed combination therapy (as discussed in Chapter 2) wherein the developed investigational compound served as an adjuvant to enhance the efficacy of existing antibiotics against multidrug-resistant (MDR) Gram-negative bacteria (GNB).

The objective of Chapter 4 is the development of short proline-rich lipopeptides (SPRLPs), consisting of seven amino acids and varying lipids, as adjuvants to potentiate the antibacterial activity of minocycline and rifampicin against MDR *Pseudomonas aeruginosa*. Proline-rich antimicrobial peptides were extensively discussed in Chapter 1. In this project, the following were investigated:

- Preparation of a library of SPRLPs through peptide synthesis

- Antibacterial activity of SPRLPs against Gram-positive and Gram-negative bacteria

- Hemolytic activity of SPRLPs towards red blood cells

- Synergism of SPRLPs with a panel of existing antibiotics against MDR clinical isolates of *P. aeruginosa*

- Cytotoxicity of lead SPRLP adjuvant

- Initial attempt to optimize the lead SPRLP adjuvant structure *via* D-amino acid replacement

Chapter 5 explores the potential of dilipid ultrashort cationic lipopeptides (dUSCLs), consisting of only four amino acids and varying dilipids, to serve as adjuvant partners to chloramphenicol and other antibiotic classes against MDR GNB. These membrane-acting ultrashort cationic lipopeptides were extensively discussed in Chapter 1. In this project, the following were investigated:

- Preparation of a library of dUSCLs through peptide synthesis

- Antibacterial activity of dUSCLs against Gram-positive and Gram-negative bacteria

- Hemolytic activity of dUSCLs towards red blood cells

- Synergism of dUSCLs with a panel of existing antibiotics against MDR clinical isolates of *P. aeruginosa*, *Acinetobacter baumannii*, *Escherichia coli*, *Klebsiella pneumoniae* and *Enterobacter cloacae*

Chapter 6 focuses on the structure-activity relationship study of the effect of hydrophobicity *via* lipid composition in dilipid polymyxin B (PMB) analogs. Moreover, this chapter also focuses on the potential for these analogs as adjuvant partners for existing antibiotics against *P. aeruginosa*. The ten amino acid-comprising polymyxin antibiotic was discussed in Chapter 1. In this chapter, the following were investigated:

- Preparation of dilipid PMBs through peptide and organic synthesis

- Antibacterial activity of dilipid PMBs against Gram-positive and Gram-negative bacteria compared to clinically-used polymyxins

- Hemolytic activity of dilipid PMBs towards red blood cells compared to clinically-used polymyxins

- Synergism of dilipid PMBs in combination with a panel of existing antibiotics against *P. aeruginosa* compared to the well-known membrane permeabilizer polymyxin B nonapeptide

- Contribution of hydrophobicity *via* lipid component towards polymyxin's ability to resist active efflux in *P. aeruginosa*

The objective of Chapter 7 is to explore the biological effect (antibacterial and adjuvant property) of covalently linking the peptide-based antibiotic polymyxin to the carbohydrate-based antibiotic aminoglycoside, therefore generating antibiotic hybrids. Specifically, polymyxin B_3 (PMB_3) was appended to tobramycin. The concept of antibiotic hybrids was extensively discussed in Chapter 2. In this chapter, the following were investigated:

- Complex preparation of antibiotic hybrids consisting of PMB_3 and tobramycin

- Antibacterial activity of PMB_3-tobramycin hybrids against Gram-positive and Gram-negative bacteria compared to PMB_3 and tobramycin

- Hemolytic activity of PMB_3-tobramycin hybrids towards red blood cells

- Synergism of PMB_3-tobramycin hybrids with a panel of existing antibiotics against *P. aeruginosa* compared to PMB_3 and tobramycin

- Enhancement of antibacterial activity of minocycline, rifampicin and vancomycin in combination with PMB_3-tobramycin hybrids against *P. aeruginosa*, *A. baumannii* and *K. pneumoniae*.

The concluding Chapter 8 summarizes my efforts in the development of these investigational peptide-based agents. Following Chapter 8 comprises of Appendices I to IV that compose of complimentary data for Chapters 4 to 7, respectively. Appendix V contains copyright permissions for used articles in this thesis.

Chapter 4: Development of short proline-rich lipopeptides as adjuvants

This chapter is based on my publication:

4.1. Introductory remarks

As discussed in Chapter 2, combination therapy is a *via*ble strategy to overcome antimicrobial resistance especially against Gram-negative bacteria to which arguably are difficult to treat due to their intrinsic resistance mechanisms (double protective membrane + overexpressed multidrug efflux systems) that are coupled to multiple chromosomal resistance mechanisms. In this chapter, synthetic proline-rich antimicrobial peptides (as discussed in Chapter 1) were acylated to yield lipopeptides that possess the ability to enhance antibacterial activity of minocycline and rifampin (also called rifampicin) against clinical isolates of multidrug- and extensively drug-resistant *Pseudomonas aeruginosa*. A lead lipopeptide candidate was identified to be non-cytotoxic and non-hemolytic, that appeared to have a chemical structure amenable to peptidomimetic modification.

4.2. Contributions of authors

Ronald Domalaon and Yaroslav Sanchak prepared, purified and characterized all lipopeptides for this study. Ronald Domalaon evaluated the microbiological activity of all the lipopeptides alone and in combination with other antibiotics in this study. George G. Zhanel and Frank Schweizer guided the antimicrobial evaluation of the compounds. Yinfeng Lyu and Ronald Domalaon assessed the hemolytic properties of the lipopeptides. Linet Cherono Koskei and Gilbert Arthur assessed the cytotoxicity of the lead lipopeptide adjuvant for this study. Ronald Domalaon interpreted all the chemical and biological data with helpful insights from George G. Zhanel, Gilbert Arthur and Frank Schweizer. All authors were responsible for the final form of this research article.

4.3. Abstract

A series of 16 short proline-rich lipopeptides (SPRLPs) were constructed to mimic longer naturally-existing proline-rich antimicrobial peptides. Antibacterial assessment revealed that lipopeptides containing hexadecanoic acid (C_{16}) possess optimal antibacterial activity relative to others with shorter lipid component. SPRLPs were further evaluated for their potential to serve as adjuvants in combination with existing antibiotics to enhance antibacterial activity against drug-resistant *Pseudomonas aeruginosa*. Out of sixteen prepared SPRLPs, C_{12}-PRP was found to significantly potentiate the antibiotics minocycline and rifampicin against multidrug- and extensively drug-resistant (MDR/XDR) *P. aeruginosa* clinical isolates. This non-hemolytic C_{12}-PRP is comprised of a heptapeptide sequence PRPRPRP-NH$_2$ acylated to dodecanoic acid (C_{12}) at the N-terminus. The adjuvant potency of C_{12}-PRP was apparent by its ability to reduce the minimum inhibitory concentration of minocycline and rifampicin below their interpretative

susceptibility breakpoints against MDR/XDR *P. aeruginosa*. An attempt to optimize C_{12}-PRP through peptidomimetic modification was performed by replacing all L- to D-amino acids. C_{12}-PRP demonstrated pliability to optimization as synergism with minocycline and rifampicin were retained. Moreover, C_{12}-PRP displayed no cytotoxicity against human liver carcinoma HepG2 and human embryonic kidney HEK-293 cell lines. Thus, the SPRLP C_{12}-PRP is a lead adjuvant candidate that warrants further optimization. Discovery of agents that are able to resuscitate the activity of existing antibiotics against drug-resistant Gram-negative pathogens, especially *P. aeruginosa* are of great clinical interest.

4.4. Introduction

The increasing incidence of multidrug-resistant (MDR) and extensively drug-resistant (XDR) *Pseudomonas aeruginosa* infection impose significant burden in our current health care system (1, 2). Infections caused by *P. aeruginosa* are difficult to treat as this pathogen often harbors multiple resistance mechanisms against most currently-used antibiotics (3, 4). Intrinsic resistance in *P. aeruginosa* is a major hurdle to overcome. The protective outer membrane (OM) of *P. aeruginosa* is comprised of selective porins and a polar lipopolysaccharide (LPS) barrier that is 12-100 times less permeable than *Escherichia coli* (5). Compounds which are able to cross the OM and enter the periplasm are prone to efflux by up to twelve overexpressed multidrug efflux systems that prevent most antibiotics from reaching the required intracellular concentration for their antibacterial action (6, 7). As a result, there is currently a strong interest to identify novel agents that are able to enhance membrane permeability and compromise active efflux in Gram-negative bacillary pathogens such as *P. aeruginosa* (8).

Proline-rich antimicrobial peptides (PRAMPs) are amphiphilic cationic peptides typically possessing potent Gram-negative but poor Gram-positive antibacterial activity (9, 10). They are characterized by an unusually high amount of L-proline residues (typically 25-50% sequence composition) and frequently contain a repeating PXP or PXXP motif where X may be any amino acid but typically is L-arginine (9, 10). Well-known examples include mammalian-derived Bac7(1-35) (11) (sequence: RRIRPRPRLPRPRPRPLPFPRPGPRPIPRPLPFP) and PR-39 (12) (sequence: RRRPRPPYLPRPRPPPFFPPRLPPRIPPGFPPRFPPRFP-NH2), and insect-derived apidaecins (13). PRAMPs eradicate bacteria in a dose-dependent bimodular fashion. At low concentrations, they are believed to target the 70S ribosome and the DnaK chaperone (14, 15). Conversely, they eradicate pathogen *via* lysis at high concentrations (15). PRAMPs enter the OM *via* a poorly understood mechanism (presumably through a 'self-promoted' uptake mechanism similar to most cationic peptides) (16). Inner membrane transporters Sbma and MdtM proteins facilitate their promiscuous cytosolic uptake (17, 18). However, the Gram-negative *P. aeruginosa* does not express both Sbma and MdtM therefore PRAMPs mode of action is restricted to membrane rupture and lysis (19). With the urgent need for new therapeutic agents/strategies to treat drug-resistant Gram-negative bacterial infections, PRAMPs are considered as an emerging source of potential new antibiotics.

Aside antimicrobials that directly kill bacteria, adjuvants that sensitize resistant pathogens to existing antibiotics are widely studied (20, 21). In fact, several combinations of β-lactamase inhibitor (adjuvant) and β-lactam (antibiotic) are already used to treat drug-resistant Gram-negative bacillary infections (22, 23). Adjuvants act on bacterial processes that may elicit direct or indirect advantageous effects towards its partner antibiotic. For instance, adjuvants that inhibit β-

lactamase enzymes prevent the degradation of β-lactam antibiotics. Adjuvants that disrupt the bacterial membrane may enhance cellular permeation of otherwise membrane-impermeable antibiotics.

In this study, we evaluate the antibacterial activity of synthetic short proline-rich lipopeptides (SPRLPs) against clinically-relevant Gram-positive and Gram-negative pathogens. The short peptide sequence of SPRLPs were inspired by the repeating PXP motif apparent in longer PRAMPs. Moreover, we assess the potential of these SPRLPs to serve as adjuvants in combination with clinically-used antibiotics against *P. aeruginosa*. Our results revealed an amphiphilic non-hemolytic non-cytotoxic L-lipopeptide lead sequence that strongly potentiates minocycline and rifampicin against MDR/XDR *P. aeruginosa*. Furthermore, the adjuvant potency is retained in its enantiomeric D-SPRLP counterpart.

4.5. Results and discussion

SPRLP design inspired by repeating PXP motif in PRAMPs. Inspired by peptide sequences of longer and naturally occurring PRAMPs such as Bac7(1-35) and PR-39, we prepared shorter synthetic versions possessing a lipoheptapeptide sequence of PRPZPRP; where Z denotes to either R, G, L or W (Table 4-1). The observed PXP repeats in naturally-occurring PRAMPs were retained in the heptapeptide sequence. Position Z was incorporated to introduce amino acid variability, resulting in four sequence subsets namely PRP, PGP, PLP and PWP sequences (Table 4-1). Amino acid variability was integrated in the design to 'fine-tune' the overall physicochemical property of SPRLP at the heptapeptide portion. For instance, incorporation of L-arginine imparts an additional protonatable guanidine side-chain whereas L-leucine imparts

additional hydrophobicity. L-tryptophan was added for its aromatic ring side-chain while L-

glycine was selected to see the effect of replacing the carbon-based side-chain groups with

hydrogen. Aliphatic lipids such as octanoic acid (C_8), dodecanoic acid (C_{12}) and hexadecanoic

acid (C_{16}) were ligated to the N-terminus of the cationic heptapeptide to vary the hydrophobic or

amphiphilic moment in the SPRLPs (24–26). We also included the more rigid and

conformationally-constrained lipid 1-adamantaneacetic acid (Ad) in our study. The bulky

hydrophobic adamantane moiety is perceived to be less prone to toxicity issues relative to longer

aliphatic hydrocarbons. The C-terminus of each peptide was also amidated. Sixteen acylated

SPRLPs were synthesized to explore the effect of peptide sequence and amphiphilicity to their

biological activity.

Table 4-1 SPRLPs sequences under consideration

Compound	Sequence	Molecular weight, g/mol (TFA salt)
C_8-PRP	$CH_3(CH_2)_6CO$-PRPRPRP-NH_2	1342.33
C_{12}-PRP	$CH_3(CH_2)_{10}CO$-PRPRPRP-NH_2	1398.44
C_{16}-PRP	$CH_3(CH_2)_{14}CO$-PRPRPRP-NH_2	1454.55
Ad-PRP	Adamantyl-CH_2CO-PRPRPRP-NH_2	1392.39
C_8-PGP	$CH_3(CH_2)_6CO$-PRPGPRP-NH_2	1129.17
C_{12}-PGP	$CH_3(CH_2)_{10}CO$-PRPGPRP-NH_2	1185.28
C_{16}-PGP	$CH_3(CH_2)_{14}CO$-PRPGPRP-NH_2	1241.39
Ad-PGP	Adamantyl-CH_2CO-PRPGPRP-NH_2	1179.23
C_8-PLP	$CH_3(CH_2)_6CO$-PRPLPRP-NH_2	1185.28
C_{12}-PLP	$CH_3(CH_2)_{10}CO$-PRPLPRP-NH_2	1241.39
C_{16}-PLP	$CH_3(CH_2)_{14}CO$-PRPLPRP-NH_2	1297.50
Ad-PLP	Adamantyl-CH_2CO-PRPLPRP-NH_2	1235.34
C_8-PWP	$CH_3(CH_2)_6CO$-PRPWPRP-NH_2	1258.34
C_{12}-PWP	$CH_3(CH_2)_{10}CO$-PRPWPRP-NH_2	1314.44
C_{16}-PWP	$CH_3(CH_2)_{14}CO$-PRPWPRP-NH_2	1370.55
Ad-PWP	Adamantyl-CH_2CO-PRPWPRP-NH_2	1308.40
C_{12}-prp	$CH_3(CH_2)_{10}CO$-prprprp-NH_2 (all D-peptide)	1398.44

SPRLPs composed of longer hydrocarbons demonstrate antibacterial activity. The synthesized SPRLPs were evaluated for their antibacterial potency against a panel of Gram-positive and Gram-negative bacteria (Tables 4-2 & 4-3). Some of the included pathogens were collected from patients visiting or admitted to participating Canadian hospitals through the CAN-ICU (27) and CANWARD (28) national surveillance studies. Antibacterial activity was assessed using minimum inhibitory concentration (MIC) against various clinical pathogens.

Table 4-2 Biological activity of SPRLPs belonging to PRP and PGP sequence subsets

| Organism | MIC, µg/mL | | | | | | | |
	C_8-PRP	C_{12}-PRP	C_{16}-PRP	Ad-PRP	C_8-PGP	C_{12}-PGP	C_{16}-PGP	Ad-PGP
S. aureus[a]	>128	128	8	>128	>128	>128	32	>128
MRSA[b]	>128	>128	16	>128	>128	>128	32	>128
MSSE[c]	>128	32	4	>128	>128	128	8	>128
MRSE[d]	>128	128	8	>128	>128	>128	16	>128
E. faecalis[e]	>128	>128	16	>128	>128	>128	16	>128
E. faecium[f]	>128	128	8	>128	>128	>128	16	>128
E. coli[g]	>128	>128	16	>128	>128	>128	32	>128
E. coli[h]	>128	>128	8	>128	>128	>128	32	>128
E. coli[i]	>128	>128	8	>128	>128	>128	32	>128
E. coli[j]	>128	>128	8	>128	>128	>128	32	>128
P. aeruginosa[k]	>128	>128	32	>128	>128	>128	128	>128
P. aeruginosa[l]	>128	>128	32	>128	>128	>128	128	>128
P. aeruginosa[m]	>128	>128	64	>128	>128	>128	128	>128
P. aeruginosa[n]	>512	128	32	>512	>512	>512	64	>512
S. maltophilia[o]	>128	>128	64	>128	>128	>128	128	>128
A. baumannii[p]	>128	>128	16	>128	>128	>128	32	>128
K. pneumoniae[q]	>128	>128	64	>128	>128	>128	64	>128
MHC[r]	>512	>512	16	>512	>512	>512	16	>512

[a] = ATCC 29213. [b] = methicillin-resistant *S. aureus* ATCC 33592. [c] = methicillin-susceptible *Staphylococcus epidermidis* CANWARD-2008 81388. [d] = methicillin-resistant *S. epidermidis* CAN-ICU 61589 (ceftazidime-resistant). [e] = ATCC 29212. [f] = ATCC 27270. [g] = ATCC 25922. [h] = CAN-ICU 61714 (gentamicin-resistant). [i] = CAN-ICU 63074 (amikacin-intermediate resistant). [j] = CANWARD-2011 97615 (gentamicin-, tobramycin-, ciprofloxacin-resistant) aac(3')*iia*. [k] = ATCC 27853. [l] = CAN-ICU 62308 (gentamicin-resistant). [m] = CANWARD-2011 96846 (gentamicin-, tobramycin-resistant). [n] = wild-type PAO1 [o] = CAN-ICU 62584. [p] = CAN-ICU 63169. [q] = ATCC 13883. [r] = minimum concentration in µg/mL that resulted in 5% red blood cell hemolysis.

The Gram-negative-specific antibacterial activity of naturally-existing PRAMPs was not observed for the synthesized SPRLPs. Among the four sequence subsets, peptides acylated with C_{16} displayed better antibacterial activity relative to C_8, C_{12} or Ad. Three out of the four C_{16}-comprising peptides showed promising activity. C_{16}-PRP displayed broad-spectrum activity (Table 4-2) with an MIC range of 4-16 µg/mL against Gram-positive bacteria and an MIC range of 8-16 µg/mL against the Gram-negative bacteria *E. coli*. Moderate activity against Gram-positive bacteria (MIC range of 8-32 µg/mL) was demonstrated by C_{16}-PGP (Table 4-2). The lipopeptide C_{16}-PWP also exhibited good activity (MIC range of 4-8 µg/mL) against Gram-positive bacteria (Table 4-3). Overall, these SPRLPs reported herein appeared to be mostly active against Gram-positive organisms.

Table 4-3 Biological activity of SPRLPs belonging to PLP and PWP sequence subsets

Organism	MIC, µg/mL							
	C_8-PLP	C_{12}-PLP	C_{16}-PLP	Ad-PLP	C_8-PWP	C_{12}-PWP	C_{16}-PWP	Ad-PWP
S. aureus[a]	>128	128	64	>128	>128	32	8	>128
MRSA[b]	>128	128	64	>128	>128	32	8	>128
MSSE[c]	>128	64	32	>128	>128	16	4	>128
MRSE[d]	>128	64	64	>128	>128	16	8	>128
E. faecalis[e]	>128	128	64	>128	>128	32	8	>128
E. faecium[f]	>128	128	64	>128	>128	32	8	>128
E. coli[g]	>128	>128	128	>128	>128	128	32	>128
E. coli[h]	>128	>128	64	>128	>128	128	32	>128
E. coli[i]	>128	>128	64	>128	>128	128	16	>128
E. coli[j]	>128	>128	128	>128	>128	128	64	>128
P. aeruginosa[k]	>128	>128	>128	>128	>128	>128	64	>128
P. aeruginosa[l]	>128	>128	>128	>128	>128	>128	64	>128
P. aeruginosa[m]	>128	>128	>128	>128	>128	>128	64	>128
P. aeruginosa[n]	>512	512	32	>512	>512	64	32	>512
S. maltophilia[o]	>128	>128	>128	>128	>128	>128	64	>128
A. baumannii[p]	>128	>128	128	>128	>128	128	64	>128
K. pneumoniae[q]	>128	>128	128	>128	>128	>128	64	>128
MHC[r]	>512	>512	16	>512	>512	64	16	>512

[a] = ATCC 29213. [b] = methicillin-resistant *S. aureus* ATCC 33592. [c] = methicillin-susceptible *Staphylococcus epidermidis* CANWARD-2008 81388. [d] = methicillin-resistant *S. epidermidis* CAN-ICU 61589 (ceftazidime-resistant). [e] = ATCC 29212. [f] = ATCC 27270. [g] = ATCC 25922. [h] = CAN-ICU 61714 (gentamicin-resistant). [i] = CAN-ICU 63074 (amikacin-intermediate resistant). [j] = CANWARD-2011 97615 (gentamicin-, tobramycin-, ciprofloxacin-resistant) aac(3')*iia*. [k] = ATCC 27853. [l] = CAN-ICU 62308 (gentamicin-resistant). [m] = CANWARD-2011 96846 (gentamicin-, tobramycin-resistant). [n] = wild-type PAO1 [o] = CAN-ICU 62584. [p] = CAN-ICU 63169. [q] = ATCC 13883. [r] = minimum concentration in µg/mL that resulted in 5% red blood cell hemolysis.

Non-specific membrane lysis limits therapeutic potential. Since PRAMPs are able to kill bacteria through membrane lysis, it is imperative to evaluate whether these synthesized SPRLPs also lyse eukaryotic membranes. The ability to lyse porcine red blood cells was assessed and the minimum concentration to result in 5% erythrocyte hemolysis (MHC) was reported (Tables 4-2 & 4-3). SPRLPs acylated with the long hydrocarbon C_{16} showed high hemolytic activity. C_{16}-PRP, C_{16}-PGP, C_{16}-PLP and C_{16}-PWP resulted in 5% red blood cell hemolysis at 16 µg/mL. These data corroborate that the observed antibacterial activity of these four SPRLPs is through non-specific

membrane lysis; and therefore greatly limits their therapeutic potential. The lipopeptide C_{12}-PWP demonstrated marginal hemolytic activity with a MHC of 64 µg/mL. However, all other SPRLPs were non-hemolytic (MHC >512 µg/mL).

Potentiation of minocycline and rifampicin by an SPRLP against MDR/XDR *P. aeruginosa*.

Adjuvants typically do not kill the pathogens directly but are able to help their antibiotic partner broaden their antibacterial spectrum or maximize antibacterial activity. A literature search revealed only one report of a PRAMP that can synergize a clinically-used antibiotic against Gram-negative bacilli. The long proline-rich peptide dimer A3-APO, consisting of 41 amino acids, was found to potentiate chloramphenicol against *Klebsiella pneumoniae* using a checkerboard assay (29). However, an amphiphilic lysine-based peptide-like agent was reported to potentiate rifampicin in *E. coli* (30). We therefore were interested to study whether our short proline-rich heptapeptide-based SPRLPs possessed adjuvant properties. Certainly, it is advantageous to have a lead molecule of shorter peptide sequence as it is more cost-effective and more pliable to peptidomimetic modifications for further optimization.

We evaluated the activity of SPRLPs in combination with fifteen clinically-used antibiotics (see Appendix Table I-1 to I-3 in Appendix I) against *P. aeruginosa*. Antibiotics tested included fluoroquinolones (moxifloxacin, ciprofloxacin and levofloxacin), aminoglycosides (gentamicin, tobramycin and amikacin), cephalosporins (ceftazidime and cefotaxime), carbapenems (meropenem and doripenem), aztreonam, rifampicin, minocycline, colistin and fosfomycin. The SPRLPs were screened initially at a fixed concentration of 8 µg/mL (5 µM) in combination with antibiotics against wild-type *P. aeruginosa* PAO1. We assessed potentiation by at least a four-

fold absolute MIC reduction of the antibiotic, after which synergism was further validated by a conventional checkerboard assay. A fractional inhibitory concentration (FIC) index of ≤0.5, 0.5<x≤4 or >4 was interpreted as synergistic, indifferent or antagonistic interaction, respectively (31). FIC index was obtained by adding the FIC values of the antibiotic and the SPRLP adjuvant. FIC of antibiotics was calculated by dividing the MIC of the antibiotic in the presence of the adjuvant by the MIC of the antibiotic alone. Similarly, the FIC of the adjuvant was calculated *via* dividing the MIC of the adjuvant in the presence of the antibiotic by the MIC of the adjuvant alone.

Out of the fifteen clinically-used antibiotics and sixteen short synthetic SPRLPs, initial screening revealed potentiation of minocycline and rifampicin with the amphiphilic lipopeptide C_{12}-PRP (see Appendix Table I-1 in Appendix I). Further validation by checkerboard assay confirmed the synergistic combinations against wild-type *P. aeruginosa* PAO1 strain. C_{12}-PRP with either minocycline or rifampicin yielded an FIC index of 0.19 or 0.14, respectively. These findings warranted further studies as C_{12}-PRP is non-hemolytic even up to a high concentration of 512 µg/mL (Table 4-2). Note that rifampicin and minocycline are not typically used to treat infections caused by *P. aeruginosa*. We then evaluated whether the observed synergism was retained against MDR/XDR *P. aeruginosa* clinical isolates. But also, the capability of C_{12}-PRP to reduce the absolute MIC of minocycline and rifampicin below their interpretative susceptibility breakpoint was investigated. No established minocycline and rifampicin susceptibility breakpoints currently exist for *P. aeruginosa* from neither CLSI nor the European Committee on Antimicrobial Susceptibility Testing (EUCAST). Therefore we cautiously used established breakpoints for other organisms as similar as possible to *P. aeruginosa* for our

comparison. According to CLSI (32), the susceptibility breakpoint of minocycline for *Acinetobacter spp*. is ≤4 µg/mL while the susceptibility breakpoint of rifampicin for *Staphylococcus spp*. is ≤1 µg/mL.

The combination of minocycline and C_{12}-PRP was found to be strongly synergistic against all eight tested MDR/XDR *P. aeruginosa* isolates (Table 4-4). Moreover, the MIC of minocycline in the presence of 8 µg/mL (5 µM) C_{12}-PRP was reduced below susceptibility breakpoint in seven out of nine strains. Significant potentiation was also observed for the combination of rifampicin and C_{12}-PRP against MDR/XDR *P. aeruginosa* isolates (Table 4-5). At 8 µg/mL (5 µM) C_{12}-PRP, the MIC of rifampicin reached susceptibility breakpoint in five out of nine strains. Indeed, the SPRLP C_{12}-PRP was able to enhance the antibacterial potency of minocycline and rifampicin against wild-type and clinical isolates of *P. aeruginosa*. The potential of this SPRLP as a lead adjuvant candidate is apparent. The mechanism of antibiotic potentiation certainly warrants further study in the future. However, membrane perturbation that results in an enhanced antibiotic uptake is a likely possibility. PRAMPs are known to disrupt bacterial membranes, and is more pronounced in *P. aeruginosa* relative to other Gram-negative bacilli (19). Suggestively, the SPRLP C_{12}-PRP may potentiate minocycline and rifampicin through OM permeabilization of *P. aeruginosa*. Membrane perturbation may also compromise the activity of integral membrane proteins such as multidrug efflux pumps, essentially halting antibiotic resistance through active efflux.

Table 4-4 Adjuvant potency of amphiphilic C_{12}-PRP in combination with minocycline (MIN) against wild-type and MDR/XDR *P. aeruginosa*.

P. aeruginosa strain	MIC_{MIN}, µg/mL	$MIC_{C12-PRP}$, µg/mL	FIC index	Absolute MIC_{MIN},[a] µg/mL	Potentiation[b]
PAO1	8	128	0.19	1	8-fold
259-96918	16	>128	0.12<x<0.19	2	8-fold
260-97103	16	128	0.12	1	16-fold
262-101856	64	>128	0.12<x<0.25	16	4-fold
264-104354	32	>128	0.06<x<0.12	2	16-fold
91433[c]	32	>128	0.12<x<0.25	8	4-fold
100036	16	>128	0.12<x<0.25	4	4-fold
101243[c]	2	128	0.31	0.5	4-fold
101885	16	64	0.37	4	4-fold

[a] = MIC of minocycline in the presence of 8 µg/mL (5 µM) C_{12}-PRP. [b] = degree of antibiotic potentiation in the presence of 8 µg/mL (5 µM) C_{12}-PRP. [c] = colistin-resistant. MDR = multidrug-resistant. XDR = extensively drug-resistant.

The type of fatty acyl ligated to the peptide sequence PRPRPRP-NH2 is important for adjuvant activity. Since the lead adjuvant C_{12}-PRP was discovered from a synergy scan having a fixed 8 µg/mL (5 µM) SPRLP concentration, combinations of minocycline or rifampicin with other PRP subset lipopeptides warranted further investigation. Therefore, we assessed the interaction of either C_8-PRP, C_{16}-PRP or Ad-PRP with minocycline or rifampicin by checkerboard assay. The three synthetic SPRLPs displayed indifferent interaction with minocycline and rifampicin (see Appendix Table I-4 in Appendix I). Interestingly, C_{16}-PRP did not display synergism with both antibiotics even though our initial data suggested that it can disrupt and lyse membranes. These data suggest that the aliphatic lipid C_{12} is optimal for amphiphilic SPRLPs to potentiate minocycline and rifampicin against *P. aeruginosa*.

The D-lipopeptide counterpart of C12-PRP retains adjuvant potency. The amphiphilic C_{12}-PRP is considered susceptible to non-specific proteolytic degradation as host enzymes (e.g. human proteases) easily recognize L-amino acid peptide bonds. Therefore, lead peptide agents typically

undergo peptidomimetic modifications to increase serum stability (10, 33). We explored one

approach to optimize C_{12}-PRP by synthesizing the same sequence but with D- instead of L-amino

acids, yielding the D-lipopeptide analog C_{12}-prp. Peptide bonds formed by D-amino acids are

less prone to mammalian proteases (34). Similar to C_{12}-PRP, C_{12}-prp was found to be inactive

(MIC >128 µg/mL) against wild-type and clinical isolates of *P. aeruginosa*. The adjuvant

properties of C_{12}-PRP were retained but the potency was slightly reduced in the D-lipopeptide

analog. C_{12}-prp potentiated minocycline and rifampicin against wild-type and MDR/XDR *P.*

aeruginosa (Tables 4-6 & 4-7). Furthermore, 8 µg/mL (5 µM) of C_{12}-prp reduced the MIC of

minocycline (Table 4-6) and rifampicin (Table 4-7) below susceptibility breakpoints in some

MDR/XDR *P. aeruginosa* clinical isolates. These results suggest that C_{12}-PRP is pliable to

peptidomimetic alterations and that further lead optimizations are possible.

Table 4-5 Adjuvant potency of amphiphilic C_{12}-PRP in combination with rifampicin (RMP) against wild-type and MDR/XDR *P. aeruginosa*.

P. aeruginosa strain	MIC$_{RMP}$, µg/mL	MIC$_{C12-PRP}$, µg/mL	FIC index	Absolute MIC$_{RMP}$,[a] µg/mL	Potentiation[b]
PAO1	8	128	0.14	1	8-fold
259-96918	16	>128	0.01<x<0.14	2	8-fold
260-97103	16	128	0.16	2	8-fold
262-101856	512	>128	0.25<x<0.37	512	none
264-104354	8	>128	0.06<x<0.12	0.5	16-fold
91433[c]	16	>128	0.06<x<0.09	1	16-fold
100036	16	>128	0.01<x<0.14	1	16-fold
101243[c]	4	128	0.09	0.125	32-fold
101885	16	64	0.25	2	8-fold

[a] = MIC of rifampicin in the presence of 8 µg/mL (5 µM) C_{12}-PRP. [b] = degree of antibiotic potentiation in the presence of 8 µg/mL (5 µM) C_{12}-PRP. [c] = colistin-resistant. MDR = multidrug-resistant. XDR = extensively drug-resistant.

Table 4-6 Adjuvant potency of amphiphilic C_{12}-prp in combination with minocycline (MIN) against wild-type and MDR/XDR *P. aeruginosa*.

P. aeruginosa strain	MIC_{MIN}, µg/mL	$MIC_{C12\text{-}prp}$, µg/mL	FIC index	Absolute MIC_{MIN},[a] µg/mL	Potentiation[b]
PAO1	8	>128	0.25<x<0.31	2	4-fold
259-96918	16	>128	0.12<x<0.25	4	4-fold
260-97103	16	>128	0.12<x<0.19	2	8-fold
262-101856	64	>128	0.12<x<0.25	16	4-fold
264-104354	32	>128	0.12<x<0.19	4	8-fold
91433[c]	32	>128	0.12<x<0.19	4	8-fold
100036	16	>128	0.25<x<0.37	8	2-fold
101243[c]	4	>128	0.12<x<0.37	2	2-fold
101885	16	>128	0.25<x<0.37	8	2-fold

[a] = MIC of minocycline in the presence of 8 µg/mL (5 µM) C_{12}-prp. [b] = degree of antibiotic potentiation in the presence of 8 µg/mL (5 µM) of all D-lipopeptide C_{12}-prp. [c] = colistin-resistant. MDR = multidrug-resistant. XDR = extensively drug-resistant.

Amphiphilic C12-PRP is not cytotoxic to eukaryotic cells. Our initial assessment on the effect of

SPRLPs to eukaryotic membranes revealed that C_{12}-PRP is non-hemolytic. In fact, the

concentration that results in 5% red blood cell hemolysis for C_{12}-PRP was >512 µg/mL. At 512

µg/mL (366 µM), C_{12}-PRP only resulted in $4.6 \pm 0.2\%$ hemolysis (Fig. 4-1A). We then evaluated

the potential toxicity of C_{12}-PRP against two eukaryotic cell lines, which include human liver

carcinoma HepG2 and human embryonic kidney HEK-293, by its ability to inhibit cellular

proliferation and cellular viability (see Appendix Table I-5 in Appendix I). We used colistin

(also known as polymyxin E) and adriamycin® as internal controls to represent clinically-used

peptide antibiotics and anticancer drugs, respectively. Amphiphilic C_{12}-PRP did not inhibit

cellular proliferation of both cell lines (Fig. 4-1B and 4-1C) up to the highest concentration

tested (50 µM), notably 10-fold higher than the C_{12}-PRP's adjuvant working concentration (5

µM). Interestingly, 1.5 µM of the antibiotic colistin inhibited proliferation of HepG2 cells to

50% (IC_{50}). The anticancer drug adriamycin® inhibited growth of both cell lines at very low

concentrations. We further evaluated cytotoxicity by assessing the effect of the agents on the

global oxidoreductive metabolism of cells through MTS assay (Fig. 4-1D and 4-1E). Both C_{12}-

PRP and colistin did not kill both cell lines up to the highest concentration tested (50 µM).

Congruent with results from the proliferation assay, adriamycin® drastically reduced viability of

both cell lines at low concentration. Our data presented herein strongly suggest that the

amphiphilic C_{12}-PRP is not cytotoxic to eukaryotic cells.

Table 4-7 Adjuvant potency of amphiphilic C_{12}-prp in combination with rifampicin (RMP) against wild-type and MDR/XDR *P. aeruginosa*.

P. aeruginosa strain	MIC_{RMP}, µg/mL	$MIC_{C12-prp}$, µg/mL	FIC index	Absolute MIC_{RMP},[a] µg/mL	Potentiation[b]
PAO1	8	>128	0.12<x<0.19	1	8-fold
259-96918	16	>128	0.03<x<0.16	2	8-fold
260-97103	16	>128	0.06<x<0.19	4	4-fold
262-101856	512	>128	0.12<x<0.25	256	2-fold
264-104354	8	>128	0.12<x<0.25	2	4-fold
91433[c]	16	>128	0.12<x<0.14	2	8-fold
100036	16	>128	0.06<x<0.19	4	4-fold
101243[c]	4	>128	0.06<x<0.19	0.5	8-fold
101885	16	>128	0.12<x<0.25	4	4-fold

[a] = MIC of rifampicin in the presence of 8 µg/mL (5 µM) C_{12}-prp. [b] = degree of antibiotic potentiation in the presence of 8 µg/mL (5 µM) of all D-lipopeptide C_{12}-prp. [c] = colistin-resistant. MDR = multidrug-resistant. XDR = extensively drug-resistant.
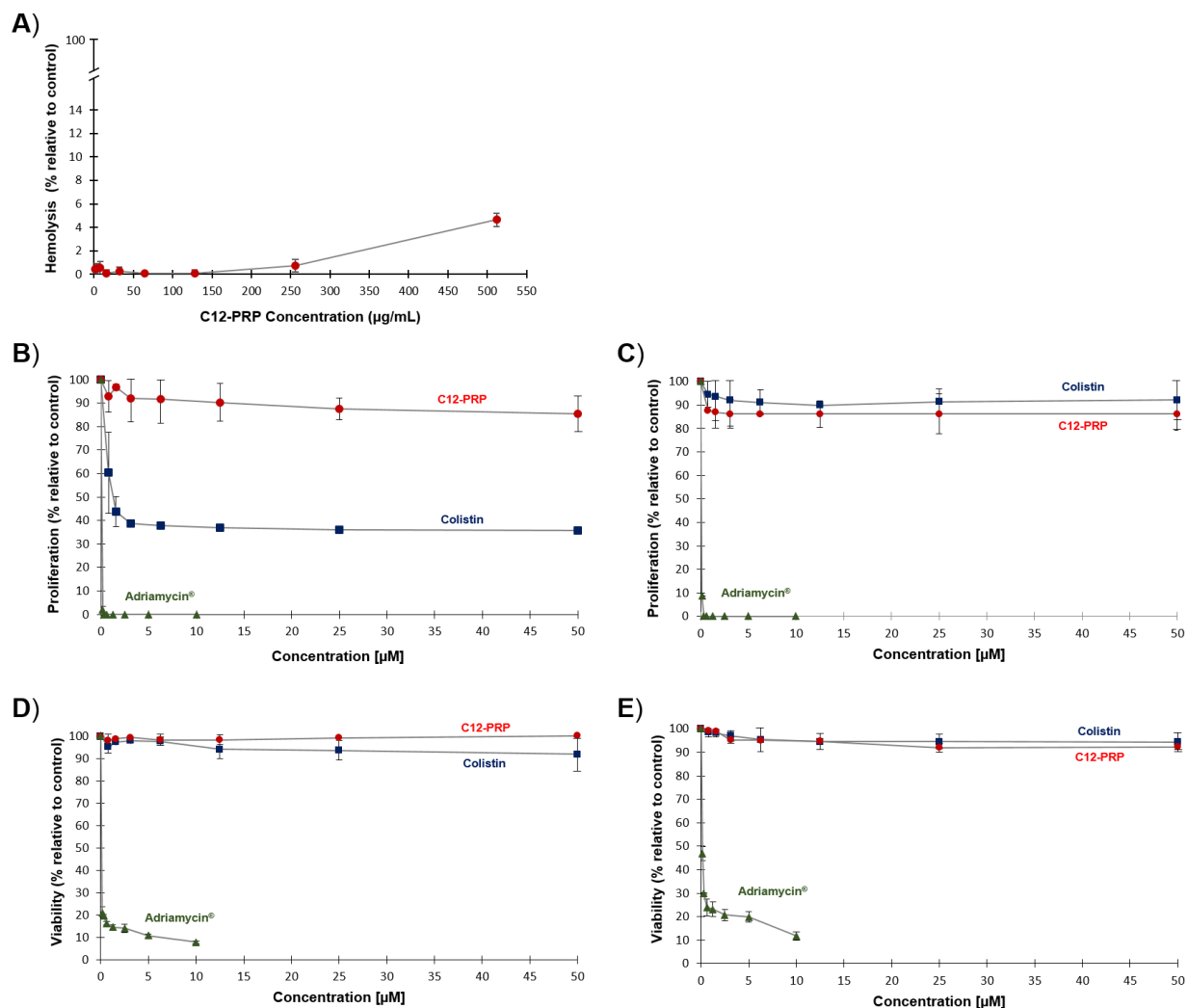
Figure 4-1 Evaluation for cytotoxicity of amphiphilic C12-PRP.

Cytotoxicity assessment of C_{12}-PRP (red circle) *via* (A) hemolytic activity against erythrocytes, (B) inhibition of cellular proliferation against human liver carcinoma HepG2 cells, (C) inhibition of cellular proliferation against human embryonic kidney HEK-293 cells, (D) cytotoxic effects against human liver carcinoma HepG2 cells and (E) cytotoxic effects against human embryonic kidney HEK-293 cells. All experiments were performed in three or more replicates. Colistin (blue square) and adriamycin® (green triangle) were used to represent clinically-used peptide antibiotics and anticancer drugs, respectively. Error bars indicate standard de*via*tion from three independent experiments ($n = 3$).

4.6. Conclusion

An amphiphilic short proline-rich lipopeptide that synergizes with two clinically-used antibiotics was identified for the first time. The non-hemolytic lipopeptide C_{12}-PRP, with a short sequence of C_{12}-PRPRPRP-NH$_2$, potentiates minocycline and rifampicin against wild-type and multidrug-/extensively drug-resistant *P. aeruginosa*. More importantly, C_{12}-PRP significantly reduced the MIC of minocycline and rifampicin against *P. aeruginosa* below their interpretative susceptibility breakpoints. Furthermore, our data strongly suggest that C_{12}-PRP is non-cytotoxic. However, instability to proteases remains a drawback. Our initial attempt of optimization by incorporating D-amino acids retained the desired adjuvant property of the lipopeptide; and therefore C_{12}-PRP appeared to be amenable to peptidomimetic modification. Envisioned future work includes further optimization to bestow protease stability and to enhance the adjuvant profile of C_{12}-PRP, by incorporating peptoids and unnatural amino acids to the C_{12}-PRP structure. The *in vivo* efficacy of the lipopeptide – antibiotic combination and mechanism of potentiation would then be elucidated for the resulting optimized agent. Indeed, peptide-based antibacterial drug candidates such as murepavadin (also known as POL7080) (35) and brilacidin (36), both in Phase-2 clinical trials, were optimized to remove their 'peptide-like' nature prior to clinical validation.

4.7. Materials and methods

Peptide preparation. All lipopeptides were synthesized on solid-phase methylbenzhydrylamine (MBHA) Rink amide resin following standard fluorenylmethyloxycarbonyl (Fmoc) chemistry protocol (37, 38). Amino acids with reactive side-chain functional group were masked with protecting groups inert to solid-phase peptide synthesis conditions yet labile upon peptide cleavage from the solid support. Therefore, Fmoc-Arg(Pbf)-OH and Fmoc-Trp(Boc)-OH were

purchased to prevent the guanidine and indole side-chains, respectively, to cause unwanted reactions. The coupling reagent O-(benzotriazol-1-yl)-*N*,*N*,*N*′,*N*′-tetramethyluronium tetrafluoroborate (TBTU) and *N*-methylmorpholine were used to induce peptide bond formation between amino acids. All reagents and solvents were purchased from commercially available sources and used without further purification.

SPRLPs were purified *via* reverse-phase flash chromatography using C18 (40-63 µm) silica gel purchased from Silicycle (USA). Purity was assessed by high-performance liquid chromatography (HPLC) and were determined to be >95%. Each peptide was characterized using nuclear magnetic resonance (NMR) and mass spectrometry (MS). One (^{1}H and ^{13}C) and two dimensional NMR experiments were performed on either a Bruker AMX-500 or AMX-300 (Germany). Electrospray ionization mass spectrometry (ESI-MS) experiments were performed on Varian 500-MS ion trap mass spectrometer (USA) and high-resolution matrix-assisted laser desorption ionization mass spectrometry (MALDI-MS) experiments were done on Bruker Ultraflextreme mass spectrometer (Germany) coupled to a time-of-flight mass analyzer.

Bacterial strains. Isolates used in this study were either obtained from the American Type Culture Collection (ATCC), the Canadian National Intensive Care Unit (CAN-ICU) surveillance study (27) or the Canadian Ward Surveillance (CANWARD) study (28). Clinical isolates belonging to the CAN-ICU and CANWARD studies were recovered from patients suffering presumed infectious diseases entering or admitted in a participating medical center across Canada during the time of study. MDR *P. aeruginosa* strains in this study refer to those that are resistant to aminoglycosides, fluoroquinolones, cephalosporins, and carbapenems while XDR

strains are those that are resistant to aminoglycosides, fluoroquinolones, cephalosporins, carbapenems, aztreonam and penicillin + β-lactamase inhibitor combination (37, 39).

Antimicrobial susceptibility assay. Microbroth dilution susceptibility test following the Clinical and Laboratory Standards Institute (CLSI) guidelines (32) was performed to assess the *in vitro* antibacterial activity of SPRLPs. Overnight grown bacterial cultures were diluted in saline (0.85% NaCl) to achieve a 0.5 McFarland turbidity, followed by 1:50 dilution in Mueller-Hinton broth (MHB) for inoculation to a final concentration of 5×10^5 colony forming units/mL. The assay was done on a 96-well plates to which the agents of interest were 2-fold serially diluted in MHB and incubated with equal volumes of inoculum at 37 °C for 18 hours. MIC was determined as the lowest concentration to inhibit visible bacterial growth in form of turbidity, which was confirmed using EMax Plus microplate reader (Molecular Devices, USA) at a wavelength of 590 nm. The well containing MHB broth with or without bacterial cells was used as positive or negative controls, respectively.

Hemolytic assay. The ability of SPRLPs to lyse eukaryotic red blood cells was quantified by the amount of hemoglobin released upon incubation with pig erythrocytes, following published protocols (37, 40). Fresh pig blood drawn from pig antecubital vein was centrifuged at $1000 \times g$ for 5 minutes at 4 °C, washed with PBS three times and re-suspended in the same buffer, consecutively. Then, agents of interest were 2-fold serially diluted in phosphate-buffered saline (PBS) on 96-well plate and mixed with equal volumes of erythrocyte solution. Post 1-hour incubation at 37 °C, intact cells were pelleted by centrifugation at $1000 \times g$ for 5 minutes at 4 °C. The supernatant was then transferred to a new 96-well plate. The hemoglobin released was

measured *via* EMax Plus microplate reader (Molecular Devices, USA) at 570 nm wavelength. Erythrocytes in PBS with or without 0.1% Triton X-100 were used as negative or positive controls, respectively.

Synergy scan testing. The assay was performed on a 96-well plate, to which the agents of interest were 2-fold serially diluted in working MHB. Prior to serial dilution, SPRLP was added to the working MHB media so that a fixed final concentration of 8 µg/mL (5 µM) SPRLP per well was achieved. To ensure that the assay was working, the MIC determination test of the studied antibiotic (without SPRLP) was included on the same plate. Similar MIC results between the assay comparator and an independent MIC determination test (on a different plate) ensured validity of the synergy test. Overnight grown bacterial cultures were diluted in saline (0.85% NaCl) to 0.5 McFarland turbidity, followed by 1:50 dilution in MHB (without SPRLP) and inoculation into each well to a final concentration of approximately 5×10^5 colony forming units/mL. Wells containing only MHB (without SPRLP) with or without bacterial cells were used as positive or negative controls, respectively. The plate was then incubated at 37 °C for 18 hours and examined for visible turbidity, which was confirmed using EMax Plus microplate reader (Molecular Devices, USA) at a wavelength of 590 nm. A 4-fold or more MIC reduction of antibiotic in the presence of 8 µg/mL (5 µM) SPRLP denoted a positive synergy result and was further validated by a checkerboard assay.

Checkerboard assay. The assay was done on a 96-well plate as previously described (39, 41). The agent of interest was 2-fold serially diluted along the x-axis, while the adjuvant was 2-fold serially diluted along the y-axis to create a matrix in which each well consists of a combination

of both at different concentrations. Overnight grown bacterial cultures were diluted in saline (0.85% NaCl) to 0.5 McFarland turbidity, followed by 1:50 dilution in MHB and inoculation on each well to a final concentration of approximately 5×10^5 colony forming units/mL. Wells containing only MHB with or without bacterial cells were used as positive or negative controls, respectively. The plate was incubated at 37 °C for 18 hours and examined for visible turbidity, which was confirmed using EMax Plus microplate reader (Molecular Devices, USA) at a wavelength of 590 nm. Fractional inhibitory concentration (FIC) of antibiotic was calculated by dividing the MIC of antibiotic in the presence of adjuvant by the MIC of antibiotic alone. Similarly, the FIC of adjuvant was calculated *via* dividing the MIC of adjuvant in the presence of antibiotic by the MIC of adjuvant alone. FIC index was obtained by the summation of both FIC values. FIC index was interpreted as synergistic, indifferent or antagonistic for values of ≤0.5, 0.5<x≤4 or >4, respectively (31).

Proliferation assay. The CyQuant Direct cell proliferation assay kit (ThermoFisher, Canada) was used to assess the effect of C_{12}-PRP on cell proliferation according to the manufacturer's protocol. Briefly, human embryonic kidney cells (HEK-293) and HepG2 cells were grown in Dulbecco's Modified Eagle's Medium supplemented with 10% fetal bovine serum. The cells were dispersed into 96-well plates (8000 cells/well in 100 μl). Wells with media but no cells were used as blanks. After 24 hours, varying concentrations of C_{12}-PRP, colistin and Adriamycin® were added to the wells containing cells but also the blanks. After incubation of the cells with the compounds for 48 hours, the CyQuant Direct detection reagent was added to the wells. Plates were incubated at 37 °C for 1 hour and the fluorescence (Excitation 480nm / Emission 535nm) was read using a SpectraMax M2e (Molecular Devices, USA). As a positive

control, CyQuant Direct detection reagent was added to a plate with untreated cells, incubated for 1 hour followed by fluoresecence reading. The number of cells in each well was determined by detaching the cells by trypsin followed by counting on a CoulterZM counter to ensure an approximate equal number of cells per well.

Cytotoxicity assay. The cytotoxic effect of C12-PRP was assessed by measuring their effect on the viability of HEK-293 or HepG2 cells. The cells were dispersed into 96-well plates, and after 24 hours, C12-PRP, colistin or Adriamycin® were added as described in the proliferation assay. After incubation for 48 hours, the viability of the cells was determined with the MTS reagent (Promega, Canada) as previously described (42).

Statistical analysis. Data herein represents the mean ± standard de*via*tion (error bars) of at least three independent experiments. The null hypothesis was evaluated *via* one-way analysis of variance (ANOVA), where the confidence interval was set to be 95% (*$p < 0.05$).

4.8. Acknowledgements

4.9. References

1.   Safaei HG, Moghim S, Isfahani BN, Fazeli H, Poursina F, Yadegari S, Nasirmoghadas P,

Hosseininassab Nodoushan SA. 2017. Distribution of the strains of multidrug-resistant, extensively drug-resistant, and pandrug-resistant *Pseudomonas aeruginosa* isolates from burn patients. Adv Biomed Res 6:74.

2. Cerceo E, Deitelzweig SB, Sherman BM, Amin AN. 2016. Multidrug-resistant Gram-negative bacterial infections in the hospital setting: Overview, implications for clinical practice, and emerging treatment options. Microb Drug Resist 22:412–431.

3. Potron A, Poirel L, Nordmann P. 2015. Emerging broad-spectrum resistance in *Pseudomonas aeruginosa* and Acinetobacter baumannii: Mechanisms and epidemiology. Int J Antimicrob Agents 45:568–585.

4. Gellatly SL, Hancock REW. 2013. *Pseudomonas aeruginosa*: new insights into pathogenesis and host defenses. Pathog Dis 67:159–173.

5. Breidenstein EBM, de la Fuente-Nunez C, Hancock REW. 2011. *Pseudomonas aeruginosa*: all roads lead to resistance. Trends Microbiol 19:419–426.

6. Kumar A, Schweizer HP. 2005. Bacterial resistance to antibiotics: active efflux and reduced uptake. Adv Drug Deliv Rev 57:1486–1513.

7. Silver LL. 2016. A Gestalt approach to Gram-negative entry. Bioorg Med Chem 24:6379–6389.

8. Huwaitat R, McCloskey AP, Gilmore BF, Laverty G. 2016. Potential strategies for the eradication of multidrug-resistant Gram-negative bacterial infections. Future Microbiol 11:955–972.

9. Li W, Tailhades J, O'Brien-Simpson NM, Separovic F, Otvos LJ, Hossain MA, Wade JD.

2014. Proline-rich antimicrobial peptides: potential therapeutics against antibiotic-resistant bacteria. Amino Acids 46:2287–2294.

10.   Domalaon R, Zhanel GG, Schweizer F. 2016. Short antimicrobial peptides and peptide scaffolds as promising antibacterial agents. Curr Top Med Chem 16:1217–1230.

11.   Benincasa M, Scocchi M, Podda E, Skerlavaj B, Dolzani L, Gennaro R. 2004. Antimicrobial activity of Bac7 fragments against drug-resistant clinical isolates. Peptides 25:2055–2061.

12.   Holani R, Shah C, Haji Q, Inglis GD, Uwiera RRE, Cobo ER. 2016. Proline-arginine rich (PR-39) cathelicidin: Structure, expression and functional implication in intestinal health. Comp Immunol Microbiol Infect Dis 49:95–101.

13.   Li W-F, Ma G-X, Zhou X-X. 2006. Apidaecin-type peptides: biodiversity, structure-function relationships and mode of action. Peptides 27:2350–2359.

14.   Krizsan A, Volke D, Weinert S, Strater N, Knappe D, Hoffmann R. 2014. Insect-derived proline-rich antimicrobial peptides kill bacteria by inhibiting bacterial protein translation at the 70S ribosome. Angew Chem Int Ed Engl 53:12236–12239.

15.   Podda E, Benincasa M, Pacor S, Micali F, Mattiuzzo M, Gennaro R, Scocchi M. 2006. Dual mode of action of Bac7, a proline-rich antibacterial peptide. Biochim Biophys Acta 1760:1732–1740.

16.   Holfeld L, Hoffmann R, Knappe D. 2017. Correlating uptake and activity of proline-rich antimicrobial peptides in Escherichia coli. Anal Bioanal Chem.

17.   Runti G, Lopez Ruiz M del C, Stoilova T, Hussain R, Jennions M, Choudhury HG, Benincasa M, Gennaro R, Beis K, Scocchi M. 2013. Functional characterization of SbmA,

a bacterial inner membrane transporter required for importing the antimicrobial peptide Bac7(1-35). J Bacteriol 195:5343–5351.

18.   Graf M, Mardirossian M, Nguyen F, Seefeldt AC, Guichard G, Scocchi M, Innis CA, Wilson DN. 2017. Proline-rich antimicrobial peptides targeting protein synthesis. Nat Prod Rep 34:702–711.

19.   Runti G, Benincasa M, Giuffrida G, Devescovi G, Venturi V, Gennaro R, Scocchi M. 2017. The mechanism of killing by the proline-rich peptide Bac7(1-35) against clinical strains of *Pseudomonas aeruginosa* differs from that against other Gram-negative bacteria. Antimicrob Agents Chemother 61.

20.   Gill EE, Franco OL, Hancock REW. 2015. Antibiotic adjuvants: diverse strategies for controlling drug-resistant pathogens. Chem Biol Drug Des 85:56–78.

21.   Bernal P, Molina-Santiago C, Daddaoua A, Llamas MA. 2013. Antibiotic adjuvants: identification and clinical use. Microb Biotechnol 6:445–449.

22.   Toussaint KA, Gallagher JC. 2015. beta-lactam/beta-lactamase inhibitor combinations: from then to now. Ann Pharmacother 49:86–98.

23.   Shlaes DM. 2013. New beta-lactam-beta-lactamase inhibitor combinations in clinical development. Ann N Y Acad Sci 1277:105–114.

24.   Sivertsen A, Isaksson J, Leiros H-KS, Svenson J, Svendsen J-S, Brandsdal BO. 2014. Synthetic cationic antimicrobial peptides bind with their hydrophobic parts to drug site II of human serum albumin. BMC Struct Biol 14:4.

25.   Findlay B, Szelemej P, Zhanel GG, Schweizer F. 2012. Guanidylation and tail effects in

cationic antimicrobial lipopeptoids. PLoS One 7:e41141.

26. Svenson J, Brandsdal B-O, Stensen W, Svendsen JS. 2007. Albumin binding of short cationic antimicrobial micropeptides and its influence on the in vitro bactericidal effect. J Med Chem 50:3334–3339.

27. Zhanel GG, DeCorby M, Laing N, Weshnoweski B, Vashisht R, Tailor F, Nichol K a., Wierzbowski A, Baudry PJ, Karlowsky J a., Lagacé-Wiens P, Walkty A, McCracken M, Mulvey MR, Johnson J, Hoban DJ. 2008. Antimicrobial-resistant pathogens in intensive care units in Canada: results of the Canadian National Intensive Care Unit (CAN-ICU) study, 2005-2006. Antimicrob Agents Chemother 52:1430–1437.

28. Zhanel GG, Adam HJ, Baxter MR, Fuller J, Nichol KA, Denisuik AJ, Lagacé-Wiens PRS, Walkty A, Karlowsky JA, Schweizer F, Hoban DJ, Canadian Antimicrobial Resistance Alliance. 2013. Antimicrobial susceptibility of 22746 pathogens from Canadian hospitals: results of the CANWARD 2007-11 study. J Antimicrob Chemother 68 Suppl 1:7–22.

29. Cassone M, Vogiatzi P, La Montagna R, De Olivier Inacio V, Cudic P, Wade JD, Otvos LJ. 2008. Scope and limitations of the designer proline-rich antibacterial peptide dimer, A3-APO, alone or in synergy with conventional antibiotics. Peptides 29:1878–1886.

30. Jammal J, Zaknoon F, Kaneti G, Goldberg K, Mor A. 2015. Sensitization of Gram-negative bacteria to rifampin and OAK combinations. Sci Rep 5:9216.

31. Meletiadis J, Pournaras S, Roilides E, Walsh TJ. 2010. Defining fractional inhibitory concentration index cutoffs for additive interactions based on self-drug additive combinations, Monte Carlo simulation analysis, and in vitro-in vivo correlation data for antifungal drug combinations against Aspergillus fumi. Antimicrob Agents Chemother

54:602–609.

32. The Clinical and Laboratory Standards Institute. 2016. Performance Standards for Antimicrobial Susceptibility Testing CLSI supplement M100S 26th ed. Clin Lab Stand Institute, Wayne, PA.

33. Qvit N, Rubin SJS, Urban TJ, Mochly-Rosen D, Gross ER. 2017. Peptidomimetic therapeutics: scientific approaches and opportunities. Drug Discov Today 22:454–462.

34. Weinstock MT, Francis JN, Redman JS, Kay MS. 2012. Protease-resistant peptide design-empowering nature's fragile warriors against HIV. Biopolymers 98:431–442.

35. Srinivas N, Jetter P, Ueberbacher BJ, Werneburg M, Zerbe K, Steinmann J, Van der Meijden B, Bernardini F, Lederer A, Dias RLA, Misson PE, Henze H, Zumbrunn J, Gombert FO, Obrecht D, Hunziker P, Schauer S, Ziegler U, Kach A, Eberl L, Riedel K, DeMarco SJ, Robinson JA. 2010. Peptidomimetic antibiotics target outer-membrane biogenesis in *Pseudomonas aeruginosa*. Science 327:1010–1013.

36. Mensa B, Howell GL, Scott R, DeGrado WF. 2014. Comparative mechanistic studies of brilacidin, daptomycin, and the antimicrobial peptide LL16. Antimicrob Agents Chemother 58:5136–5145.

37. Lyu Y, Yang X, Goswami S, Gorityala BK, Idowu T, Domalaon R, Zhanel GG, Shan A, Schweizer F. 2017. Amphiphilic tobramycin-lysine conjugates sensitize multidrug resistant Gram-negative bacteria to rifampicin and minocycline. J Med Chem 60:3684–3702.

38. Domalaon R, Yang X, O'Neil J, Zhanel GG, Mookherjee N, Schweizer F. 2014. Structure-activity relationships in ultrashort cationic lipopeptides: the effects of amino acid ring

constraint on antibacterial activity. Amino Acids 46:2517–2530.

39.   Yang X, Goswami S, Gorityala BK, Domalaon R, Lyu Y, Kumar A, Zhanel GG, Schweizer F. 2017. A tobramycin vector enhances synergy and efficacy of efflux pump inhibitors against multidrug-resistant Gram-negative bacteria. J Med Chem 60:3913–3932.

40.   Domalaon R, Findlay B, Ogunsina M, Arthur G, Schweizer F. 2016. Ultrashort cationic lipopeptides and lipopeptoids: Evaluation and mechanistic insights against epithelial cancer cells. Peptides 84:58–67.

41.   Domalaon R, Yang X, Lyu Y, Zhanel GG, Schweizer F. 2017. Polymyxin B3-tobramycin hybrids with *Pseudomonas aeruginosa*-selective antibacterial activity and strong potentiation of rifampicin, minocycline, and vancomycin. ACS Infect Dis 3:941–954.

42.   Ogunsina M, Samadder P, Idowu T, Arthur G, Schweizer F. 2017. Replacing D-glucosamine with its L-enantiomer in glycosylated antitumor ether lipids (GAELs) retains cytotoxic effects against epithelial cancer cells and cancer stem cells. J Med Chem 60:2142–2147.

4.10. Concluding remarks

This chapter highlighted my efforts in developing short peptide-based adjuvants that were inspired by proline-rich antimicrobial peptides. The lead short proline-rich lipopeptide C_{12}-PRPRPRP-NH$_2$ appeared to be a potent adjuvant partner that revitalize the activity of minocycline and rifampin against *P. aeruginosa*, to which lipopeptide showed no sign of cytotoxicity and hemolytic activity. Indeed, combination therapy of this lipopeptide with partner antibiotics may be a *via*ble treatment for *P. aeruginosa* infections in the future.

Note that complimentary data for this Chapter is provided in Appendix I.

Chapter 5: Development of dilipid ultrashort cationic lipopeptides as adjuvants

This chapter is based on my publication:

Ronald Domalaon, Marc Brizuela, Benjamin Eisner, Brandon Findlay, George G. Zhanel, Frank Schweizer. **2018**. Dilipid ultrashort cationic lipopeptides as adjuvants for chloramphenicol and other conventional antibiotics against Gram-negative bacteria. Amino Acids (Epub ahead of print). doi: 10.1007/s00726-018-2673-9.

Reproduced with permission.

5.1. Introductory remarks

As discussed in Chapter 1, ultrashort cationic lipopeptides were developed to mimic wanted biological activity of naturally-occurring antimicrobial peptides but in a much shorter scaffold of ≤ 5 amino acids. In this chapter, an additional lipid component (with varying carbon-length) was appended to ultrashort cationic lipopeptides to yield dilipid compounds in order to modulate warranted biological activity relative to toxicity that may result from increasing hydrophobicity. Moreover, the viability of these dilipid ultrashort cationic lipopeptides as adjuvant partner in combination with chloramphenicol, and other clinically-used antibiotics, against multidrug-resistant Gram-negative bacteria was explored.

5.2. Contributions of authors

Benjamin Eisner, with the guidance of Brandon Findlay, prepared and purified all lipopeptides for this study. Ronald Domalaon and Benjamin Eisner characterized all purified compounds. Ronald

Domalaon and Marc Brizuela evaluated the microbiological activity of all the lipopeptides alone and in combination with other antibiotics in this study. George G. Zhanel and Frank Schweizer guided the antimicrobial evaluation of the compounds. Ronald Domalaon evaluated the hemolytic activity of the compounds. Ronald Domalaon interpreted all the chemical and biological data with helpful insights from George G. Zhanel and Frank Schweizer. All authors were responsible for the final form of this research article.

5.3. Abstract

The necessity to develop therapeutic agents and strategies to abate the spread of antibiotic-resistant pathogens is prominent. Antimicrobial peptides (AMPs) provide scaffolds and inspirations for antibiotic development. As an AMP of shorter scaffold, eight dilipid ultrashort cationic lipopeptides (dUSCLs) were prepared consisting of only four amino acids and varying dilipids. Lipids were acylated at the peptide N-terminus and the ε-amine side-chain of the N-terminal L-lysine. Compounds that possess aliphatic dilipids of ≥11 carbons-long showed significant hemolysis and therefore limited therapeutic application. Several non-hemolytic dUSCLs were identified to enhance the activity of chloramphenicol and other conventional antibiotics against Gram-negative bacteria. Compounds **2** and **6** that have a short peptide sequence of KKKK and KKGK, respectively, and are both acylated with an aliphatic dilipid of nine carbons-long potentiated chloramphenicol against MDR clinical isolates of *Pseudomonas aeruginosa*, *Acinetobacter baumannii* and *Enterobacteriaceae*. Both dUSCLs showed comparable adjuvant potency in combination with chloramphenicol. However, dUSCL **2** synergized with a wider span of antibiotic classes against *P. aeruginosa* relative to dUSCL **6** that included rifampicin, trimethoprim, minocycline, fosfomycin, piperacillin, ciprofloxacin, levofloxacin, moxifloxacin,

linezolid and vancomycin. Our data revealed that dUSCLs can indirectly disrupt active efflux of chloramphenicol in *P. aeruginosa*. This along with their membrane permeabilizing properties may explain the dUSCLs synergistic combination with conventional antibiotics against Gram-negative bacteria.

5.4. Introduction

Antimicrobial peptides (AMPs) present an attractive reservoir of potential therapeutic agents to treat infectious diseases (1). These naturally-occurring AMPs are produced by animals and bacteria to defend themselves from invading pathogens. Most AMPs, especially those with inherent overall positive charge at physiological pH, eradicate bacteria *via* membrane permeabilization and cell lysis (2, 3). However, protease instability limits their therapeutic usage. Moreover, the sheer size of typical AMPs (normally ≥10 amino acids-long) confers a disadvantage on their production cost. Ultrashort cationic lipopeptides (USCLs) mimic the bioactivity of longer AMPs through a small peptide composed of ≤5 amino acids that is acylated at the N-terminus (4), providing drug candidates with a relatively short scaffold to optimize. An overall amphiphilic character is crucial to the activity of AMPs and thus is incorporated in the USCL design through the use of hydrophilic amino acids and hydrophobic lipids.

Several structure-activity relationship studies have been reported by our group and others that provide meaningful insights to guide the development of bioactive USCLs. For instance, the presence of at least two protonatable amine groups (perceived to be protonated at physiological pH and therefore bestow cationic charge) was found crucial to yield agents with antibacterial activity (5). Constraining the typically flexible amino acid side-chain in a rigidified cyclic ring

seemed to be detrimental for activity (6). Hydrophobic lipids of ≥14 carbons-long appeared necessary to eradicate pathogens (7). However, substantial hemolysis of red blood cells occurred with lipids of ≥16 carbons-long (7). In an attempt to adjust hydrophobicity, dilipid USCLs (dUSCLs) have been developed possessing two shorter instead of one longer lipid to modulate antibacterial activity relative to unwanted toxicity. So far, several membrane-acting dUSCLs have been reported to possess potent antibacterial activity against Gram-positive and Gram-negative bacteria with little hemolytic activity (8, 9).

Combination therapy of AMPs and conventional antibiotics has been identified as a *via*ble strategy to eradicate antibiotic-resistant pathogens (10, 11). In this approach, the antibacterial activity of AMPs may work in synergy with an antibiotic and thus achieve enhanced bacterial killing. However, it is also possible that AMPs with limited activity may still help maximize antibiotic potency by allowing enhanced membrane permeation of the antibiotic resulting in an increased intracellular accumulation. The naturally-occurring 18-residue cationic peptide novicidin was reported to synergize with rifampicin, ceftriaxone and ceftazidime against antibiotic-resistant *Enterobacteriaceae* (12). Other naturally-occurring AMPs such as nisin Z and pediocin PA-1 were also described to potentiate several classes of antibiotics, including chloramphenicol, against antibiotic-resistant *Pseudomonas fluorescens* (13). Synthetic AMPs that act on bacterial membranes were also reported in combination with antibiotics. For instance, the synthetic 18-residue leucine-lysine-rich peptide P5 was found to synergize with chloramphenicol against Gram-positive and Gram-negative bacteria (14). Moreover, the synthetic 26-residue α-helical peptide PL5 was demonstrated to enhance the efficacy of levofloxacin in a *Staphylococcus aureus* wound infection mouse model (15). Since most AMPs act on bacterial membranes, synergy with

antibiotics was likely due to membrane permeabilization and disorganization that led to an increased intracellular antibiotic concentration.

Most reported AMPs that enhanced the activity of conventional antibiotics have been composed of ≥10 amino acids. However, we recently demonstrated that even a short proline-rich lipopeptide, consisting of only 7 amino acids linked to a 12 carbons-long lipid, can synergize with rifampicin and minocycline against multidrug-resistant (MDR) *Pseudomonas aeruginosa* clinical isolates (16). We wondered whether even shorter AMPs such as USCLs have the ability to potentiate conventional antibiotics against antibiotic-resistant bacteria. Herein, we report the development of new dUSCLs (Fig. 5-1) with varying lipid components (Fig. 5-2) and their antibacterial evaluation against Gram-positive and Gram-negative pathogens. More importantly, we demonstrate that dUSCLs can potentiate chloramphenicol and other conventional antibiotics against wild-type and MDR clinical isolates of Gram-negative bacteria.
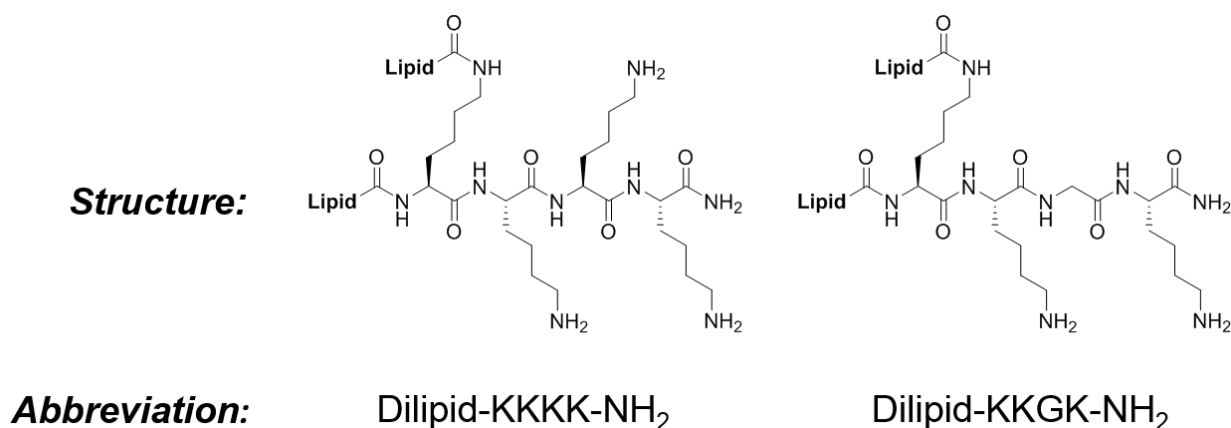
Figure 5-1 General chemical structure and abbre*via*tion of dilipid ultrashort cationic lipopeptides (dUSCLs) in this study.

Peptide N-terminus and ε-amine side-chain of L-lysine at position 1 were acylated with various lipids while peptide C-terminus was amidated.
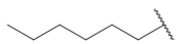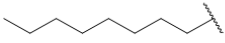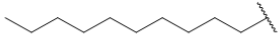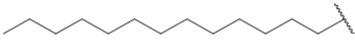
Lipid component	(C_n)	Compound	
		Dilipid-KKKK-NH$_2$	Dilipid-KKGK-NH$_2$
	(C_7)	(1)	(5)
	(C_9)	(2)	(6)
	(C_{11})	(3)	(7)
	(C_{14})	(4)	(8)

Figure 5-2 Eight dilipid ultrashort cationic lipopeptides (dUSCLs) differing in their lipid component.

Aliphatic lipids used ranged from seven (C_7) to fourteen (C_{14}) carbons-long.

5.5. Results and discussion

Dilipid ultrashort cationic lipopeptides (dUSCLs) acylated with two aliphatic lipids. Adequate lipid hydrophobicity is crucial for USCLs to effectively lyse bacterial cells (7). This selective action is due to the cationic peptide portion of USCL that electrostatically interact with the anionic bacterial membranes over zwitterionic eukaryotic membranes. However, too high hydrophobic moment leads to non-specific membrane lysis of eukaryotic cells such as red blood cells resulting in toxicity. To work around this conundrum, dUSCLs are prepared by acylating two shorter instead of one longer lipid to maximize hydrophobic input for better antibacterial activity while minimizing the propensity for toxicity (17).

All the dUSCLs were synthesized *via* solid-phase peptide synthesis following an Fmoc-strategy on an MBHA Rink amide resin. We incorporated our previously reported USCL tripeptide sequence of KKK and KGK (7), where K indicate L-lysine and G indicates glycine, into the dUSCL design (Fig. 5-1) and added another K at amino acid position 1 (K_1) as a point of attachment of the dilipid. The peptide N-terminus and ε-amine side-chain of K_1 were then acylated with various lipids (Fig. 5-2) consisting of seven (C_7) to fourteen (C_{14}) carbons-long, affording us eight dUSCLs. As a result of using an MBHA-based resin, the C-terminus of dUSCLs were amidated.

Peptide sequence and dilipid length of dUSCL influenced antibacterial activity. The antibacterial activity of dUSCLs was evaluated against Gram-positive and Gram-negative bacteria (Table 5-1), most of which were MDR clinical isolates. Minimum inhibitory concentration (MIC) or the lowest concentration of the agent to inhibit bacterial growth were assessed. Out of the eight dUSCLs, compound **3** displayed good broad spectrum activity (MIC of 8 μg/mL) against all Gram-positive bacteria and *Escherichia coli* isolates in the panel. Moderate activity (MIC of 32 μg/mL) was observed for dUSCL **3** against *P. aeruginosa* strains while limited activity was found against the rest of the Gram-negative bacteria in the panel. The peptide sequence KKKK appeared to be better as dUSCLs with the KKGK sequence displayed relatively poor antibacterial activity (Table 5-1). For instance, dUSCL **7** displayed poor activity (MIC of 64 or 128 μg/mL) against Gram-positive bacteria and *E. coli* even though it was a direct counterpart of **3**, both consisting of eleven carbons-long (C_{11}) dilipids but different peptide sequences (Fig. 5-2). This difference in activity may be attributed to the number of protonatable amine side-chain groups (thus, possible cationic charges) in KKKK (+3 charges) relative to KKGK (+2 charges) sequences. It should be noted that the ε-

amine side-chain of K_1 was acylated and therefore did not have a protonatable group. Compound **2** demonstrated moderate activity (MIC of 16-32 µg/mL) against Gram-positive bacteria only. The length of the dilipid was found to influence antibacterial activity. Hydrophobicity in dUSCLs appeared to have a certain threshold that aliphatic dilipids consisting of nine (C_9) to eleven (C_{11}) carbons were optimal to yield favorable antibacterial activity (Table 5-1).

Table 5-1 Antibacterial activity of dilipid USCLs (dUSCLs) against laboratory reference and multidrug-resistant clinical isolates of Gram-positive and Gram-negative bacteria

Organism	MIC, µg/mL							
	1	**2**	**3**	**4**	**5**	**6**	**7**	**8**
S. aureus ATCC 29213	>512	32	8	128	128	64	64	>256
MRSA[a] ATCC 33592	512	32	8	128	128	64	64	>256
MSSE[b] CANWARD-2008 81388	512	32	8	64	128	32	64	256
MRSE[c] CAN-ICU 61589	512	16	8	64	128	32	64	256
E. faecalis ATCC 29212	512	32	8	128	256	32	64	256
E. faecium ATCC 27270	512	32	8	32	128	64	64	256
E. coli ATCC 25922	>512	256	8	256	128	256	128	>256
E. coli CAN-ICU 61714	>512	256	8	128	>512	256	128	>256
E. coli CAN-ICU 63074	512	256	8	128	512	256	128	>256
E. coli CANWARD-2011 97615	>512	128	8	256	>512	256	128	>256
P. aeruginosa ATCC 27853	>512	256	32	256	>512	256	256	>256
P. aeruginosa CAN-ICU 62308	512	128	32	128	>512	256	256	>256
P. aeruginosa CANWARD-2011 96846	>512	256	32	256	>512	256	256	>256
S. maltophilia CAN-ICU 62584	>512	512	128	256	>512	>512	512	>256
A. baumannii CAN-ICU 63169	>512	256	128	512	>512	256	512	>256
K. pneumoniae ATCC 13883	>512	512	128	512	256	128	256	>256

[a] = methicillin-resistant *Staphylococcus aureus;* [b] = methicillin-susceptible *Staphylococcus epidermidis;* [c] = methicillin-resistant *S. epidermidis*.

Dilipids of longer length resulted in hemolysis. To address the concern that augmented hydrophobicity may lead to non-specific cell lysis, we evaluated the propensity of dUSCLs to lyse eukaryotic red blood cells by measuring the amount of heme release upon addition at 50, 100 and 500 µg/mL of peptide (Table 5-2). As expected, dUSCLs comprising of longer aliphatic lipids elicited high hemolysis. For instance, compounds **4** and **8** that both contain C_{14} dilipid resulted in 42.10% and 30.50% hemolysis, respectively, at 100 µg/mL. The most potent dUSCL **3** appeared to be too hemolytic for therapeutic use, that 23.72% hemolysis was observed at 100 µg/mL. However, dUSCLs with shorter dilipid of C_7 to C_9 did not produce appreciable hemolysis at 100 µg/mL. For instance, 100 µg/mL of dUSCL **2** and **6** that both consist of C_9 dilipid resulted in only 2.07% and 3.78% hemolysis.

Table 5-2 Concentration-dependent hemolytic activity of dilipid ultrashort cationic lipopeptides (dUSCLs) against red blood cells

dUSCLs	% Hemolysis (with respect to control[a]) elicited at respective concentration		
	500 µg/mL	100 µg/mL	50 µg/mL
1	1.03	0.75	1.03
2	22.44	2.07	1.53
3	96.40	23.72	2.32
4	97.97	42.10	1.00
5	2.21	1.10	1.00
6	74.28	3.78	1.21
7	36.78	19.73	13.66
8	77.00	30.50	22.23

[a] = control used was 0.1% Triton X-100.

dUSCLs synergized with chloramphenicol against wild-type *P. aeruginosa*. We then evaluated the dUSCLs as adjuvants in combination with conventional antibiotics against Gram-negative bacteria. Adjuvants are biomolecules used in combination therapy that enhance antibacterial efficacy of antibiotics by either increasing their intracellular accumulation (e.g. membrane permeabilizers and efflux-pump inhibitors), preventing their inactivation (enzyme inhibitors) or targeting other pathways that incapacitate bacteria to resist their effect (anti-virulence and two-component system inhibitors) (18). A synergistic adjuvant-antibiotic combination is expected to exhibit enhanced bacterial killing relative to monotherapy. We decided to explore the effect of dUSCLs on the antibacterial activity of chloramphenicol against *P. aeruginosa*. Chloramphenicol is a bacteriostatic antibiotic that inhibits bacterial protein synthesis and is on the World Health Organization's list of essential medicines (19). Resistance to chloramphenicol is commonly attributed to overexpression of efflux pumps and inactivating enzymes (such as chloramphenicol acetyltransferases) but as well as to a decrease in membrane permeability, especially in Gram-negative pathogens (20).

Several large amphiphilic AMPs have been reported to enhance the antibiotic efficacy of chloramphenicol against Gram-negative bacteria (13, 14). Therefore, we were curious whether dUSCLs can also exhibit this property. Interactions between dUSCLs and chloramphenicol were assessed *via* fractional inhibitory concentration (FIC) index, to which a value of ≤0.5, 0.5<x≤4 and >4 were interpreted as synergistic, additive and antagonistic interactions, respectively. We identified five out of eight dUSCLs that synergized with chloramphenicol against wild-type *P. aeruginosa* PAO1 (Table 5-3). Compound **2** appeared to be the most promising adjuvant as it potentiated chloramphenicol the best (FIC index of 0.094) and that it induced low red blood cell hemolysis (Table 5-2). Furthermore, the MIC of chloramphenicol was reduced 32-fold (from 32 to 1 µg/mL) in the presence of only 8 µg/mL (7 µM) of dUSCL **2**.

Table 5-3 Evaluation for synergy of combinations consisting of dilipid ultrashort cationic lipopeptides (dUSCLs) and chloramphenicol (CHL) against wild-type *P. aeruginosa* PAO1

dUSCL	MIC_{dUSCL} [MIC_{combo}], µg/mL	MIC_{CHL} [MIC_{combo}], µg/mL	FIC index	Interpretation	Absolute MIC_{CHL},[a] µg/mL	Potentiation[b]
1	>128 [8]	32 [8]	0.250<x<0.312	Synergy	8	4-fold
2	128 [8]	32 [1]	0.094	Synergy	1	32-fold
3	32 [8]	32 [1]	0.281	Synergy	1	32-fold
4	>128 [0.25]	32 [16]	0.500<x<0.502	Additive	16	2-fold
5	>128 [0.25]	32 [16]	0.500<x<0.502	Additive	16	2-fold
6	64 [16]	32 [1]	0.281	Synergy	16	2-fold
7	>128 [8]	32 [8]	0.250<x<0.312	Synergy	16	2-fold
8	128 [0.25]	32 [16]	0.502	Additive	16	2-fold

[a] = MIC of CHL in the presence of 8 µg/mL dUSCL. [b] = degree of CHL potentiation in the presence of 8 µg/mL dUSCL.

Similar to the trend observed for antibacterial activity, there appeared to be a hydrophobic threshold needed for dUSCL to exhibit adjuvant property. Dilipid components of C_9 to C_{11} appeared to be optimal for dUSCLs to synergize with chloramphenicol. Interestingly, the peptide sequence seemed to affect the ability of dUSCLs to act as adjuvant. Compound **6**, which was the counterpart of **2** as both consist of the same dilipid components, displayed synergism with chloramphenicol but at a relatively higher FIC index of 0.281. The only difference between dUSCL **2** (KKKK) and dUSCL **6** (KKGK) was their peptide sequences. Hereon, we assessed both dUSCLs for their ability to enhance conventional antibiotics in Gram-negative bacteria.

Synergy between dUSCL and chloramphenicol was retained against MDR clinical isolates of *P. aeruginosa*. Synergism between dUSCLs and chloramphenicol was further assessed against five MDR clinical isolates of *P. aeruginosa*. Chloramphenicol alone had very limited activity (MIC of 128 to >512 µg/mL) against the five MDR *P. aeruginosa* strains (Table 5-4). Similar to the results observed against the wild-type *P. aeruginosa* strain PAO1, both compounds **2** and **6** potentiated chloramphenicol against all MDR *P. aeruginosa* strains tested (Table 5-4). For instance, 8 µg/mL (7 µM) of both dUSCLs **2** and **6** reduced the MIC of chloramphenicol 128-fold (from 128 to 1 µg/mL) against MDR *P. aeruginosa* PA260-97103. No difference in the degree of chloramphenicol potentiation against tested MDR *P. aeruginosa* clinical isolates was observed for both dUSCLs **2** and **6**, and therefore the slight difference in peptide sequence (KKKK vs KKGK) appeared not to play a role in their adjuvant property against clinical isolates.

Table 5-4 Evaluation for synergy of combinations consisting of dilipid ultrashort cationic lipopeptides (dUSCLs) **2** or **6** and chloramphenicol (CHL) against MDR clinical isolates of *P. aeruginosa*

Organism	dUSCL	MIC$_{dUSCL}$ [MIC$_{combo}$], µg/mL	MIC$_{CHL}$ [MIC$_{combo}$], µg/mL	FIC index	Interpretation	Absolute MIC$_{CHL}$,[a] µg/mL	Potentiation[b]
P. aeruginosa PA259-96918	**2**	>64 [16]	>512 [16]	x<0.281	Synergy	32	>16-fold
	6	64 [16]	>512 [8]	0.250<x<0.265	Synergy	16	>32-fold
P. aeruginosa PA260-97103	**2**	>64 [8]	128 [1]	0.125<x<0.133	Synergy	1	128-fold
	6	64 [8]	128 [1]	0.133	Synergy	1	128-fold
P. aeruginosa PA262-101856	**2**	>64 [2]	>512 [128]	x<0.281	Synergy	32	>16-fold
	6	>64 [8]	>512 [64]	x<0.250	Synergy	64	>8-fold
P. aeruginosa PA264-104354	**2**	>64 [16]	>512 [32]	x<0.312	Synergy	64	>8-fold
	6	>64 [2]	>512 [128]	x<0.281	Synergy	32	>16-fold
P. aeruginosa 100036	**2**	>64 [16]	512 [4]	0.008<x<0.258	Synergy	8	64-fold
	6	64 [16]	512 [8]	0.266	Synergy	16	32-fold

[a] = MIC of CHL in the presence of 8 µg/mL dUSCL. [b] = degree of CHL potentiation in the presence of 8 µg/mL dUSCL. MDR = multidrug-resistant.

dUSCLs can disrupt active efflux of chloramphenicol in *P. aeruginosa*. While amphiphilic AMPs and dUSCLs are known to permeabilize bacterial membranes (8, 13) that may result in synergism with conventional antibiotics, we wondered whether dUSCLs can also affect active efflux. This is especially important since the intracellular chloramphenicol concentration is significantly affected by efflux (20). In *P. aeruginosa*, chloramphenicol is a known substrate of MexAB-OprM, MexCD-OprJ and MexXY-OprM efflux systems (21). To study the effect of efflux, we compared the potentiation of chloramphenicol by dUSLCs **2** and **6** against wild-type PAO1 and two efflux-deficient (PAO200 and PAO750) *P. aeruginosa* strains (Fig. 5-3). *P. aeruginosa* PAO200 lacked the MexAB-OprM efflux pump while *P. aeruginosa* PAO750 lacked five clinically-relevant pumps (MexAB-OprM, MexCD-OprJ, MexEF-OprN, MexJK and MexXY) and outer membrane protein OpmH. As expected, chloramphenicol was greatly affected by efflux as we observed a 32-fold decrease in MIC from wild-type PAO1 (MIC of 32 µg/mL) to both efflux-deficient PAO200 and PAO750 strains (MIC of 1 µg/mL against both strains) (see Appendix Table II-1). Interestingly, the synergism found against wild-type PAO1 was not observed against PAO200 nor

143

PAO750 for the combination of dUSCLs and chloramphenicol (Fig. 5-3). It appeared that knocking-out these efflux systems in *P. aeruginosa* negated the ability of dUSCLs to enhance the antibacterial activity of chloramphenicol. This strongly suggests that amphiphilic dUSCLs can disrupt active efflux in *P. aeruginosa* that may result in potentiation of chloramphenicol. While further biochemical studies are needed, these membrane-acting dUSCLs suggestively may block efflux indirectly by either (1) sequestering lipids surrounding the transmembrane protein of efflux pumps that result in conformational change and inactivation or (2) by affecting the proton motive force in the inner membrane required to energize these efflux systems. We also do not discredit the possibility of these dUSCLs to interact directly with efflux pumps by "clogging" their pores. Nonetheless, dUSCLs can synergize with a partner antibiotic by enhancing their intracellular accumulation through permeabilization of bacterial membranes and/or disruption of active efflux leading to increased intracellular concentration.
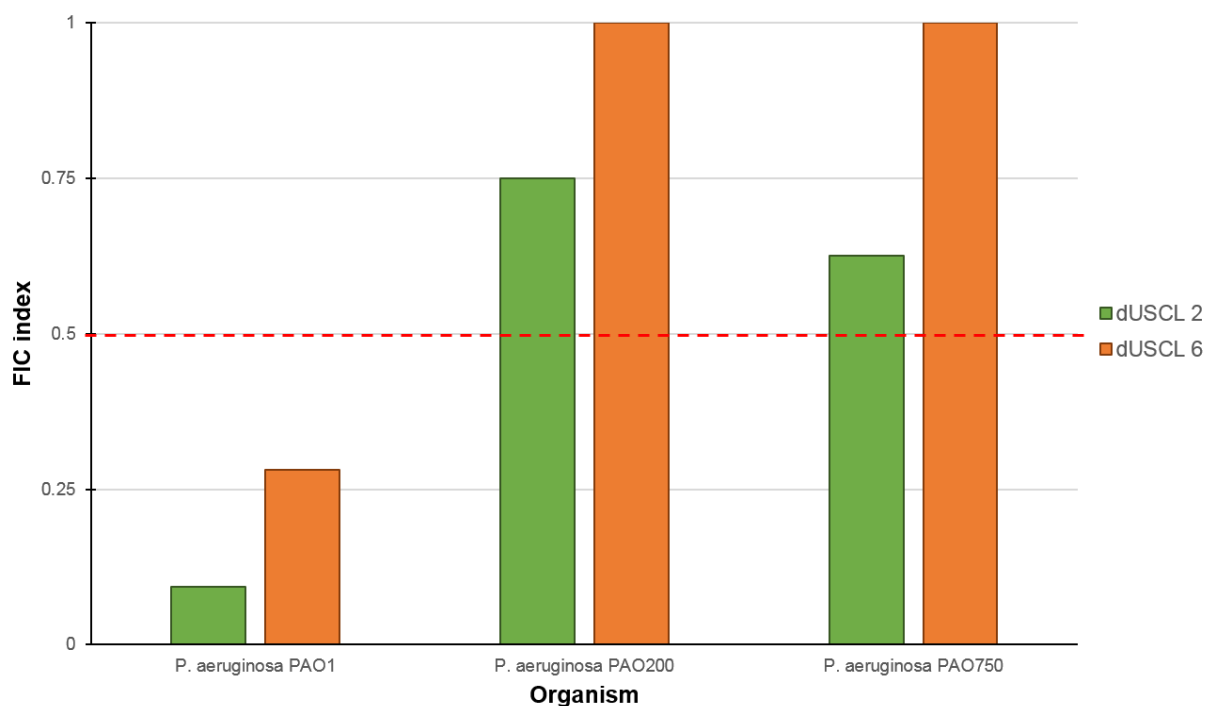
Figure 5-3 Differences in fractional inhibitory concentration (FIC) index of combinations consisting of chloramphenicol and either dilipid ultrashort cationic lipopeptides (dUSCLs) **2** or **6** against wild-type PAO1 and efflux-deficient (PAO200 and PAO750) *P. aeruginosa* strains.

Efflux-deficient strain PAO200 lacked the MexAB-OprM pump while PAO750 lacked five clinically-relevant pumps (MexAB-OprM, MexCD-OprJ, MexEF-OprN, MexJK and MexXY) and outer membrane protein OpmH. Synergy was lost in efflux-deficient *P. aeruginosa* strains. Red dashed line denotes the cutoff FIC index of ≤0.5 for synergistic interaction.

Antibacterial activity of chloramphenicol was enhanced by dUSCLs against other MDR Gram-negative bacteria. Synergy between dUSCLs and chloramphenicol was then assessed in other Gram-negative bacteria including *Acinetobacter baumannii* (5), *E. coli* (4), *Klebsiella pneumoniae* (3) and *Enterobacter cloacae* (1). Both dUSCLs **2** and **6** potentiated chloramphenicol against four out of five *A. baumannii* strains (Table 5-5), including the wild-type ATCC 17978 strain and MDR strains AB027, AB031 and 110193. Only additive interactions were found for the combinations against *A. baumannii* LAC-4 (Table 5-5), which may be attributed to phenotypic differences between the tested clinical isolates. Both dUSCLs also reduced the MIC of chloramphenicol

against *Enterobacteriaceae*. Compound **6** potentiated chloramphenicol against all strains while compound **2** was able to do so for only three out of four tested *E. coli* strains (Table 5-6). Both dUSCLs synergized with only one out of three MDR *K. pneumoniae* strains tested while they both synergized with MDR *E. cloacae* 117029 (Table 5-6). These data show that dUSCLs **2** and **6** can potentiate the antibacterial activity of chloramphenicol against a panel of Gram-negative pathogens. However, it appeared that phenotypic variations between isolates affected the observed activity of the combination, suggesting that other resistance mechanisms besides reduced permeability and efflux were likely operational such as expression of chloramphenicol-inactivating enzymes.

Table 5-5 Evaluation for synergy of combinations consisting of dilipid ultrashort cationic lipopeptides (dUSCLs) **2** or **6** and chloramphenicol (CHL) against wild-type and MDR clinical isolates of *A. baumannii*

Organism	dUSCL	MIC_{dUSCL} $[MIC_{combo}]$, µg/mL	MIC_{CHL} $[MIC_{combo}]$, µg/mL	FIC index	Interpretation	Absolute MIC_{CHL},[a] µg/mL	Potentiation[b]
A. baumannii	**2**	64 [2]	128 [32]	0.281	Synergy	32	4-fold
ATCC 17978	**6**	64 [8]	128 [32]	0.375	Synergy	32	4-fold
A. baumannii	**2**	64 [8]	128 [16]	0.250	Synergy	16	8-fold
AB027	**6**	>64 [8]	128 [16]	0.125<x<0.250	Synergy	16	8-fold
A. baumannii	**2**	32 [2]	128 [32]	0.312	Synergy	32	4-fold
AB031	**6**	>64 [8]	128 [32]	0.250<x<0.375	Synergy	32	4-fold
A. baumannii	**2**	8 [2]	32 [16]	0.750	Additive	NA[c]	NA[c]
LAC-4	**6**	16 [2]	32 [16]	0.625	Additive	NA[c]	NA[c]
A. baumannii	**2**	64 [2]	128 [16]	0.312	Synergy	16	8-fold
110193	**6**	>64 [8]	128 [16]	0.125<x<0.250	Synergy	16	8-fold

[a] = MIC of CHL in the presence of 8 µg/mL dUSCL. [b] = degree of CHL potentiation in the presence of 8 µg/mL dUSCL. [c] = not applicable as the MIC of dUSCL was at or 2-fold closer to 8µg/mL. MDR = multidrug-resistant.

Table 5-6 Evaluation for synergy of combinations consisting of dilipid ultrashort cationic lipopeptides (dUSCLs) **2** or **6** and chloramphenicol (CHL) against wild-type and MDR clinical isolates of *Enterobacteriaceae*

Organism	dUSCL	MIC$_{dUSCL}$ [MIC$_{combo}$], µg/mL	MIC$_{CHL}$ [MIC$_{combo}$], µg/mL	FIC index	Interpretation	Absolute MIC$_{CHL}$,[a] µg/mL	Potentiation[b]
E. coli ATCC 25922	**2**	32 [4]	4 [1]	0.375	Synergy	1	4-fold
	6	64 [4]	4 [1]	0.312	Synergy	1	4-fold
E. coli 94393	**2**	32 [0.25]	4 [2]	0.508	Additive	2	2-fold
	6	64 [8]	4 [1]	0.375	Synergy	1	4-fold
E. coli 94474	**2**	64 [2]	512 [128]	0.281	Synergy	128	4-fold
	6	64 [4]	512 [128]	0.312	Synergy	128	4-fold
E. coli 107115	**2**	64 [2]	512 [16]	0.062	Synergy	16	32-fold
	6	64 [16]	512 [16]	0.281	Synergy	32	16-fold
K. pneumoniae 113250	**2**	>64 [0.25]	4 [4]	1<x<1.004	Additive	4	1-fold
	6	>64 [16]	4 [2]	0.500<x<0.750	Additive	4	1-fold
K. pneumoniae 113254	**2**	>64 [0.25]	2 [2]	1<x<1.004	Additive	2	1-fold
	6	>64 [8]	4 [2]	0.500<x<0.625	Additive	2	2-fold
K. pneumoniae 116381	**2**	>64 [4]	>512 [128]	x<0.312	Synergy	128	>4-fold
	6	>64 [16]	>512 [128]	x<0.500	Synergy	>512	1-fold
E. cloacae 117029	**2**	>64 [8]	8 [1]	0.125<x<0.250	Synergy	1	8-fold
	6	>64 [8]	8 [1]	0.125<x<0.250	Synergy	1	8-fold

[a] = MIC of CHL in the presence of 8 µg/mL dUSCL. [b] = degree of CHL potentiation in the presence of 8 µg/mL dUSCL. MDR = multidrug-resistant.

To test whether the observed chloramphenicol potentiation was specific to dUSCLs, three clinically-used cationic amphiphile/surfactant comparators (benzethonium chloride, benzalkonium chloride and cetrimonium bromide) were assessed in combination with chloramphenicol against wild-type *P. aeruginosa* PAO1, *A. baumannii* ATCC 17978 and *E. coli* ATCC 25922. As shown in Fig. 5-4, none of the comparators were able to potentiate chloramphenicol suggesting that this adjuvant property is specific to dUSCLs **2** and **6**.
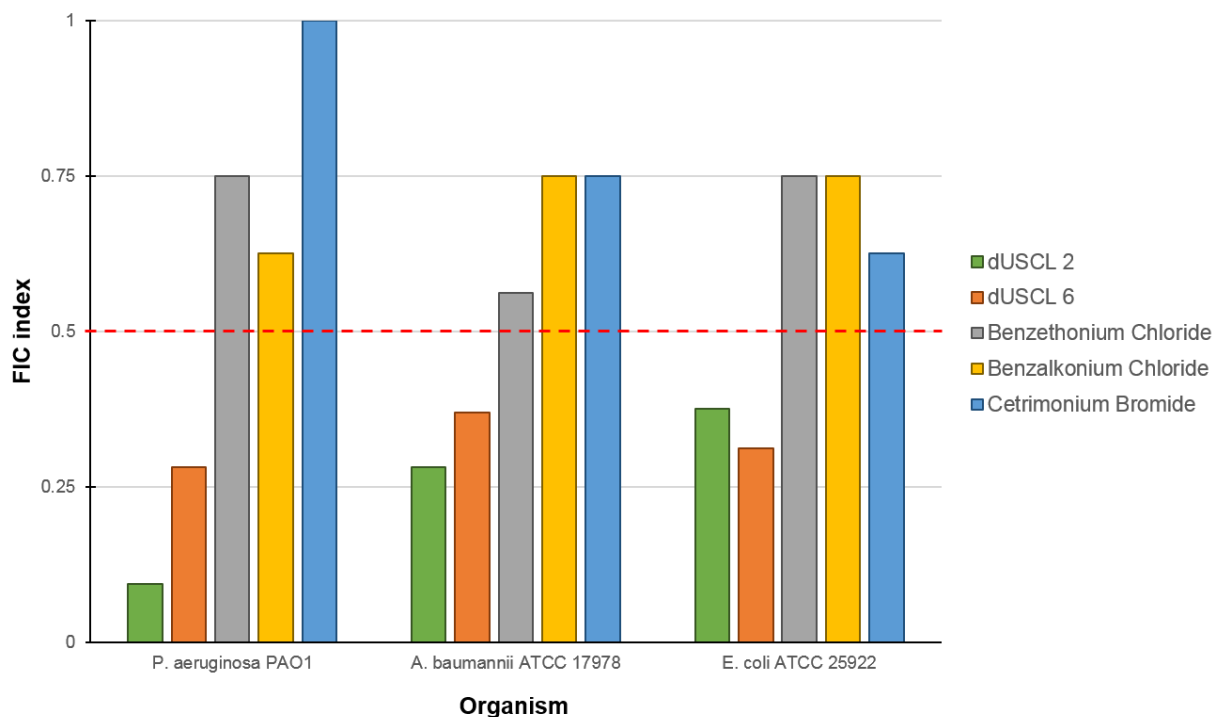
Figure 5-4 Fractional inhibitory concentration (FIC) indices of combinations consisting of chloramphenicol (CHL) and either dilipid ultrashort cationic lipopeptides (dUSCLs) or clinically-used cationic amphiphiles against wild-type Gram-negative bacteria.

Benzethonium chloride, benzalkonium chloride and cetrimonium bromide were used as comparators of commonly used antiseptics/surfactants. All used cationic amphiphile comparators did not synergize with CHL against Gram-negative bacteria. Red dashed line denotes the cutoff FIC index of ≤0.5 for synergistic interaction.

dUSCLs also potentiated other antibiotics against *P. aeruginosa.* Besides chloramphenicol, we explored whether dUSCLs **2** and **6** can potentiate other classes of antibiotics against *P. aeruginosa.* We studied a panel containing fifteen antibiotics that included aminoglycosides, β-lactams, fluoroquinolones, fosfomycin and other antibiotics that have activity only against Gram-positive bacteria (Fig. 5-5). Compound **2** potentiated ten out of fifteen clinically-used antibiotics against *P. aeruginosa* PAO1 (Fig. 5-5). Synergism was observed with antibiotics that were greatly affected by efflux (trimethoprim, minocycline, fosfomycin, piperacillin, ciprofloxacin, levofloxacin, moxifloxacin and linezolid) and those with restricted permeation across outer membrane

148

(rifampicin and vancomycin). On the other hand, dUSCL **6** only potentiated seven out of fifteen antibiotics against *P. aeruginosa* PAO1 (Fig. 5-5), including rifampicin, minocycline, fosfomycin, piperacillin, levofloxacin, moxifloxacin and linezolid. Our results suggest that the antibiotic potentiation effects are sequence-dependent and that dUSCL **2** can enhance a wider range of antibiotic classes relative to dUSCL **6** against *P. aeruginosa*, presumably by increasing their intracellular accumulation.
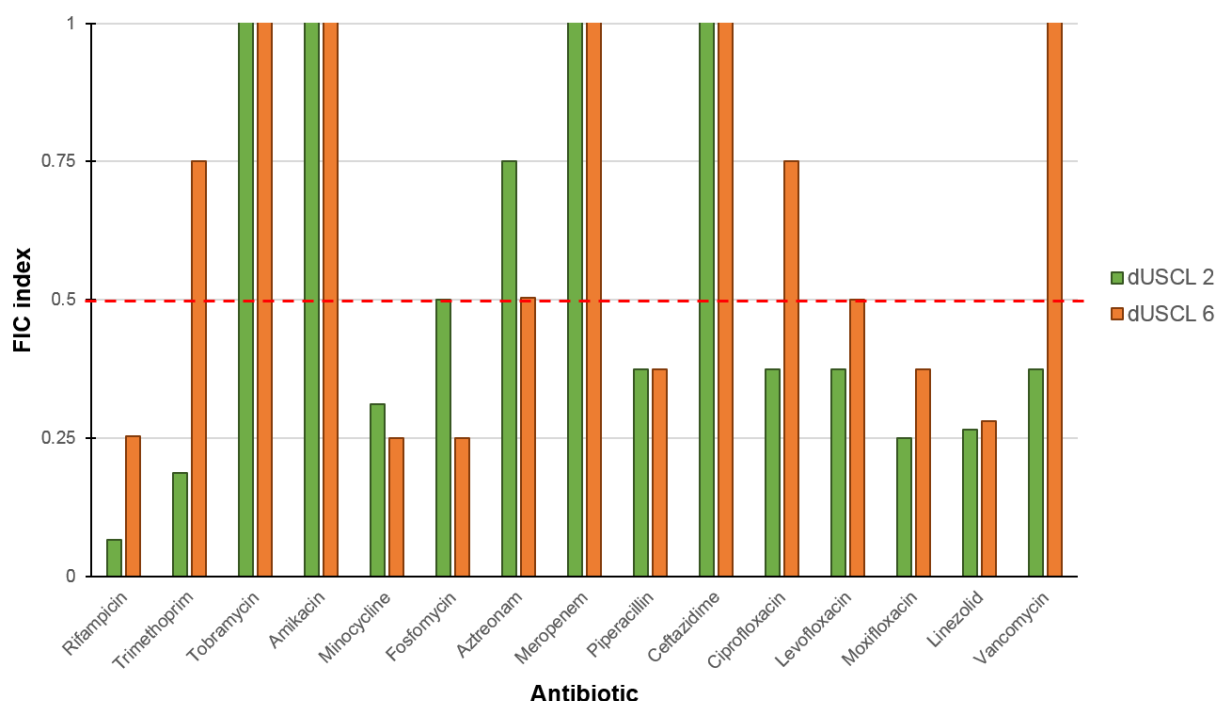
Figure 5-5 Adjuvant profile of dilipid ultrashort cationic lipopeptides (dUSCLs) 2 and 6 in combination with fifteen clinically-used antibiotics against wild-type *P. aeruginosa* PAO1 strain.

The fractional inhibitory concentration (FIC) index of aztreonam with dUSCL **6** was 0.504 and therefore not synergistic. Data for chloramphenicol not included in the figure. Red dashed line denotes the cutoff FIC index of ≤0.5 for synergistic interaction.

5.6. Conclusion

An attempt to develop dUSCLs possessing potent antibacterial activity was described. We found that dUSCLs consisting of ≥11 carbons-long aliphatic dilipids strongly lysed red blood cells at 100 µg/mL, therefore greatly limiting their therapeutic potential. However, several non-hemolytic dUSCLs appeared to be promising adjuvants in combination with chloramphenicol and other conventional antibiotics against Gram-negative bacteria. The dUSCLs **2** and **6** were identified as lead adjuvant candidates, both consisting of C_9 dilipid with peptide sequence of KKKK and KKGK, respectively. Both dUSCLs enhanced the antibacterial activity of chloramphenicol against MDR clinical isolates of *P. aeruginosa*, *A. baumannii* and *Enterobacteriaceae* with similar degrees of potency. However, dUSCL **2** synergized with a wider range of antibiotic classes against *P. aeruginosa* relative to dUSCL **6**. While dUSCLs, like AMPs, permeabilize bacterial membranes resulting in enhanced intracellular antibiotic accumulation, our data suggest that they are also able to indirectly disrupt active efflux of chloramphenicol in *P. aeruginosa*. Our study demonstrates that dUSCLs might aid conventional antibiotics, such as chloramphenicol, in combination against antibiotic-resistant Gram-negative bacteria.

5.7. Materials and methods

Peptide synthesis. All dUSCLs were prepared on a solid-support 4-methylbenzhydrylamine (MBHA) Rink amide resin following standard fluorenylmethyloxycarbonyl (Fmoc)-protection strategy (6). All ε-amine side-chains of L-lysine were protected with *tert*-butyloxycarbonyl (Boc) with the exception of L-lysine at amino acid position 1, which was masked with Fmoc. Peptide coupling was done using the coupling reagent *O*-(benzotriazol-1-yl)-*N,N,N′,N′*-tetramethyluronium tetrafluoroborate (TBTU) and the weak base *N*-methylmorpholine. The dilipid

was acylated at the peptide N-terminus and the ε-amine side-chain of L-Lysine at position 1 *via* peptide coupling reaction. Once the solid-phase peptide synthesis was completed, dUSCL were cleaved from the resin using an acidic solution of trifluoroacetic acid:water (95:5 v/v). The dUSCLs were purified using reverse-phase flash chromatography with C18-functionalized silica gel (40-63 µm) obtained from Silicycle (USA), solvents used were a gradient mixture of water and methanol (both spiked with 0.1% trifluoroacetic acid). All purified dUSCLs were in their trifluoroacetic acid salt form. Purity was measured using high-performance liquid chromatography (HPLC) on a Breeze HPLC Waters with 2998 PDA detector (1.2 nm resolution) coupled to Phenomenex Synergi Polar (50 x 2.0 mm) 4 µm reverse-phase column and were determined to be >95%. Characterization of dUSCLs was achieved using nuclear magnetic resonance (NMR) and mass spectrometry (MS). One (^{1}H and ^{13}C) and two dimensional NMR experiments were done on a Bruker AMX-500 (Germany). Electrospray ionization mass spectrometry (ESI-MS) experiments were done on a Varian 500-MS ion trap mass spectrometer (USA). NMR and MS characterization of the peptides are shown in Appendix II.

Antibacterial activity assay. Bacterial isolates used in this study were obtained from the American Type Culture Collection (ATCC), the Canadian National Intensive Care Unit (CAN-ICU) surveillance study (22) and the Canadian Ward (CANWARD) surveillance study (23). Clinical isolates belonging to the CAN-ICU and CANWARD surveillance studies were recovered from patients suffering presumed infectious diseases entering or admitted in a participating medical center across Canada during the time of study. Efflux-deficient *P. aeruginosa* PAO200 and PAO750 strains were generously provided by Dr. Ayush Kumar (University of Manitoba).

Microbroth dilution susceptibility testing was done according to the Clinical and Laboratory Standards Institute (CLSI) guidelines (24) to evaluate the *in vitro* antibacterial activity of dUSCLs. Briefly, overnight-grown bacterial culture was diluted in saline (0.85% NaCl) to achieve a 0.5 McFarland turbidity. The resulting bacterial solution was then diluted 1:50 in Mueller-Hinton broth (MHB) for inoculation to a final concentration of 5×10^5 colony forming units/mL. The assay was performed on 96-well plates where the agents were 2-fold serially diluted in MHB and incubated with equal volumes of inoculum for 18 hours at 37 °C. Antibacterial activity of the agents was determined by their minimum inhibitory concentration or the lowest concentration to inhibit visible bacterial growth in the form of turbidity, which was inspected visually and further confirmed using EMax Plus microplate reader (Molecular Devices, USA) at a wavelength of 590 nm. Wells containing MHB with or without bacterial cells were used as positive or negative control, respectively.

Hemolytic assay. The ability of dUSCLs to lyse eukaryotic cells was quantified by the amount of hemoglobin released upon incubation with pig red blood cells, following published protocols (7). Fresh pig blood that was drawn from the antecubital vein was centrifuged at $1000 \times g$ for 5 minutes at 4 °C, washed with phosphate-buffered saline (PBS) three times and re-suspended in the same buffer, consecutively, to prepare the working erythrocyte solution. The agents were then 2-fold serially diluted in PBS on 96-well plates and mixed with equal volumes of working erythrocyte solution. Post 1-hour incubation at 37 °C, intact cells on the 96-well plates were pelleted by centrifugation at $1000 \times g$ for 5 minutes at 4 °C. The supernatant was then transferred to a new 96-well plate. The released hemoglobin was then measured *via* EMax Plus microplate reader

(Molecular Devices, USA) at 570 nm wavelength. Red blood cells in PBS with or without 0.1% Triton X-100 was used as negative or positive control, respectively.

Checkerboard assay. The assay was performed on a 96-well plate as previously described (25). The antibiotic was 2-fold serially diluted along the x-axis, while the adjuvant was 2-fold serially diluted along the y-axis to create a matrix in which each well contain a combination of both agents at different concentrations. Overnight-grown bacterial culture was diluted in saline (0.85% NaCl) to 0.5 McFarland turbidity, followed by 1:50 dilution in MHB and inoculation on each well to a final concentration of approximately 5×10^5 colony forming units/mL. Wells comprising of only MHB with or without bacterial cells were used as positive or negative controls, respectively. The plate was incubated for 18 hours at 37 °C and inspected for visible turbidity, which was confirmed using EMax Plus microplate reader (Molecular Devices, USA) at a wavelength of 590 nm. Fractional inhibitory concentration (FIC) of antibiotic was calculated by dividing the MIC of antibiotic in the presence of adjuvant by the MIC of antibiotic alone. Likewise, the FIC of adjuvant was calculated *via* dividing the MIC of adjuvant in the presence of antibiotic by the MIC of adjuvant alone. The FIC index was obtained by the summation of both FIC values. The FIC index was interpreted as synergistic, indifferent or antagonistic for values of ≤0.5, 0.5<x≤4 or >4, respectively (26).

5.8. Acknowledgements

PAO750 strains. We thank Dr. Richard Hodges (University of Manitoba) for generously providing fresh red blood cells from pigs in their Animal Care and Veterinary Services facility.

5.9. References

1.   Domalaon R, Zhanel GG, Schweizer F. 2016. Short antimicrobial peptides and peptide scaffolds as promising antibacterial agents. Curr Top Med Chem 16:1217–1230.

2.   Juhaniewicz-Dębińska J, Tymecka D, Sęk S. 2018. Lipopeptide-induced changes in permeability of solid supported bilayers composed of bacterial membrane lipids. J Electroanal Chem 812:227–234.

3.   Fjell CD, Hiss JA, Hancock REW, Schneider G. 2011. Designing antimicrobial peptides: form follows function. Nat Rev Drug Discov 11:37–51.

4.   Makovitzki A, Avrahami D, Shai Y. 2006. Ultrashort antibacterial and antifungal lipopeptides. Proc Natl Acad Sci U S A 103:15997–16002.

5.   Greber KE, Dawgul M, Kamysz W, Sawicki W. 2017. Cationic net charge and counter ion type as antimicrobial activity determinant factors of short lipopeptides. Front Microbiol 8:123.

6.   Domalaon R, Yang X, O'Neil J, Zhanel GG, Mookherjee N, Schweizer F. 2014. Structure-activity relationships in ultrashort cationic lipopeptides: the effects of amino acid ring constraint on antibacterial activity. Amino Acids 46:2517–2530.

7.   Findlay B, Zhanel GG, Schweizer F. 2012. Investigating the antimicrobial peptide "window of activity" using cationic lipopeptides with hydrocarbon and fluorinated tails. Int J Antimicrob Agents 40:36–42.

8.   Ahn M, Jacob B, Gunasekaran P, Murugan RN, Ryu EK, Lee G, Hyun J-K, Cheong C, Kim N-H, Shin SY, Bang JK. 2014. Poly-lysine peptidomimetics having potent antimicrobial activity without hemolytic activity. Amino Acids 46:2259–2269.

9.   Greber KE, Dawgul M, Kamysz W, Sawicki W, Lukasiak J. 2014. Biological and surface-active properties of double-chain cationic amino acid-based surfactants. Amino Acids 46:1893–1898.

10.   Jorge P, Perez-Perez M, Perez Rodriguez G, Pereira MO, Lourenco A. 2017. A network perspective on antimicrobial peptide combination therapies: the potential of colistin, polymyxin B and nisin. Int J Antimicrob Agents 49:668–676.

11.   Steenbergen JN, Mohr JF, Thorne GM. 2009. Effects of daptomycin in combination with other antimicrobial agents: a review of in vitro and animal model studies. J Antimicrob Chemother 64:1130–1138.

12.   Soren O, Brinch KS, Patel D, Liu Y, Liu A, Coates A, Hu Y. 2015. Antimicrobial peptide novicidin synergizes with rifampin, ceftriaxone, and ceftazidime against antibiotic-resistant Enterobacteriaceae in vitro. Antimicrob Agents Chemother 59:6233–6240.

13.   Naghmouchi K, Le Lay C, Baah J, Drider D. 2012. Antibiotic and antimicrobial peptide combinations: synergistic inhibition of Pseudomonas fluorescens and antibiotic-resistant variants. Res Microbiol 163:101–108.

14.   Park Y, Park SN, Park S-C, Shin SO, Kim J-Y, Kang S-J, Kim M-H, Jeong C-Y, Hahm K-S. 2006. Synergism of Leu-Lys rich antimicrobial peptides and chloramphenicol against bacterial cells. Biochim Biophys Acta 1764:24–32.

15.   Feng Q, Huang Y, Chen M, Li G, Chen Y. 2015. Functional synergy of alpha-helical antimicrobial peptides and traditional antibiotics against Gram-negative and Gram-positive bacteria in vitro and in vivo. Eur J Clin Microbiol Infect Dis 34:197–204.

16.   Domalaon R, Sanchak Y, Koskei LC, Lyu Y, Zhanel GG, Arthur G, Schweizer F. 2018. Short proline-rich lipopeptide potentiates minocycline and rifampin against multidrug- and extensively drug-resistant *Pseudomonas aeruginosa*. Antimicrob Agents Chemother 62.

17.   Dawgul MA, Greber KE, Bartoszewska S, Baranska-Rybak W, Sawicki W, Kamysz W. 2017. In vitro evaluation of cytotoxicity and permeation study on lysine- and arginine-based lipopeptides with proven antimicrobial activity. Molecules 22.

18.   Domalaon R, Idowu T, Zhanel GG, Schweizer F. 2018. Antibiotic hybrids: the next generation of agents and adjuvants against Gram-negative pathogens? Clin Microbiol Rev 31.

19.   World Health Organization. 2015. The selection and use of essential medicines. Report of the WHO Expert Committee, 2015 (including the 19th WHO Model List of Essential Medicines and the 5th WHO Model List of Essential Medicines for Children).

20.   Schwarz S, Kehrenberg C, Doublet B, Cloeckaert A. 2004. Molecular basis of bacterial resistance to chloramphenicol and florfenicol. FEMS Microbiol Rev 28:519–542.

21.   Masuda N, Sakagawa E, Ohya S, Gotoh N, Tsujimoto H, Nishino T. 2000. Substrate specificities of MexAB-OprM, MexCD-OprJ, and MexXY-oprM efflux pumps in *Pseudomonas aeruginosa*. Antimicrob Agents Chemother 44:3322–3327.

22.   Zhanel GG, DeCorby M, Laing N, Weshnoweski B, Vashisht R, Tailor F, Nichol K a., Wierzbowski A, Baudry PJ, Karlowsky J a., Lagacé-Wiens P, Walkty A, McCracken M, Mulvey

MR, Johnson J, Hoban DJ. 2008. Antimicrobial-resistant pathogens in intensive care units in Canada: results of the Canadian National Intensive Care Unit (CAN-ICU) study, 2005-2006. Antimicrob Agents Chemother 52:1430–1437.

23.   Hoban DJ, Zhanel GG. 2013. Introduction to the CANWARD study (2007-11). J Antimicrob Chemother. England.

24.   The Clinical and Laboratory Standards Institute. 2016. Performance Standards for Antimicrobial Susceptibility Testing CLSI supplement M100S 26th ed. Clin Lab Stand Institute, Wayne, PA.

25.   Domalaon R, Berry L, Tays Q, Zhanel GG, Schweizer F. 2018. Development of dilipid polymyxins: investigation on the effect of hydrophobicity through its fatty acyl component. Bioorg Chem 80:639–648.

26.   Meletiadis J, Pournaras S, Roilides E, Walsh TJ. 2010. Defining fractional inhibitory concentration index cutoffs for additive interactions based on self-drug additive combinations, Monte Carlo simulation analysis, and in vitro-in vivo correlation data for antifungal drug combinations against Aspergillus fumi. Antimicrob Agents Chemother 54:602–609.

5.10. Concluding remarks

This chapter highlighted my efforts in developing dilipid peptide-based adjuvants that were inspired by ultrashort cationic lipopeptides. The lead non-hemolytic dilipid ultrashort cationic lipopeptide diC$_9$-KKKK-NH$_2$ appeared to be a good adjuvant partner to chloramphenicol against *P. aeruginosa*, *A. baumannii*, *E. coli*, *K. pneuomoniae* and *E. cloacae*. Another peptide diC$_9$-KKGK-NH$_2$ also showed promising adjuvant activity, which was only slightly subpar to the leading compound. These dilipid peptides also potentiated ciprofloxacin, levofloxacin, moxifloxacin, rifampicin, minocycline, trimethoprim, fosfomycin, piperacillin, vancomycin and linezolid against wild-type *P. aeruginosa*, to which combinations are currently being evaluated against other Gram-negative bacteria. Indeed, combination therapy of these two dilipid ultrashort cationic lipopeptides with chloramphenicol may be a *via*ble treatment for Gram-negative bacterial infections in the future.

Note that complimentary data for this Chapter are provided in Appendix II.

Chapter 6: Structure-activity relationship study of dilipid polymyxins

This chapter is based on my publication:

Ronald Domalaon, Liam Berry, Quinn Tays, George G. Zhanel, Frank Schweizer. **2018**. Development of dilipid polymyxins: investigation on the effect of hydrophobicity through its fatty acyl component. Bioorg Chem 80:639-648. doi: 10.1016/j.bioorg.2018.07.018.

Reproduced with permission.

6.1. Introductory remarks

The polymyxin class of antibiotics is considered one of the antibiotics of last resort to treat multidrug-resistant Gram-negative bacterial infections, as discussed in Chapter 1. As with all antibiotics, it is imperative to thoroughly understand how the chemical structure (and its fragments) affects the overall biological activity of the agent to guide future drug optimization attempts. Thus, this chapter presents a structure-activity relationship study of polymyxins to investigate the effects of hydrophobicity on their biological activity by attaching two fatty acids in the polymyxin core structure, yielding dilipid polymyxin analogs. Aside from the effect of the modification on the antibacterial activity of polymyxins, we also focused on the adjuvant property (compared to polymyxin B nonapeptide) and their ability to resist active efflux in *Pseudomonas aeruginosa*.

6.2. Contributions of authors

Liam Berry and Quinn Tays prepared, purified and characterized all dilipid polymyxins for this study, with guidance from Ronald Domalaon. Ronald Domalaon evaluated the microbiological

activity of all the compounds alone and in combination with other antibiotics in this study. George G. Zhanel and Frank Schweizer guided the antimicrobial evaluation of the compounds. Ronald Domalaon assessed the hemolytic properties of the dilipid polymyxins. Ronald Domalaon interpreted all the chemical and biological data with helpful insights from George G. Zhanel and Frank Schweizer. All authors were responsible for the final form of this research article.

6.3. Abstract

Continuous development of new antibacterial agents is necessary to counter the problem of antimicrobial resistance. Polymyxins are considered as drugs of last resort to combat multidrug-resistant Gram-negative pathogens. Structural optimization of polymyxins requires an in-depth understanding of their structure and how it relate to their antibacterial activity. Herein, the effect of hydrophobicity was explored by adding a secondary fatty acyl component of varying length onto the polymyxin structure at the amine side-chain of L-diaminobuytric acid at position 1, resulting in the development of dilipid polymyxins. The incorporation of an additional lipid was found to confer polymyxin activity against Gram-positive bacteria, to which polymyxins are inherently inactive against. The dilipid polymyxins showed selective antibacterial activity against *Pseudomonas aeruginosa*. Moreover, dilipid polymyxin **1** that consists of four carbon-long aliphatic lipids displayed the ability to enhance the antibacterial potency of other antibiotics in combination against *P. aeruginosa*, resembling the adjuvant activity of the well-known outer membrane permeabilizer polymyxin B nonapeptide (PMBN). Interestingly, our data revealed that dilipid polymyxin **1** and PMBN are substrates for the MexAB-OprM efflux system, and therefore are affected by efflux. In contrast, dilipid polymyxin analogs that consist of longer lipids and colistin were not affected by efflux, suggesting that the lipid component of polymyxin plays an

important role in resisting active efflux. Our work described herein provides an understanding of the polymyxin structure that may be used to usher the development of enhanced polymyxin analogs.

6.4. Introduction

Polymyxins are a class of antibacterials used as drugs of last resort to treat multidrug-resistant (MDR) Gram-negative bacterial infections that are non-responsive to conventional antibiotic treatments (1). Concerns with polymyxin's nephrotoxicity and neurotoxicity as well as the availability of less toxic alternatives hampered their widespread clinical usage in the past. However, a rejuvenated interest in polymyxins has been observed recently due to the alarming increase of MDR pathogens that are impervious to most antibiotics, but also due to improved understanding of polymyxin's pharmacokinetic/pharmacodynamic properties and how they relate to alle*via*ting toxicity (1, 2). Polymyxin B and E, also known as colistin, (Fig. 6-1A) are currently used in the clinic as monotherapy or as part of combination therapy with other antibiotics when standard treatment options fail (3).
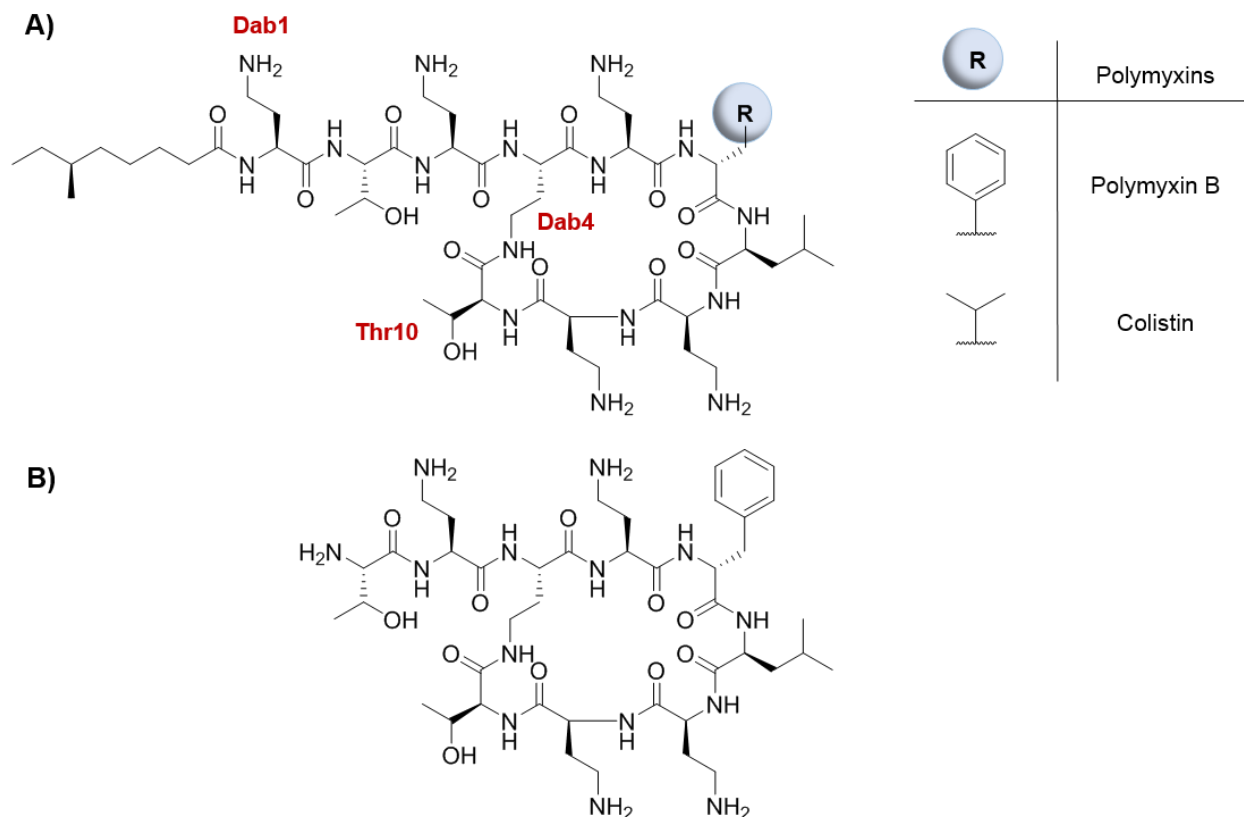
Figure 6-1 Polymyxin structures: (A) polymyxin B & colistin; (B) polymyxin B nonapeptide (PMBN)

The general structure of polymyxins consists of a cyclic heptapeptide core attached to a linear tripeptide with an acylated N-terminus to a fatty acid (Fig. 6-1A). A segregated hydrophobic and hydrophilic domains bestow polymyxins an amphiphilic nature. Polymyxin's hydrophilicity is due to the polar amine side-chains of L-2,4,-diaminobutyric acid (Dab) and hydroxyl side-chains of L-threonine (Thr). These polar side-chains, but also the peptide/amide backbone, are responsible for polymyxins' lipopolysaccharide (LPS) binding that consequently result in displacement of divalent cation bridges and outer membrane destabilization (4). The majority of polymyxins' hydrophobic character is from the fatty acid acylated to its N-terminus. This lipid component is believed to be crucial in polymyxins' insertion into the destabilized outer membrane and its transit to the periplasmic space (5), but also is responsible for disrupting the inner membrane stability (6,

7). Hydrophobicity is also imparted by L-leucine (Leu) and either D-phenylalanine (phe) in polymyxin B or D-leucine (leu) in colistin. These hydrophobic amino acids are believed to play a crucial role in LPS binding (4). Overall, the amphiphilic nature of polymyxins results in membrane disruption that leads to intracellular component leakage and bacterial cell death. Notably, polymyxins exhibit poor activity against Gram-positive bacteria as they do not bind favorably to lipoteichoic acid studded in the cytoplasmic membrane (8).

Structure-activity relationship (SAR) studies have generated a wealth of knowledge on the parameters which are critical/non-critical for polymyxins' antibacterial activity. For instance, alanine scanning of polymyxin B revealed several amino acid side-chains that are not crucial for activity (9). It also has been elucidated that aliphatic hydrocarbon lipids of seven to nine carbons-long are optimal for antibacterial activity (4). However, several aliphatic hydrocarbon non-classical isosteres such as adamantyl and aromatic functional groups may yield derivatives with similar antibacterial activity to polymyxins but with less nephrotoxicity (4, 10). Removal of the lipid and Dab at position 1 (Dab1) yields polymyxin B nonapeptide (PMBN) (Fig. 6-1B), which is known to permeabilize the outer membrane yet lacks the ability to kill bacteria (11). In fact, PMBN is known to enhance the cellular entry and therefore antibacterial activity of antibiotics that suffer limited outer membrane penetration (12). The absence of antibacterial activity in PMBN is due to the lack of lipid component crucial for interaction of polymyxins with lipid bilayers of the outer- and inner membranes of Gram-negative bacteria. Several SAR studies confirmed that hydrophobicity at certain structural points of PMBN is crucial for its outer membrane sensitization and LPS binding properties (13, 14). A derivative of PMBN called SPR741 is currently being evaluated in clinical studies as an adjuvant to enhance the efficacy of antibiotics in combination

against Gram-negative pathogens (15, 16). For instance, SPR741 potentiated an extensive panel of antibiotics against *Enterobacteriacaea* and *Acinetobacter baumannii*, but not against *Pseudomonas aeruginosa* (17). Two recently completed phase-1 clinical studies (https://clinicaltrials.gov/ct2/show/NCT03022175; https://clinicaltrials.gov/ct2/show/NCT03376529) showed SPR741 to be well-tolerated in healthy volunteers up to a single dose of 800 mg or multiple dose up to 600 mg every 8 hours for 14 consecutive days.
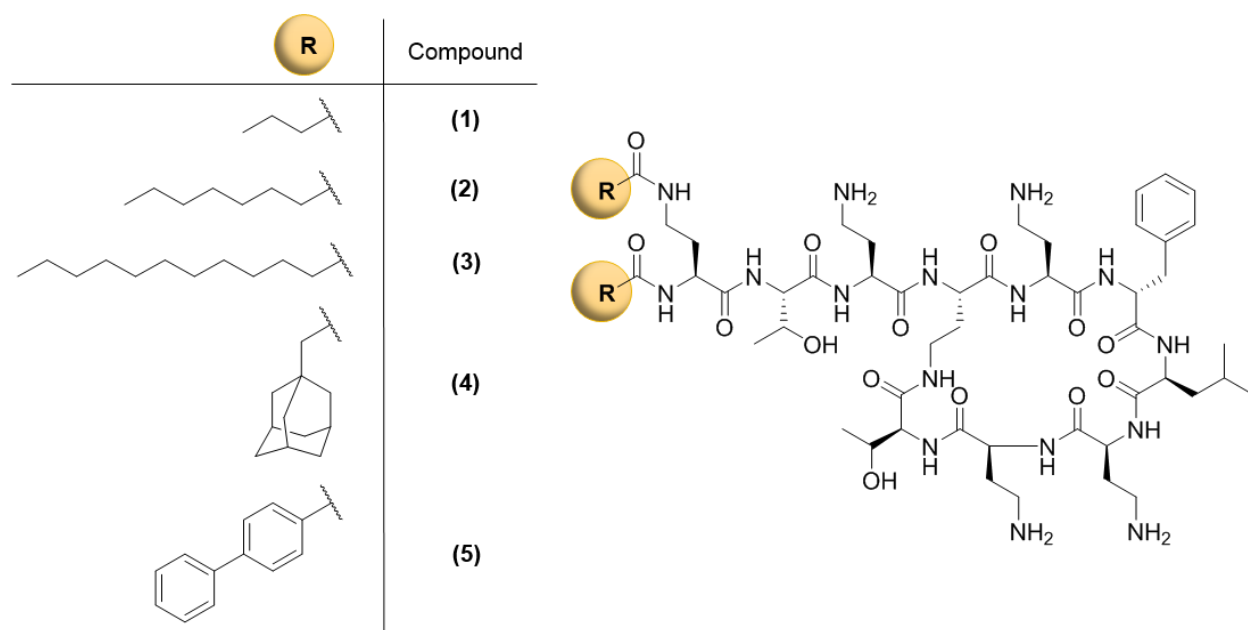
Figure 6-2 Synthesized dilipid polymyxins

It is evident that hydrophobicity plays a critical role in the antibacterial activity of polymyxins (4). A recent study revealed that remodelling of the outer membrane through *pagL*-induced lipid A deacylation resulted in decreased membrane interaction and penetration of polymyxins (18). The removal of an acyl group from the typically hexa-acylated lipid A occurred in the presence of sub-inhibitory polymyxin concentrations in both polymyxin-susceptible and -resistant organisms,

resulting in a more efficient lipid packing that prevent polymyxins from inserting into the bilayer and traversing into the periplasm (18). We hypothesize that the addition of hydrophobic functional groups into the polymyxin structure may enhance its ability to insert into membranes and therefore enhance its activity against Gram-negative but also Gram-positive bacteria. An effort to elucidate the effect of hydrophobicity on polymyxin's antipseudomonal activity by replacing the primary amine side-chain of Dab to tertiary *N,N*-dimethylamine was recently reported (19). In this study, we explore the effect of adding hydrophobicity to the polymyxin structure by acylating the amine side-chain of Dab1 with different fatty acids. These dilipid polymyxins (Fig. 6-2) were then evaluated for their antibacterial activity against wild-type and multidrug-resistant clinical isolates of Gram-positive and Gram-negative bacteria. Moreover, their ability to potentiate the efficacy of other antibiotics in combination, as observed with PMBN, was also assessed. Furthermore, we explored whether the lipid component affects the ability of polymyxin to resist active efflux. To address the concern that an enhanced hydrophobicity may result in non-specific lysis of membranes including eukaryotic membranes, we measured the dilipid polymyxin's lytic activity against red blood cells. Our study provides valuable information for optimization of the polymyxin class of antibiotics as stand-alone antibiotics but also as antimicrobial adjuvant to potentiate other classes of antibiotics.

6.5. Results and discussion

Design and synthesis of dilipid polymyxins. To study the effect of hydrophobicity on polymyxin's bioactivity, we prepared five dilipid polymyxins with varying lipid components (Fig. 6-2). Aside from an acylated N-terminus typically observed in polymyxins, we decided to incorporate another lipid to the amine side-chain of Dab1. Previous alanine scanning of the polymyxin structure

suggested that the side-chain of Dab1 is not crucial for its activity (9). We selected to install aliphatic hydrocarbon lipids with lengths of four- (**1**), eight- (**2**) or twelve- (**3**) carbons-long. We also included lipids that contain a bulky caged-hydrocarbon adamantyl group (**4**) and an aromatic bi-phenyl group (**5**) to explore the effect of hydrophobicity from non-aliphatic hydrocarbon chains.
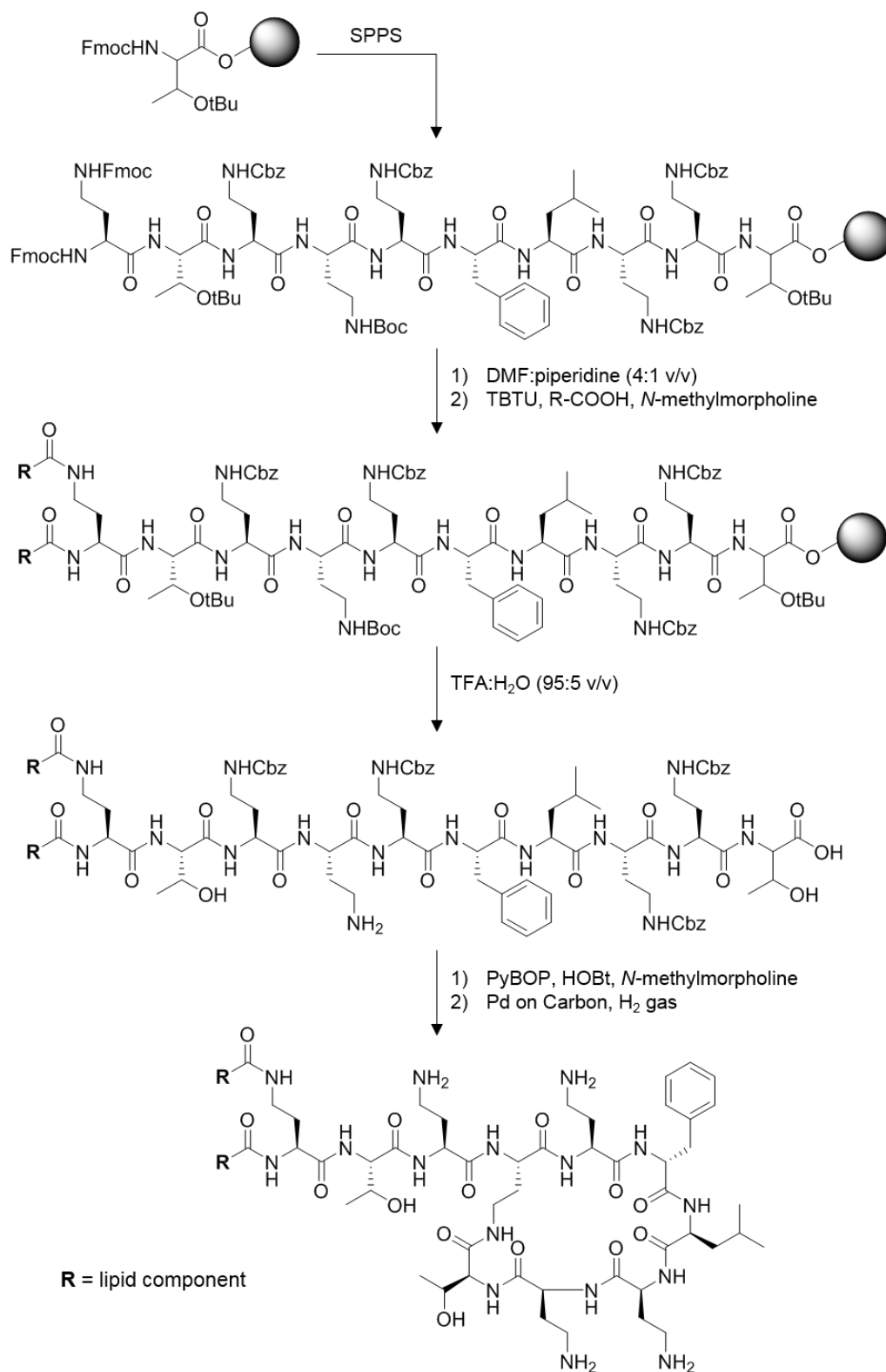
Scheme 6-1 Synthesis of dilipid polymyxins by solid-phase peptide synthesis (SPPS) and intramolecular cyclization.

Solid-phase peptide synthesis followed by solution-phase intramolecular amide bond formation were performed to synthesize the dilipid polymyxins (Scheme 6-1) following our previously reported protocol with minor de*via*tions (20). Briefly, amino acids were immobilized on a Wang resin following a fluorenylmethyloxycarbonyl (Fmoc)-protection strategy. Dab containing an Fmoc-group at the Nα and amine side-chain was immobilized in amino acid position 1. Fmoc deprotection of this Dab1 resulted in two free amine groups, which were then acylated with the lipid component. The resin was then subjected to an acidic solution of trifluoroacetic acid (TFA): water (95:5 v/v) to release the linear dilipid peptide with a free carboxyl C-terminus and amine side-chain of Dab at position 4 (Dab4). These two key functional groups were then reacted together to form an intramolecular amide bond that effectively cyclized the dilipid peptide. Removal of residual side-chain protecting groups yielded five dilipid polymyxins (Fig. 6-2).

Table 6-1 Antimicrobial activity of dilipid polymyxins against laboratory reference and multidrug-resistant clinical isolates of Gram-positive bacteria

| Organism | MIC, µg/mL | | | | | |
	1	2	3	4	5	Colistin
S. aureus ATCC 29213	>128	16	>128	16	8	256
MRSA[a] ATCC 33592	>128	16	>128	32	16	512
MSSE[b] CANWARD-2008 81388	>128	8	64	16	8	256
MRSE[c] CAN-ICU 61589	>128	16	64	16	8	128
E. faecalis ATCC 29212	>128	32	64	32	16	256
E. faecium ATCC 27270	>128	16	8	16	8	256
S. pneumoniae ATCC 49619	>128	32	64	32	32	512

[a] = methicillin-resistant *Staphylococcus aureus;* [b] = methicillin-susceptible *Staphylococcus epidermidis;* [c] = methicillin-resistant *S. epidermidis*.

Addition of another lipid bestows polymyxin activity against Gram-positive bacteria. The antibacterial activity of the dilipid polymyxins were evaluated against a panel of Gram-positive (Table 6-1) and Gram-negative bacteria (Table 6-2), some of which are MDR clinical isolates

collected through the Canadian National Intensive Care Unit (CAN-ICU) surveillance study (21) or the Canadian Ward Surveillance (CANWARD) study (22). Antibacterial activity was measured *via* minimum inhibitory concentration (MIC), which is the lowest concentration of the agent to inhibit bacterial growth. It was evident that the presence of a second lipid component bestows dilipid polymyxins superior activity against Gram-positive bacteria relative to colistin (Table 6-1). For instance, compounds **2** and **5** exhibited 32-fold better MIC than colistin against methicillin-resistant *Staphylococcus aureus* and methicillin-susceptible *Staphylococcus epidermidis*. This suggests that imparting another hydrophobic region within the polymyxin structure may afford favorable interaction with lipoteichoic acid in Gram-positive bacterial membranes, presumably through the hydrophobic effect, resulting in enhanced antibacterial activity.

Table 6-2 Antimicrobial activity of dilipid polymyxins against laboratory reference and multidrug-resistant clinical isolates of Gram-negative bacteria

Organism	MIC, µg/mL					
	1	2	3	4	5	Colistin
E. coli ATCC 25922	>128	4	16	4	8	0.5
E. coli CAN-ICU 61714	>128	32	128	64	32	0.5
E. coli CAN-ICU 63074	>128	64	64	64	32	≤0.5
E. coli CANWARD-2011 97615	>128	64	64	64	32	NT
E. coli 107115	128	2	8	4	4	0.5
P. aeruginosa ATCC 27853	>128	8	>128	16	32	2
P. aeruginosa PAO1	128	4	32	4	8	1
P. aeruginosa CAN-ICU 62308	>128	8	64	16	16	2
P. aeruginosa CANWARD-2011 96846	>128	8	>128	32	64	NT
P. aeruginosa PA259-96918	64	2	16	8	8	0.25
P. aeruginosa PA260-97103	2	2	32	4	8	0.5
P. aeruginosa PA262-101856	>128	8	32	8	8	2
P. aeruginosa PA264-104354	128	4	64	8	8	2
P. aeruginosa PA095	64	2	8	4	4	0.25
P. aeruginosa PA100036	>128	4	32	8	8	1
P. aeruginosa PA101885	128	4	32	8	8	1
S. maltophilia CAN-ICU 62584	>128	32	128	64	64	64
A. baumannii ATCC 17978	>128	32	>128	32	16	0.25
A. baumannii CAN-ICU 63169	>128	64	128	128	64	32
A. baumannii 110193	>128	16	>128	32	16	0.25
A. baumannii LAC-4	128	16	>128	16	16	0.125
A. baumannii AB027	>128	32	128	64	6	0.25
A. baumannii AB031	>128	8	64	16	8	0.25
K. pneumoniae ATCC 13883	>128	>128	>128	>128	>128	≤0.25
K. pneumoniae 116381	>128	>128	>128	>128	>128	1
E. cloacae 117029	64	2	16	4	8	0.125

Dilipid polymyxins display selective antibacterial activity against *P. aeruginosa* among other Gram-negative bacteria. Evaluation of the dilipid polymyxins against Gram-negative bacteria revealed an interesting trend (Table 6-2). Addition of another lipid component to the amine side-chain of Dab1 seemed to reduce polymyxin's activity against *Escherichia coli*, *P. aeruginosa*, *Stenotrophomonas maltophilia*, *A. baumannii*, *Klebsiella pneumoniae* and *Enterobacter cloacae*. However, it seemed that the reduction of activity against *P. aeruginosa* was not as drastic relative

to other Gram-negative pathogens. For instance, polymyxin **2** diacylated with octanoic acid displayed only 4-8 fold lower MIC than colistin against all eleven *P. aeruginosa* strains tested (Table 6-2). An apparent hydrophobic threshold to retain antibacterial activity against *P. aeruginosa* was observed, where an eight carbons-long lipid as seen in **2** appeared to be optimal compared to shorter (four carbons-long in **1**) or longer (twelve carbons-long in **3**) lipid components. Dilipid polymyxins **4** and **5** that consist of caged adamantyl and aromatic biphenyl lipids, respectively, displayed 2-4 fold lower MIC against *P. aeruginosa* relative to **2**. While this needs to be further elucidated, we believe that this selectivity for *P. aeruginosa* may be due to differences in exopolysaccharides and lipopolysaccharides between Gram-negative bacteria. This finding may imply the possibility of developing antipseudomonal polymyxins for pathogen-specific therapy.

Addition of another lipid do not enhance the activity of polymyxin against colistin-resistant Gram-negative bacteria. We then addressed the possibility for the dilipid polymyxins to display enhanced antibacterial activity against colistin-resistant Gram-negative pathogens. Resistance to polymyxins is mainly due to outer membrane/LPS structural modifications (such as conjugation of ethanolamine and 4-aminoarabinose or lipid A deacylation) that result in reduced binding affinity, and hence lowered antibacterial activity (23). The extended hydrophobic region of the dilipid polymyxin may provide additional hydrophobic interactions to the outer membrane of colistin-resistant organisms. Eight MDR colistin-resistant Gram-negative bacterial isolates were tested, including two *E. coli* isolates harboring the *mcr-1* plasmid-encoded polymyxin resistance gene (24). We found no difference between the antibacterial activity of dilipid polymyxins and colistin

against colistin-resistant Gram-negative bacteria (Table 6-3). Therefore, addition of a second lipid

component to the polymyxin structure does not impart activity against colistin-resistant organisms.

Table 6-3 Antimicrobial activity of dilipid polymyxins against colistin-resistant multidrug-resistant Gram-negative bacterial isolates

Organism	MIC, µg/mL					
	1	2	3	4	5	Colistin
E. coli 94393	>64	4	32	16	16	4
E. coli 94474	>64	4	>64	8	8	16
P. aeruginosa 91433	>128	4	8	8	8	4
P. aeruginosa 101243	>128	32	16	64	>128	1024
P. aeruginosa 114228	>128	4	>128	8	16	4
A. baumannii 92247	>64	8	32	8	8	4
K. pneumoniae 113250	>64	>64	>64	>64	>64	256
K. pneumoniae 113254	>64	>64	>64	>64	>64	256

Table 6-4 Evaluation for synergism of dilipid polymyxins or polymyxin B nonapeptide (PMBN) and clinically-used antibiotics against *P. aeruginosa* PAO1

Drug	FIC index[a] 1	2	3	4	5	PMBN
Ceftazidime	0.37	1.00	1.00	0.53	0.62	0.19
Piperacillin	0.75	0.51	1.00	1.03	1.00	0.31
Aztreonam	0.37	0.53	0.75	0.51	0.62	0.16
Meropenem	0.50	0.56	1.00	1.00	1.00	0.37
Doripenem	0.75	0.62	1.00	0.56	1.00	0.31
Minocycline	0.08	0.50	0.62	0.75	0.62	0.09
Doxycycline	0.08	0.51	0.62	1.00	0.53	0.05
Tobramycin	1.00	1.03	1.01	1.01	1.01	1.00
Streptomycin	0.75	0.75	1.01	1.03	1.00	0.50[c]
Gentamicin	1.00	2.01	1.01	1.03	2.01	1.50
Moxifloxacin	0.25	1.50	1.00	1.50	0.75	0.37
Ciprofloxacin	0.50	0.75	1.01	1.03	1.00	0.50
Fosfomycin	0.25	0.51	0.75	0.75	0.56	0.37
Trimethoprim	0.25	0.56	0.62	1.00	0.62	0.09
Chloramphenicol	0.09	0.37	0.62	0.62	0.50	0.07
Novobiocin	0.09	0.26	0.50[b]	0.50	0.50	0.04
Vancomycin	0.28	0.51	1.00	0.75	0.51	0.02
Clindamycin	0.09	0.31	0.56	0.62	0.53	0.03
Linezolid	0.09	0.50[b]	1.00	1.00	0.53	0.06
Pleuromutilin	0.07	0.51	0.51	0.51	0.50[c]	0.03
Rifampicin	0.02	0.75	0.75	0.51	0.31	0.01

[a] = yellow shaded box indicate FIC index of ≤0.5 therefore is synergistic; [b] = FIC index is 0.500977 therefore not synergistic; [c] = FIC index is 0.503906 therefore not synergistic

Dilipid polymyxins can enhance the activity of other antibiotics. The potential of the dilipid polymyxins to serve as an adjuvant in combination with other antibiotics was evaluated against *P. aeruginosa* PAO1 strain (Table 6-4 and Appendix III). We hypothesize that the ability to permeabilize the outer membrane, as seen in PMBN, is retained in dilipid polymyxins. Checkerboard assays were performed with the dilipid polymyxins in combination with twenty-one clinically-used antibiotics. The panel included representatives from the β-lactam, carbapenem, tetracycline, aminoglycoside and fluoroquinolone antibiotic families. Other agents that are used to treat Gram-negative bacterial infection such as fosfomycin, trimethoprim and chloramphenicol

were also included. Moreover, agents with potent activity against Gram-positive bacteria but poor activity against Gram-negative bacteria such as novobiocin, vancomycin, clindamycin, linezolid, pleuromutilin and rifampicin were included. Fractional inhibitory concentration (FIC) index was calculated for each combination to measure potential synergism between the two agents. FIC was obtained by dividing the MIC of antibiotic/adjuvant in combination by the MIC of antibiotic/adjuvant alone, while FIC index was calculated by the summation of FIC indices for the antibiotic and adjuvant. An FIC index of ≤ 0.5, $0.5 < x \leq 4$, or >4 denotes for synergistic, additive or antagonistic interaction, respectively (25). Initially, we assessed the adjuvant properties of PMBN against the panel of 21 antibiotics. PMBN potentiated all antibiotics tested except for those belonging to the aminoglycoside family (Table 6-4). Interestingly, dilipid polymyxin **1** that is diacylated with butyric acid exhibited similar adjuvant potency as PMBN (Table 6-4). Both **1** and PMBN possessed poor activity against *P. aeruginosa* alone (MIC of 128 µg/mL for both) but are able to enhance the activity of other antibiotics in combination presumably through outer membrane permeabilization. Since **1** and PMBN are structurally similar, this observation may imply that amino acid Dab1 and short lipid component of four carbons-long do not affect the ability of polymyxin to permeabilize the outer membrane. This finding may imply the development of polymyxin-based adjuvants where the Dab1 and lipid component are used as molecular scaffolds in appending further functional groups to modulate the desired activity. However, not all the dilipid polymyxins potentiated the tested panel of antibiotics. For instance, the dilipid polymyxin **3** diacylated with twelve carbons-long and its isosteric bulky adamantyl counterpart **4** did not enhance the activity of any antibiotics. This may suggest that longer and bulky lipids may not be beneficial to the adjuvant properties of the polymyxins.

Length of lipid component affects the ability of polymyxins to resist efflux. To our curiosity, we explored whether efflux can affect the activity of polymyxins. It is widely accepted that polymyxins disrupt Gram-negative bacterial membranes that results in intracellular component leakage and bacterial cell death (4). However, for this to occur requires the agent to reach the periplasmic space to interact and disrupt the inner membrane. Active efflux may potentially expel polymyxins out of the periplasm, effectively reducing its periplasmic and intracellular concentrations. To study the effect of efflux on polymyxins in Gram-negative pathogens, we used *P. aeruginosa* as they inherently overexpressed efflux systems such as MexAB-OprM, MexCD-OprJ and MexXY-OprM. Moreover, antibiotic substrates for these efflux systems are mostly characterized (26, 27). We evaluated and compared the activity of the dilipid polymyxins, colistin and PMBN against wild-type PAO1 and two efflux-deficient *P. aeruginosa* isogenic mutants (Table 6-5). The strain PAO200 lacks the MexAB-OprM efflux system while strain PAO750 lacks five clinically-relevant pumps (MexAB-OprM, MexCD-OprJ, MexEF-OprN, MexJK and MexXY) and outer membrane protein OpmH. In agreement with a previous report (26), colistin was not affected by efflux as there was no difference in its MIC among the three *P. aeruginosa* strains tested (Table 6-5). Surprisingly, both **1** and PMBN appeared to be greatly affected by the MexAB-OprM efflux system (Table 6-5) as there was a 32- and 64-fold difference, respectively, in MIC of the agents against wild-type PAO1 and efflux-deficient PAO200. Deletion of other efflux systems seemed not to further alter the susceptibility of *P. aeruginosa* to **1** and PMBN as their MIC against PAO200 and PAO750 were comparable (Table 6-5). While not as potent compared to colistin (MIC of 0.5 µg/mL against PAO200), dilipid polymyxin **1** (MIC of 4 µg/mL against PAO200) and PMBN (MIC of 2 µg/mL against PAO200) displayed good antibacterial activity against MexAB-OprM deletion mutants. This suggests that **1** and PMBN may possess the

ability to disrupt the inner membrane and/or have another periplasmic target but fall short in their ability to resist efflux. This finding certainly warrants further biochemical studies. However, we could imply from our data that the length of the lipid component affected the ability of polymyxin to resist active efflux as derivatives of more than eight carbons-long (such as in colistin and **2**) displayed no difference in MIC against the three *P. aeruginosa* strains tested. To our knowledge, this is the first reported evidence to show that active efflux in *P. aeruginosa* may affect the activity of a polymyxin derivative.

Table 6-5 Antimicrobial activity of dilipid polymyxins, colistin and polymyxin B nonapeptide (PMBN) against efflux-deficient *P. aeruginosa*

Organism	MIC, µg/mL						
	1	**2**	**3**	**4**	**5**	Colistin	PMBN
P. aeruginosa PAO1[a]	128	4	32	4	8	1	128
P. aeruginosa PAO200[b]	4	2	32	4	4	0.5	2
P. aeruginosa PAO750[c]	8	2	32	8	4	0.5	4

[a] = wild type; [b] = efflux-deficient strain that lacks the MexAB-OprM pump; [c] = efflux-deficient strain that lacks five clinically-relevant pumps (MexAB-OprM, MexCD-OprJ, MexEF-OprN, MexJK and MexXY) and outer membrane protein OpmH
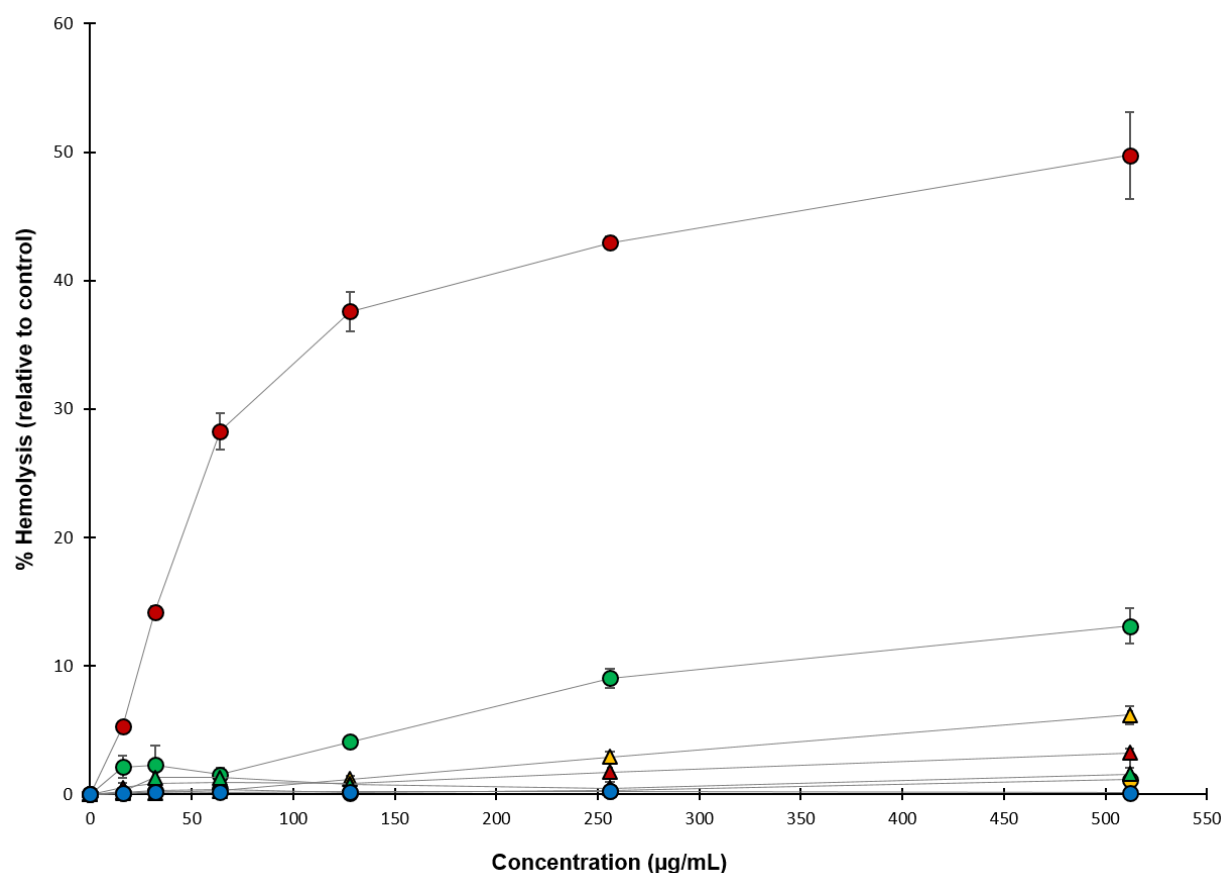
Figure 6-3 Concentration-dependent hemolysis of red blood cells induced by dilipid polymyxins, colistin and polymyxin B nonapeptide.

Yellow circle = dilipid polymyxin **1**; yellow triangle = dilipid polymyxin **2**; red circle = dilipid polymyxin **3**; red triangle = dilipid polymyxin **4**; green circle = dilipid polymyxin **5**; green triangle = colistin; blue circle = polymyxin B nonapeptide (PMBN). Experiment performed in at least triplicates.

Table 6-6 Hemolytic properties of dilipid polymyxins, colistin and polymyxin B nonapeptide (PMBN)

Polymyxin	MHC$_5$[a]	% Hemolysis at 512 µg/mL of polymyxin
1	>512	1.1 ± 1.6
2	512	6.2 ± 0.7
3	16	49.7 ± 3.3
4	>512	3.2 ± 0.4
5	128	13.1 ± 1.4
colistin	>512	1.6 ± 0.5
PMBN	>512	1.1 ± 0.1

[a] minimum concentration (µg/mL) that resulted in 5% red blood cell hemolysis

Length of lipid component affects the hemolytic activity of polymyxins. To address concerns of non-specific lysis that may arise from an enhanced hydrophobicity especially against eukaryotic cells, we evaluated the propensity of dilipid polymyxins to lyse eukaryotic red blood cells and compared them with colistin and PMBN. The length of hydrocarbon dilipid component was found to positively correlate with red blood cell hemolysis (Fig. 6-3). We quantified each compound's hemolytic activity by their MHC_5, or the minimum concentration to elicit 5% red blood cell hemolysis (Table 6-6). Compound **3** that is diacylated with twelve carbons-long lipid induced the most hemolysis (MHC_5 of 16 µg/mL) while compound **1** induced the least (MHC_5 of >512 µg/mL). In fact, the hemolytic activity of **1** resembles colistin and PMBN which show no hemolytic activity up to the highest concentration tested of 512 µg/mL (Table 6-6). While substantially non-hemolytic in comparison to **3**, dilipid polymyxin **2** only elicted 6.2% hemolysis at 512 µg/mL. Interestingly, we found that the hemolysis induced by a twelve carbons-long aliphatic dilipid can be reduced by replacing the alkyl chain by isosteric caged or aromatic moieties. For instance, the bulky adamantyl dilipid seen in **4** (MHC_5 of >512 µg/mL) and the aromatic biphenyl dilipid seen in **5** (MHC_5 of 128 µg/mL) yielded significantly lower hemolysis compared to **3**. We could infer from our data that the addition of either short-length aliphatic (eight carbons-long or less), caged or aromatic lipid is preferred to develop polymyxin-based agents that are non-hemolytic.

6.6. Conclusion

Our efforts herein have elucidated several important points useful for the rational optimization of the polymyxin structure. The addition of an extra lipid component conferred polymyxin activity against Gram-positive bacteria and selectivity against the Gram-negative bacteria *P. aeruginosa*.

The increased hydrophobicity through the additional lipid component most likely enabled membrane lysis of Gram-positive bacteria, similar to the mode of action of cationic amphiphiles. Similar to PMBN, the dilipid polymyxins can also enhance the activity of other antibiotics in combination. The lipid component appeared to modulate the ability of polymyxins to resist efflux, where derivatives acylated with shorter fatty acids and PMBN are greatly affected by the MexAB-OprM efflux system. However, lipid components of longer fatty acids may promote unwanted non-specific lysis and therefore cytotoxicity. Aliphatic lipids of eight carbons or less, caged or aromatic hydrocarbons are preferred. Overall, these data provide useful insights that may guide the optimization of the polymyxin structure.

6.7. Materials and methods

General information. All reagents and solvents were purchased from common commercial suppliers and were used without further purifications unless otherwise stated. Synthesized compounds were purified, as specified in their synthesis, by reverse-phase flash chromatography using C18 silica gel (40-63 μm) purchased from Silicycle (USA). TLC was performed on silica gel 60 F254 (0.25 mm) obtained from Merck (USA) to check the presence of compound in each fraction and was visualized by both ultraviolet light and ninhydrin staining solution. The purity of all compounds was determined to be ≥95% *via* high-performance liquid chromatography (HPLC) analysis *via* Breeze HPLC Waters with 2998 PDA detector (1.2 nm resolution) coupled to Phenomenex Synergi Polar (50 × 2.0 mm) 4 μm reverse-phase column with phenyl ether-linked stationary phase. All purified compounds were characterized *via* 1-dimensional and 2-dimensional NMR experiments. NMR experiments were performed on a Bruker AMX-500 (500 MHz) instrument (Germany). The molecular weights for all synthesized compounds were recorded by

Matrix-assisted Laser Desorption Ionization coupled to a time of flight mass analyzer and mass spectrometer (MALDI-TOF-MS) on a Bruker Ultraflextreme (Germany), using 2,5-dehydroxybenzoic acid as the matrix.

Peptide synthesis. Solid-phase peptide synthesis was performed following our previously reported protocol (20, 28). All linear diacylated peptides were synthesized on solid-support following an Fmoc-protection strategy. Wang *p*-alkoxybenzyl alcohol resin containing an already immobilized L-threonine was used to grow the peptide. Fmoc deprotection was done using a weak basic solution of *N,N*-dimethylformamide (DMF):piperidine (4:1 v/v). Peptide coupling reactions were performed by reacting the free amine of the immobilized amino acid with the free carboxylic acid of the incoming amino acid, *via* the peptide coupling reagent O-(benzotriazol-1-yl)-*N,N,N′,N′*-tetramethyluronium tetrafluoroborate (TBTU) (3 mol. equiv.) and *N*-methylmorpholine (3 mol. equiv.). Peptide coupling reactions were done in DMF with constant gentle agitation for 45 minutes. An acidic solution of TFA:water (95:5 v/v) was added to the resin and reacted for 30 minutes to cleave the peptide, followed by immediate evaporation *in vacuo* to afford the crude peptide. MALDI-TOF-MS confirmed the presence and relative purity of the linear diacylated peptides.

Intramolecular cyclization and deprotection. The linear diacylated peptide was then mixed with benzotriazole-1-yl-oxy-trispyrrolidino-phosphonium hexafluorophosphate (PyBOP) (4 mol. equiv.), hydroxybenzotriazole (HOBt) (4 mol. equiv.),and *N*-methymorpholine (10 mol. equiv.) in anhydrous DMF under very dilute conditions, which was then vigorously stirred for 2 h to induce intramolecular cyclization *via* amide bond formation between the carboxyl end of L-threonine at

position 10 (Thr10) and the amine side-chain of Dab4. The solvent was then removed *in vacuo*. The cyclized diacylated peptide was precipitated from the crude by addition of cold water. It was then filtered to obtain a pale brown solid. Dichloromethane (DCM) was added to result in a partially dissolved product and co-distilled *in vacuo* to dryness. MALDI-TOF-MS was then used to confirm the product. The cyclized diacylated peptide was then subjected to catalytic hydrogenolysis. The compound was dissolved in a mixture of 4:5:1 methanol/acetic acid/water. Palladium on carbon was then added, followed by H_2 gas (balloon) to remove the remaining carboxybenzyl (Cbz) protecting groups. The resulting solution was then filtered *via* Nylon filter, and the filter was then washed with methanol. The filtrate was evaporated to dryness *in vacuo*. The crude was purified *via* reverse-phase flash chromatography with an eluent mixture of water and methanol (both solvents spiked with 0.1% TFA), following a gradient of 0% to 50% methanol in water ratio (2.5% stepwise), to afford compounds **1-5**.

*Dibutyric acid (Di-C4) polymyxin (**1**).* ^{1}H NMR (500 MHz, Methanol-d_4) δ: 7.32 – 7.19 (m, 5H D-Phe$_6$ aromatic), 4.51 (dd, J = 8.7, 4.4 Hz 1H, Dab$_{5\alpha}$), 4.49 – 4.24 (m, 7H, Dab$_{1\alpha}$ + Dab$_{3\alpha}$ + Dab$_{4\alpha}$ + Dab$_{8\alpha}$ + Dab$_{8\alpha}$ + D-Phe$_{6\alpha}$ + Thr$_{2\beta}$), 4.21 (d, J = 3.2 Hz, 1H, Thr$_{2\alpha}$), 4.20 – 4.16 (m, 1H, Thr$_{10\beta}$), 4.11 (dd, J = 11.5, 3.8 Hz, 1H, Leu$_{7\alpha}$), 4.06 (d, J = 4.9 Hz, 1H, Thr$_{10\alpha}$), 3.67 – 3.57 (m, 1H, Dab$_{4\gamma1}$), 3.42 – 3.34 (m, 1H, Dab$_{4\gamma2}$), 3.23 – 2.85 (m, 12H, Dab$_{1\gamma2}$ + Dab$_{3\gamma}$ + Dab$_{8\gamma}$ + Dab$_{9\gamma}$ + Dab$_{4\gamma2}$ + D-Phe$_{6\beta}$ + Dab$_{5\gamma}$), 2.52 – 2.42 (m, 1H, Dab$_{3\beta1}$), 2.31 – 1.90 (m, 14H, Dab$_{1\beta1}$ + Dab$_{3\beta2}$ + Dab$_{8\beta}$ + Dab$_{9\beta}$ + Dab$_{4\beta}$ + Dab$_{5\beta}$ + Di-C$_4$ CO-C$\underline{H}_2$-CH$_2$-CH$_3$), 1.84 – 1.75 (m, 1H, Dab$_{1\beta2}$), 1.69 – 1.59 (m, 4H, Di-C$_4$ CO-CH$_2$-C$\underline{H}_2$-CH$_3$), 1.54 – 1.46 (m, 1H Leu$_{7\beta1}$), 1.40 – 1.31 (m, 1H Leu$_{7\beta2}$), 1.29 – 1.15 (m, 6H, Thr$_{2\gamma}$ + Thr$_{10\gamma}$), 0.98 – 0.91 (m, 6H, Di-C$_4$ C$\underline{H}_3$), 0.88 – 0.58 (m, 7H, Leu$_{7\gamma}$ + Leu$_{7\delta}$). ^{13}C NMR (126 MHz, Methanol-d_4) δ: 175.60, 175.09, 173.87, 173.40, 172.60, 172.41, 172.33, 172.14,

171.83, 171.46, 171.32, 170.85, 135.84 (D-Phe$_6$ C without H), 128.85, 128.34, 126.72, 66.28, 65.77, 60.21, 59.32, 56.42, 51.94, 51.90, 51.84, 51.66, 51.49, 50.70, 49.92, 39.29, 37.64 (Di-C$_4$ CO-C$\underline{H}_2$-CH$_2$-CH$_3$), 37.21 (Di-C$_4$ CO-C$\underline{H}_2$-CH$_2$-CH$_3$), 36.64, 36.61, 36.44, 36.36, 35.96, 35.58, 34.90, 30.81, 30.25, 30.02, 28.70, 28.39, 23.52, 22.77, 22.17, 20.01, 19.15, 18.99 (Di-C$_4$ CO-CH$_2$-C$\underline{H}_2$-CH$_3$), 18.88 (Di-C$_4$ CO-CH$_2$-C$\underline{H}_2$-CH$_3$), 18.79, 12.67 (Di-C$_4$ CO-CH$_2$-CH$_2$-C$\underline{H}_3$), 12.63 (Di-C$_4$ CO-CH$_2$-CH$_2$-C$\underline{H}_3$). MALDI-TOF-MS m/z calcd for C$_{55}$H$_{95}$N$_{16}$O$_{14}$ (M + H)$^+$ monoisotopic peak: 1203.721; found 1203.717.

Dioctanoic acid (Di-C8) polymyxin (2). ^{1}H NMR (500 MHz, Methanol-d_4) δ 7.31 − 7.19 (m, 5H, D-Phe$_6$ aromatic), 4.51 (dd, J = 8.8, 4.4 Hz, 1H, Dab$_{5\alpha}$), 4.46 − 4.38 (m, 2H, Dab$_{1\alpha}$ + Dab$_{3\alpha}$), 4.38 − 4.24 (m, 5H, Dab$_{4\alpha}$ + Dab$_{8\alpha}$ + Dab$_{8\alpha}$ + D-Phe$_{6\alpha}$ + Thr$_{2\beta}$), 4.24 − 4.20 (m, 1H, Thr$_{2\alpha}$), 4.20 − 4.14 (m, 1H, Thr$_{10\beta}$), 4.14 − 4.09 (m, 1H, Leu$_{7\alpha}$), 4.06 (d, J = 3.1 Hz, 1H, Thr$_{10\alpha}$), 3.67 − 3.53 (m, 1H, Dab$_{4\gamma1}$), 3.42 − 3.34 (m, 1H, Dab$_{1\gamma1}$), 3.23 − 3.12 (m, 2H, Dab$_{1\gamma2}$ + Dab$_{4\gamma2}$), 3.12 − 2.87 (m, 10H, Dab$_{3\gamma}$ + Dab$_{8\gamma}$ + Dab$_{9\gamma}$ + D-Phe$_{6\beta}$ + Dab$_{5\gamma}$), 2.53 − 2.41 (m, 1H, Dab$_{3\beta1}$), 2.33 − 2.16 (m, 7H, Dab$_{1\beta1}$ + Dab$_{5\beta}$ + Di-C$_8$ CO-C$\underline{H}_2$-), 2.16 − 1.92 (m, 7H, Dab$_{3\beta2}$ + Dab$_{8\beta}$ + Dab$_{9\beta}$ + Dab$_{4\beta}$), 1.82 − 1.73 (m, 1H, Dab$_{1\beta2}$), 1.67 − 1.56 (m, 4H, Di-C$_8$ CO-CH$_2$-C$\underline{H}_2$-), 1.54 − 1.46 (m, 1H, Leu$_{7\beta1}$), 1.40 − 1.25 (m, 17H, Leu$_{7\beta2}$ + Di-C$_8$ alkyl), 1.25 − 1.08 (m, 6H, Thr$_{2\gamma}$ + Thr$_{10\gamma}$), 0.89 (t, J = 6.6 Hz, 6H, Di-C$_8$ C$\underline{H}_3$), 0.84 − 0.78 (m, 1H, Leu$_{7\gamma}$), 0.78 − 0.57 (m, 6H, Leu$_{7\delta}$). ^{13}C NMR (126 MHz, Methanol-d$_4$) δ 175.68, 175.29, 173.88, 173.36, 172.59, 172.40, 172.38, 172.12, 171.82, 171.45, 171.32, 170.82, 135.85(D-Phe$_6$ C without H), 128.85, 128.34, 126.72, 66.32, 65.79, 59.30, 56.39, 51.81, 51.67, 51.58, 51.48, 51.45, 49.91, 48.19, 48.02, 47.85, 47.68, 39.33, 39.30, 36.64, 36.61, 36.47, 36.43, 36.36, 35.96(Di-C$_8$ CO-C$\underline{H}_2$-), 35.80(Di-C$_8$ CO-C$\underline{H}_2$-), 35.62, 35.38, 34.92, 31.46, 30.85, 30.24, 30.01, 29.99, 28.93, 28.86, 28.71, 28.37, 25.68(Di-C$_8$ CO-CH$_2$-C$\underline{H}_2$-), 25.65(Di-C$_8$ CO-CH$_2$-C$\underline{H}_2$-

), 25.57, 23.56, 23.53, 22.25, 22.16, 20.02, 19.16, 18.78, 13.01(Di-C$_8$ $\underline{C}$H$_3$), 12.97(Di-C$_8$ $\underline{C}$H$_3$).

MALDI-TOF-MS m/z calcd for C$_{63}$H$_{111}$N$_{16}$O$_{14}$ (M + H)$^+$ monoisotopic peak: 1315.846; found 1315.865.

Didodecanoic acid (Di-C12) polymyxin (3). ^{1}H NMR (500 MHz, Methanol-d_4) δ: 7.31 − 7.17 (m, 5H, D-Phe$_6$ aromatic), 4.59 − 4.50 (m, 1H, Dab$_{5α}$), 4.50 − 4.26 (m, 7H, Dab$_{1α}$ + Dab$_{3α}$ + Dab$_{4α}$ + Dab$_{8α}$ + D-Phe$_{6α}$ + Thr$_{2β}$ + Dab$_{9α}$), 4.23 (d, J = 3.4 Hz, 1H, Thr$_{2α}$), 4.21 − 4.15 (m, 1H, Thr$_{10β}$), 4.15 − 4.09 (m, 1H, Leu$_{7α}$), 4.03 (d, J = 3.7 Hz, 1H, Thr$_{10α}$), 3.73 − 3.58 (m, 1H, Dab$_{4γ1}$), 3.41 − 3.34 (m, 1H, Dab$_{1γ1}$), 3.21 − 2.82 (m, 12H, Dab$_{1γ2}$ + Dab$_{4γ2}$ + Dab$_{3γ}$ + Dab$_{8γ}$ + Dab$_{9γ}$ + D-Phe$_{6β}$ + Dab$_{5γ}$), 2.76 − 2.67 (m, 1H), 2.51 − 2.36 (m, 1H, Dab$_{3β1}$), 2.33 − 1.93 (m, 14H. Dab$_{1β1}$ + Dab$_{5β}$ + Di-C$_{12}$ CO-C$\underline{H}$$_2$- + Dab$_{3β2}$ + Dab$_{8β}$ + Dab$_{9β}$ + Dab$_{4β}$), 1.85 − 1.78 (m, 1H, Dab$_{1β2}$), 1.64 − 1.56 (m, 4H, Di-C$_{12}$ CO-CH$_2$-C$\underline{H}$$_2$-), 1.54 − 1.47 (m, 1H, Leu$_{7β1}$), 1.46 − 1.41 (m, 1H, Leu$_{7β2}$), 1.34 − 1.25 (m, 32H, Di-C$_{12}$ alkyl), 1.23 − 1.13 (m, 6H, Thr$_{2γ}$ + Thr$_{10γ}$), 0.95 − 0.63 (m, 13H, Di-C$_{12}$ C$\underline{H}$$_{3}$ $_+$, Leu$_{7γ}$ $_+$ Leu$_{7δ}$).^{13}C NMR (126 MHz Methanol-d_4) δ: 175.68, 175.30, 173.89, 173.37, 173.10, 172.80, 172.58, 172.18, 171.84, 171.47, 171.32, 171.24, 129.05(D-Phe$_6$ C without H), 128.90, 128.88, 128.34, 128.23, 126.72, 76.43, 75.43, 74.83, 73.01, 66.35, 65.79, 59.30, 56.43, 51.60, 51.46, 49.98, 49.64, 39.30, 36.67, 36.48, 36.45(Di-C$_{12}$ CO-$\underline{C}$H$_2$-), 36.36(Di-C$_{12}$ CO-$\underline{C}$H$_2$-), 35.81, 35.64, 35.40, 31.63, 29.33, 29.31, 29.23, 29.06, 29.03, 28.98, 28.66, 25.69(Di-C$_{12}$ CO-CH$_2$-$\underline{C}$H$_2$-), 25.66(Di-C$_{12}$ CO-CH$_2$-$\underline{C}$H$_2$-), 25.57, 23.53, 22.29, 22.17, 20.02, 19.40, 19.16, 18.79, 13.00(Di-C$_{12}$ $\underline{C}$H$_3$), 12.99(Di-C$_{12}$ $\underline{C}$H$_3$) MALDI-TOF-MS m/z calcd for C$_{71}$H$_{127}$N$_{16}$O$_{14}$ (M + H)$^+$ monoisotopic peak: 1427.971; found 1428.006

Diadamantane acetic acid (Di-adamantyl) polymyxin (4). ^{1}H NMR (500 MHz, Methanol-d_4) δ: 7.32 − 7.20 (m, 5H, D-Phe$_6$ aromatic), 4.51 (dd, J = 8.7, 4.3 Hz, 1H, Dab$_{5α}$), 4.47 − 4.32 (m, 5H,

Dab$_{1\alpha}$ + Dab$_{3\alpha}$ + Dab$_{4\alpha}$ + Dab$_{8\alpha}$ + D-Phe$_{6\alpha}$), 4.32 − 4.26 (m, 2H, Dab$_{9\alpha}$ + Thr$_{2\beta}$), 4.25 − 4.22 (m,

Thr$_{2\alpha}$ 1H), 4.22 − 4.15 (m, 1H, Thr$_{10\beta}$), 4.12 (dd, J = 11.5, 3.4 Hz, 1H, Leu$_{7\alpha}$), 4.07 (d, J = 4.6 Hz,

1H, Thr$_{10\alpha}$), 3.69 − 3.54 (m, 1H, Dab$_{4\gamma1}$), 3.43 − 3.35 (m, 1H, Dab$_{1\gamma1}$), 3.19 − 2.86 (m, 12H, Dab$_{1\gamma2}$

+ Dab$_{4\gamma2}$ + Dab$_{3\gamma}$ + Dab$_{5\gamma}$ + Dab$_{8\gamma}$ + Dab$_{9\gamma}$ + D-Phe$_{6\beta}$), 2.55 − 2.41 (m, 1H, Dab$_{3\beta1}$), 2.30 − 2.20 (m,

2H, Dab$_{8\beta}$), 2.20 − 2.05 (m, 5H, Dab$_{1\beta1}$ + Dab$_{5\beta1}$ + Dab$_{3\beta2}$ + Dab$_{9\beta}$), 2.04 − 1.91 (m, 13H, Dab$_{5\beta2}$ +

Dab$_{4\beta}$ + Di-adamantyl CO-C$\underline{H}_2$- + Di-adamantyl -C$\underline{H}$-), 1.82 − 1.76 (m, 1H, Dab$_{1\beta2}$), 1.75 − 1.59

(m, 24H, Di-adamantyl -C$\underline{H}_2$-), 1.54 − 1.47 (m, 1H, Leu$_{7\beta1}$), 1.39 − 1.32 (m, 1H, Leu$_{7\beta2}$), 1.29 −

1.15 (m, 6H, Thr$_{2\gamma}$ + Thr$_{10\gamma}$), 1.00 − 0.86 (m, 1H, Leu$_{7\gamma}$), 0.82 − 0.62 (m, 6H, Leu$_{7\delta}$). ^{13}C NMR (126

MHz, Methanol-d_4) δ: 173.89, 173.31, 173.20, 172.85, 172.62, 172.47, 172.33, 172.26, 171.91,

171.56, 171.39, 171.30, 135.82(D-Phe$_6$ C without H), 128.88, 128.35, 128.18, 126.72, 126.67,

66.43, 65.71, 59.36, 59.12, 56.45, 51.96, 51.87, 51.64, 51.54, 50.59(Di-adamantyl CO-$\underline{C}$H$_2$),

50.55(Di-adamantyl CO-$\underline{C}$H$_2$), 49.99, 42.40(Di-adamantyl -$\underline{C}$H$_2$-), 42.30(Di-adamantyl -$\underline{C}$H$_2$-),

39.26, 36.67, 36.43, 36.40, 36.01, 35.68, 34.93, 32.67(Di-adamantyl -$\underline{C}$-), 32.48(Di-adamantyl -

$\underline{C}$-), 31.02, 28.73(Di-adamantyl -$\underline{C}$H-), 28.71(Di-adamantyl -$\underline{C}$H-), 23.49, 22.20, 20.03, 19.16,

18.89. MALDI-TOF-MS m/z calcd for $C_{71}H_{115}N_{16}O_{14}$ (M + H)$^+$ monoisotopic peak: 1415.877;

found 1415.865

Dibiphenyl-4-carboxylic acid (Di-biphenyl) polymyxin (5). ^{1}H NMR (500 MHz, Methanol-d_4) δ:

8.01 − 7.89 (m, 4H, Di-biphenyl aromatic), 7.76 − 7.57 (m, 8H, Di-biphenyl aromatic), 7.47 − 7.36

(m, 6H, Di-biphenyl aromatic), 7.29 − 7.18 (m, 5H, D-Phe$_6$ aromatic), 4.73 − 4.66 (m, 1H, Dab$_{5\alpha}$),

4.52 − 4.39 (m, 3H, Dab$_{1\alpha}$ + Dab$_{3\alpha}$ + D-Phe$_{6\alpha}$), 4.40 − 4.24 (m, 5H, Dab$_{4\alpha}$ + Dab$_{8\alpha}$ + Dab$_{9\alpha}$ + Thr$_{2\beta}$

+ Thr$_{2\alpha}$), 4.21 − 4.10 (m, 2H, Thr$_{10\beta}$ + Leu$_{7\alpha}$), 4.05 (d, J = 4.8 Hz, 1H, Thr$_{10\alpha}$), 3.78 − 3.71 (m, 1H,

Dab$_{1\gamma1}$), 3.69 − 3.60 (m, 1H, Dab$_{4\gamma1}$), 3.57 − 3.51 (m, 1H, Dab$_{1\gamma2}$), 3.19 − 2.88 (m, 11H, Dab$_{4\gamma2}$ +

$Dab_{3\gamma} + Dab_{5\gamma} + Dab_{8\gamma} + Dab_{9\gamma} + D\text{-}Phe_{6\beta}$), 2.50 − 2.41 (m, 1H, $Dab_{3\beta1}$), 2.39 − 2.31 (m, 2H, $Dab_{8\beta}$), 2.30 − 2.25 (m, 1H, + $Dab_{5\beta1}$), 2.22 − 2.11 (m, 4H, $Dab_{1\beta1} + Dab_{3\beta2} + Dab_{4\beta}$), 2.04 − 1.92 (m, 3H, $Dab_{5\beta2} + Dab_{9\beta}$), 1.87 − 1.80 (m, 1H, $Dab_{1\beta2}$), 1.54 − 1.47 (m, 1H, $Leu_{7\beta1}$), 1.38 − 1.32 (m, 1H, $Leu_{7\beta2}$), 1.26 − 1.11 (m, 6H, $Thr_{2\gamma} + Thr_{10\gamma}$), 0.95 − 0.87 (m, 1H, $Leu_{7\gamma}$), 0.82 − 0.60 (m, 6H, $Leu_{7\delta}$). ^{13}C NMR (126 MHz, Methanol-d_4) δ: 173.91, 173.81, 173.71, 173.68, 173.51, 172.44, 171.48, 171.46, 171.27, 170.94, 169.31(Di-biphenyl carbonyl), 168.81(Di-biphenyl carbonyl), 144.81(Di-biphenyl C without H), 144.77(Di-biphenyl C without H), 144.39(Di-biphenyl C without H), 144.35(Di-biphenyl C without H), 139.71(Di-biphenyl C without H), 139.64(Di-biphenyl C without H), 135.82(D-Phe_6 C without H), 132.66, 132.62, 131.88, 128.90, 128.86, 128.63, 128.62, 128.34, 128.20, 127.92, 127.81, 127.72, 127.58, 126.68, 119.99, 117.70, 117.65, 115.36, 115.30, 66.37, 66.35, 59.67, 59.58, 56.22, 52.66, 51.91, 51.89, 51.87, 51.53, 51.11, 50.96, 45.93, 39.29, 36.73, 36.65, 36.61, 36.56, 36.44, 36.39, 36.00, 30.66, 30.13, 29.30, 28.94, 28.69, 28.43, 25.88, 23.54, 23.31, 22.17, 20.02, 19.13, 18.80. MALDI-TOF-MS m/z calcd for $C_{73}H_{99}N_{16}O_{14}$ $(M + H)^+$ monoisotopic peak: 1423.752; found 1423.767

Biological studies. Bacterial strains were either obtained from the American Type Culture Collection (ATCC), Canadian National Intensive Care Unit (CAN-ICU) surveillance study (21) or the Canadian Ward Surveillance (CANWARD) study (22). Strains from both CAN-ICU and CANWARD are isolates recovered from patients diagnosed with a presumed infectious disease that were admitted in a participating medical center across Canada. Efflux-deficient strain PAO200 (lacking MexAB-OprM efflux system) and PAO750 (lacking MexAB-OprM, MexCD-OprJ, MexEF-OprN, MexJK and MexXY efflux systems, and the outer membrane protein OpmH) were kindly gifted by Dr. Ayush Kumar (University of Manitoba).

Antimicrobial susceptibility assay. The *in vitro* antibacterial activity of the compounds under study were assessed by broth microdilution susceptibility testing following CLSI guidelines (29). Bacterial cultures were grown overnight prior to the assay. The overnight grown cultures were diluted in saline (0.85% NaCl) to 0.5 McFarland turbidity, followed by 1:50 dilution in Mueller-Hinton broth (MHB) for inoculation to a final concentration of approximately 5×10^5 colony forming units/mL. Testing was performed on 96-well plates where the tested compounds were 2-fold serially diluted in MHB and incubated with equal volumes of bacterial inoculum at 37 °C for 18 h. The MIC was determined as the lowest concentration of the compound to inhibit visible bacterial growth in the form of turbidity, which was confirmed *via* an EMax Plus microplate reader (Molecular Devices, USA) at a wavelength of 590 nm. Wells containing MHB with or without bacterial cells were used as positive or negative controls, respectively.

Checkerboard assay. The assay was performed on 96-well plates as previously described (20, 30). Briefly, the antibiotic under study was 2-fold serially diluted along the x-axis, while the adjuvant was 2-fold serially diluted along the y-axis to create a matrix in which each well consists of a combination of both at different concentrations. Overnight grown bacterial cultures were diluted in saline (0.85% NaCl) to 0.5 McFarland turbidity, followed by 1:50 dilution in MHB and inoculation on each well to a final concentration of approximately 5×10^5 colony forming units/mL. Wells containing only MHB with or without bacterial cells were used as positive or negative controls, respectively. Plates were incubated at 37 °C for 18 h and examined for visible turbidity, which was confirmed *via* an EMax Plus microplate reader (Molecular Devices, USA) at a wavelength of 590 nm. The fractional inhibitory concentration (FIC) of the antibiotic was

calculated by dividing the MIC of antibiotic in the presence of adjuvant by the MIC of antibiotic alone. Similarly, the FIC of adjuvant was calculated *via* dividing the MIC of adjuvant in the presence of antibiotic by the MIC of adjuvant alone. The FIC index was obtained by the summation of both FIC values. The FIC index was then interpreted as synergistic, additive, or antagonistic for values of $\leq$0.5, 0.5 < x < 4, or $\geq$4, respectively (25).

Hemolytic assay. The ability of the compounds to lyse eukaryotic red blood cells was measured by the amount of hemoglobin released upon incubation with pig erythrocytes, following a published protocol (30). Briefly, fresh pig blood (generously provided by Dr. Richard Hodges, Director of Animal Care and Veterinary Services of the University of Manitoba) drawn from a pig's antecubital vein was centrifuged at 1000g for 5 min at 4 °C, washed with phosphate-buffered saline (PBS) three times, and re-suspended in the same buffer, consecutively. Compounds under study were 2-fold serially diluted in PBS on a 96-well plate and mixed with equal volumes of erythrocyte solution. Post 1 h incubation at 37 °C, the intact cells were pelleted by centrifugation at 1000g for 5 min at 4 °C. The resulting supernatant was then transferred to a new 96-well plate. The hemoglobin released was then measured *via* an EMax Plus microplate reader (Molecular Devices, USA) at 570 nm wavelength. Erythrocytes in PBS with or without 0.1% Triton X-100 were used as positive or negative control, respectively.

6.8. Acknowledgements

6.9. References

1. Pogue JM, Ortwine JK, Kaye KS. 2017. Clinical considerations for optimal use of the polymyxins: A focus on agent selection and dosing. Clin Microbiol Infect 23:229–233.

2. Pogue JM, Ortwine JK, Kaye KS. 2016. Are there any ways around the exposure-limiting nephrotoxicity of the polymyxins? Int J Antimicrob Agents 48:622–626.

3. Zusman O, Altunin S, Koppel F, Dishon Benattar Y, Gedik H, Paul M. 2017. Polymyxin monotherapy or in combination against carbapenem-resistant bacteria: systematic review and meta-analysis. J Antimicrob Chemother 72:29–39.

4. Velkov T, Thompson PE, Nation RL, Li J. 2010. Structure-activity relationships of polymyxin antibiotics. J Med Chem 53:1898–1916.

5. Velkov T, Soon RL, Chong PL, Huang JX, Cooper MA, Azad MAK, Baker MA, Thompson PE, Roberts K, Nation RL, Clements A, Strugnell RA, Li J. 2013. Molecular basis for the increased polymyxin susceptibility of Klebsiella pneumoniae strains with under-acylated lipid A. Innate Immun 19:265–277.

6. Dixon RA, Chopra I. 1986. Polymyxin B and polymyxin B nonapeptide alter cytoplasmic membrane permeability in Escherichia coli. J Antimicrob Chemother 18:557–563.

7. Deris ZZ, Swarbrick JD, Roberts KD, Azad MAK, Akter J, Horne AS, Nation RL, Rogers KL, Thompson PE, Velkov T, Li J. 2014. Probing the penetration of antimicrobial polymyxin lipopeptides into Gram-negative bacteria. Bioconjug Chem 25:750–760.

8. Scott MG, Gold MR, Hancock RE. 1999. Interaction of cationic peptides with lipoteichoic acid and gram-positive bacteria. Infect Immun 67:6445–6453.

9.   Kanazawa K, Sato Y, Ohki K, Okimura K, Uchida Y, Shindo M, Sakura N. 2009. Contribution of each amino acid residue in polymyxin B(3) to antimicrobial and lipopolysaccharide binding activity. Chem Pharm Bull (Tokyo) 57:240–244.

10.   Gallardo-Godoy A, Muldoon C, Becker B, Elliott AG, Lash LH, Huang JX, Butler MS, Pelingon R, Kavanagh AM, Ramu S, Phetsang W, Blaskovich MAT, Cooper MA. 2016. Activity and predicted nephrotoxicity of synthetic antibiotics based on polymyxin B. J Med Chem 59:1068–1077.

11.   Danner RL, Joiner KA, Rubin M, Patterson WH, Johnson N, Ayers KM, Parrillo JE. 1989. Purification, toxicity, and antiendotoxin activity of polymyxin B nonapeptide. Antimicrob Agents Chemother 33:1428–1434.

12.   Ofek I, Cohen S, Rahmani R, Kabha K, Tamarkin D, Herzig Y, Rubinstein E. 1994. Antibacterial synergism of polymyxin B nonapeptide and hydrophobic antibiotics in experimental gram-negative infections in mice. Antimicrob Agents Chemother 38:374–377.

13.   Tsubery H, Ofek I, Cohen S, Fridkin M. 2000. Structure-function studies of polymyxin B nonapeptide: implications to sensitization of gram-negative bacteria. J Med Chem 43:3085–3092.

14.   Tsubery H, Ofek I, Cohen S, Eisenstein M, Fridkin M. 2002. Modulation of the hydrophobic domain of polymyxin B nonapeptide: effect on outer-membrane permeabilization and lipopolysaccharide neutralization. Mol Pharmacol 62:1036–1042.

15.   Vaara M, Siikanen O, Apajalahti J, Fox J, Frimodt-Moller N, He H, Poudyal A, Li J, Nation RL, Vaara T. 2010. A novel polymyxin derivative that lacks the fatty acid tail and

carries only three positive charges has strong synergism with agents excluded by the intact outer membrane. Antimicrob Agents Chemother 54:3341–3346.

16.   Domalaon R, Idowu T, Zhanel GG, Schweizer F. 2018. Antibiotic hybrids: the next generation of agents and adjuvants against Gram-negative pathogens? Clin Microbiol Rev 31.

17.   Corbett D, Wise A, Langley T, Skinner K, Trimby E, Birchall S, Dorali A, Sandiford S, Williams J, Warn P, Vaara M, Lister T. 2017. Potentiation of antibiotic activity by a novel cationic peptide: potency and spectrum of activity of SPR741. Antimicrob Agents Chemother 61.

18.   Han M-L, Velkov T, Zhu Y, Roberts KD, Le Brun AP, Chow SH, Gutu AD, Moskowitz SM, Shen H-H, Li J. 2018. Polymyxin-induced lipid A deacylation in *Pseudomonas aeruginosa* perturbs polymyxin penetration and confers high-level resistance. ACS Chem Biol 13:121–130.

19.   Kinoshita Y, Yakushiji F, Matsui H, Hanaki H, Ichikawa S. 2018. Study of the structure-activity relationship of polymyxin analogues. Bioorg Med Chem Lett.

20.   Domalaon R, Yang X, Lyu Y, Zhanel GG, Schweizer F. 2017. Polymyxin B3-tobramycin hybrids with *Pseudomonas aeruginosa*-selective antibacterial activity and strong potentiation of rifampicin, minocycline, and vancomycin. ACS Infect Dis 3:941–954.

21.   Zhanel GG, DeCorby M, Laing N, Weshnoweski B, Vashisht R, Tailor F, Nichol K a., Wierzbowski A, Baudry PJ, Karlowsky J a., Lagacé-Wiens P, Walkty A, McCracken M, Mulvey MR, Johnson J, Hoban DJ. 2008. Antimicrobial-resistant pathogens in intensive care units in Canada: results of the Canadian National Intensive Care Unit (CAN-ICU)

study, 2005-2006. Antimicrob Agents Chemother 52:1430–1437.

22. Zhanel GG, Adam HJ, Baxter MR, Fuller J, Nichol KA, Denisuik AJ, Lagacé-Wiens PRS, Walkty A, Karlowsky JA, Schweizer F, Hoban DJ, Canadian Antimicrobial Resistance Alliance. 2013. Antimicrobial susceptibility of 22746 pathogens from Canadian hospitals: results of the CANWARD 2007-11 study. J Antimicrob Chemother 68 Suppl 1:7–22.

23. Velkov T, Deris ZZ, Huang JX, Azad MAK, Butler M, Sivanesan S, Kaminskas LM, Dong Y-D, Boyd B, Baker MA, Cooper MA, Nation RL, Li J. 2014. Surface changes and polymyxin interactions with a resistant strain of Klebsiella pneumoniae. Innate Immun 20:350–363.

24. Walkty A, Karlowsky JA, Adam HJ, Lagace-Wiens P, Baxter M, Mulvey MR, McCracken M, Poutanen SM, Roscoe D, Zhanel GG. 2016. Frequency of MCR-1-mediated colistin resistance among Escherichia coli clinical isolates obtained from patients in Canadian hospitals (CANWARD 2008-2015). C open 4:E641–E645.

25. Meletiadis J, Pournaras S, Roilides E, Walsh TJ. 2010. Defining fractional inhibitory concentration index cutoffs for additive interactions based on self-drug additive combinations, Monte Carlo simulation analysis, and in vitro-in vivo correlation data for antifungal drug combinations against Aspergillus fumi. Antimicrob Agents Chemother 54:602–609.

26. Masuda N, Sakagawa E, Ohya S, Gotoh N, Tsujimoto H, Nishino T. 2000. Substrate specificities of MexAB-OprM, MexCD-OprJ, and MexXY-oprM efflux pumps in *Pseudomonas aeruginosa*. Antimicrob Agents Chemother 44:3322–3327.

27. Chuanchuen R, Narasaki CT, Schweizer HP. 2002. The MexJK efflux pump of

Pseudomonas aeruginosa requires OprM for antibiotic efflux but not for efflux of triclosan. J Bacteriol 184:5036–5044.

28. Domalaon R, Yang X, O'Neil J, Zhanel GG, Mookherjee N, Schweizer F. 2014. Structure-activity relationships in ultrashort cationic lipopeptides: the effects of amino acid ring constraint on antibacterial activity. Amino Acids 46:2517–2530.

29. The Clinical and Laboratory Standards Institute. 2016. Performance Standards for Antimicrobial Susceptibility Testing CLSI supplement M100S 26th ed. Clin Lab Stand Institute, Wayne, PA.

30. Domalaon R, Sanchak Y, Koskei LC, Lyu Y, Zhanel GG, Arthur G, Schweizer F. 2018. Short proline-rich lipopeptide potentiates minocycline and rifampin against multidrug- and extensively drug-resistant *Pseudomonas aeruginosa*. Antimicrob Agents Chemother 62.

6.10. Concluding remarks

This chapter highlighted my efforts in exploring the effect of hydrophobicity on polymyxin's biological activity through their fatty acid component. Several interesting biological trends were discovered, such as the presence of dilipid fragments upon polymyxin resulted in an enhancement of antibacterial activity against Gram-positive bacteria. Moreover, this study revealed a dilipid polymyxin analog that possessed the ability to potentiate other classes of antibiotics, in combination, similar to the adjuvant properties of the well-known polymyxin B nonapeptide. Interestingly, we disclosed, for the first time, data suggesting that the length of the lipid component in polymyxins to be responsible on their ability to resist active efflux in *P. aeruginosa*.

Note that complimentary data for this Chapter is provided in Appendix I.

My interest in polymyxins continues in Chapter 7 where I successfully covalently attached polymyxin B_3 to the aminoglycoside antibiotic tobramycin, yielding for the first time polymyxin-aminoglycoside antibiotic hybrids.

Chapter 7: Development of polymyxin B$_3$-tobramycin hybrid as antipseudomonal agent and adjuvant

This chapter is based on my publication:

7.1. Introductory remarks

Antibiotic hybrids, as discussed in chapter 2, are agents composed of two covalently linked antibiotics bound together by a molecular linker/tether. My interest in the peptide antibiotic polymyxin is apparent from the previous chapter, where I performed a structure-activity relationship study on the effects of the fatty acid component on the biological activity (antibacterial, adjuvant and resistance to efflux) of polymyxins. In this chapter, polymyxin B$_3$ was covalently appended to the aminoglycoside tobramycin to yield polymyxin-aminoglycoside antibiotic hybrids for the first time in the literature. Their antibacterial activities as a stand-alone drug and as an adjuvant partner to clinically-used antibiotics were assessed against multidrug-resistant *Pseudomonas aeruginosa* clinical isolates.

7.2. Contributions of authors

Ronald Domalaon prepared, purified and characterized all hybrid compounds for this study, with minor help in synthesizing one of the tobramycin intermediates from Xuan Yang. Ronald Domalaon evaluated the microbiological activity of all the compounds alone and in combination with other antibiotics in this study. George G. Zhanel and Frank Schweizer guided the antimicrobial evaluation of the compounds. Ronald Domalaon and Yinfeng Lyu assessed the hemolytic properties of all the hybrid compounds. Ronald Domalaon interpreted all the chemical and biological data with helpful insights from George G. Zhanel and Frank Schweizer. All authors were responsible for the final form of this research article.

7.3. Abstract

There is an urgent need to develop novel antibacterial agents able to eradicate drug-resistant Gram-negative pathogens such as *Pseudomonas aeruginosa*. Antimicrobial hybrids have emerged as a promising strategy to combat bacterial resistance, as a stand-alone drug but also as an adjuvant in combination with existing antibiotics. Herein, we report for the first time the synthesis and biological evaluation of polymyxin-aminoglycoside heterodimers composed of polymyxin B$_3$ covalently linked to tobramycin *via* an aliphatic hydrocarbon linker. The polymyxin B$_3$-tobramycin hybrids demonstrate potent activity against carbapenem-resistant as well as multidrug- or extensively drug-resistant (MDR/XDR) *P. aeruginosa* clinical isolates. Furthermore, the most potent hybrid was able to synergize with currently-used antibiotics against wild-type and MDR/XDR *P. aeruginosa*, but as well against *Acinetobacter baumannii*. The promising biological activity described herein warrants additional studies into design and development of new antimicrobial hybrids able to surmount the problem of antimicrobial resistance.

7.4. Introduction

Antimicrobial resistance is a pressing concern worldwide (1–3). An increasing incidence rate of drug-resistant bacterial infections has been observed in the past decade, to which effective antibiotics are dwindling down to a few (4, 5). Recently, the WHO released a list of priority pathogens that necessitate new and effective antibiotic treatments (6). Carbapenem-resistant Gram-negative *Acinetobacter baumannii*, *Pseudomonas aeruginosa* and *Enterobacteriaceae* lead the list, with new treatments for these pathogens tagged as of critical importance. A major hurdle in developing antimicrobials against Gram-negative pathogens is attaining sufficient intracellular accumulation. Intrinsic resistance, including a highly impermeable outer membrane (OM) and overexpressed efflux pumps, of Gram-negative bacteria prevent antimicrobials from achieving intracellular concentrations required to induce the desired biological effect. Moreover, the optimized physicochemical properties required for a molecule to traverse the OM are orthogonal to that for the inner membrane (7). As a result of insufficient permeability, many agents with potent (low nanomolar) activity against isolated enzymatic targets frequently exhibit poor whole cell activity in Gram-negative bacteria.

Scientific ingenuity has led to various strategies in drug discovery. The covalent fusion of two known drugs/pharmacophores or drug + delivery vehicle to form a unified heterodimer construct known as an antimicrobial hybrid is a promising strategy that has yielded several drug candidates (8–10). At least four antimicrobial hybrids are currently in clinical trials (11). The β-lactam-siderophore conjugate Cefiderocol (12) is currently in phase III clinical trials for the treatment of carbapenem-resistant Gram-negative bacterial infections, as well as for complicated urinary tract

infections. Cadazolid (13), consisting of a fused fluoroquinolone and oxazolidinone pharmacophores, is also currently in phase III clinical trials for the treatment *Clostridium difficile*-associated diarrhea. Two more hybrids (TD-1607 and MCB3837) are in Phase 1 trials (11).

Our group recently reported tobramycin-fluoroquinolone hybrids that are able to potentiate multiple classes of antibiotics against resistant Gram-negative bacilli (14, 15). For instance, we described tobramycin-ciprofloxacin (14) and tobramycin-moxifloxacin (15) hybrids that are able to sensitize fluoroquinolone-resistant multidrug- or extensively drug-resistant (MDR/XDR) *P. aeruginosa* to ciprofloxacin, moxifloxacin and levofloxacin. We also developed tobramycin-efflux pump inhibitor hybrids (16) and tobramycin-amphiphilic lysine peptoid hybrids (17) that were found to synergize with antibiotics subjected to intrinsic resistance in *P. aeruginosa*. Our results indicated that tobramycin attached to a twelve carbons-long (C12) aliphatic hydrocarbon linker (considered as an amphiphilic aminoglycoside) possesses intrinsic physicochemical properties for potentiating multiple classes of antibiotics; while the second pharmacophore enhances the antibacterial (biocidal) and/or adjuvant potency of the hybrid. Aminoglycosides are known to possess concentration-dependent bacterial killing. The aminoglycoside tobramycin eradicates Gram-negative bacteria by inhibition of protein translation at low concentrations while membrane rupture occurs at higher concentrations (18). Mechanistic studies of the tobramycin-fluoroquinolone hybrids revealed that the protein translation inhibitory effects of tobramycin were abolished while its membrane effects were significantly enhanced (14, 15). In addition, we have shown that tobramycin-based hybrids disrupt the outer membrane and affect the proton motive force of the cytoplasmic membrane in *P. aeruginosa* (15–17). Similar membrane actions were reported for other amphiphilic aminoglycosides (19, 20, 29, 21–28). Amphiphilic aminoglycosides

were also reported to possess beneficial immunomodulatory properties (30), which may be retained in tobramycin-based hybrids.

Polymyxin is a membrane-targeting decalipopeptide antibiotic used to treat MDR/XDR Gram-negative bacterial infections. It is known to exhibit synergistic interactions with other antibiotics by enhancing OM permeability (31) and is inert to efflux (32). Similar to the tobramycin-hybrid scaffold, polymyxin is also known to disrupt bacterial membranes and affect the proton motive force (33, 34). We therefore hypothesized that linking these two membranotropic pharmacophores would result in a hybrid with augmented antibacterial and adjuvant properties against MDR/XDR Gram-negative pathogens. To the best of our knowledge, there has not been any report of an antimicrobial hybrid containing an aminoglycoside fused to a polymyxin pharmacophore. Herein, we describe for the first time the synthesis and biological evaluation of polymyxin B_3-tobramycin hybrids.

7.5. Results and discussion

Design and synthesis of polymyxin B_3-tobramycin hybrids. The point of covalent attachment between the two chosen drugs is important to retain meaningful antimicrobial activity. Literature data suggests that the *C*-5 position of the cyclitol ring on tobramycin (**TOB**) is amenable to chemical modifications (19, 35). Alanine scanning of polymyxin B_3 (**PMB3**) found the amine side-chain of L-2,4-diaminobutyric acid (Dab) at amino acid position 1 to be pliable as it does not contribute to polymyxin's antibacterial activity (36). Therefore, we decided to fuse **TOB** and **PMB3** at the above-mentioned position *via* copper-assisted azide alkyne cycloaddition (Fig. 7-1).

The spatial distance between the two fused pharmacophores was also explored by incorporating hydrocarbon linkers of varying carbon-lengths, from four to twelve carbons-long.

n = 4; (**1a**)
n = 6; (**1b**)
n = 8; (**1c**)
n = 10; (**1d**)
n = 12; (**1e**)

Polymyxin B$_3$ (**PMB3**)
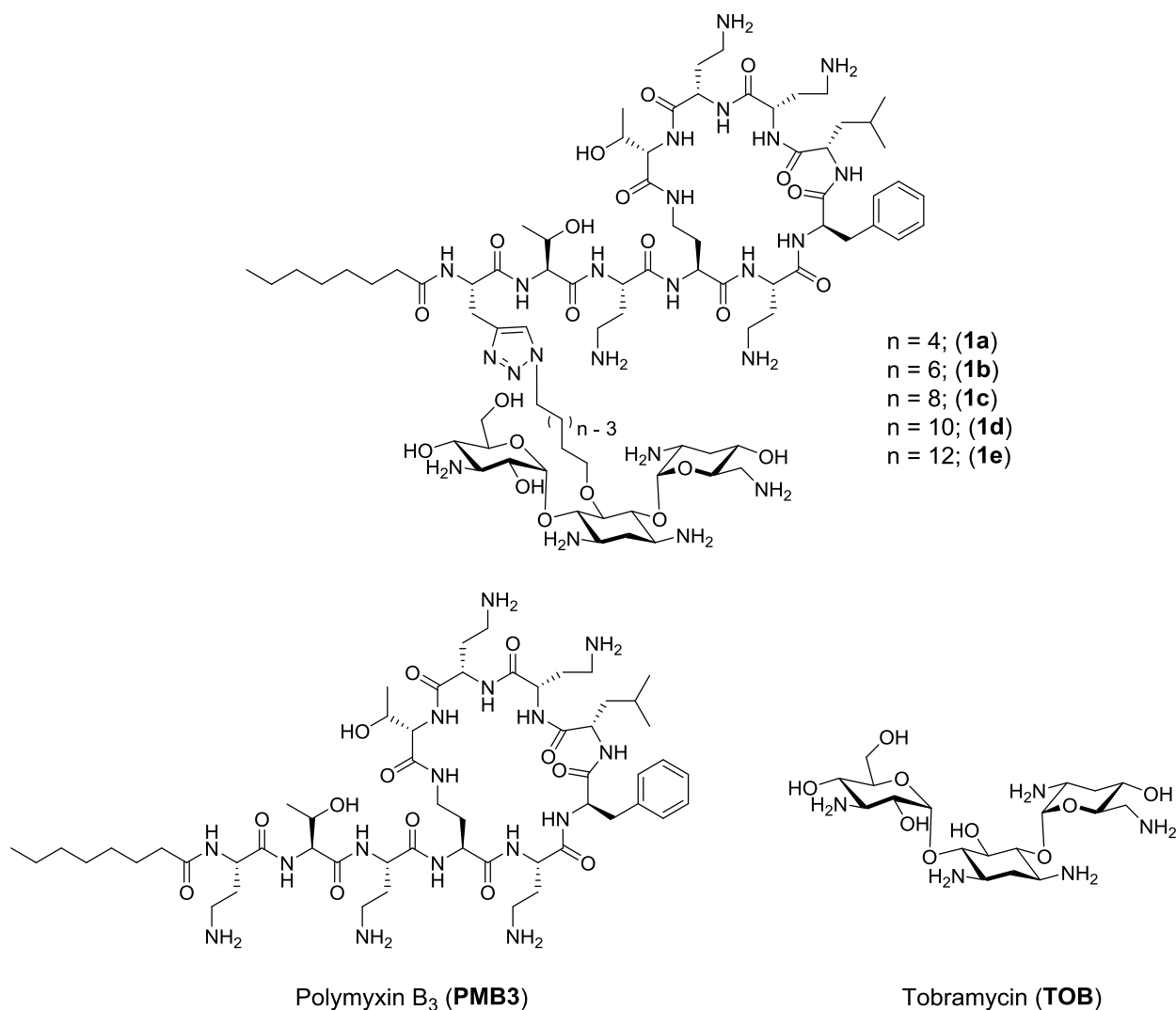
Tobramycin (**TOB**)

Figure 7-1 Chemical structure of polymyxin B$_3$-tobramycin hybrids (**1a-1e**), polymyxin B$_3$ (**PMB3**) and tobramycin (**TOB**).

The clinically-used polymyxin B is naturally-isolated as a mixture of chemically-related structures with minor differences on its fatty acyl group, among which polymyxin B$_1$ with 6-(S)-methyloctanoic acid and B$_2$ with 6-methylheptanoic acid as the major components of the mixture

(37). Polymyxin B$_3$ has an octanoic acid lipid portion that is more readily commercially available relative to the other fatty acyls. Given that all components in the polymyxin B mixture display similar antibacterial activity and do not interact synergistically with one another (38), we therefore decided to synthesize **PMB3** (see Appendix IV) as a reference. Following a reported protocol (39), standard solid-phase peptide synthesis on a Wang resin and subsequent solution-phase peptide intramolecular cyclization enabled the preparation of **PMB3**. The polymyxin B$_3$ to be fused with tobramycin (**3**) was synthesized similarly, with L-propargylglycine (Pra) instead of Dab at amino acid position 1, to effectively install an alkyne moiety (Scheme 7-1).
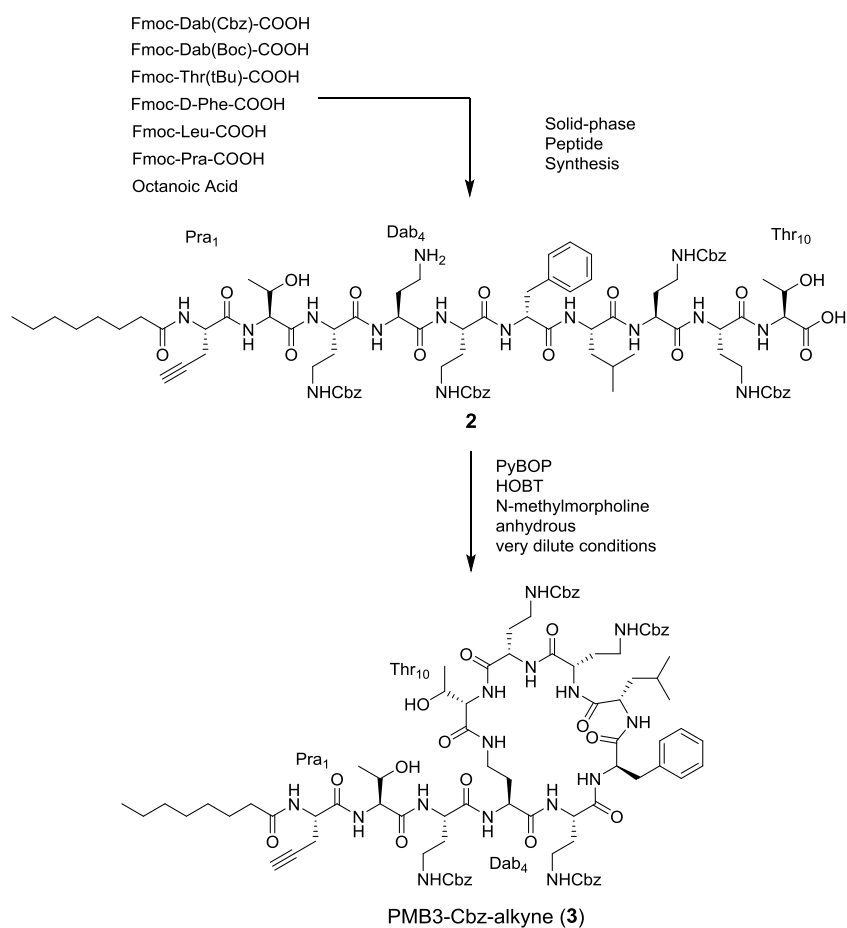
Scheme 7-1 Synthesis of polymyxin B$_3$ intermediate containing an alkyne functional group at amino acid position 1.
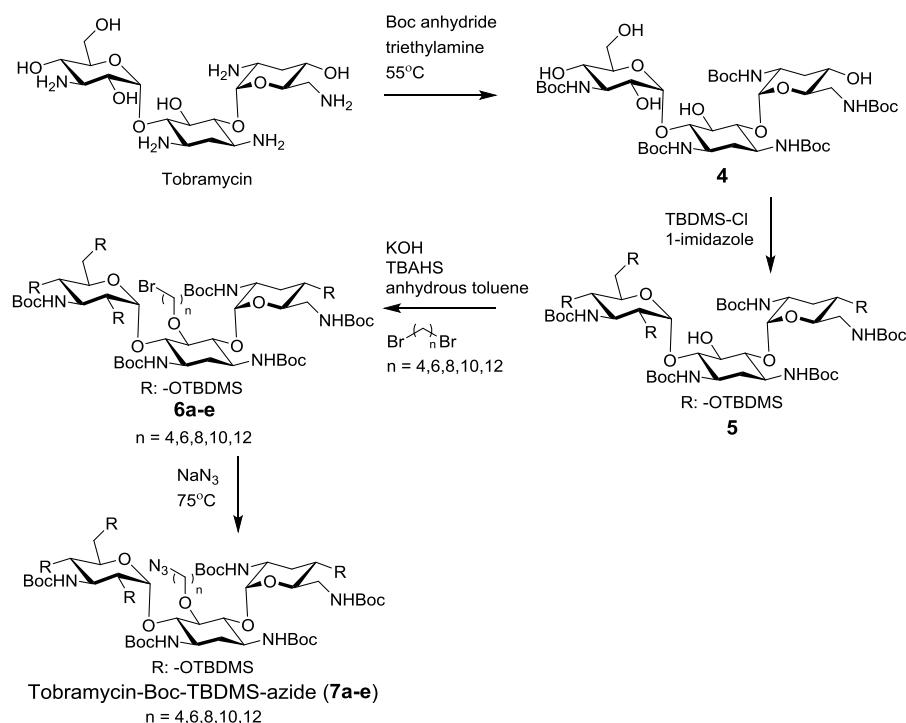
Scheme 7-2 Synthesis of tobramycin intermediate appended to the linker and azide functional group.

An azide moiety was installed on the tobramycin intermediates (**7a-e**) as outlined in Scheme 7-2.

All the reactive amine and alcohol groups, with the exception of the sterically-hindered *C*-5

alcohol, were masked following a published protocol (16). The aliphatic hydrocarbon, in the

form of a dibromoalkane, was appended to the free alcohol by phase-transfer catalysis using

tetrabutylammonium hydrogen sulfate (TBAHS) in anhydrous toluene. This resulted in a

tobramycin-intermediate that is already attached to the molecular linker (**6a-e**). The bromide was

then replaced by an azide to yield the desired intermediate.
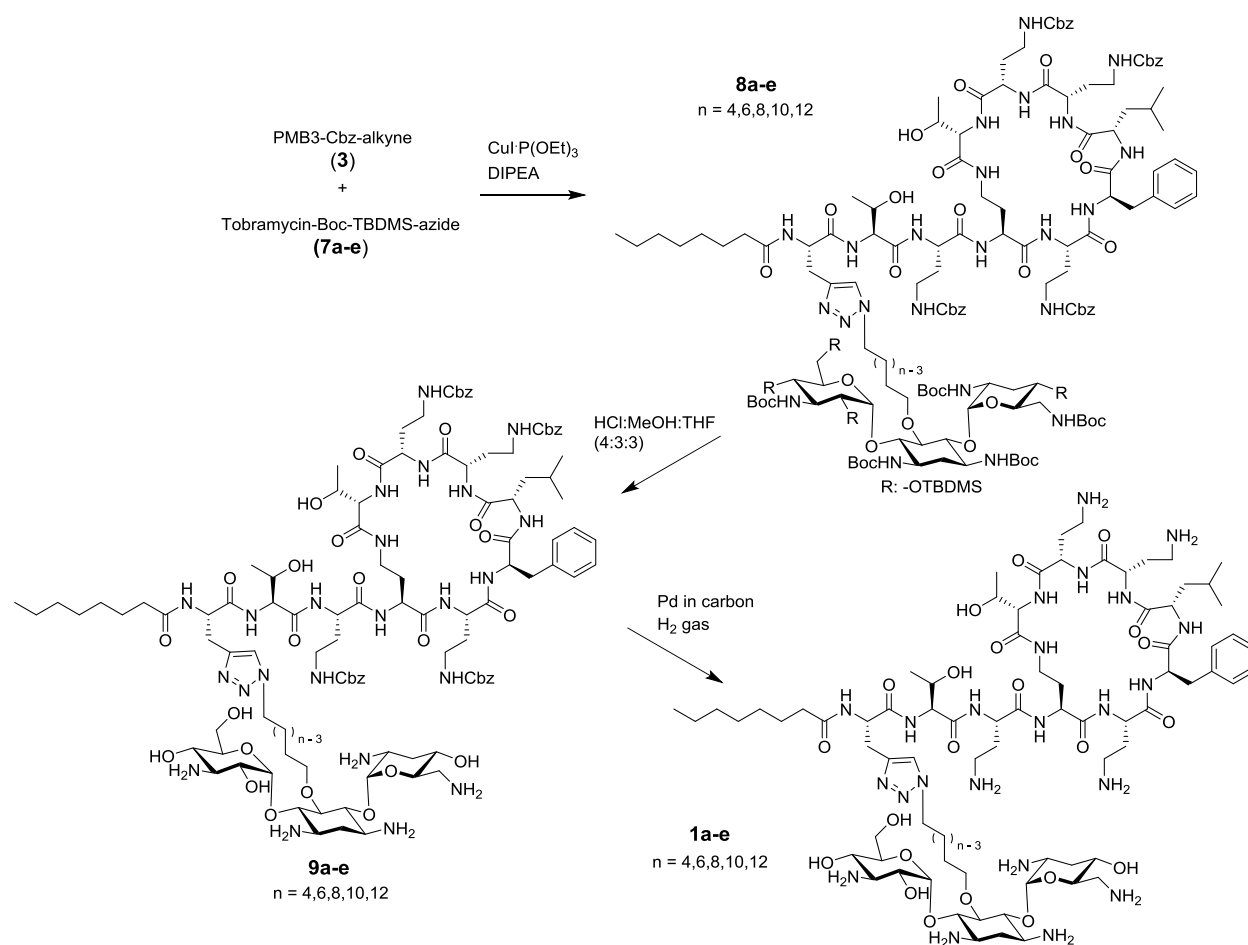
Scheme 7-3 Conjugation of polymyxin B$_3$ and tobramycin intermediates *via* copper-assisted azide alkyne cycloaddition.

The alkyne- and azide-containing intermediates were then fused together *via* copper-assisted azide alkyne cycloaddition to form a 1,2,3-triazole ring linkage (Scheme 7-3). Copper iodide triethylphosphite (CuI•P(OEt)$_3$) was used as an efficient copper source in DMF, along with the weak base diisopropylethylamine (DIPEA). The resulting heterodimer was then deblocked using HCl in a methanol and tetrahydrofuran mixture to remove the Boc- and TBDMS-protecting groups of the tobramycin portion. Subsequently, catalytic hydrogenolysis was used to deblock the remaining Cbz protecting groups of the polymyxin portion. Using this strategy, we were able to

prepare five polymyxin B_3-tobramycin hybrids (Fig. 7-1) containing a four (**1a**), six (**1b**), eight (**1c**), ten (**1d**) or twelve (**1e**) carbons-long aliphatic hydrocarbon linker.

Polymyxin B_3-tobramycin hybrids possess strong *Pseudomonas aeruginosa*-selective activity. We assessed the antibacterial activity of the polymyxin B_3-tobramycin hybrids against a panel of Gram-positive and Gram-negative pathogens (Table 7-1). The panel included clinical isolates from Canadian hospitals obtained through the Canadian National Intensive Care Unit (CAN-ICU) (40) and Canadian Ward Surveillance (CANWARD) (41) national surveillance studies. Minimum inhibitory concentration (MIC) values are reported both in µg/mL and µM for comparison. Antimicrobial hybrids have higher (2-fold or more) molecular weight relative to their respective parent antimicrobials and therefore would produce a higher MIC (less active) in µg/mL as the value is dependent on the molecular weight. For instance, the molecular weight of hybrid **1d** (2859.46 g/mol) is double than the commercially-available polymyxin B (1301.56 g/mol) and 5-fold higher than tobramycin (565.59 g/mol). An MIC value in µM would factor out the molecular weight bias, to which should be used for comparison of the hybrids and parent antibiotics. Previously reported amphiphilic tobramycin **TOB-C12** (30), having a 12-carbons long aliphatic chain attached to the *C*-5 position of tobramycin, was also included for comparison. Similar to **PMB3** and **TOB-C12**, the hybrids demonstrated moderate to poor activity against Gram-positive bacteria. Notably, **1d** (8-32 µg/mL or 2.8-11.2 µM) and **1e** (8-16 µg/mL or 2.8-5.5 µM) displayed moderate activity across staphylococcal species that include methicillin-resistant strains. Against Gram-negative bacteria, the hybrids exhibited potent antibacterial activity against *P. aeruginosa* relative to other Gram-negative bacilli. Compounds **1b** and **1d** were the most potent hybrids and displayed equipotency compared to both **PMB3** and **TOB** against susceptible strains. For instance,

PMB3, **1b** and **1d** demonstrated similar MICs (2 µg/mL or 0.7-1.1 µM) against a tobramycin-resistant *P. aeruginosa* (CANWARD-2011 96846) clinical isolate. All hybrids were notably potent relative to amphiphilic tobramycin reference **TOB-C12** against *P. aeruginosa* isolates in the panel. Since **TOB-C12** closely resembles the tobramycin-hydrocarbon linker portion of the hybrid, this data clearly showed the essentiality of polymyxin B_3 pharmacophore on the hybrid's antibacterial activity. However, the activity of even the most potent hybrid **1d** was 8- or 16-fold less relative to **PMB3** and **TOB** against all susceptible *Escherichia coli* isolates. Weak to poor activity was observed against *Stenotrophomonas maltophilia*, *A. baumannii* and *Klebsiella pneumoniae*. Indeed, the polymyxin-tobramycin hybrids displayed a relatively narrow spectrum Gram-negative antibacterial activity limited to *P. aeruginosa*. Conversely, **PMB3** has broad spectrum activity against Gram-negative bacilli but poor activity against Gram-positive organisms, while **TOB** demonstrated activity against both Gram-positive and Gram-negative pathogens. While our current data cannot fully explain the observed *P. aeruginosa*-specific antibacterial activity of the hybrids, variations in the exopolysaccharides and the lipopolysaccharides between Gram-negative bacilli may be considered. We postulate that these components in *P. aeruginosa* allow efficient interaction (either through hydrogen bonding or electrostatic interaction) of the hybrid and the outer membrane resulting in disruption and bacterial cell death.

Table 7-1 Biological activity assessment of polymyxin B₃-tobramycin hybrids, along with **PMB3** and **TOB**.

Organism	MIC, µg/mL [µM]							
	PMB3	**1a**	**1b**	**1c**	**1d**	**1e**	**TOB**	**TOB-C12[r]**
S. aureus[a]	128 [72.7]	128 [46.1]	64 [22.8]	32 [11.3]	16 [5.6]	16 [5.5]	≤0.25 [≤0.4]	64 [78.2]
MRSA[b]	>128 [>72.7]	>128 [>46.1]	128 [45.7]	128 [45.2]	32 [11.2]	16 [5.5]	≤0.25 [≤0.4]	128 [156.4]
MSSE[c]	128 [72.7]	64 [23.1]	16 [5.7]	16 [5.6]	8 [2.8]	8 [2.8]	≤0.25 [≤0.4]	16 [19.5]
MRSE[d]	128 [72.7]	128 [46.1]	32 [11.4]	32 [11.3]	16 [5.6]	8 [2.8]	1 [1.8]	16 [19.5]
E. faecalis[e]	>128 [>72.7]	>128 [>46.1]	>128 [45.7]	>128 [>45.2]	>128 [>44.8]	128 [44.3]	8 [14.1]	16 [19.5]
E. faecium[f]	>128 [>72.7]	>128 [>46.1]	>128 [45.7]	>128 [>45.2]	32 [11.2]	32 [11.1]	8 [14.1]	32 [39.1]
E. coli[g]	1 [0.6]	64 [23.1]	32 [11.4]	32 [11.3]	16 [5.6]	16 [5.5]	0.5 [0.9]	128 [156.4]
E. coli[h]	1 [0.6]	64 [23.1]	16 [5.7]	32 [11.3]	8 [2.8]	16 [5.5]	8 [14.1]	128 [156.4]
E. coli[i]	1 [0.6]	64 [23.1]	16 [5.7]	32 [11.3]	8 [2.8]	16 [5.5]	8 [14.1]	128 [156.4]
E. coli[j]	1 [0.6]	64 [23.1]	16 [5.7]	16 [5.6]	8 [2.8]	16 [5.5]	128 [226.3]	128 [156.4]
P. aeruginosa[k]	1 [0.6]	16 [5.8]	4 [1.4]	8 [2.8]	4 [1.4]	8 [2.8]	0.5 [0.9]	512 [625.8]
P. aeruginosa[l]	2 [1.1]	8 [2.9]	2 [0.7]	8 [2.8]	2 [0.7]	4 [1.4]	16 [28.3]	256 [312.9]
P. aeruginosa[m]	2 [1.1]	8 [2.9]	2 [0.7]	8 [2.8]	2 [0.7]	8 [2.8]	256 [452.6]	512 [625.8]
S. maltophilia[n]	32 [18.2]	>128 [>46.1]	>128 [>45.7]	>128 [>45.2]	>128 [>44.8]	>128 [>44.3]	>512 [>905.2]	>512 [>625.8]
A. baumannii[o]	16 [9.1]	>128 [>46.1]	128 [45.7]	32 [11.3]	16 [5.6]	32 [11.1]	32 [56.6]	>512 [>625.8]
K. pneumoniae[p]	0.5 [0.3]	>128 [>46.1]	128 [45.7]	>128 [>45.2]	128 [44.8]	128 [44.3]	≤0.25 [≤0.4]	64 [78.2]
MHC[q]	>128 [>72.7]	>128 [>46.1]	>128 [>45.7]	>128 [>45.2]	>128 [>44.8]	128 [44.3]	ND	ND

[a] = ATCC 29213. [b] = methicillin-resistant *S. aureus* ATCC 33592. [c] = methicillin-susceptible *Staphylococcus epidermidis* CANWARD-2008 81388. [d] = methicillin-resistant *S. epidermidis* CAN-ICU 61589 (ceftazidime-resistant). [e] = ATCC 29212. [f] = ATCC 27270. [g] = ATCC 25922. [h] = CAN-ICU 61714 (gentamicin-resistant). [i] = CAN-ICU 63074 (amikacin-intermediate resistant). [j] = CANWARD-2011 97615 (gentamicin-, tobramycin-, ciprofloxacin-resistant) aac(3')*iia*. [k] = ATCC 27853. [l] = CAN-ICU 62308 (gentamicin-resistant). [m] = CANWARD-2011 96846 (gentamicin-, tobramycin-resistant). [n] = CAN-ICU 62584. [o] = CAN-ICU 63169. [p] = ATCC 13883. [q] = minimum hemolytic concentration that result to 1% red blood cell hemolysis. [r] = data reported on ref.[30]. ND = not determined

All polymyxin B₃-tobramycin hybrids did not induce red blood cell hemolysis. The possibility of non-specific membranolytic action had to be addressed (42) as some of the hybrids exhibited activity against both Gram-positive (albeit moderate to weak) and Gram-negative bacteria. The ability of the hybrids to lyse eukaryotic membrane through hemolysis of red blood cells was explored (Table 7-1). The concentration to induce 1% hemolysis (MHC) was evaluated. No hemolysis was observed for any of the hybrids, nor for the membrane-active **PMB3**, even at the

highest concentration tested of 128 µg/mL. Therefore, the antibacterial activity observed was most

likely specific to bacterial membranes.

Table 7-2 Antibacterial activity of polymyxin B$_3$-tobramycin hybrids **1b** and **1d**, in comparison with **PMB3**, **TOB**, imipenem (**IMI**) and meropenem (**MER**), against carbapenem-resistant[a] MDR/XDR *P. aeruginosa* clinical isolates[b].

P. aeruginosa strain	MIC, µg/mL [µM]					
	1b	**1d**	**PMB3**	**TOB**	**IMI**	**MER**
79199	4 [1.4]	4 [1.4]	1 [0.6]	2 [3.5]	4 [12.6]	16 [36.6]
79352	16 [5.7]	8 [2.8]	4 [2.3]	>64 [>113.2]	32 [100.8]	32 [73.1]
80621	8 [2.8]	8 [2.8]	4 [2.3]	2 [3.5]	32 [100.8]	16 [36.6]
83182	16 [5.7]	8 [2.8]	2 [1.1]	1 [1.8]	16 [50.4]	16 [36.6]
84745	4 [1.4]	4 [1.4]	2 [1.1]	1 [1.8]	16 [50.4]	16 [36.6]
85322	8 [2.8]	8 [2.8]	2 [1.1]	1 [1.8]	32 [100.8]	16 [36.6]
86053	8 [2.8]	8 [2.8]	2 [1.1]	1 [1.8]	16 [50.4]	>32 [>73.1]
86079	4 [1.4]	4 [1.4]	1 [0.6]	2 [3.5]	16 [50.4]	32 [73.1]
86141	4 [1.4]	4 [1.4]	1 [0.6]	2 [3.5]	16 [50.4]	16 [36.6]
88949	8 [2.8]	8 [2.8]	2 [1.1]	2 [3.5]	32 [100.8]	16 [36.6]
92014	4 [1.4]	4 [1.4]	1 [0.6]	1 [1.8]	8 [25.2]	8 [18.3]
100036	ND	8 [2.8]	2 [1.1]	64 [113.2]	8 [25.2]	4 [9.1]
101885	ND	8 [2.8]	0.5 [0.3]	≤0.5 [≤0.9]	1 [3.2]	1 [2.3]
108590	2 [0.7]	2 [0.7]	1 [0.6]	4 [7.1]	32 [100.8]	8 [18.3]
109084	16 [5.7]	8 [2.8]	4 [2.3]	2 [3.5]	16 [50.4]	8 [18.3]
110112	16 [5.7]	8 [2.8]	2 [1.1]	8 [14.1]	32 [100.8]	16 [36.6]
259-96918	ND	4 [1.4]	0.25 [0.1]	>64 [>113.2]	32 [100.8]	>32 [>73.1]
260-97103	ND	2 [0.7]	0.5 [0.3]	32 [56.6]	32 [100.8]	16 [36.6]
262-101856	ND	16 [5.6]	4 [2.3]	>64 [>113.2]	32 [100.8]	32 [73.1]
264-104354	ND	16 [5.6]	0.5 [0.3]	64 [113.2]	32 [100.8]	>32 [>73.1]
PAO1	ND	2 [0.7]	0.5 [0.3]	1 [1.8]	ND	1 [2.3]

[a] = except 101885 and PAO1 strain. [b] = except wild-type PAO1 strain. ND = not determined. MDR = multidrug-resistant. XDR = extensively drug-resistant.

Antipseudomonal activity of polymyxin B$_3$-tobramycin hybrids was retained against MDR/XDR

P. aeruginosa clinical isolates. The antipseudomonal potency of **1b** and **1d** was further tested

against clinical isolates, all (except two) were carbapenem-resistant, MDR/XDR strains (Table 7-

2). According to the Clinical and Laboratory Standards Institute (CLSI) (43), the susceptibility

breakpoint for both imipenem (**IMI**) and meropenem (**MER**) in *P. aeruginosa* is ≤2 µg/mL (~ ≤6 µM). As expected, **1b** and **1d** demonstrated relatively potent activity (MIC of 2-16 µg/ml or 0.7-5.7 µM) against MDR/XDR *P. aeruginosa* strains, which was significantly more potent than the MICs obtained with **IMI** and **MER**. It was apparent that among the two hybrids, **1d** possessed slightly better activity relative to **1b**. Hybrid **1d** displayed similar MIC to **PMB3** in most *P. aeruginosa* clinical isolates (except for 101885, 259-96918 and 264-104354 strains). Similarly, **1d** displayed similar MICs to **TOB** in tobramycin-susceptible and significantly lower MICs in tobramycin-resistant strains.

Table 7-3 Antibacterial activity of polymyxin B$_3$-tobramycin hybrid **1b** and **1d**, in comparison with **PMB3** and colistin (**COL**), against colistin-resistant *P. aeruginosa*.

P. aeruginosa strain	MIC, µg/mL [µM]			
	1b	**1d**	**PMB3**	**COL**[a]
91433	4 [1.4]	8 [2.8]	4 [2.3]	4 [3.2]
95937	16 [5.7]	16 [5.6]	16 [9.1]	8 [6.3]
98516	16 [5.7]	8 [2.8]	8 [4.5]	4 [3.2]
98749	16 [5.7]	16 [5.6]	8 [4.5]	8 [6.3]
100403	16 [5.7]	16 [5.6]	32 [18.2]	16 [12.6]
101243	32 [11.4]	16 [5.6]	128 [72.7]	1024 [807.9]
108833	8 [2.8]	8 [2.8]	4 [2.3]	4 [3.2]

[a] = [µM] calculated for colistin sulfate salt.

Polymyxin B$_3$-tobramycin hybrids possessed enhanced membrane effects relative to polymyxins but was still vulnerable to polymyxin resistance mechanisms. All the strains tested at this point were colistin-susceptible and warranted assessment in colistin-resistant strains. Colistin (**COL**), also known as polymyxin E, displays a resistance breakpoint of ≥4 µg/mL (~ ≥3.2 µM) in *P. aeruginosa* according to CLSI (43). The antibacterial activity of polymyxin B$_3$-tobramycin hybrids was then evaluated in seven colistin-resistant *P. aeruginosa* clinical isolates (Table 7-3). Compounds **1b** (4-32 µg/mL or 1.4-11.4 µM) and **1d** (8-16 µg/mL or 2.8-5.6 µM) displayed

slightly better or similar MICs to **PMB3** (4-128 µg/mL or 2.3-72.7 µM) and **COL** (4-1024 µg/mL or 3.2-807.9 µM) against most isolates. It was not surprising as the major polymyxin resistance mechanism is through membrane modification, resulting in the loss of overall negative charge in lipopolysaccharides studded on the OM (44–46). This effectively confers resistance to most cationic membrane-targeting antimicrobials such as polymyxins and antimicrobial peptides. Since we fused two OM-acting cationic pharmacophores (amphiphilic tobramycin and polymyxin), we expected that resistance due to OM modification would lead to reduced activity of the hybrids. However, both **1b** and **1d** displayed lower MICs relative to **PMB3** and **COL** against colistin-resistant *P. aeruginosa* 101243 clinical isolate. Specifically, **1d** displayed an MIC (16 µg/mL or 5.6 µM) of ~8-fold better than **PMB3** (128 µg/mL or 72.7 µM) and ~128-fold better than **COL** (1024 µg/mL or 807.9 µM). Subtly, both hybrids also displayed a ~4-fold lower MIC than **PMB3** against strain 100403. This observation suggests that the polymyxin B$_3$-tobramycin hybrids possess enhanced membrane effects relative to polymyxins alone.

Polymyxin B$_3$-tobramycin hybrid **1d** demonstrated superior adjuvant properties relative to polymyxin B$_3$ and tobramycin against *P. aeruginosa.* We recently described antimicrobial hybrids that are able to potentiate clinically-used antibiotics against MDR/XDR *P. aeruginosa* clinical isolates (14–17). Encouraged by these results, but also from reports of polymyxins interacting synergistically with select antibiotics (31), we evaluated the most potent polymyxin B$_3$-tobramycin hybrid **1d** as a potential adjuvant in *P. aeruginosa*. We assessed the synergy of **1d** with a panel of 26 clinically-used antibiotics in wild-type *P. aeruginosa* PAO1 (Fig 7-2). Synergistic combinations were scored by their fractional inhibitory concentration (FIC) index. FIC values of ≤ 0.5, $0.5 < x < 4$ or ≥ 4 denote synergistic, additive or antagonistic interactions, respectively.(47)

Polymyxin B_3-tobramycin hybrid **1d** was found to be synergistic with tetracycline antibiotics minocycline, doxycycline and tigecycline. It also potentiated the outer membrane-impermeable antibiotics rifampicin, vancomycin and novobiocin, but also the efflux-susceptible trimethoprim, chloramphenicol, clindamycin and linezolid. **PMB3** and **TOB** were assessed in combination with the ten above-mentioned antibiotics (Fig. 7-3A and 7-3B) to investigate whether the adjuvant property of the hybrid stems from either parent pharmacophores. Both **PMB3** and **TOB** were not able to potentiate all ten antibiotics, suggesting the fusion of both pharmacophores to be causal of the observed adjuvant property. To validate these observations, we performed the same checkerboard study using the ten antibiotics in combination with either **1d**, **PMB3** and **TOB** against MDR *P. aeruginosa* 259-96918 clinical isolate (Fig. 7-3C, 7-3D and 7-3E). Similarly, hybrid **1d** displayed strong synergy, yet neither **PMB3** nor **TOB** were able to potentiate all of the ten antibiotics. Therefore, our results indicate that the potent adjuvant property of polymyxin B_3-tobramycin heterodimer **1d** arises from the hybridization of **PMB3** and **TOB**.
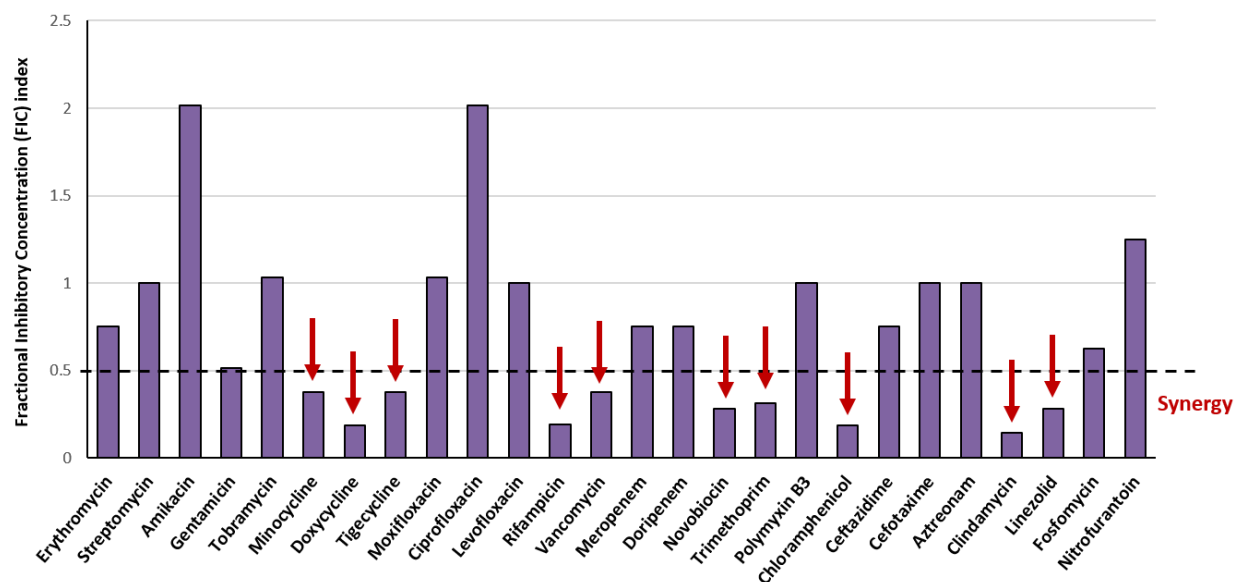
Figure 7-2 Interaction of hybrid **1d** with various antibiotics, in combination, against wild-type *P. aeruginosa* PAO1.

Fractional inhibitory concentration (FIC) index value of ≤0.5 denotes a synergistic interaction. Dashed line represents the FIC cut-off. Red arrow indicates those antibiotics that exhibit synergy with hybrid.
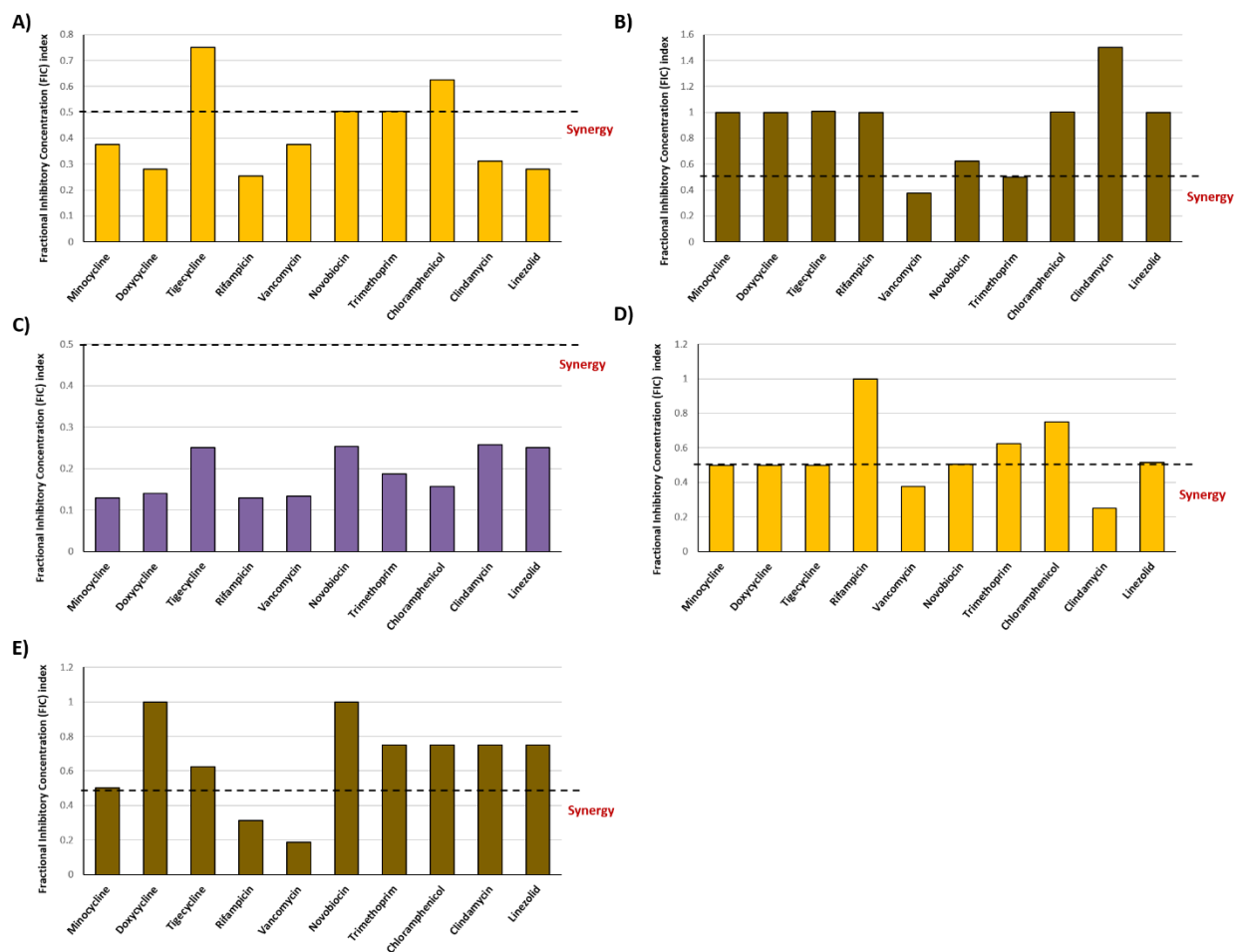
Figure 7-3 Interaction of either **PMB3**, **TOB** or hybrid **1d** with in combination with various antibiotics.

(A) **PMB3** against wild-type *P. aeruginosa* PAO1, (B) **TOB** against wild-type *P. aeruginosa* PAO1, (C) **1d** against MDR *P. aeruginosa* 259-96918 clinical isolate, (D) **PMB3** against MDR *P. aeruginosa* 259-96918 clinical isolate, (E) **TOB** against MDR *P. aeruginosa* 259-96918 clinical isolate. Fractional inhibitory concentration (FIC) index value of ≤0.5 denotes synergistic interaction. Dashed line represents the FIC cut-off.

The potential of polymyxin B₃-tobramycin hybrid **1d** as an adjuvant partner to minocycline, rifampicin and vancomycin was evident. Out of the ten antibiotics, we decided to pursue further evaluation of hybrid **1d** in combination with either minocycline (Table 7-4), rifampicin (Table 7-5) or vancomycin (Table 7-6) against MDR/XDR *P. aeruginosa* clinical isolates. Notably, we included colistin- and tobramycin-resistant MDR *P. aeruginosa* 101243 in the panel. The three

antibiotics were chosen due to their strong synergism; but also that the presence of $\leq\frac{1}{4} \times$ MIC (≤ 4 µg/mL) of hybrid **1d** brought down the antibiotic's MIC in PAO1 and/or 259-96918 strains below their interpretative susceptibility breakpoint. There are no established susceptibility breakpoints for the three chosen antibiotics in *P. aeruginosa* (neither CLSI nor European Committee on Antimicrobial Susceptibility Testing [EUCAST]). Therefore, we have used the established susceptibility breakpoint for other organisms as representative of clinically achievable concentrations as comparison for *Pseudomonas* spp. According to CLSI (43), the minocycline breakpoint in *Acinetobacter* spp. is ≤ 4 µg/mL, rifampicin breakpoint in *Staphylococcus* spp. is ≤ 1 µg/mL and vancomycin breakpoint in *Enterococcus* spp. is ≤ 4 µg/mL. Hybrid **1d** brought down the MIC of minocycline in all tested *P. aeruginosa* strains below its susceptibility breakpoint. We previously reported that the tobramycin-hybrid scaffold, indiscriminate of the other appended pharmacophore, affected the electrical component ($\Delta\Psi$) of the proton motive force resulting in an increase in the ΔpH component for compensation (16, 17). This leads to an enhanced tetracycline (such as minocycline) uptake as it is known to be ΔpH-dependent (48). Our results corroborate that the intrinsic nature of the tobramycin scaffold to influence the proton motive force is retained in polymyxin B$_3$-tobramycin hybrids. The outer membrane-impermeable rifampicin was also found to be synergistic with **1d** across the panel of MDR/XDR *P. aeruginosa* clinical isolates. Rifampicin's MIC dropped below its susceptibility breakpoint in almost all (except one) clinical *P. aeruginosa* strains in the presence of $\leq\frac{1}{4} \times$ MIC (≤ 4 µg/mL) **1d**. In fact, we observed 8- to $\geq$2048-fold potentiation of rifampicin against the MDR/XDR *P. aeruginosa* panel. The combination of vancomycin and **1d** was found to be synergistic in seven out of eight *P. aeruginosa* strains. Compound **1d** reduced the MIC of vancomycin below its susceptibility breakpoint in half of the strains tested. The degree of vancomycin potentiation by **1d** appeared to be strain-specific.

For instance, vancomycin only demonstrated a 4-fold potentiation in strain 101243 while it resulted in a 1024-fold potentiation in strain 264-104354. Combination of **PMB3** with the three antibiotics exhibited slightly weaker to similar effects relative to **1d** across the panel (see Appendix IV). **TOB** combination with the three antibiotics mostly showed additive interactions although synergy with rifampicin was observed in half of the strains and weak synergy with vancomycin was found in two strains tested (see Appendix IV). Our data support the notion that the potent adjuvant properties of polymyxin B_3-tobramycin hybrids in *P. aeruginosa* arise from the conjugation of both **PMB3** and **TOB** components.

Table 7-4 Adjuvant potency of hybrid **1d** in combination with minocycline against wild-type and MDR/XDR *P. aeruginosa*.

P. aeruginosa strain	$MIC_{Minocycline}$, µg/mL	MIC_{1d}, µg/mL	FIC index	Absolute $MIC_{Minocycline}$,[a] µg/mL	Potentiation[b]
PAO1	8	4	0.37	1	8-fold
259-96918	32	8	0.13	0.125	256-fold
260-97103	16	2	0.37	2	8-fold
262-101856	64	16	0.19	4	16-fold
264-104354	32	16	0.12	1	32-fold
100036	16	8	0.25	1	16-fold
101243[c]	4	16	0.28	1	4-fold
101885	16	8	0.25	2	8-fold

[a] = MIC of minocycline in the presence of ¼ MIC_{1d} or 4 µg/mL of hybrid **1d**. [b] = degree of antibiotic potentiation in the presence of $\leq$¼ × MIC_{1d} ($\leq$ 4 µg/mL) of hybrid **1d**. [c] = colistin- and tobramycin-resistant. MDR = multidrug-resistant. XDR = extensively drug-resistant.

Table 7-5 Adjuvant potency of hybrid **1d** in combination with rifampicin against wild-type and MDR/XDR *P. aeruginosa*.

P. aeruginosa strain	MIC$_{Rifampicin}$, µg/mL	MIC$_{1d}$, µg/mL	FIC index	Absolute MIC$_{Rifampicin}$,[a] µg/mL	Potentiation[b]
PAO1	16	4	0.19	≤0.0625	≥256-fold
259-96918	16	8	0.13	≤0.0625	≥256-fold
260-97103	16	2	0.37	2	8-fold
262-101856	512	32	0.08	≤2	≥256-fold
264-104354	8	16	0.07	≤0.007813	≥1024-fold
100036	16	8	0.13	≤0.007813	≥2048-fold
101243[c]	8	16	0.04	≤0.007813	≥1024-fold
101885	16	8	0.07	0.015625	1024-fold

[a] = MIC of rifampicin in the presence of ¼ MIC$_{1d}$ or 4 µg/mL of hybrid **1d**. [b] = degree of antibiotic potentiation in the presence of ≤¼ × MIC$_{1d}$ (≤ 4 µg/mL) of hybrid **1d**. [c] = colistin- and tobramycin-resistant. MDR = multidrug-resistant. XDR = extensively drug-resistant.

Table 7-6 Adjuvant potency of hybrid **1d** in combination with vancomycin against wild-type and MDR/XDR *P. aeruginosa*.

P. aeruginosa strain	MIC$_{Vancomycin}$, µg/mL	MIC$_{1d}$, µg/mL	FIC index	Absolute MIC$_{Vancomycin}$,[a] µg/mL	Potentiation[b]
PAO1	1024	4	0.37	128	8-fold
259-96918	1024	4	0.13	2	512-fold
260-97103	512	2	0.50[d]	256	2-fold
262-101856	1024	16	0.16	4	256-fold
264-104354	512	16	0.14	0.5	1024-fold
100036	512	8	0.19	2	256-fold
101243[c]	128	16	0.31	32	4-fold
101885	512	8	0.28	16	32-fold

[a] = MIC of vancomycin in the presence of ¼ MIC$_{1d}$ or 4 µg/mL of hybrid **1d**. [b] = degree of antibiotic potentiation in the presence of ≤¼ × MIC$_{1d}$ (≤ 4 µg/mL) of hybrid **1d**. [c] = colistin- and tobramycin-resistant. [d] = exact FIC index value is 0.500977 and therefore not synergistic. MDR = multidrug-resistant. XDR = extensively drug-resistant.

Potentiation of minocycline, rifampicin and vancomycin by polymyxin B$_3$-tobramycin hybrid **1d** was retained in other Gram-negative bacilli. Synergism of compound **1d** with either minocycline, rifampicin or vancomycin against other Gram-negative bacilli was then explored (Table 7-7). Checkerboard assay was performed against three *A. baumannii* strains, including ATCC reference

strain and two clinical isolates. Compound **1d** displayed poor antibacterial activity by itself (MIC

of >64 µg/mL). Interestingly, minocycline was not potentiated against the three isolates (Table 7-

7). We believe that this might be due to the fact that the three organisms were already susceptible

(below MIC breakpoint) to minocycline. However, 4 µg/mL of hybrid **1d** reduced the MIC of

rifampicin (3/3 strains) and vancomycin (2/3 strains) below their susceptibility breakpoint. Similar

to our previous observations in *P. aeruginosa*, synergism with vancomycin against *A. baumannii*

appeared to be strain-specific. The adjuvant potency of **1d** was also evaluated against an MDR *K.*

pneumoniae strain, to which hybrid **1d** exhibited poor activity by itself (MIC of >64 µg/mL).

Minocycline, rifampicin and vancomycin were all synergistic with **1d** against the *K. pneumoniae*

strain (Table 7-7).

Table 7-7 Adjuvant potency of hybrid **1d** in combination with either minocycline (MIN), rifampicin (RMP) or vancomycin (VAN) against wild-type and MDR/XDR Gram-negative bacilli.

Organism	Antibiotic	$MIC_{Antibiotic}$, µg/mL	MIC_{1d}, µg/mL	FIC index	Absolute $MIC_{Antibiotic}$,[a] µg/mL	Potentiation[b]
A. baumannii[c]	MIN	1	>64	1.000<x<1.002	1	none
A. baumannii[c]	RMP	2	>64	0.008<x<0.039	0.03125	64-fold
A. baumannii[c]	VAN	128	>64	0.016<x<0.047	4	32-fold
A. baumannii[d]	MIN	4	>64	1.00<x<1.002	4	none
A. baumannii[d]	RMP	1	>64	0.016<x<0.047	0.015625	64-fold
A. baumannii[d]	VAN	128	>64	0.031<x<0.047	4	32-fold
A. baumannii[e]	MIN	1	>64	0.500<x<0.502	0.5	2-fold
A. baumannii[e]	RMP	1	>64	0.008<x<0.023	≤0.003906	≥256-fold
A. baumannii[e]	VAN	128	>64	1.000<x<1.002	128	none
K. pneumoniae[f]	MIN	128	>64	0.062<x<0.078	8	16-fold
K. pneumoniae[f]	RMP	512	>64	0.002<x<0.033	0.5	1024-fold
K. pneumoniae[f]	VAN	256	>64	0.250<x<0.312	64	4-fold

[a] = MIC of antibiotic in the presence of 4 µg/mL hybrid **1d**. [b] = degree of antibiotic potentiation in the presence of 4 µg/mL hybrid **1d**. [c] = strain ATCC 17978. [d] = strain 110193. [e] = strain LAC-4. [f] = strain 116381. MDR = multidrug-resistant. XDR = extensively drug-resistant.

7.6. Conclusion

The synthesis of polymyxin-aminoglycoside hybrids possessing meaningful biological activity was achieved. Specifically, polymyxin B_3 was covalently linked to tobramycin using copper-assisted azide alkyne cycloaddition at functional sites amenable to modification. The polymyxin B_3-tobramycin hybrids displayed potent *P. aeruginosa*-selective activity. We speculate that differences in the exopolysaccharides and lipopolysaccharides between Gram-negative bacilli are responsible for the observed differences. The most potent hybrid **1d** also synergized clinically-used antibiotics in wild-type and MDR/XDR *P. aeruginosa*, with MIC reductions (minocycline, rifampicin and vancomycin) below susceptibility breakpoints. Furthermore, hybrid **1d** reduced the MIC of rifampicin and vancomycin below their susceptibility breakpoint in *A. baumannii*. We highlight the potential of this class of antimicrobial hybrids not only as a stand-alone antimicrobial but also in combination with other existing antibiotic classes.

7.7. Materials and methods

General information. Reagents and solvents were purchased commercially and used without purification unless otherwise noted. Compounds were purified, as specified in their synthesis, by either normal-phase flash chromatography, using Kiesel gel 40 (40-63 µm) purchased from Merck, or reverse-phase flash chromatography, using C18 silica gel (40-63 µm) purchased from Silicycle (USA). TLC was performed on silica gel 60 F254 (0.25 mm) acquired from Merck (USA) to monitor reactions and was visualized by both ultraviolet light and ninhydrin staining solution. All reported hybrids/final compounds were found to have purity of ≥ 95% as determined by high-performance liquid chromatography (HPLC) analysis *via* Breeze HPLC Waters with 2998 PDA detector (1.2 nm resolution) coupled to Phenomenex Synergi Polar (50 x 2.0 mm) 4 micron

reverse-phase column with phenyl ether-linked stationary phase. All purified compounds were characterized using 1-dimensional and 2-dimensional NMR experiments such as ^{1}H, ^{13}C, homonuclear correlation spectroscopy (COSY), heteronuclear single-quantum correlation spectroscopy (HSQC) and heteronuclear multiple-bond correlation spectroscopy (HMBC). All NMR measurements were recorded from either AMX-500 (500 MHz) or AMX-300 (300 MHz) Bruker instrument (Germany). The molecular weights for all compounds were recorded by either electrospray ionization mass spectrometer (ESI-MS) on a Varian 500-MS Ion Trap Mass Spectrometer (USA) or matrix-assisted laser desorption ionization mass spectrometer coupled to time-of-flight mass analyzer (MALDI-TOF-MS) on a Bruker Ultraflextreme (Germany), using 2,5-dehydroxybenzoic acid as the matrix.

Chemistry. The synthesis of intermediate compounds **4, 5** and **6a-e** follows our previously reported protocol (16) and is described in Appendix IV.

Synthesis of uncyclized PMB3-Cbz-alkyne (2). Solid-phase peptide synthesis following a standard fluorenylmethyloxycarbonyl (Fmoc) protection strategy on a Wang *p*-alkoxybenzyl alcohol resin was utilized. A published protocol (39) was followed with several modifications. Amino acids with protected functional groups were purchased and used to yield the uncyclized lipopeptide, having a free carboxylic acid C-terminus of Thr_{10} and free amine side-chain of Dab_4. Therefore, all the Dab amino side-chains, with the exception of Dab_4 which was protected with Boc, were protected with Cbz protecting group. The two Thr hydroxyl side-chains were protected with *t*-Bu. Pra was used instead of Dab for amino acid position 1 to effectively install an alkyne functional group. Briefly, the protocol is as follows. Fmoc removal was done by subjecting the resin to 4:1

DMF:piperidine solution for 15 minutes, and repeated twice to ensure complete Fmoc removal. Coupling was achieved by the addition of a pre-activated coupling solution [Fmoc-amino acid or lipid tail (3 mol. eq.) was pre-mixed with the coupling reagent *N,N,N',N'*-tetramethyl-*O*-(benzotriazol-1-yl)uronium tetrafluoroborate (TBTU) (3 mol. eq.) and *N*-methylmorpholine (8 mol. eq.) in DMF 5 minutes prior] to the immobilized peptide on solid support followed by gentle agitation using N_2 gas for 45 minutes. Both Fmoc removal and coupling steps were followed with thorough washing of the beads using DMF (3x), DCM (3x) and DMF (3x). A small amount of resin was subjected to Kaiser test (5% chloranil in DMF) after each coupling and Fmoc removal step to qualitatively ensure that the reaction went to completion. Consecutive Fmoc removal and coupling steps were performed to yield the resin-immobilized desired lipopeptide. Cleavage from the solid support was performed by the addition of 95:5 TFA:water solution followed by gentle stirring for 30 minutes. The solvent was removed *in vacuo* to obtain a dry crude. MALDI-TOF-MS was performed to check for the presence of **2**.

Synthesis of PMB3-Cbz-alkyne (3). The crude containing compound **2** was mixed with benzotriazole-1-yl-oxy-tris-pyrrolidino-phosphonium hexafluorophosphate (PyBOP) (4 mol. eq.), hydroxybenzotriazole (HOBt) (4 mol. eq.) and *N*-methymorpholine (10 mol. eq.) in DMF under very dilute and anhydrous conditions, followed by vigorous stirring for 2 hours, to afford the intramolecular cyclization *via* amide bond formation between the Thr_{10} carboxyl end and Dab_4 amine side-chain. The solvent was removed *in vacuo*. Precipitation of the product from the crude was induced by addition of cold water. The precipitate was filtered and obtained as a pale brown solid. DCM was added to partially dissolve the product and was evaporated *in vacuo* to dryness. MALDI-TOF-MS was performed to confirm product **3**.

*General Procedure for the conversion of bromo- to azido-tobramycin intermediate (**7a-e**).* The bromoalkylated tobramycin intermediate (**6a-e)** and sodium azide (3 mol. eq.) were dissolved in DMF. The resulting solution was stirred at 75 °C for 3 hours and transferred to a separatory funnel. Cold water was added followed by an extraction with ethyl acetate (3x). The combined organic layers were washed with brine and dried over anhydrous sodium sulfate. The solvent was removed *in vacuo* and the resulting solid was dried under high vacuum for more than 24 hours to afford **7a-e** as an opaque solid (91-97% yield). R_f = 0.52 (hexanes/ethyl acetate = 4:1). Detailed characterization of compounds **7a-e** are described in Appendix IV.

*Synthesis of polymyxin B$_3$-tobramycin hybrids (**1a-e**).* The Cu$^+$ source iodo(triethyl phosphite)copper (I) was utilized for the formation of a 1,2,3-triazole ring linkage *via* copper-assisted azide alkyne cycloaddition between the intermediate compounds **7a-e** and **3**. Unfortunately, the resulting compounds **8a-e** proved to have very limited solubility that it did not permit a proper purification using neither normal- nor reverse-phase flash chromatography. Therefore, the crude was co-distilled with toluene (3x) and left drying under high-vacuum for at least 24 hours. No further steps were taken and the compounds were used as is in the consecutive steps.

Deprotections were done systematically. First, removal of Boc- and TBDMS- protecting groups were performed. Compounds **8a-e** were dissolved in methanol (3 volume ratio eq.) followed by the addition of HCl (4 volume ratio eq.) and tetrahydrofuran (3 volume ratio eq.). The acidic solution was stirred for 2.5 hours. The solvent was then removed *in vacuo* followed by co-

distillation with toluene (3x). The resulting dry compound was crudely purified as the Boc- and TBDMS-deprotection procedure also resulted to the partial deprotection of Cbz-protecting groups. The partial deprotection of Cbz groups, which occurred at a slow rate, was deemed negligible as the subsequent step entailed their global deprotection. Therefore, reverse-phase flash chromatography was performed using an eluent mixture of water and methanol (both spiked with 0.1% TFA), from 25% to 100% methanol in water ratio (12.5% step-wise), to afford compound **9a-e** that also contained a minor amount of partially Cbz-deprotected product.

Finally, Cbz-deprotection of the hybrid was achieved by catalytic hydrogenolysis. The resulting material **9a-e** (from the prior step) was dissolved in a mixture of 4:5:1 methanol:acetic acid:water. Palladium on carbon (Pd/C) was added and the compound was subjected to H_2 gas (balloon) with constant stirring until all the Cbz groups were removed. It was then filtered *via* Nylon filter followed by washing with ample amounts of methanol. The filtrate was evaporated to dryness *in vacuo*. The crude product was then purified using reverse-phase flash chromatography having an eluent mixture of water and methanol (both spiked with 0.1% TFA), from 0% to 50% methanol in water ratio (12.5% step-wise), to afford compounds **1a-e** as an opaque solid.

*PMB3-triazole-C$_4$-Tobramycin (**1a**).* ^{1}H NMR (500 MHz, Methanol-d_4) δ 7.91 − 7.83 (m, 1H, triazole), 7.32 − 7.20 (m, 5H, D-Phe$_6$ aromatic), 5.48 − 5.38 (m, 1H, H-1'), 5.09 (d, J = 3.2 Hz, 1H, H-1''), 4.74 − 4.66 (m, 1H, Pra$_{1\alpha}$), 4.53 (dd, J = 8.8, 4.4 Hz, 1H, Dab$_{5\alpha}$), 4.50 − 4.42 (m, 2H, D-Phe$_{6\alpha}$ + Dab$_{8\alpha}$), 4.42 − 4.08 (m, 11H, Thr$_{2\alpha}$ + Thr$_{2,10\beta}$ + Leu$_{7\alpha}$ + Dab$_{3,4,9\alpha}$ + C$_4$'s -C$\underline{H}_2$-N=N- + H-4 + H-5'), 4.05 (d, J = 4.6 Hz, 1H, Thr$_{10\alpha}$), 3.95 − 3.62 (m, 11H, C$_4$'s -C$\underline{H}_2$-O- + H-5 + H-6 + H-2' + H-4' + H-2'' + H-4'' + H-5'' + H-6''), 3.56 − 3.40 (m, 4H, Dab$_{4\gamma1}$ + H-1 + H-3 + H-3''),

3.28 – 3.19 (m, 3H, Pra$_{1\beta1}$ + H-6'), 3.17 – 2.91 (m, 12H, Pra$_{1\beta2}$ + Dab$_{4\gamma2}$ + D-Phe$_{6\beta}$ + Dab$_{3,5,8,9\gamma}$), 2.52 – 2.42 (m, 2H, Dab$_{3\beta1}$ + H-2$_{eq}$), 2.29 – 1.90 (m, 16H, Dab$_{3\beta2}$ + Dab$_{4,5,8,9\beta}$ + PMB3 C$_8$'s -CH$_2$CO- + C$_4$'s -CH$_2$CH$_2$-N=N- + H-2$_{ax}$ + H-3'), 1.69 – 1.47 (m, 5H, Leu$_{7\beta1}$ + C$_4$'s -CH$_2$CH$_2$-O- + PMB3 C$_8$'s -CH$_2$CH$_2$CO-), 1.38 – 1.26 (m, 9H, Leu$_{7\beta2}$ + PMB3 C$_8$'s -CH$_2$-), 1.25 – 1.02 (m, 6H, Thr$_{2,10\gamma}$), 0.89 (t, J = 7.2 Hz, 3H, PMB3 C$_8$'s -CH$_3$), 0.87 – 0.58 (m, 7H, Leu$_{7\gamma}$ + Leu$_{7\delta}$). ^{13}C NMR (126 MHz, Methanol-d_4) δ 175.48 (PMB3 C$_8$'s carbonyl), 173.91, 172.88, 172.58, 172.50, 172.29, 171.98, 171.87, 171.54, 171.32, 170.98, 143.19 (triazole C without H), 135.82 (D-Phe$_6$ C without H), 128.86, 128.34, 126.72, 123.42 (triazole C with H), 101.07 (C-1''), 92.78 (C-1'), 82.50, 81.72 (C-6), 76.81, 76.17, 74.08, 72.02, 69.05, 66.41, 65.83, 65.29, 63.50, 59.86, 59.71, 56.46, 55.03, 53.51 (Pra$_{1\alpha}$), 51.79, 51.67, 51.49, 49.97 (Dab$_{5\alpha}$), 49.67, 49.62, 48.46, 48.42, 39.27 (Leu$_{7\beta}$), 38.45, 38.39, 38.35, 36.65, 36.60, 36.44, 36.36, 36.17, 36.00, 35.39, 31.43, 30.25, 28.88, 28.67, 28.34, 27.69, 26.96, 26.48, 26.38, 25.91, 25.84, 25.51, 23.51, 22.24, 22.17, 20.02, 19.81, 19.76, 19.18, 18.69, 12.98 (PMB$_3$ C$_8$'s -CH$_3$). MALDI-TOF-MS m/z calcd for C$_{72}$H$_{138}$N$_{23}$O$_{22}$ (M+H)$^+$ monoisotopic peak: 1749.039, found: 1749.012.

PMB3-triazole-C$_6$-Tobramycin (1b). ^{1}H NMR (500 MHz, Methanol-d_4) δ 7.91 – 7.84 (m, 1H, triazole), 7.34 – 7.19 (m, 5H, D-Phe$_6$ aromatic), 5.43 (d, J = 2.7 Hz, 1H, H-1'), 5.11 (d, J = 3.3 Hz, 1H, H-1''), 4.69 – 4.62 (m, 1H, Pra$_{1\alpha}$), 4.52 (dd, J = 8.7, 4.3 Hz, 1H, Dab$_{5\alpha}$), 4.46 (dd, J = 8.7, 4.7 Hz, 1H, Dab$_{8\alpha}$), 4.42 (dd, J = 9.4, 6.7 Hz, 1H, D-Phe$_{6\alpha}$), 4.40 – 4.14 (m, 10H, Thr$_{2\alpha}$ + Thr$_{2,10\beta}$ + Dab$_{3,4,9\alpha}$ + C$_6$'s -CH$_2$-N=N- + H-4 + H-5'), 4.14 – 4.09 (m, 1H, Leu$_{7\alpha}$), 4.07 (d, J = 4.6 Hz, 1H, Thr$_{10\alpha}$), 3.94 – 3.88 (m, 1H, H-6), 3.85 – 3.64 (m, 8H, C$_6$'s -CH$_2$-O- + H-5 + H-4' + H-2'' + H-4'' + H-6''), 3.61 – 3.55 (m, 2H, H-2' + H-5''), 3.54 – 3.43 (m, 4H, Dab$_{4\gamma1}$ + H-1 + H-3 + H-3''), 3.34 – 3.31 (m, 1H, H-6'$_{eq}$), 3.25 – 3.19 (m, 2H, Pra$_{1\beta1}$ + H-6'$_{ax}$), 3.19 – 2.88 (m, 12H, Pra$_{1\beta2}$ +

Dab$_{4\gamma2}$ + D-Phe$_{6\beta}$ + Dab$_{3,5,8,9\gamma}$), 2.53 – 2.43 (m, 2H, Dab$_{3\beta1}$ + H-2$_{eq}$), 2.29 – 1.85 (m, 16H, Dab$_{3\beta2}$ + Dab$_{4,5,8,9\beta}$ + PMB3 C$_8$'s -C$\underline{H}_2$CO- + C$_6$'s -C$\underline{H}_2$CH$_2$-N=N- + H-2$_{ax}$ + H-3'), 1.66 – 1.60 (m, 2H, C$_6$'s -C$\underline{H}_2$CH$_2$-O-), 1.59 – 1.47 (m, 3H, Leu$_{7\beta1}$ + PMB3 C$_8$'s -C$\underline{H}_2$CH$_2$CO-), 1.44 – 1.26 (m, 13H, Leu$_{7\beta2}$ + PMB3 C$_8$'s -C$\underline{H}_2$- + C$_6$'s -C$\underline{H}_2$-), 1.24 – 1.03 (m, 6H, Thr$_{2,10\gamma}$), 0.89 (t, J = 7.2 Hz, 3H, PMB3 C$_8$'s -CH$_3$), 0.87 – 0.59 (m, 7H, Leu$_{7\gamma}$ + Leu$_{7\delta}$). ^{13}C NMR (126 MHz, Methanol-d_4) δ 175.64 (PMB3 C$_8$'s carbonyl), 175.38, 174.53, 172.74, 172.64, 172.62, 172.48, 172.17, 171.91, 171.74, 171.47, 142.12 (triazole C without H), 135.51 (D-Phe$_6$ C without H), 128.85, 128.34, 126.72, 123.53 (triazole C with H), 101.07 (C-1''), 92.70 (C-1'), 82.24, 81.56 (C-6), 76.37, 75.62, 73.95, 72.59, 69.07, 66.33, 66.04, 65.06, 63.64, 59.92, 59.82, 56.41, 55.00, 53.43 (Pra$_{1\alpha}$), 52.18, 51.94, 51.67, 50.03 (Dab$_{5\alpha}$), 49.73, 48.41, 47.50, 39.30 (Leu$_{7\beta}$), 38.54, 36.61, 36.45, 36.28, 36.01, 35.40, 31.43, 29.71, 29.47, 28.87, 28.83, 28.69, 28.60, 28.54, 27.69, 25.54, 24.85, 22.25, 22.15, 20.05, 19.19, 18.73, 12.99 (PMB$_3$ C$_8$'s -C$\underline{H}_3$). MALDI-TOF-MS m/z calcd for C$_{80}$H$_{142}$N$_{23}$O$_{22}$ (M+H)$^+$ monoisotopic peak: 1777.070, found: 1777.073.

PMB3-triazole-C$_8$-Tobramycin (1c). ^{1}H NMR (500 MHz, Methanol-d_4) δ 7.88 – 7.81 (m, 1H, triazole), 7.35 – 7.18 (m, 5H, D-Phe$_6$ aromatic), 5.43 (d, J = 2.7 Hz, 1H, H-1'), 5.12 (d, J = 3.3 Hz, 1H, H-1''), 4.70 – 4.62 (m, 1H, Pra$_{1\alpha}$), 4.52 (dd, J = 8.8, 4.4 Hz, 1H, Dab$_{5\alpha}$), 4.49 – 4.44 (m, 1H, Dab$_{8\alpha}$), 4.42 (dd, J = 9.7, 6.8 Hz, 1H, D-Phe$_{6\alpha}$), 4.39 – 4.14 (m, 10H, Thr$_{2\alpha}$ + Thr$_{2,10\beta}$ + Dab$_{3,4,9\alpha}$ + C$_8$'s -C$\underline{H}_2$-N=N- + H-4 + H-5'), 4.13 – 4.08 (m, 1H, Leu$_{7\alpha}$), 4.06 (d, J = 4.6 Hz, 1H, Thr$_{10\alpha}$), 3.91 (t, J = 9.3 Hz, 1H, H-6), 3.83 – 3.64 (m, 8H, C$_8$'s -C$\underline{H}_2$-O- + H-5 + H-4' + H-2'' + H-4'' + H-6''), 3.61 – 3.56 (m, 2H, H-2' + H-5''), 3.56 – 3.43 (m, 4H, Dab$_{4\gamma1}$ + H-1 + H-3 + H-3''), 3.29 – 3.25 (m, 1H, H-6'$_{eq}$), 3.25 – 3.19 (m, 2H, Pra$_{1\beta1}$ + H-6'$_{ax}$), 3.19 – 2.85 (m, 12H, Pra$_{1\beta2}$ + Dab$_{4\gamma2}$ + D-Phe$_{6\beta}$ + Dab$_{3,5,8,9\gamma}$), 2.54 – 2.43 (m, 2H, Dab$_{3\beta1}$ + H-2$_{eq}$), 2.31 – 1.85 (m, 16H, Dab$_{3\beta2}$ +

Dab$_{4,5,8,9\beta}$ + PMB3 C$_8$'s -C$\underline{H}_2$CO- + C$_8$'s -C$\underline{H}_2$CH$_2$-N=N- + H-2$_{ax}$ + H-3'), 1.67 − 1.60 (m, 2H, C$_8$'s -C$\underline{H}_2$CH$_2$-O-), 1.59 − 1.47 (m, 3H, Leu$_{7\beta1}$ + PMB3 C$_8$'s -C$\underline{H}_2$CH$_2$CO-), 1.41 − 1.25 (m, 17H, Leu$_{7\beta2}$ + PMB3 C$_8$'s -C$\underline{H}_2$- + C$_8$'s -C$\underline{H}_2$-), 1.24 − 1.02 (m, 6H, Thr$_{2,10\gamma}$), 0.90 (t, J = 7.3 Hz, 3H, PMB3 C$_8$'s -CH$_3$), 0.88 − 0.58 (m, 7H, Leu$_{7\gamma}$ + Leu$_{7\delta}$). ^{13}C NMR (126 MHz, Methanol-d_4) δ 175.34 (PMB3 C$_8$'s carbonyl), 173.91, 173.16, 172.64, 172.50, 172.20, 171.97, 171.81, 171.48, 171.28, 170.95, 142.97 (triazole C without H), 135.85 (D-Phe$_6$ C without H), 128.86, 128.34, 126.71, 123.28 (triazole C with H), 101.10 (C-1''), 92.67 (C-1'), 82.22, 81.57 (C-6), 76.41, 75.56, 73.93, 72.58, 69.07, 66.28, 65.26, 63.66, 59.94, 59.82, 56.41, 54.99, 53.53 (Pra$_{1\alpha}$), 52.01, 51.73, 51.45, 50.00 (Dab$_{5\alpha}$), 49.95, 49.76, 48.48, 47.68, 39.28 (Leu$_{7\beta}$), 38.58, 36.67, 36.60, 36.52, 36.45, 36.40, 36.00, 35.38, 31.43, 29.88, 29.84, 29.70, 29.62, 29.39, 29.31, 29.26, 28.86, 28.83, 28.70, 28.60, 28.33, 27.70, 26.13, 26.06, 26.01, 25.54, 25.51, 25.48, 25.44, 23.54, 22.25, 22.16, 20.04, 19.18, 18.74, 12.99 (PMB$_3$ C$_8$'s -C$\underline{H}_3$). MALDI-TOF-MS m/z calcd for C$_{82}$H$_{146}$N$_{23}$O$_{22}$ (M+H)$^+$ monoisotopic peak: 1805.101, found: 1805.104.

PMB3-triazole-C$_{10}$-Tobramycin (1d). ^{1}H NMR (500 MHz, Methanol-d_4) δ 7.87 − 7.82 (m, 1H, triazole), 7.32 − 7.19 (m, 5H, D-Phe$_6$ aromatic), 5.41 (d, J = 2.6 Hz, 1H, H-1'), 5.12 (d, J = 3.4 Hz, 1H, H-1''), 4.68 − 4.62 (m, 1H, Pra$_{1\alpha}$), 4.52 (dd, J = 8.8, 4.5 Hz, 1H, Dab$_{5\alpha}$), 4.48 − 4.39 (m, 2H, D-Phe$_{6\alpha}$ + Dab$_{8\alpha}$), 4.39 − 4.13 (m, 10H, Thr$_{2\alpha}$ + Thr$_{2,10\beta}$ + Dab$_{3,4,9\alpha}$ + C$_{10}$'s -C$\underline{H}_2$-N=N- + H-4 + H-5'), 4.13 − 4.08 (m, 1H, Leu$_{7\alpha}$), 4.06 (d, J = 4.7 Hz, 1H, Thr$_{10\alpha}$), 3.91 (t, J = 9.2 Hz, 1H, H-6), 3.84 − 3.63 (m, 8H, C$_{10}$'s -C$\underline{H}_2$-O- + H-5 + H-4' + H-2'' + H-4'' + H-6''), 3.61 − 3.56 (m, 2H, H-2' + H-5''), 3.55 − 3.43 (m, 4H, Dab$_{4\gamma1}$ + H-1 + H-3 + H-3''), 3.28 − 3.25 (m, 1H, H-6'$_{eq}$), 3.25 − 3.18 (m, 2H, Pra$_{1\beta1}$ + H-6'$_{ax}$), 3.17 − 2.87 (m, 12H, Pra$_{1\beta2}$ + Dab$_{4\gamma2}$ + D-Phe$_{6\beta}$ + Dab$_{3,5,8,9\gamma}$), 2.54 − 2.43 (m, 2H, Dab$_{3\beta1}$ + H-2$_{eq}$), 2.29 − 1.86 (m, 16H, Dab$_{3\beta2}$ + Dab$_{4,5,8,9\beta}$ + PMB3 C$_8$'s -C$\underline{H}_2$CO- +

C$_{10}$'s -C$\underline{H}_2$CH$_2$-N=N- + H-2$_{ax}$ + H-3'), 1.67 − 1.59 (m, 2H, C$_{10}$'s -C$\underline{H}_2$CH$_2$-O-), 1.59 − 1.48 (m, 3H, Leu$_{7\beta1}$ + PMB3 C$_8$'s -C$\underline{H}_2$CH$_2$CO-), 1.39 − 1.25 (m, 21H, Leu$_{7\beta2}$ + PMB3 C$_8$'s -C$\underline{H}_2$- + C$_{10}$'s -C$\underline{H}_2$-), 1.23 − 1.02 (m, 6H, Thr$_{2,10\gamma}$), 0.89 (t, J = 7.2 Hz, 3H, PMB3 C$_8$'s -CH$_3$), 0.87 − 0.58 (m, 7H, Leu$_{7\gamma}$ + Leu$_{7\delta}$). ^{13}C NMR (126 MHz, Methanol-d_4) δ 175.31 (PMB3 C$_8$'s carbonyl), 173.91, 173.20, 172.64, 172.49, 172.17, 171.98, 171.70, 171.45, 171.27, 170.93, 142.96 (triazole C without H), 135.86 (D-Phe$_6$ C without H), 128.86, 128.33, 126.71, 123.27 (triazole C with H), 101.10 (C-1''), 92.68 (C-1'), 82.19, 81.57 (C-6), 76.43, 75.62, 73.92, 72.65, 69.07, 66.26, 65.27, 63.64, 59.97, 59.81, 56.36, 54.98, 53.48 (Pra$_{1\alpha}$), 51.93, 51.75, 51.45, 50.02 (Dab$_{5\alpha}$), 49.91, 49.76, 48.48, 47.56, 39.29 (Leu$_{7\beta}$), 38.55, 36.68, 36.59, 36.53, 36.45, 36.00, 35.38, 31.43, 30.31, 29.95, 29.78, 29.56, 29.38, 29.25, 28.86, 28.79, 28.70, 28.58, 28.48, 28.32, 27.70, 26.90, 26.21, 26.16, 25.66, 25.54, 23.56, 22.25, 22.15, 20.05, 19.17, 18.74, 12.99 (PMB$_3$ C$_8$'s -$\underline{C}$H$_3$). MALDI-TOF-MS m/z calcd for C$_{84}$H$_{150}$N$_{23}$O$_{22}$ (M+H)$^+$ monoisotopic peak: 1833.133, found: 1833.192.

PMB3-triazole-C$_{12}$-Tobramycin (1e). ^{1}H NMR (500 MHz, Methanol-d_4) δ 7.87 − 7.83 (m, 1H, triazole), 7.34 − 7.18 (m, 5H, D-Phe$_6$ aromatic), 5.42 (d, J = 2.7 Hz, 1H, H-1'), 5.12 (d, J = 3.2 Hz, 1H, H-1''), 4.70 − 4.62 (m, 1H, Pra$_{1\alpha}$), 4.52 (dd, J = 8.8, 4.3 Hz, 1H, Dab$_{5\alpha}$), 4.48 − 4.40 (m, 2H, D-Phe$_{6\alpha}$ + Dab$_{8\alpha}$), 4.39 − 4.14 (m, 10H, Thr$_{2\alpha}$ + Thr$_{2,10\beta}$ + Dab$_{3,4,9\alpha}$ + C$_{12}$'s -C$\underline{H}_2$-N=N- + H-4 + H-5') 4.14 − 4.08 (m, 1H, Leu$_{7\alpha}$), 4.06 (d, J = 4.6 Hz, 1H, Thr$_{10\alpha}$), 3.91 (t, J = 9.4 Hz, 1H, H-6), 3.84 − 3.65 (m, 8H, C$_{12}$'s -C$\underline{H}_2$-O- + H-5 + H-4' + H-2'' + H-4'' + H-6''), 3.61 − 3.55 (m, 2H, H-2' + H-5''), 3.54 − 3.43 (m, 4H, Dab$_{4\gamma1}$ + H-1 + H-3 + H-3''), 3.29 − 3.26 (m, 1H, H-6'$_{eq}$), 3.24 − 3.18 (m, 2H, Pra$_{1\beta1}$ + H-6'$_{ax}$), 3.17 − 2.87 (m, 12H, Pra$_{1\beta2}$ + Dab$_{4\gamma2}$ + D-Phe$_{6\beta}$ + Dab$_{3,5,8,9\gamma}$), 2.53 − 2.44 (m, 2H, Dab$_{3\beta1}$ + H-2$_{eq}$), 2.29 − 1.86 (m, 16H, Dab$_{3\beta2}$ + Dab$_{4,5,8,9\beta}$ + PMB3 C$_8$'s -C$\underline{H}_2$CO- + C$_{12}$'s -C$\underline{H}_2$CH$_2$-N=N- + H-2$_{ax}$ + H-3'), 1.68 − 1.60 (m, 2H, C$_{12}$'s -C$\underline{H}_2$CH$_2$-O-), 1.59 − 1.48 (m,

3H, Leu$_{7\beta1}$ + PMB$_3$ C$_8$'s -C$\underline{H}_2$CH$_2$CO-), 1.38 – 1.24 (m, 25H, Leu$_{7\beta2}$ + PMB3 C$_8$'s -C$\underline{H}_2$- + C$_{12}$'s -C$\underline{H}_2$-), 1.24 – 1.04 (m, 6H, Thr$_{2,10\gamma}$), 0.89 (t, J = 7.3 Hz, 3H, PMB3 C$_8$'s -CH$_3$), 0.88 – 0.59 (m, 7H, Leu$_{7\gamma}$ + Leu$_{7\delta}$). ^{13}C NMR (126 MHz, Methanol-d_4) δ 175.30 (PMB3 C$_8$'s carbonyl), 174.84, 174.39, 173.92, 173.21, 172.64, 172.51, 172.16, 172.00, 171.46, 170.94, 143.08 (triazole C without H), 135.86 (D-Phe$_6$ C without H), 128.86, 128.33, 126.71, 120.82 (triazole C with H), 101.11 (C-1''), 92.66 (C-1'), 82.33, 82.19, 81.58 (C-6), 80.61, 76.40, 75.59, 73.92, 72.66, 69.07, 66.27, 65.80, 65.26, 63.65, 63.12, 59.97, 59.81, 56.00, 54.98, 53.46 (Pra$_{1\alpha}$), 52.66, 52.01, 51.74, 51.47, 50.03 (Dab$_{5\alpha}$), 49.77, 48.48, 47.51, 39.31 (Leu$_{7\beta}$), 38.55, 36.68, 36.66, 36.62, 36.53, 36.44, 36.00, 35.39, 31.44, 29.95, 29.79, 29.62, 29.49, 29.43, 29.35, 29.26, 29.16, 28.91, 28.87, 28.81, 28.77, 28.71, 28.58, 28.32, 27.69, 26.21, 26.16, 25.70, 25.55, 23.56, 22.26, 22.16, 20.05, 19.17, 18.75, 13.00 (PMB$_3$ C$_8$'s -C$\underline{H}_3$). MALDI-TOF-MS m/z calcd for C$_{86}$H$_{154}$N$_{23}$O$_{22}$ (M+H)$^+$ monoisotopic peak: 1861.164, found: 1861.144.

Biological studies. Bacterial isolates were either obtained from the American Type Culture Collection (ATCC), Canadian National Intensive Care Unit (CAN-ICU) surveillance study (40) or the Canadian Ward Surveillance (CANWARD) study (41). Strains from CAN-ICU and CANWARD are clinical isolates recovered from patients suffering from a presumed infectious disease admitted in a participating medical center across Canada.

Antimicrobial susceptibility assay. The *in vitro* antibacterial activity was assessed by microbroth dilution susceptibility testing following the CLSI guidelines (43). Overnight grown bacterial cultures were diluted in saline (0.85% NaCl) to achieve a 0.5 McFarland turbidity, followed by 1:50 dilution in Mueller-Hinton broth (MHB) for inoculation to a final concentration of

approximately 5×10^5 colony forming units/mL. The assay was performed on a 96-well plates to which the tested agents were 2-fold serially diluted in MHB and incubated with equal volumes of inoculum at 37 °C for 18 hours. The MIC was determined as the lowest concentration to inhibit visible bacterial growth in form of turbidity, which was confirmed using EMax Plus microplate reader (Molecular Devices, USA) at a wavelength of 590 nm. The broth with or without bacterial cells was used as positive or negative control, respectively.

Checkerboard Assay. The assay was performed in a 96-well plate as previously described (16, 17). Briefly, the antibiotic of interest was 2-fold serially diluted along the x-axis, while the adjuvant was 2-fold serially diluted along the y-axis to create a matrix in which each well consists of a combination of both at different concentrations. Bacterial cultures grown overnight were diluted in saline (0.85% NaCl) to 0.5 McFarland turbidity, followed by 1:50 dilution in MHB and inoculation in each well to a final concentration of approximately 5×10^5 colony forming units/mL. Wells containing only MHB with or without bacterial cells were used as positive or negative controls, respectively. The plates were incubated at 37 °C for 18 hours and examined for visible turbidity, which was confirmed using EMax Plus microplate reader (Molecular Devices, USA) at a wavelength of 590 nm. The fractional inhibitory concentration (FIC) of the antibiotic was calculated *via* dividing the MIC of antibiotic in the presence of adjuvant by the MIC of antibiotic alone. Similarly, the FIC of adjuvant was calculated *via* dividing the MIC of adjuvant in the presence of antibiotic by the MIC of adjuvant alone. FIC index was obtained by the summation of both FIC values. FIC index was interpreted as synergistic, additive or antagonistic for values of $\leq$ 0.5, $0.5 < x < 4$ or ≥ 4, respectively (47).

Hemolytic assay. The ability of the agents to lyse eukaryotic red blood cells was quantified by the amount of hemoglobin released upon incubation with pig erythrocytes, following a published protocol (17). Briefly, fresh pig blood (generously provided by Dr. Charles M. Nyachoti from University of Manitoba) drawn from pig antecubital vein was centrifuged at $1000 \times$ g for 5 minutes at 4 °C, washed with PBS three times and re-suspended in the same buffer, consecutively. Agents were 2-fold serially diluted in phosphate-buffered saline (PBS) on a 96-well plate and mixed with equal volumes of erythrocyte solution. Post 1-hour incubation at 37 °C, intact cells were pelleted by centrifugation at $1000 \times$ g for 5 minutes at 4 °C. The resulting supernatant was then transferred to a new 96-well plate. The hemoglobin released was measured *via* EMax Plus microplate reader (Molecular Devices, USA) at 570 nm wavelength. Erythrocytes in PBS with or without 0.1% Triton X-100 were used as negative or positive controls, respectively.

7.8. Acknowledgements

7.9. References

1.   de Smalen AW, Ghorab H, Abd El Ghany M, Hill-Cawthorne GA. 2017. Refugees and antimicrobial resistance: A systematic review. Travel Med Infect Dis 15:23–28.

2.   Ayukekbong JA, Ntemgwa M, Atabe AN. 2017. The threat of antimicrobial resistance in developing countries: causes and control strategies. Antimicrob Resist Infect Control 6:47.

3.   Brown ED, Wright GD. 2016. Antibacterial drug discovery in the resistance era. Nature 529:336–343.

4.   Bartsch SM, McKinnell JA, Mueller LE, Miller LG, Gohil SK, Huang SS, Lee BY. 2017. Potential economic burden of carbapenem-resistant Enterobacteriaceae (CRE) in the United States. Clin Microbiol Infect 23:48.e9-48.e16.

5.   Cooper MA, Shlaes D. 2011. Fix the antibiotics pipeline. Nature 472:32.

6.   World Health Organization. 2017. Global Priority List of Antibiotic-Resistant Bacteria to Guide Research, Discovery, and Development of New Antibiotics. Febr 27.

7.   Silver LL. 2016. A Gestalt approach to Gram-negative entry. Bioorg Med Chem 24:6379–6389.

8.   Pokrovskaya V, Baasov T. 2010. Dual-acting hybrid antibiotics: a promising strategy to combat bacterial resistance. Expert Opin Drug Discov 5:883–902.

9.   Parkes AL, Yule IA. 2016. Hybrid antibiotics - clinical progress and novel designs. Expert Opin Drug Discov 11:665–680.

10.   Klahn P, Bronstrup M. 2017. Bifunctional antimicrobial conjugates and hybrid antimicrobials. Nat Prod Rep 34:832–885.

11.   The PEW Charitable Trust. 2017. Antibiotics Currently in Clinical Development. March.

12.   Katsube T, Echols R, Arjona Ferreira JC, Krenz HK, Berg JK, Galloway C. 2017. Cefiderocol, a siderophore cephalosporin for Gram-negative bacterial infections: pharmacokinetics and safety in subjects with renal impairment. J Clin Pharmacol 57:584–591.

13. Endres BT, Basseres E, Alam MJ, Garey KW. 2017. Cadazolid for the treatment of Clostridium difficile. Expert Opin Investig Drugs 26:509–514.

14. Gorityala BK, Guchhait G, Fernando DM, Deo S, McKenna SA, Zhanel GG, Kumar A, Schweizer F. 2016. Adjuvants based on hybrid antibiotics overcome resistance in *Pseudomonas aeruginosa* and enhance fluoroquinolone efficacy. Angew Chem Int Ed Engl 55:555–559.

15. Gorityala BK, Guchhait G, Goswami S, Fernando DM, Kumar A, Zhanel GG, Schweizer F. 2016. Hybrid antibiotic overcomes resistance in *P. aeruginosa* by enhancing outer membrane penetration and reducing efflux. J Med Chem 59:8441–8455.

16. Yang X, Goswami S, Gorityala BK, Domalaon R, Lyu Y, Kumar A, Zhanel GG, Schweizer F. 2017. A tobramycin vector enhances synergy and efficacy of efflux pump inhibitors against multidrug-resistant Gram-negative bacteria. J Med Chem 60:3913–3932.

17. Lyu Y, Yang X, Goswami S, Gorityala BK, Idowu T, Domalaon R, Zhanel GG, Shan A, Schweizer F. 2017. Amphiphilic tobramycin-lysine conjugates sensitize multidrug resistant Gram-negative bacteria to rifampicin and minocycline. J Med Chem 60:3684–3702.

18. Hancock RE. 1981. Aminoglycoside uptake and mode of action-with special reference to streptomycin and gentamicin. II. Effects of aminoglycosides on cells. J Antimicrob Chemother 8:429–445.

19. Berkov-Zrihen Y, Herzog IM, Benhamou RI, Feldman M, Steinbuch KB, Shaul P, Lerer S, Eldar A, Fridman M. 2015. Tobramycin and nebramine as pseudo-oligosaccharide scaffolds for the development of antimicrobial cationic amphiphiles. Chemistry 21:4340–

4349.

20.   Shaul P, Benhamou RI, Herzog IM, Louzoun Zada S, Ebenstein Y, Fridman M. 2016.
        Synthesis and evaluation of membrane permeabilizing properties of cationic amphiphiles
        derived from the disaccharide trehalose. Org Biomol Chem 14:3012–3015.

21.   Sautrey G, Zimmermann L, Deleu M, Delbar A, Souza Machado L, Jeannot K, Van
        Bambeke F, Buyck JM, Decout J-L, Mingeot-Leclercq M-P. 2014. New amphiphilic
        neamine derivatives active against resistant *Pseudomonas aeruginosa* and their
        interactions with lipopolysaccharides. Antimicrob Agents Chemother 58:4420–4430.

22.   Sautrey G, El Khoury M, Dos Santos AG, Zimmermann L, Deleu M, Lins L, Decout J-L,
        Mingeot-Leclercq M-P. 2016. Negatively Charged Lipids as a Potential Target for New
        Amphiphilic Aminoglycoside Antibiotics: A BIOPHYSICAL STUDY. J Biol Chem
        291:13864–13874.

23.   Dhondikubeer R, Bera S, Zhanel GG, Schweizer F. 2012. Antibacterial activity of
        amphiphilic tobramycin. J Antibiot (Tokyo) 65:495–8.

24.   Zimmermann L, Das I, Desire J, Sautrey G, Barros R S V, El Khoury M, Mingeot-
        Leclercq M-P, Decout J-L. 2016. New broad-spectrum antibacterial amphiphilic
        aminoglycosides active against resistant bacteria: from neamine derivatives to smaller
        neosamine analogues. J Med Chem 59:9350–9369.

25.   Bera S, Dhondikubeer R, Findlay B, Zhanel GG, Schweizer F. 2012. Synthesis and
        antibacterial activities of amphiphilic neomycin B-based bilipid conjugates and
        fluorinated neomycin B-based lipids. Molecules 17:9129–9141.

26.   Bera S, Zhanel GG, Schweizer F. 2010. Antibacterial activities of aminoglycoside antibiotics-derived cationic amphiphiles. Polyol-modified neomycin B-, kanamycin A-, amikacin-, and neamine-based amphiphiles with potent broad spectrum antibacterial activity. J Med Chem 53:3626–3631.

27.   Bera S, Zhanel GG, Schweizer F. 2010. Antibacterial activity of guanidinylated neomycin B- and kanamycin A-derived amphiphilic lipid conjugates. J Antimicrob Chemother 65:1224–1227.

28.   Bera S, Zhanel GG, Schweizer F. 2008. Design, synthesis, and antibacterial activities of neomycin-lipid conjugates: polycationic lipids with potent Gram-positive activity. J Med Chem 51:6160–6164.

29.   Udumula V, Ham YW, Fosso MY, Chan KY, Rai R, Zhang J, Li J, Chang C-WT. 2013. Investigation of antibacterial mode of action for traditional and amphiphilic aminoglycosides. Bioorg Med Chem Lett 23:1671–1675.

30.   Guchhait G, Altieri A, Gorityala B, Yang X, Findlay B, Zhanel GG, Mookherjee N, Schweizer F. 2015. Amphiphilic tobramycins with immunomodulatory properties. Angew Chemie Int Ed 54:6278–6282.

31.   Lenhard JR, Nation RL, Tsuji BT. 2016. Synergistic combinations of polymyxins. Int J Antimicrob Agents 48:607–613.

32.   Masuda N, Sakagawa E, Ohya S, Gotoh N, Tsujimoto H, Nishino T. 2000. Substrate specificities of MexAB-OprM, MexCD-OprJ, and MexXY-oprM efflux pumps in *Pseudomonas aeruginosa*. Antimicrob Agents Chemother 44:3322–3327.

33.   Velkov T, Thompson PE, Nation RL, Li J. 2010. Structure-activity relationships of polymyxin antibiotics. J Med Chem 53:1898–1916.

34.   Velkov T, Roberts KD, Nation RL, Thompson PE, Li J. 2013. Pharmacology of polymyxins: new insights into an "old" class of antibiotics. Future Microbiol 8:711–724.

35.   Hanessian S, Tremblay M, Swayze EE. 2003. Tobramycin analogues with C-5 aminoalkyl ether chains intended to mimic rings III and IV of paromomycin. Tetrahedron 59:983–993.

36.   Kanazawa K, Sato Y, Ohki K, Okimura K, Uchida Y, Shindo M, Sakura N. 2009. Contribution of each amino acid residue in polymyxin B(3) to antimicrobial and lipopolysaccharide binding activity. Chem Pharm Bull (Tokyo) 57:240–244.

37.   Orwa JA, Govaerts C, Busson R, Roets E, Van Schepdael A, Hoogmartens J. 2001. Isolation and structural characterization of colistin components. J Antibiot (Tokyo) 54:595–599.

38.   Kassamali Z, Prince RA, Danziger LH, Rotschafer JC, Rhomberg PR, Jones RN. 2015. Microbiological assessment of polymyxin B components tested alone and in combination. Antimicrob Agents Chemother 59:7823–7825.

39.   Tsubery H, Ofek I, Cohen S, Fridkin M. 2000. Structure-function studies of polymyxin B nonapeptide: implications to sensitization of gram-negative bacteria. J Med Chem 43:3085–3092.

40.   Zhanel GG, DeCorby M, Laing N, Weshnoweski B, Vashisht R, Tailor F, Nichol K a., Wierzbowski A, Baudry PJ, Karlowsky J a., Lagacé-Wiens P, Walkty A, McCracken M,

Mulvey MR, Johnson J, Hoban DJ. 2008. Antimicrobial-resistant pathogens in intensive care units in Canada: results of the Canadian National Intensive Care Unit (CAN-ICU) study, 2005-2006. Antimicrob Agents Chemother 52:1430–1437.

41.   Hoban DJ, Zhanel GG. 2011. Introduction to the CANWARD Study (2007-2009). Diagn Microbiol Infect Dis. United States.

42.   Hurdle JG, O'Neill AJ, Chopra I, Lee RE. 2011. Targeting bacterial membrane function: an underexploited mechanism for treating persistent infections. Nat Rev Microbiol 9:62–75.

43.   The Clinical and Laboratory Standards Institute. 2016. Performance Standards for Antimicrobial Susceptibility Testing CLSI supplement M100S 26th ed. Clin Lab Stand Institute, Wayne, PA.

44.   Velkov T, Deris ZZ, Huang JX, Azad MAK, Butler M, Sivanesan S, Kaminskas LM, Dong Y-D, Boyd B, Baker MA, Cooper MA, Nation RL, Li J. 2014. Surface changes and polymyxin interactions with a resistant strain of Klebsiella pneumoniae. Innate Immun 20:350–363.

45.   Anaya-Lopez JL, Lopez-Meza JE, Ochoa-Zarzosa A. 2013. Bacterial resistance to cationic antimicrobial peptides. Crit Rev Microbiol 39:180–195.

46.   Poirel L, Jayol A, Nordmann P. 2017. Polymyxins: antibacterial activity, susceptibility testing, and resistance mechanisms encoded by plasmids or chromosomes. Clin Microbiol Rev 30:557–596.

47.   Meletiadis J, Pournaras S, Roilides E, Walsh TJ. 2010. Defining fractional inhibitory

concentration index cutoffs for additive interactions based on self-drug additive combinations, Monte Carlo simulation analysis, and in vitro-in vivo correlation data for antifungal drug combinations against Aspergillus fumi. Antimicrob Agents Chemother 54:602–609.

48.   Yamaguchi A, Ohmori H, Kaneko-Ohdera M, Nomura T, Sawai T. 1991. Delta pH-dependent accumulation of tetracycline in Escherichia coli. Antimicrob Agents Chemother 35:53–56.

7.10. Concluding remarks

This chapter highlighted my efforts in the development of antibiotic hybrids composed of polymyxins and aminoglycosides. Specifically, I successfully linked polymyxin B_3 to tobramycin through an aliphatic hydrocarbon molecular linker that yielded five different polymyxin B_3-tobramycin hybrids (only differing in the length of the linker). We identified several hybrids with potent antipseudomonal activity, that also possessed the ability to enhance other antibiotics as a partner adjuvant against Gram-negative bacteria, especially against *P. aeruginosa*. Importantly, the polymyxin-tobramycin hybrid exhibited superior (or similar in few strains) membrane effects and adjuvant properties relative to either polymyxin B_3 or tobramycin.

Note that complimentary data for this Chapter is provided in Appendix IV.

Chapter 8: Conclusion and outlook

8.1. Summary

It is of utmost importance to address the problem of antimicrobial resistance. Significant efforts have been taken by the government, academia and private companies, alike, to raise public awareness of this issue and stimulate the development of new strategies that either may mitigate the spread or may eradicate these recalcitrant pathogens (1, 2). Several therapeutic strategies that may overcome these problematic multidrug-resistant (MDR) bacteria were extensively discussed in Chapters 1 and 2, which included the development of membrane-targeting peptides, antibiotic hybrids and drug combinations.

Through my doctoral research, I have identified several lead peptides with potential as adjuvant partners to clinically-used antibiotics against MDR Gram-negative bacteria. For instance, a short proline-rich lipopeptide (SPRLP) was found to enhance the antibacterial activity of minocycline and rifampin (also known as rifampicin) against MDR *P. aeruginosa*, as discussed in Chapter 4. This SPRLP was evaluated to be non-hemolytic and non-cytotoxic. Our initial attempt to optimize the chemical scaffold of this SPRLP revealed that its adjuvant property was amenable to modifications. Another lead peptide adjuvant was identified in Chapter 5 to be a dilipid ultrashort cationic lipopeptide (dUSCL) that demonstrated the ability to enhance the antibacterial activity of chloramphenicol against Gram-negative bacteria. Our initial assessment revealed that this non-hemolytic dUSCL potentiated chloramphenicol against wild-type and MDR clinical isolates of *P. aeruginosa*, *A. baumannii*, and *Enterobacteriaceae*. Moreover, this dUSCL also synergized with

other clinically-used antibiotics such as fluoroquinolones, rifampicin, minocycline, trimethoprim, fosfomycin, piperacillin, vancomycin and linezolid against wild-type *P. aeruginosa*. Further assessment is currently undergoing for these observed synergistic combinations of dUSCL in other Gram-negative bacteria.

Polymyxin is a clinically-used peptide antibiotic to treat multidrug-resistant Gram-negative bacterial infections that are non-responsive to conventional antibiotic therapy. My interest in polymyxins was apparent in Chapters 6 and 7. In chapter 6, we explored the effect of hydrophobicity on the biological activity (antibacterial, adjuvant and ability to resist active efflux) of polymyxin by introducing an additional fatty acid onto its typical monolipid fragment. Dilipid polymyxins exhibited enhanced antibacterial activity against Gram-positive bacteria relative to polymyxins. We also identified a dilipid polymyxin that possessed similar adjuvant properties to the well-known membrane permeabilizer polymyxin B nonapeptide. Importantly, we disclosed for the first time that the lipid component of polymyxin was responsible for their ability to resist efflux systems in *P. aeruginosa*. The polymyxin core structure was covalently fused with an aminoglycoside to generate antibiotic hybrids in Chapter 7. The complex preparation of polymyxin B_3 linked to the aminoglycoside tobramycin *via* an aliphatic hydrocarbon tether was disclosed. Interestingly, this antibiotic hybrid exhibited potent antipseudomonal activity, and the antibacterial effect is specific only against *P. aeruginosa* relative to other Gram-negative bacteria. The polymyxin B_3-tobramycin hybrid also displayed promising adjuvant properties, better than either polymyxin B_3 or tobramycin, against *P. aeruginosa*. The combinations of the hybrid and either minocycline, rifampicin or vancomycin, among other antibiotics, were found to be strongly synergistic against multidrug-resistant *P. aeruginosa* and other Gram-negative bacterial isolates.

8.2. Future outlook

Overall, these described contributions on the development of investigational peptide-based therapeutic agents may hold the key to future therapeutic strategies to overcome MDR Gram-negative bacteria. However, these lead peptide candidates require further optimization attempts to increase their potency and stability (especially those lipopeptide compounds) to be considered for clinical trials. For instance, peptidomimetic modifications (as discussed in Chapter 1) may be imparted to the peptide to remove their "peptide-like" nature. Such modifications may involve stereochemical transformations (from L- to D-amino acids) or replacement with unnatural amino acids. Aside from the possibility that these changes may enhance biological activity, removing the "peptide-like" nature of these agents may render endogenous/host enzymes, such as proteases, unable to recognize them and therefore impart enhanced serum stability. Moving forward with the optimization of these reported investigational peptide-based agents in this thesis, peptidomimetics optimization is certainly warranted.

As we expect that these agents' action is membranotropic (permeabilize bacterial membranes), similarly observed in other antimicrobial peptides, biochemical assays that evaluate these membrane effects should be performed in the future to validate our assumption. A suggested membrane permeabilization assay might include the use of 1-*N*-phenylnaphthylamine (NPN) dye to explore the perturbation of the outer membrane. Moreover, 3,3′-dipropylthiadicarbocyanine iodide [DiSC3(5)] dye might be used to explore the effects of these agents on the inner membrane and the transmembrane potential. The latter is very important as the bacterial transmembrane potential also known as the proton motive force (3), including the electrochemical and proton

gradient, generates bacterial energy in the form of adenosine triphosphate (ATP). In turn, ATP powers all bacterial cellular functions that include important drug resistance mechanisms such as efflux systems and drug inactivating/modifying enzymes. Other modes of action may also be explored in the future. For instance, the SPRLP reported in Chapter 4 may be evaluated for their potential protein translation inhibitory activities as other proline-rich peptides are known to interact with ribosomes. Furthermore, polymyxins and the aminoglycoside tobramycin are also known to affect protein translation. Thus, the dilipid polymyxins in Chapter 6 and polymyxin B$_3$-tobramycin hybrids in Chapter 7 should also be assessed for protein translation inhibition. A protein translation assay utilizing the oxidative enzyme luciferase may be used for this assessment.

All the data presented herein are *in vitro* evaluations and thus require *in vivo* assessment to validate whether these biological activities are retained in complex biological systems. While further optimization is expected for these investigational peptide-based agents and considering that testing in animal models such as mice or rats is rather costly, one may assess *in vivo* efficacy of these peptides, in their current form, in *Galleria mellonella* wax worm infection model. The *G. mellonella* infection model is considerably inexpensive but still a valid model that emulates the immune systems of higher organisms (4, 5). Therefore, this is a potential future experiment for these peptide-based agents. Other *in vivo* assessments will soon follow once these drug candidates undergo optimization, especially to increase their serum/protease stability.

8.3. Perspective

There is absolutely an urgent need to develop new therapeutic strategies that can overcome antibiotic resistance, especially against MDR Gram-negative pathogens. However, it has been

proven difficult to generate these much needed lifeline. My collective work in the field of investigative peptide-based therapeutics published in this thesis represents an effort, among thousands of contributions, by academia to develop new strategies and agents able to eradicate MDR pathogens. I foresee that these investigational peptide-based agents will take part in the future as next generation therapeutics.

Development of novel therapeutic strategies should not cease, especially in the field of antibacterial drugs. This is very important as bacteria continuously evolve to counter and disarm our antibiotic weaponry. Scientific ingenuity is humankind's best weaponry in our crusade to repel the looming threat of antimicrobial resistance!

8.4. References

1.   Boucher HW, Talbot GH, Bradley JS, Edwards JE, Gilbert D, Rice LB, Scheld M, Spellberg B, Bartlett J. 2009. Bad bugs, no drugs: no ESKAPE! An update from the Infectious Diseases Society of America. Clin Infect Dis 48:1–12.

2.   Boucher HW, Talbot GH, Benjamin DKJ, Bradley J, Guidos RJ, Jones RN, Murray BE, Bonomo RA, Gilbert D. 2013. 10 x '20 Progress--development of new drugs active against gram-negative bacilli: an update from the Infectious Diseases Society of America. Clin Infect Dis 56:1685–1694.

3.   Kashket ER. 1985. The proton motive force in bacteria: a critical assessment of methods. Annu Rev Microbiol 39:219–242.

4.   Tsai CJ, Loh JM, Proft T. 2016. Galleria mellonella infection models for the study of

bacterial diseases and for antimicrobial drug testing. Virulence 7:214–229.

5.   Wojda I. 2017. Immunity of the greater wax moth Galleria mellonella. Insect Sci 24:342–357.

Appendix I: Supporting information for Chapter 4

Additional data shown below are complimentary to Chapter 4 and are based on my publication:

I-1. Characterization of synthesized short proline-rich lipopeptides (SPRLPs)

C8-PRP (C8-PRPRPRP-NH2)

^{1}H NMR (300 MHz, Methanol-d4) δ 4.73 – 4.56 (m, 3H, Arg$_\alpha$), 4.54 – 4.35 (m, 4H, Pro$_\beta$), 3.92 – 3.42 (m, 8H, Pro$_\delta$), 3.28 – 3.08 (m, 6H, Arg$_\delta$), 2.37 (t, J = 7.0 Hz, 2H, C8's -C$\underline{H}_2$CO-), 2.30 – 1.83 (m, 20H, Pro$_\beta$, Pro$_\gamma$, Arg$_\beta$, Arg$_\gamma$), 1.79 – 1.66 (m, 8H, Arg$_\beta$, Arg$_\gamma$), 1.62 – 1.51 (m, 2H, C8's -C$\underline{H}_2$CH$_2$CO-), 1.43 – 1.21 (m, 8H, C8's -CH$_2$-), 0.96 – 0.79 (m, 3H, C8's -CH$_3$).

^{13}C NMR (75 MHz, Methanol-d4) δ 176.94, 174.79, 174.74, 174.26, 174.15, 172.21, 172.10, 172.03, 158.91, 158.72, 158.67, 61.50, 61.45, 61.35, 61.12, 52.16, 52.12, 51.96, 49.96, 49.76, 49.44, 48.94, 48.86, 42.18, 42.07, 42.03, 35.39, 32.86, 30.91, 30.79, 30.70, 30.63, 30.50, 30.36, 30.32, 30.19, 29.32, 29.24, 25.99, 25.87, 25.81, 25.71, 25.64, 23.63, 23.30, 14.39.

MS-ESI m/z calculated for C$_{46}$H$_{82}$N$_{17}$O$_8$ (M+H)$^+$: 1001.27 found 1001.01.

C$_{12}$-PRP (C$_{12}$-PRPRPRP-NH$_2$)

^{1}H NMR (300 MHz, Methanol-d_4) δ 4.69 – 4.56 (m, 3H, Arg$_\alpha$), 4.51 – 4.37 (m, 4H, Pro$_\alpha$), 3.88 – 3.54 (m, 8H, Pro$_\delta$), 3.26 – 3.10 (m, 6H, Arg$_\delta$), 2.37 (t, J = 7.5 Hz, 2H, C12's -C$\underline{H}_2$CO-), 2.32 – 1.80 (m, 20H, Pro$_\beta$, Pro$_\gamma$, Arg$_\beta$, Arg$_\gamma$), 1.74 (m, 8H, Arg$_\beta$, Arg$_\gamma$), 1.63 – 1.54 (m, 2H, C12's -C$\underline{H}_2$CH$_2$CO-), 1.31 (m, 16H, C12's -CH$_2$-), 0.89 (t, J = 6.6 Hz, 3H, C12's -CH$_3$).

^{13}C NMR (75 MHz, Methanol-d_4) δ 176.92, 174.81, 174.79, 174.32, 174.18, 172.25, 172.14, 172.01, 158.76, 158.71, 158.69, 61.46, 61.36, 61.32, 61.16, 52.29, 52.18, 51.93, 49.74, 48.88, 48.59, 48.35, 42.16, 42.09, 42.03, 40.85, 35.45, 33.08, 30.99, 30.81, 30.76, 30.72, 30.68, 30.59, 30.48, 30.43, 29.41, 29.36, 29.29, 29.24, 26.03, 25.93, 25.88, 25.78, 25.75, 25.69, 25.63, 25.56, 23.74, 14.44.

MALDI-MS m/z calculated for C$_{50}$H$_{90}$N$_{17}$O$_8$ (M+H)$^+$: 1056.72, found 1056.722.

C$_{16}$-PRP (C$_{16}$-PRPRPRP-NH$_2$)

^{1}H NMR (300 MHz, Methanol-d_4) δ 4.65 – 4.52 (m, 3H, Arg$_\alpha$), 4.46 – 4.30 (m, 4H, Pro$_\alpha$), 3.82 – 3.67 (m, 3H, Pro$_\delta$), 3.66 – 3.49 (m, 5H, Pro$_\delta$), 3.22 – 3.09 (m, 6H, Arg$_\delta$), 2.33 (t, J = 7.5 Hz, 2H, C16's -C$\underline{H}_2$CO-), 2.24 – 1.52 (m, 30H, Pro$_\beta$, Pro$_\gamma$, Arg$_\beta$, Arg$_\gamma$, C16's -C$\underline{H}_2$CH$_2$CO-), 1.34 – 1.18 (m, 24H, C16's -CH$_2$-), 0.85 (t, J = 6.9 Hz, 3H, C16's -CH$_3$).

^{13}C NMR (126 MHz, Methanol-d_4, rotamers observed) δ 175.47, 173.35, 173.33, 172.87, 172.82, 172.79, 172.72, 170.79, 170.67, 170.56, 157.31, 157.26, 157.23, 60.03, 60.01, 59.90, 59.86, 59.74, 59.70, 50.75, 50.73, 50.48, 48.19, 48.02, 47.85, 47.68, 40.71, 40.67, 40.63, 33.99, 31.63,

29.54, 29.34, 29.31, 29.26, 29.23, 29.14, 29.03, 28.98, 27.95, 27.85, 27.83, 24.58, 24.48, 24.43, 24.40, 24.32, 24.18, 22.29, 12.99.

MS-ESI m/z calculated for $C_{54}H_{98}N_{17}O_8$ (M+H)$^+$: 1113.49, found 1113.40.

Ad-PRP (Ad-PRPRPRP-NH$_2$)

^{1}H NMR (300 MHz, Methanol-d_4) δ 4.72 – 4.54 (m, 3H, Arg$_α$), 4.53 – 4.32 (m, 4H, Pro$_α$), 3.90 – 3.43 (m, 8H, Pro$_δ$), 3.29 – 3.06 (m, 6H, Arg$_δ$), 2.40 – 2.11 (m, 6H, Pro$_β$, Adamantyl's -C$\underline{H}_2$CO-), 2.11 – 1.82 (m, 18H, Pro$_β$, Pro$_γ$, Arg$_β$, Arg$_γ$, Adamantyl), 1.82 – 1.56 (m, 21H, Arg$_β$, Arg$_γ$, Adamantyl).

^{13}C NMR (75 MHz, Methanol-d_4) δ 176.92, 174.72, 174.28, 174.14, 172.86, 172.22, 172.07, 172.01, 158.75, 158.70, 158.68, 61.57, 61.46, 61.34, 61.22, 52.17, 52.13, 51.90, 50.14, 49.78, 48.96, 48.56, 48.30, 43.78, 43.63, 42.21, 42.10, 41.93, 37.85, 35.09, 34.73, 30.93, 30.85, 30.68, 30.65, 30.52, 30.47, 30.36, 30.26, 30.16, 29.94, 29.48, 29.40, 29.27, 29.25, 26.03, 26.00, 25.82, 25.73, 25.63.

MALDI-MS m/z calculated for $C_{50}H_{84}N_{17}O_8$ (M+H)$^+$: 1049.66, found 1050.680.

C$_8$-PGP (C$_8$-PRPGPRP-NH$_2$)

^{1}H NMR (500 MHz, Methanol-d_4) δ 4.75 – 4.65 (m, 2H, Arg$_α$), 4.54 – 4.37 (m, 4H, Pro$_α$), 4.15 – 3.96 (m, 2H, Gly$_α$), 3.83 – 3.55 (m, 8H, Pro$_δ$), 3.27 – 3.16 (m, 4H, Arg$_δ$), 2.37 (t, J = 7.6 Hz, 2H, C8's -C$\underline{H}_2$CO-), 2.30 – 1.86 (m, 18H, Pro$_β$, Pro$_γ$, Arg$_β$, Arg$_γ$), 1.80 – 1.69 (m, 6H, Pro$_γ$, Arg$_β$,

Arg$_\gamma$), 1.60 (m, 2H, C8's -C$\underline{H}_2$CH$_2$CO-), 1.40 – 1.25 (m, 8H, C8's -CH$_2$-), 0.91 (t, J = 7.0 Hz, 3H C8's -CH$_3$).

^{13}C NMR (126 MHz, Methanol-d_4) δ 176.94, 174.78, 174.70, 174.54, 174.36, 172.18, 171.84, 169.38, 158.66, 158.64, 61.53, 61.47, 61.28, 61.16, 52.03, 51.93, 49.63, 49.46, 49.28, 48.49, 47.88, 42.85, 42.10, 42.05, 35.43, 32.92, 30.98, 30.74, 30.73, 30.63, 30.38, 30.25, 29.37, 29.34, 25.99, 25.92, 25.86, 25.84, 25.64, 25.63, 23.69, 14.41.

MALDI-MS m/z calculated for C$_{42}$H$_{73}$N$_{14}$O$_8$ (M+H)$^+$: 900.57, found 901.586.

C$_{12}$-PGP (C$_{12}$-PRPGPRP-NH$_2$)

^{1}H NMR (300 MHz, Methanol-d_4) δ 4.76 – 4.59 (m, 2H, Arg$_\alpha$), 4.57 – 4.34 (m, 4H, Pro$_\alpha$), 4.17 – 3.89 (m, 2H, Gly$_\alpha$), 3.88 – 3.46 (m, 8H, Pro$_\delta$), 3.27 – 3.04 (m, 4H, Arg$_\delta$), 2.42 – 2.30 (t, J = 7.5 Hz, 2H, C12's -C$\underline{H}_2$CO-), 2.27 – 1.65 (m, 24H, Pro$_\beta$, Pro$_\gamma$, Arg$_\beta$, Arg$_\gamma$), 1.63 – 1.52 (m, 2H, C12's -C$\underline{H}_2$CH$_2$CO-), 1.43 – 1.15 (m, 16H, C12's -CH$_2$-), 0.95 – 0.78 (m, 3H, C12's -CH$_3$).

^{13}C NMR (75 MHz, Methanol-d_4) 176.94, 174.74, 174.68, 174.51, 174.36, 172.22, 171.89, 169.35, 158.65, 158.56, 61.49, 61.32, 61.18, 61.13, 52.15, 51.95, 49.41, 49.15, 48.86, 47.86, 42.84, 42.06, 35.40, 33.03, 30.94, 30.84, 30.71, 30.62, 30.54, 30.42, 30.40, 29.44, 29.39, 29.34, 29.31, 29.25, 29.18, 26.06, 25.97, 25.88, 25.82, 25.69, 25.62, 23.69, 23.63, 14.42.

MALDI-MS m/z calculated for C$_{46}$H$_{81}$N$_{14}$O$_8$ (M+H)$^+$: 957.64, found 957.656.

C$_{16}$-PGP (C$_{16}$-PRPGPRP-NH$_2$)

^{1}H NMR (300 MHz, Methanol-d_4) δ 4.54 – 4.41 (m, 2H, Arg$_α$), 4.37 – 4.14 (m, 4H, Pro$_α$), 3.96 – 3.73 (m, 2H, Gly$_α$), 3.65 – 3.28 (m, 8H, Pro$_δ$), 3.07 – 2.90 (m, 4H, Arg$_δ$), 2.17 (t, J = 7.6 Hz, 2H, C16's -CH$_2$CO-), 2.11 – 1.61 (m, 18H, Pro$_β$, Pro$_γ$, Arg$_β$, Arg$_γ$), 1.59 – 1.33 (m, 8H, Pro$_γ$, Arg$_β$, Arg$_γ$, C16's -C$\underline{H}_2$CH$_2$CO-), 1.19 – 1.01 (m, 24H, C16's -CH$_2$-), 0.68 (t, J = 6.7 Hz, 3H, C16's -CH$_3$).

^{13}C NMR (75 MHz, Methanol-d_4) δ 176.97, 174.81, 174.72, 174.56, 174.38, 172.21, 171.87, 169.40, 158.75, 158.68, 61.55, 61.50, 61.31, 61.18, 52.17, 51.96, 48.93, 48.58, 48.30, 47.90, 42.87, 42.12, 42.07, 35.45, 33.08, 31.00, 30.95, 30.93, 30.91, 30.80, 30.77, 30.68, 30.66, 30.59, 30.48, 30.44, 29.50, 29.39, 29.37, 26.08, 26.01, 25.94, 25.87, 25.76, 25.74, 25.67, 25.59, 25.57, 23.74, 14.45.

MALDI-MS m/z calculated for C$_{50}$H$_{89}$N$_{14}$O$_8$ (M+H)$^+$: 1013.70, found 1013.704.

Ad-PGP (C8-PRPGPRP-NH$_2$)

^{1}H NMR (300 MHz, Methanol-d_4) δ 4.73 – 4.61 (m, 2H, Arg$_α$), 4.59 – 4.37 (m, 4H, Pro$_α$), 4.17 – 3.94 (m, 2H, Gly$_α$), 3.84 – 3.52 (m, 8H, Pro$_δ$), 3.26 – 3.13 (m, 4H, Arg$_δ$), 2.39 – 2.13 (m, 6H, Pro$_β$, Adamantyl's -C$\underline{H}_2$CO-), 2.12 – 1.82 (m, 17H, Pro$_β$, Pro$_γ$, Arg$_β$, Arg$_γ$, Adamantyl), 1.81 – 1.57 (m, 18H, Arg$_β$, Arg$_γ$, Adamantyl).

^{13}C NMR (75 MHz, Methanol-d_4) δ 176.94, 174.67, 174.55, 174.35, 172.90, 172.14, 171.82, 169.38, 61.53, 61.46, 61.31, 61.26, 51.94, 51.90, 49.99, 49.78, 49.73, 49.44, 49.42, 49.15, 48.99, 48.61, 48.31, 48.28, 48.06, 42.85, 42.17, 42.12, 42.07, 41.72, 41.64, 37.87, 35.12, 30.99, 30.73, 30.70, 30.66, 30.64, 30.20, 29.48, 29.38, 29.36, 26.07, 26.01, 25.99, 25.96, 25.91, 25.84, 25.80, 25.63

MALDI-MS m/z calculated for $C_{46}H_{75}N_{14}O_8$ (M+H)$^+$: 950.58, found 951.604.

C$_8$-PLP (C$_8$-PRPLPRP-NH$_2$)

^{1}H NMR (300 MHz, Methanol-d_4) δ 4.73 – 4.55 (m, 3H, Arg$_\alpha$, Leu$_\alpha$), 4.54 – 4.34 (m, 4H, Pro$_\alpha$), 3.91 – 3.46 (m, 8H, Pro$_\delta$), 3.27 – 3.12 (m, 4H, Arg$_\delta$), 2.36 (t, J = 7.5 Hz, 2H, C8's -C$\underline{H}_2$CO-), 2.30 – 1.80 (m, 19H, Pro$_\beta$, Pro$_\gamma$, Arg$_\beta$, Leu$_\gamma$), 1.79 – 1.66 (m, 6H, Arg$_\beta$, Arg$_\gamma$), 1.64 – 1.50 (m, 4H, Leu$_\beta$, C8's -C$\underline{H}_2$CH$_2$CO-), 1.41 – 1.21 (m, 8H, C8's -CH$_2$-), 0.97 (m, 6H, Leu$_\delta$), 0.90 (t, J = 6.2 Hz, 3H, C8's -CH$_3$).

^{13}C NMR (75 MHz, Methanol-d_4) δ 176.96, 174.76, 174.73, 174.38, 174.34, 174.12, 173.29, 172.00, 158.71, 158.70, 61.35, 61.28, 61.21, 61.17, 52.04, 51.89, 51.19, 49.97, 49.76, 49.47, 48.91, 42.13, 42.11, 41.21, 35.44, 32.92, 30.97, 30.81, 30.55, 30.45, 30.43, 30.39, 30.25, 29.41, 29.31, 26.01, 25.92, 25.86, 25.74, 25.68, 25.60, 23.79, 23.69, 21.96, 14.43.

MALDI-MS m/z calculated for $C_{46}H_{81}N_{14}O_8$ (M+H)$^+$: 957.63, found 957.632.

C$_{12}$-PLP (C$_{12}$-PRPLPRP-NH$_2$)

^{1}H NMR (300 MHz, Methanol-d_4) δ 4.73 – 4.55 (m, 3H, Arg$_\alpha$, Leu$_\alpha$), 4.53 – 4.35 (m, 4H, Pro$_\alpha$), 3.93 – 3.40 (m, 8H, Pro$_\delta$), 3.28 – 3.06 (m, 4H, Arg$_\delta$), 2.37 (t, J = 7.6 Hz, 2H, C12's –C$\underline{H}_2$CO-), 2.30 – 1.83 (m, 18H, Pro$_\beta$, Pro$_\gamma$, Arg$_\beta$), 1.83 – 1.65 (m, 7H, Arg$_\beta$, Arg$_\gamma$, Leu$_\gamma$), 1.65 – 1.50 (m, 4H, Leu$_\beta$, C12's -C$\underline{H}_2$CH$_2$CO-), 1.40 – 1.23 (m, 16H, C12's -CH$_2$-), 0.97 (m, 6H, Leu$_\delta$), 0.89 (t, J = 6.7 Hz, 3H, C12's -CH$_3$).

^{13}C NMR (75 MHz, Methanol-d_4) δ 176.92, 174.79, 174.71, 174.69, 174.33, 174.11, 173.23, 172.01, 158.70, 158.65, 61.56, 61.31, 61.27, 61.16, 52.04, 51.89, 51.15, 49.85, 49.72, 49.46, 48.87, 42.09, 41.16, 35.40, 35.30, 33.18, 33.03, 30.92, 30.77, 30.71, 30.63, 30.54, 30.43, 30.39, 30.30, 29.35, 29.24, 25.97, 25.87, 25.82, 25.71, 25.65, 25.61, 25.51, 23.77, 23.70, 23.64, 21.93, 14.43.

MALDI-MS m/z calculated for $C_{50}H_{89}N_{14}O_8$ (M+H)$^+$: 1013.70, found 1013.699.

C$_{16}$-PLP (C$_{16}$-PRPLPRP-NH$_2$)

^{1}H NMR (300 MHz, Methanol-d_4) δ 6.77 – 6.57 (m, 3H, Arg$_α$, Leu$_α$), 6.57 – 6.38 (m, 4H, Pro$_α$), 5.96 – 5.44 (m, 8H, Pro$_δ$), 5.31 – 5.08 (m, 4H, Arg$_δ$), 4.38 (t, J = 7.5 Hz, 2H, C16's -C$\underline{H}_2$CO-), 4.31 – 3.86 (m, 18H, Pro$_β$, Pro$_γ$, Arg$_β$), 3.86 – 3.68 (m, 7H, Arg$_β$, Arg$_γ$, Leu$_γ$), 3.68 – 3.53 (m, 4H, Leu$_β$, C16's -C$\underline{H}_2$CH$_2$CO-), 3.42 – 3.24 (m, 24H, C16's -CH$_2$-), 3.06 – 2.95 (m, 6H, Leu$_δ$), 2.91 (t, J = 6.7 Hz, 3H, C16's -CH$_3$).

^{13}C NMR (75 MHz, Methanol-d_4) δ 176.91, 174.78, 174.68, 174.30, 174.12, 173.18, 172.05, 158.68, 158.63, 61.53, 61.29, 61.19, 61.13, 52.08, 51.93, 51.14, 50.06, 49.96, 49.72, 48.86, 42.07, 41.95, 41.16, 35.40, 35.28, 33.03, 30.91, 30.74, 30.72, 30.63, 30.53, 30.43, 30.39, 29.34, 29.21, 26.18, 25.97, 25.87, 25.81, 25.71, 25.66, 25.51, 25.47, 23.77, 23.70, 23.21, 23.17, 22.13, 22.08, 22.04, 21.94, 21.86, 14.44.

MALDI-MS m/z calculated for $C_{54}H_{97}N_{14}O_8$ (M+H)$^+$: 1069.76, found 1069.736.

Ad-PLP (Ad-PRPLPRP-NH$_2$)

^{1}H NMR (300 MHz, Methanol-d_4) δ 4.72 – 4.54 (m, 3H, Arg$_α$, Leu$_α$), 4.53 – 4.35 (m, 4H, Pro$_α$), 3.94 – 3.36 (m, 8H, Pro$_δ$), 3.28 – 3.10 (m, 4H, Arg$_δ$), 2.37 – 2.12 (m, 6H Pro$_β$, Adamantyl's -CH$_2$CO-), 2.12 – 1.86 (m, 17H, Pro$_β$, Pro$_γ$, Arg$_β$, Leu$_γ$, Adamantyl), 1.80 – 1.48 (m, 21H, Arg$_β$, Arg$_γ$, Adamantyl), 1.03-0.88 (m, 6H, Leu$_δ$).

^{13}C NMR (75 MHz, Methanol-d_4) δ 176.92, 174.66, 174.33, 174.09, 173.25, 172.83, 171.99, 171.95, 158.72, 158.67, 61.43, 61.31, 61.27, 61.13, 52.02, 51.85, 51.15, 50.13, 50.02, 49.99, 49.72, 43.76, 43.63, 42.09, 41.87, 41.17, 37.84, 35.07, 34.71, 33.17, 33.09, 30.92, 30.74, 30.66, 30.59, 30.50, 30.35, 30.30, 30.15, 29.47, 29.26, 26.01, 25.97, 25.70, 25.63, 25.59, 23.76, 22.21, 21.92.

MALDI-MS m/z calculated C$_{50}$H$_{83}$N$_{14}$O$_8$ (M+H)$^+$: 1007.65 found, 1006.64.

C$_8$-PWP (C$_8$-PRPWPRP-NH$_2$)

^{1}H NMR (500 MHz, Methanol-d_4) δ 7.68 – 7.00 (m, 5H, Trp aromatic), 5.00 – 4.86 (m, 1H, Trp$_α$), 4.72 – 4.57 (m, 2H, Arg$_α$), 4.55 – 4.29 (m, 4H, Pro$_α$), 3.87 – 3.35 (m, 8H, Pro$_δ$), 3.29 – 3.07 (m, 6H, Arg$_δ$, Trp$_β$), 2.37 (t, J = 7.6 Hz, 2H, C8's -CH$_2$CO-), 2.30 – 1.83 (m, 16H, Pro$_β$, Pro$_γ$), 1.82 – 1.44 (m, 10H, Arg$_β$, Arg$_γ$, C8's -CH$_2$CH$_2$CO-), 1.43 – 1.25 (m, 8H, C8's -CH$_2$-), 0.89 (t, J = 6.8 Hz, 3H, C8's -CH$_3$).

^{13}C NMR (126 MHz, Methanol-d_4) δ 176.96, 176.93, 174.86, 174.76, 174.73, 174.67, 174.57, 174.33, 174.12, 173.96, 173.33, 173.26, 172.89, 172.08, 172.06, 171.96, 158.66, 158.60, 137.98, 128.79, 125.11, 122.49, 119.88, 119.05, 112.37, 110.53, 61.62, 61.59, 61.32, 61.29, 61.27, 61.25, 61.22, 61.18, 53.64, 53.55, 52.01, 51.98, 51.92, 51.84, 49.63, 49.45, 49.28, 49.11, 49.04, 48.96, 48.87, 48.70, 42.12, 42.11, 42.06, 42.02, 35.42, 32.91, 30.99, 30.94, 30.82, 30.77, 30.46, 30.37,

30.32, 30.29, 30.25, 30.19, 30.09, 29.67, 29.59, 29.42, 29.41, 29.39, 29.35, 28.33, 28.31, 28.27, 26.01, 25.99, 25.95, 25.92, 25.89, 25.86, 25.81, 25.70, 25.57, 23.68, 14.41.

MALDI-MS m/z calculated for $C_{51}H_{80}N_{15}O_8$ (M+H)$^+$: 1030.63, found 1030.640.

C_{12}-PWP (C_{12}-PRPWPRP-NH$_2$)

^{1}H NMR (300 MHz, Methanol-d_4) δ 7.71 – 6.95 (m, 5H, Trp aromatic), 4.93 – 4.88 (m, 1H, Trp$_\alpha$), 4.72 – 4.56 (m, 2H, Arg$_\alpha$), 4.56 – 4.34 (m, 4H, Pro$_\alpha$), 3.88 – 3.34 (m, 8H, Pro$_\delta$), 3.29 – 3.03 (m, 6H, Arg$_\delta$, Trp$_\beta$), 2.36 (t, J = 7.6 Hz, 2H, C12's -C$\underline{H}_2$CO-), 2.31 – 1.83 (m, 16H, Pro$_\beta$, Pro$_\gamma$), 1.82 – 1.48 (m, 10H, Arg$_\beta$, Arg$_\gamma$, C12's -C$\underline{H}_2$CH$_2$CO-), 1.42 – 1.20 (m, 16H, C12's -CH$_2$-), 0.88 (t, J = 6.5 Hz, 3H, C12's -CH$_3$).

^{13}C NMR (75 MHz, Methanol-d_4, rotamers present) δ 176.96, 174.85, 174.74, 174.66, 174.04, 173.98, 173.31, 173.27, 172.81, 172.75, 172.54, 172.16, 172.01, 171.85, 158.64, 158.59, 137.93, 128.80, 128.62, 125.15, 124.99, 122.81, 122.47, 120.04, 119.88, 119.25, 119.04, 112.59, 112.40, 110.46, 110.17, 61.71, 61.57, 61.41, 61.38, 61.30, 61.15, 61.04, 54.29, 53.50, 52.35, 52.05, 51.95, 51.86, 49.97, 49.71, 48.95, 48.86, 48.27, 42.10, 42.03, 35.46, 35.41, 35.32, 35.30, 33.03, 31.93, 30.94, 30.89, 30.71, 30.63, 30.54, 30.43, 30.39, 30.29, 30.15, 29.59, 29.33, 28.82, 28.78, 28.72, 28.29, 28.21, 25.99, 25.95, 25.89, 25.83, 25.72, 25.62, 25.59, 23.70, 23.11, 23.06, 14.42.

MALDI-MS m/z calculated for $C_{55}H_{88}N_{15}O_8$ (M+H)$^+$: 1086.69, found 1086.679.

C_{16}-PWP (C_{16}-PRPWPRP-NH$_2$)

^{1}H NMR (300 MHz, Methanol-d_4) δ 7.75 – 6.89 (m, 5H, Trp aromatic), 4.98 – 4.87 (m, 1H, Trp$_\alpha$), 4.73 – 4.56 (m, 2H, Arg$_\alpha$), 4.56 – 4.25 (m, 4H, Pro$_\alpha$), 3.91 – 3.34 (m, 8H, Pro$_\delta$), 3.29 – 2.96 (m, 6H, Arg$_\delta$, Trp$_\beta$), 2.37 (t, J = 7.5 Hz, 2H, C16's -C$\underline{H}_2$CO-), 2.32 – 1.83 (m, 16H, Pro$_\beta$, Pro$_\gamma$), 1.82 – 1.41 (m, 10H, Arg$_\beta$, Arg$_\gamma$, C16's -C$\underline{H}_2$CH$_2$CO-), 1.40 – 1.17 (m, 24H, C16's -CH$_2$-), 0.90 (t, J = 6.7 Hz, 3H, C16's -CH$_3$).

^{13}C NMR (75 MHz, Methanol-d_4, rotamers present) δ 176.96, 174.76, 174.66, 174.25, 174.07, 174.04, 173.97, 173.32, 173.27, 172.84, 172.75, 172.56, 172.23, 172.14, 172.00, 171.82, 158.65, 158.60, 137.95, 128.81, 128.64, 125.14, 124.97, 122.83, 122.48, 120.05, 119.88, 119.27, 119.05, 112.60, 112.39, 110.49, 110.18, 61.74, 61.58, 61.17, 53.52, 52.34, 52.23, 52.04, 51.86, 48.96, 48.88, 42.11, 42.05, 35.42, 33.05, 30.96, 30.91, 30.76, 30.64, 30.55, 30.44, 30.41, 30.32, 29.34, 28.87, 28.83, 28.78, 28.24, 26.00, 25.95, 25.90, 25.84, 25.71, 25.60, 23.71, 23.07, 14.43.

MALDI-MS m/z calculated for $C_{59}H_{96}N_{15}O_8$ (M+H)$^+$: 1142.76, found 1142.758.

Ad-PWP (C8-PRPWPRP-NH$_2$)

^{1}H NMR (300 MHz, Methanol-d_4) δ 7.70 – 6.96 (m, 5H, Trp aromatic), 5.06 – 4.92 (m, 1H, Trp$_\alpha$), 4.71 – 4.55 (m, 2H, Arg$_\alpha$), 4.55 – 4.24 (m, 4H, Pro$_\alpha$), 3.97 – 3.37 (m, 8H, Pro$_\delta$), 3.26 – 2.83 (m, 6H, Arg$_\delta$, Trp$_\beta$), 2.36 – 2.07 (m, 6H, Pro$_\beta$, Adamantyl's -C$\underline{H}_2$CO-), 2.06 – 1.80 (m, 15H, Pro$_\beta$, Pro$_\gamma$, Arg$_\beta$, Adamantyl), 1.79 – 1.16 (m, 20H, Arg$_\beta$, Arg$_\gamma$, Adamantyl).

^{13}C NMR (75 MHz, Methanol-d_4, rotamers present) δ 176.95, 174.73, 174.64, 174.10, 174.03, 173.98, 173.31, 173.27, 172.94, 172.82, 172.74, 172.62, 172.50, 172.15, 172.02, 171.86, 158.62, 158.59, 138.07, 137.91, 128.80, 128.61, 125.14, 124.99, 123.45, 122.80, 122.47, 120.04, 119.88, 119.60, 119.56, 119.25, 119.04, 115.74, 112.60, 112.41, 110.62, 110.45, 110.15, 61.68, 61.65,

61.56, 61.46, 61.31, 61.25, 61.11, 60.91, 54.29, 53.49, 52.36, 52.15, 52.06, 51.93, 51.85, 50.12, 48.94, 48.59, 43.75, 43.62, 42.16, 42.08, 41.97, 37.82, 35.06, 34.72, 31.92, 30.93, 30.87, 30.72, 30.55, 30.44, 30.32, 30.26, 30.13, 30.04, 29.70, 29.42, 29.32, 28.74, 28.19, 25.98, 25.85, 25.72, 25.63, 25.58, 23.05.

MALDI-MS m/z calculated for $C_{55}H_{82}N_{15}O_8$ (M+H)$^+$: 1079.64, found 1081.685.

C_{12}-prp (C_{12}-prprprp-NH$_2$) – all D-peptide

^{1}H NMR (300 MHz, Methanol-d_4) δ 4.70 – 4.55 (m, 3H, Arg$_\alpha$), 4.53 – 4.35 (m, 4H, Pro$_\alpha$), 3.87 – 3.46 (m, 8H, Pro$_\delta$), 3.28 – 3.10 (m, 6H, Arg$_\delta$), 2.37 (t, J = 7.6 Hz, 2H, C12's -C$\underline{H}_2$CO-), 2.30 – 1.83 (m, 19H, Pro$_\beta$, Pro$_\gamma$, Arg$_\gamma$, Arg$_\beta$), 1.83 – 1.66 (m, 9H, Arg$_\beta$, Arg$_\gamma$), 1.65 – 1.54 (m, 2H, C12's -C$\underline{H}_2$CH$_2$CO-), 1.40 – 1.22 (m, 16H, C12's -CH$_2$-), 0.89 (t, J = 6.5 Hz, 3H, C12's -CH$_3$).

^{13}C NMR (75 MHz, Methanol-d_4) δ 176.93, 174.76, 174.73, 174.28, 174.17, 172.20, 172.16, 172.01, 158.73, 158.69, 158.64, 61.49, 61.40, 61.35, 61.12, 52.19, 52.12, 52.01, 49.78, 49.69, 49.17, 48.95, 48.88, 42.24, 42.11, 41.95, 35.50, 35.41, 35.31, 33.03, 30.94, 30.84, 30.72, 30.63, 30.57, 30.55, 30.43, 30.39, 29.27, 26.13, 26.03, 25.99, 25.93, 25.88, 25.83, 25.76, 25.71, 25.61, 23.70, 14.42.

MALDI-MS m/z calculated for $C_{50}H_{90}N_{17}O_8$ (M+H)$^+$: 1056.35, found 1056.736.

I-2. Synergy scan for combinations of clinically-used antibiotics with SPRLPs against wild-type *Pseudomonas aeruginosa* PAO1

Note: A ≥four-fold reduction of the antibiotic's minimum inhibitory concentration (MIC) at a fixed 8 µg/mL (5 µM) SPRLP concentration denotes for a potential synergistic interaction.

Appendix Table I-1 Synergy scan for combinations of rifampicin, minocycline, moxifloxacin, ceftazidime, and gentamicin with SPRLPs against wild-type *P. aeruginosa* PAO1.

	Rifampicin	Minocycline	Moxifloxacin	Ceftazidime	Gentamicin
MIC, µg/mL	8	8	1	2	1

Absolute MIC in the presence of 8 µg/mL (5 µM) SPRLP adjuvant, µg/mL					
Adjuvant	Rifampicin	Minocycline	Moxifloxacin	Ceftazidime	Gentamicin
C$_8$-PRP	8	8	4	2	2
C$_{12}$-PRP	1	1	1	2	4
C$_{16}$-PRP	8	8	2	2	4
Ad-PRP	8	8	2	2	2
C$_8$-PGP	8	8	2	2	2
C$_{12}$-PGP	4	8	2	2	4
C$_{16}$-PGP	4	8	2	2	4
Ad-PGP	8	8	1	4	2
C$_8$-PLP	8	8	2	2	2
C$_{12}$-PLP	8	8	2	2	4
C$_{16}$-PLP	8	8	2	2	4
Ad-PLP	8	8	2	2	2
C$_8$-PWP	8	8	2	2	4
C$_{12}$-PWP	4	8	2	2	4
C$_{16}$-PWP	8	8	2	2	4
Ad-PWP	8	8	2	2	2

Appendix Table I-2 Synergy scan for combinations of meropenem, ciprofloxacin, colistin, tobramycin, and aztreonam with SPRLPs against wild-type *P. aeruginosa* PAO1.

	Meropenem	Ciprofloxacin	Colistin	Tobramycin	Aztreonam
MIC, µg/mL	1	0.125	0.5	1	4

Absolute MIC in the presence of 8 µg/mL (5 µM) SPRLP adjuvant, µg/mL					
Adjuvant	Meropenem	Ciprofloxacin	Colistin	Tobramycin	Aztreonam
C_8-PRP	1	0.25	0.25	0.5	2
C_{12}-PRP	2	0.0625	1	0.5	2
C_{16}-PRP	1	0.125	0.25	1	2
Ad-PRP	2	0.125	0.5	1	4
C_8-PGP	2	0.125	0.5	1	4
C_{12}-PGP	2	0.25	0.25	1	4
C_{16}-PGP	2	0.125	0.5	1	4
Ad-PGP	2	0.125	0.5	1	2
C_8-PLP	2	0.125	0.5	1	4
C_{12}-PLP	1	0.125	0.25	1	2
C_{16}-PLP	1	0.125	0.25	1	4
Ad-PLP	1	0.125	0.5	0.5	2
C_8-PWP	2	0.25	0.5	>1	4
C_{12}-PWP	2	0.125	0.5	0.5	2
C_{16}-PWP	2	0.25	0.25	1	2
Ad-PWP	1	0.125	0.5	0.5	2

Appendix Table I-3 Synergy scan for combinations of doripenem, levofloxacin, fosfomycin, amikacin, and cefotaxime with SPRLPs against wild-type *P. aeruginosa* PAO1.

	Doripenem	Levofloxacin	Fosfomycin	Amikacin	Cefotaxime
MIC, µg/mL	0.5	0.25	16	1	16

Absolute MIC in the presence of 8 µg/mL (5 µM) SPRLP adjuvant, µg/mL					
Adjuvant	Doripenem	Levofloxacin	Fosfomycin	Amikacin	Cefotaxime
C_8-PRP	0.5	1	16	4	16
C_{12}-PRP	0.5	0.5	16	4	16
C_{16}-PRP	1	1	16	4	16
Ad-PRP	0.5	0.5	16	1	16
C_8-PGP	0.5	0.5	16	1	16
C_{12}-PGP	0.5	1	32	2	16
C_{16}-PGP	0.5	0.5	16	2	16
Ad-PGP	0.5	0.5	16	1	16
C_8-PLP	0.5	0.5	16	1	16
C_{12}-PLP	0.5	0.5	16	4	16
C_{16}-PLP	0.5	0.5	16	2	16
Ad-PLP	0.5	0.5	16	1	16
C_8-PWP	1	1	32	2	16
C_{12}-PWP	0.5	0.5	16	2	16
C_{16}-PWP	0.5	1	16	2	16
Ad-PWP	0.5	0.5	16	2	16

I-3. Checkerboard assay for combinations of minocycline and rifampicin with SPRLPs belonging to the PRP sequence subset.

Appendix Table I-4 Synergy evaluation for combinations of minocycline and rifampicin with either C_8-PRP, C_{16}-PRP or Ad-PRP in wild-type *P. aeruginosa* PAO1.

Antibiotic	$MIC_{Antibiotic}$, µg/mL	Adjuvant	$MIC_{Adjuvant}$, µg/mL	FIC index	Interpretation
Minocycline	8	C_8-PRP	>512	1<x<1.004	Indifferent
Minocycline	8	C_{16}-PRP	32	1	Indifferent
Minocycline	8	Ad-PRP	>512	0.50<x<0.75	Indifferent
Rifampicin	8	C_8-PRP	>512	0.50<x<0.504	Indifferent
Rifampicin	8	C_{16}-PRP	32	0.75	Indifferent
Rifampicin	8	Ad-PRP	>512	0.25<x<0.75	Indifferent

I-4. Assessment for cytotoxicity of C12-PRP along with control drugs.

Appendix Table I-5 Cytotoxicity evaluation of amphiphilic C12-PRP, colistin and adriamycin® against human liver carcinoma HepG2 and human embryonic kidney HEK-293 cell lines.

Agent	HepG2		HEK-293	
	IC_{50}^{a}, μM	CC_{50}^{b}, μM	IC_{50}^{a}, μM	CC_{50}^{b}, μM
C12-PRP	>50	>50	>50	>50
Colistin[c]	1.5	>50	>50	>50
Adriamycin®[d]	<0.16	<0.16	<0.16	0.16

[a] = concentration needed to inhibit cell proliferation to 50% (IC_{50}); [b] = concentration needed to reduce cell viability to 50% (CC_{50}); [c] = colistin is used as an internal control for a clinically-used peptide antibiotic; [d] = adriamycin® is used as an internal control for a clinically-used anticancer drug.

Appendix II: Supporting information for Chapter 5

Additional data shown below are complimentary to Chapter 5 and are based on my publication:

Ronald Domalaon, Marc Brizuela, Benjamin Eisner, Brandon Findlay, George G. Zhanel, Frank Schweizer. **2018**. Dilipid ultrashort cationic lipopeptides as adjuvants for chloramphenicol and other conventional antibiotics against Gram-negative bacteria. Amino Acids (Epub ahead of print). doi: 10.1007/s00726-018-2673-9.

Reproduced with permission.

II-1. Chemical characterization of dilipid ultrashort cationic lipopeptides (dUSCLs)

Di-C$_7$-KKKK-NH$_2$ (1)

^{1}H NMR (500 MHz, Deuterium Oxide) δ = 4.38 – 4.14 (m, 4H), 3.15 (t, J=6.2, 2H), 2.97 (t, J=6.6, 10H), 2.37 – 2.12 (m, 4H), 1.94 – 1.11 (m, 41H), 0.92 – 0.74 (m, 6H).

^{13}C NMR (126 MHz, Deuterium Oxide) δ = 177.54, 177.20, 176.33, 174.52, 173.66, 173.65, 53.84, 53.51, 53.46, 53.37, 39.20, 38.98, 35.83, 35.42, 30.74, 30.70, 30.50, 30.48, 30.44, 30.39, 27.92, 27.86, 27.81, 26.33, 26.26, 25.44, 25.33, 22.58, 22.13, 22.11, 22.07, 21.99, 21.92, 21.90, 13.36.

MS (ESI) m/z calcd for C$_{38}$H$_{76}$N$_9$O$_6$ (M+H)$^+$: 755.07 found: 754.9.

Di-C$_9$-KKKK-NH$_2$ (2)

¹H NMR (500 MHz, Deuterium Oxide) δ = 4.32 – 4.10 (m, 4H), 3.11 (t, *J*=6.6, 5H), 2.92 (t, *J*=6.6, 18H), 2.30 – 2.02 (m, 4H), 1.81 – 1.08 (m, 48H), 0.82 – 0.72 (m, 6H).

¹³C NMR (126 MHz, Deuterium Oxide) δ = 176.83, 176.40, 176.30, 174.48, 173.70, 173.62, 53.68, 53.52, 53.49, 53.41, 39.21, 38.70, 36.05, 35.63, 31.50, 30.59, 30.56, 30.50, 30.45, 30.39, 28.88, 28.70, 28.00, 27.26, 26.40, 26.35, 26.31, 25.75, 25.70, 25.63, 22.59, 22.34, 22.14, 22.06, 20.43, 20.38, 13.66.

MS (ESI) m/z calcd for $C_{42}H_{85}N_9O_6$ $(M+2H)^{2+}$: 406.09 found: 406.1.

Di-C₁₁-KKKK-NH₂ (3)

¹H NMR (500 MHz, Deuterium Oxide) δ = 4.38 – 4.17 (m, 4H), 3.24 – 3.11 (m, 2H), 3.05 – 2.91 (m, 6H), 2.40 – 2.12 (m, 4H), 1.90 – 1.12 (m, 56H), 0.90 – 0.79 (m, 6H).

¹³C NMR (126 MHz, Deuterium Oxide) δ = 176.25, 176.11, 175.57, 174.42, 173.72, 173.58, 53.62, 53.54, 53.50, 44.61, 39.32, 39.22, 38.54, 36.27, 35.86, 31.99, 30.72, 30.58, 30.52, 30.47, 29.87, 29.84, 29.77, 29.61, 29.55, 29.50, 29.35, 29.23, 28.29, 28.21, 26.36, 26.33, 26.11, 25.93, 22.66, 22.27, 22.15, 22.09, 22.05, 21.53, 13.86, 13.80.

MS (ESI) m/z calcd for $C_{46}H_{92}N_9O_6$ $(M+H)^+$: 867.27 found: 866.9.

Di-C₁₄-KKKK-NH₂ (4)

¹H NMR (500 MHz, Methanol-*d₄*) δ = 4.42 – 4.05 (m, 4H), 3.17 (td, *J*=6.8, 3.3, 2H), 3.01 – 2.87 (m, 6H), 2.21 (dt, *J*=39.5, 7.0, 4H), 1.90 – 1.25 (m, 68H), 0.90 (t, *J*=6.8, 6H).

^{13}C NMR (126 MHz, Methanol-*d$_4$*) δ = 176.92, 176.67, 176.50, 175.24, 174.43, 174.11, 55.51, 54.77, 54.74, 54.27, 40.72, 40.63, 40.60, 40.05, 37.36, 36.91, 33.21, 32.71, 32.30, 32.27, 32.15, 30.93, 30.91, 30.84, 30.80, 30.64, 30.61, 30.55, 30.51, 30.22, 28.19, 28.14, 28.11, 28.05, 27.27, 27.09, 24.41, 23.89, 23.87, 23.77, 14.59.

MS (ESI) m/z calcd for $C_{52}H_{103}N_9O_6$ (M+2H)$^{2+}$: 476.21 found: 476.1.

Di-C$_7$-KKGK-NH$_2$ (5)

^{1}H NMR (500 MHz, Deuterium Oxide) δ 4.35 – 4.18 (m, 3H), 3.96 (s, 2H), 3.17 (t, *J* = 6.7 Hz, 2H), 2.99 (t, *J* = 7.6 Hz, 4H), 2.35 – 2.15 (m, 4H), 1.94 – 1.13 (m, 34H), 0.92 – 0.77 (m, 6H).

^{13}C NMR (126 MHz, Deuterium Oxide) δ 177.43, 176.97, 176.61, 174.58, 174.34, 171.19, 53.81, 53.65, 53.31, 42.37, 39.33, 39.23, 38.92, 35.92, 35.50, 30.84, 30.81, 30.52, 30.45, 30.28, 28.03, 28.00, 27.90, 26.28, 26.25, 25.51, 25.41, 22.59, 22.26, 22.10, 22.08, 21.99, 13.43.

MS (ESI) m/z calcd for $C_{34}H_{67}N_8O_6$ (M+H)$^+$: 683.94 found: 683.6.

Di-C$_9$-KKGK-NH$_2$ (6)

^{1}H NMR (500 MHz, Deuterium Oxide) δ 4.36 – 4.23 (m, 3H), 4.03 – 3.89 (m, 2H), 3.25 – 3.12 (m, 2H), 3.00 (t, *J* = 7.4 Hz, 4H), 2.38 – 2.12 (m, 4H), 1.92 – 1.17 (m, 42H), 0.91 – 0.77 (m, 6H).

^{13}C NMR (126 MHz, Deuterium Oxide) δ 176.57, 176.34, 175.78, 174.46, 174.35, 171.11, 53.72, 53.60, 53.37, 42.35, 39.23, 38.61, 36.20, 35.81, 31.78, 31.77, 30.70, 30.51, 30.40, 29.29,

29.23, 29.18, 29.11, 29.05, 28.98, 28.16, 26.34, 26.29, 25.99, 25.84, 22.63, 22.54, 22.46, 22.40, 22.12, 21.97, 13.79, 13.75.

MS (ESI) m/z calcd for $C_{38}H_{74}N_8O_6Na$ (M+Na)$^+$: 762.03 found: 761.7.

Di-C$_{11}$-KKGK-NH$_2$ (7)

^{1}H NMR (500 MHz, Methanol-d_4) δ 4.35 (dd, J = 9.4, 4.8 Hz, 1H), 4.28 (dd, J = 8.8, 5.5 Hz, 1H), 4.21 (dd, J = 8.9, 5.3 Hz, 1H), 3.97 – 3.81 (m, 2H), 3.17 (t, J = 6.9 Hz, 2H), 3.02 – 2.86 (m, 4H), 2.32 – 2.22 (m, 2H), 2.17 (t, J = 7.6 Hz, 2H), 1.96 – 1.23 (m, 50H), 0.90 (t, J = 6.9 Hz, 6H).

^{13}C NMR (126 MHz, Methanol-d_4) δ 176.88, 176.69, 176.33, 175.08, 174.74, 171.51, 55.23, 54.82, 54.10, 49.00, 43.64, 40.52, 40.47, 39.92, 37.21, 36.77, 33.05, 32.30, 32.14, 31.82, 30.71, 30.69, 30.68, 30.64, 30.48, 30.45, 30.43, 30.39, 30.35, 30.07, 27.96, 27.91, 27.11, 26.94, 24.27, 23.74, 23.72, 23.66, 14.43.

MS (ESI) m/z calcd for $C_{42}H_{82}N_8O_6Na$ (M+Na)$^+$: 818.14 found: 818.9.

Di-C$_{14}$-KKGK-NH$_2$ (8)

^{1}H NMR (500 MHz, Methanol-d_4) δ 4.36 (dd, J = 9.2, 4.7 Hz, 1H), 4.28 (dd, J = 8.6, 5.5 Hz, 1H), 4.20 (dd, J = 8.7, 5.3 Hz, 1H), 3.97 – 3.81 (m, 2H), 3.17 (t, J = 6.6 Hz, 2H), 3.00 – 2.85 (m, 4H), 2.33 – 2.11 (m, 4H), 1.97 – 1.20 (m, 62H), 0.90 (t, J = 6.7 Hz, 6H).

^{13}C NMR (126 MHz, Methanol-d_4) δ 176.89, 176.68, 176.35, 175.08, 174.74, 171.49, 55.23, 54.77, 54.08, 43.63, 40.53, 39.91, 37.23, 36.79, 33.15, 32.33, 32.13, 31.85, 30.80, 30.70, 30.66, 30.50, 30.48, 30.41, 30.38, 30.09, 27.98, 27.94, 27.13, 26.96, 24.27, 23.73, 23.67, 14.44.

MS (ESI) m/z calcd for $C_{48}H_{94}N_8O_6Na$ (M+Na)$^+$: 902.32 found: 902.4.

II-2. Effect of efflux on combinations consisting of chloramphenicol and dUSCLs **2** or **6** against *Pseudomonas aeruginosa*

Appendix Table II-1 Evaluation for synergy of combinations consisting of chloramphenicol and dilipid ultrashort cationic lipopeptides (dUSCLs) **2** or **6** against wild-type PAO1 and efflux-deficient (PAO200 and PAO750) *P. aeruginosa* strains.

Organism	dUSCL	MIC$_{dUSCL}$ [MIC$_{combo}$], µg/mL	MIC$_{CHL}$ [MIC$_{combo}$], µg/mL	FIC index	Interpretation
P. aeruginosa PAO1	**2**	128 [8]	32 [1]	0.094	Synergy
	6	64 [16]	32 [1]	0.281	Synergy
P. aeruginosa PAO200[a]	**2**	32 [16]	1 [0.25]	0.750	Additive
	6	64 [32]	1 [0.5]	1.000	Additive
P. aeruginosa PAO750[b]	**2**	16 [8]	1 [0.125]	0.625	Additive
	6	16 [8]	1 [0.5]	1.000	Additive

[a] = efflux-deficient strain PAO200 lacked the MexAB-OprM pump. [b] = efflux-deficient strain PAO750 lacked five clinically-relevant pumps (MexAB-OprM, MexCD-OprJ, MexEF-OprN, MexJK and MexXY) and outer membrane protein OpmH

II-3. Checkerboard studies with cationic amphiphiles and chloramphenicol against wild-type strains of *P. aeruginosa*, *Acinetobacter baumannii* and *Escherichia coli*

Appendix Table II-2 Evaluation for synergy of combinations consisting of chloramphenicol and cationic amphiphiles against wild-type strains of *P. aeruginosa*, *Acinetobacter baumannii* and *Escherichia coli*.

Organism	Amphiphile	$MIC_{amphiphile}$ [MIC_{combo}], μg/mL	MIC_{CHL} [MIC_{combo}], μg/mL	FIC index	Interpretation
P. aeruginosa PAO1	Benzethonium Chloride	32 [16]	32 [8]	0.750	Additive
	Benzalkonium Chloride	64 [32]	32 [4]	0.625	Additive
	Cetrimonium Bromide	128 [64]	32 [16]	1.000	Additive
A. baumannii ATCC 17978	Benzethonium Chloride	16 [8]	64 [4]	0.562	Additive
	Benzalkonium Chloride	8 [4]	64 [16]	0.750	Additive
	Cetrimonium Bromide	32 [8]	64 [32]	0.750	Additive
E. coli ATCC 25922	Benzethonium Chloride	64 [32]	4 [1]	0.750	Additive
	Benzalkonium Chloride	8 [2]	4 [2]	0.750	Additive
	Cetrimonium Bromide	4 [0.5]	4 [2]	0.625	Additive

II-4. Checkerboard studies with dUSCLs **2** or **6** in combination with other classes of clinically-used antibiotics against *P. aeruginosa*

Appendix Table II-3 Evaluation for synergy of combinations consisting of dilipid ultrashort cationic lipopeptides (dUSCLs) **2** and various antibiotics against wild-type PAO1.

Antibiotic	MIC$_2$ [MIC$_{combo}$], µg/mL	MIC$_{Antibiotic}$ [MIC$_{combo}$], µg/mL	FIC index	Interpretation	Absolute MIC$_{Antibiotic}$,[a] µg/mL	Potentiation[b]
Rifampicin	128 [8]	16 [0.062]	0.066	Synergy	0.062	256-fold
Trimethoprim	128 [16]	64 [4]	0.187	Synergy	16	4-fold
Tobramycin	128 [0.5]	1 [1]	1.004	Additive	1	1-fold
Amikacin	128 [0.5]	4 [4]	1.004	Additive	4	1-fold
Minocycline	128 [32]	8 [0.5]	0.312	Synergy	1	8-fold
Fosfomycin	128 [32]	16 [4]	0.500	Synergy	8	2-fold
Aztreonam	128 [32]	4 [2]	0.750	Additive	4	1-fold
Meropenem	128 [0.5]	0.5 [0.5]	1.004	Additive	0.5	1-fold
Piperacillin	128 [32]	4 [0.5]	0.375	Synergy	1	4-fold
Ceftazidime	128 [0.5]	2 [2]	1.004	Additive	2	1-fold
Ciprofloxacin	128 [16]	0.125 [0.031]	0.375	Synergy	0.062	2-fold
Levofloxacin	128 [32]	0.25 [0.031]	0.375	Synergy	0.125	2-fold
Moxifloxacin	128 [16]	2 [0.25]	0.250	Synergy	0.5	4-fold
Linezolid	128 [32]	1024[16]	0.266	Synergy	128	8-fold
Vancomycin	128 [32]	256 [32]	0.375	Synergy	256	1-fold

[a] = MIC of antibiotic in the presence of 8 µg/mL dUSCL **2**. [b] = degree of antibiotic potentiation in the presence of 8 µg/mL dUSCL **2**.

Appendix Table II-4 Evaluation for synergy of combinations consisting of dilipid ultrashort cationic lipopeptides (dUSCLs) **6** and various antibiotics against wild-type PAO1.

Antibiotic	MIC$_6$ [MIC$_{combo}$], µg/mL	MIC$_{Antibiotic}$ [MIC$_{combo}$], µg/mL	FIC index	Interpretation	Absolute MIC$_{Antibiotic}$,[a] µg/mL	Potentiation[b]
Rifampicin	64 [16]	16 [0.062]	0.254	Synergy	0.062	256-fold
Trimethoprim	64 [16]	64 [32]	0.750	Additive	64	1-fold
Tobramycin	64 [0.25]	1 [1]	1.004	Additive	2	½-fold
Amikacin	64 [0.25]	4 [4]	1.004	Additive	4	1-fold
Minocycline	64 [8]	8 [1]	0.250	Synergy	1	8-fold
Fosfomycin	64 [16]	16 [4]	0.250	Synergy	16	1-fold
Aztreonam	64 [0.25]	8 [4]	0.504	Additive	4	1-fold
Meropenem	64 [0.25]	0.5 [0.5]	1.004	Additive	0.5	1-fold
Piperacillin	64 [8]	4 [1]	0.375	Synergy	1	4-fold
Ceftazidime	64 [0.25]	2 [2]	1.004	Additive	2	1-fold
Ciprofloxacin	64 [16]	0.125 [0.062]	0.750	Additive	0.125	1-fold
Levofloxacin	64 [16]	0.25 [0.062]	0.500	Synergy	0.25	1-fold
Moxifloxacin	64 [16]	2 [0.25]	0.375	Synergy	2	1-fold
Linezolid	64 [16]	1024[32]	0.281	Synergy	1024	1-fold
Vancomycin	64 [0.25]	256 [256]	1.004	Additive	256	1-fold

[a] = MIC of antibiotic in the presence of 8 µg/mL dUSCL **6**. [b] = degree of antibiotic potentiation in the presence of 8 µg/mL dUSCL **6**.

Appendix III: Supporting information for Chapter 6

Additional data shown below are complimentary to Chapter 6 and are based on my publication:

Ronald Domalaon, Liam Berry, Quinn Tays, George G. Zhanel, Frank Schweizer. **2018**. Development of dilipid polymyxins: investigation on the effect of hydrophobicity through its fatty acyl component. Bioorg Chem 80:639-648. doi: 10.1016/j.bioorg.2018.07.018.

Reproduced with permission.

III-1. Checkerboard studies of dilipid polymyxin B with clinically used antibiotics

Appendix Table III-1 Evaluation for synergism of **1** and clinically-used antibiotics against *P. aeruginosa* PAO1.

Drug	MIC$_{Drug}$ (MIC$_{Drug}$ in combo)	MIC$_1$ (MIC$_1$ in combo)	FIC index	Interpretation
Ceftazidime	2 (0.25)	128 (32)	0.37	Synergy
Piperacillin	4 (2)	128 (32)	0.75	Additive
Aztreonam	4 (0.5)	128 (32)	0.37	Synergy
Meropenem	1 (0.25)	128 (32)	0.50	Synergy
Doripenem	1 (0.5)	128 (32)	0.75	Additive
Minocycline	16 (1)	128 (2)	0.08	Synergy
Doxycycline	8 (0.5)	128 (2)	0.08	Synergy
Tobramycin	1 (1)	128 (0.5)	1.00	Additive
Streptomycin	16 (8)	128 (32)	0.75	Additive
Gentamicin	2 (2)	128 (0.0625)	1.00	Additive
Moxifloxacin	1 (0.125)	128 (16)	0.25	Synergy
Ciprofloxacin	0.25 (0.0625)	128 (32)	0.50	Synergy
Fosfomycin	16 (2)	128 (16)	0.25	Synergy
Trimethoprim	128 (16)	128 (16)	0.25	Synergy
Chloramphenicol	32 (2)	128 (4)	0.09	Synergy
Novobiocin	512 (16)	128 (8)	0.09	Synergy
Vancomycin	256 (8)	128 (32)	0.28	Synergy
Clindamycin	1024 (32)	128 (8)	0.09	Synergy
Linezolid	1024 (64)	128 (4)	0.09	Synergy
Pleuromutilin	512 (4)	128 (8)	0.07	Synergy
Rifampicin	16 (0.125)	128 (2)	0.02	Synergy

Appendix Table III-2 Evaluation for synergism of **2** and clinically-used antibiotics against *P. aeruginosa* PAO1.

Drug	MIC$_{Drug}$ (MIC$_{Drug}$ in combo)	MIC$_2$ (MIC$_2$ in combo)	FIC index	Interpretation
Ceftazidime	2 (1)	4 (2)	1.00	Additive
Piperacillin	4 (0.0625)	8 (4)	0.51	Additive
Aztreonam	4 (0.125)	8 (4)	0.53	Additive
Meropenem	1 (0.0625)	8 (4)	0.56	Additive
Doripenem	1 (0.125)	8 (4)	0.62	Additive
Minocycline	16 (4)	8 (2)	0.50	Synergy
Doxycycline	8 (0.125)	8 (4)	0.51	Additive
Tobramycin	1 (1)	4 (0.125)	1.03	Additive
Streptomycin	16 (4)	8 (4)	0.75	Additive
Gentamicin	2 (4)	8 (0.125)	2.01	Additive
Moxifloxacin	1 (1)	4 (2)	1.50	Additive
Ciprofloxacin	0.25 (0.0625)	8 (4)	0.75	Additive
Fosfomycin	16 (0.125)	8 (4)	0.51	Additive
Trimethoprim	128 (8)	8 (4)	0.56	Additive
Chloramphenicol	32 (4)	8 (2)	0.37	Synergy
Novobiocin	512 (8)	8 (2)	0.26	Synergy
Vancomycin	256 (2)	8 (4)	0.51	Additive
Clindamycin	1024 (64)	8 (2)	0.31	Synergy
Linezolid	1024 (1)	8 (4)	0.50[a]	Additive
Pleuromutilin	512 (4)	4 (2)	0.51	Additive
Rifampicin	16 (8)	4 (1)	0.75	Additive

[a] = FIC index is 0.500977 therefore not synergistic

Appendix Table III-3 Evaluation for synergism of **3** and clinically-used antibiotics against *P. aeruginosa* PAO1.

Drug	MIC$_{Drug}$ (MIC$_{Drug}$ in combo)	MIC$_3$ (MIC$_3$ in combo)	FIC index	Interpretation
Ceftazidime	2 (1)	32 (16)	1.00	Additive
Piperacillin	4 (2)	32 (16)	1.00	Additive
Aztreonam	4 (1)	32 (16)	0.75	Additive
Meropenem	1 (0.5)	32 (16)	1.00	Additive
Doripenem	1 (0.5)	32 (16)	1.00	Additive
Minocycline	16 (2)	32 (16)	0.62	Additive
Doxycycline	8 (1)	32 (16)	0.62	Additive
Tobramycin	1 (1)	32 (0.25)	1.01	Additive
Streptomycin	16 (16)	32 (0.25)	1.01	Additive
Gentamicin	2 (2)	32 (0.25)	1.01	Additive
Moxifloxacin	1 (0.5)	32 (16)	1.00	Additive
Ciprofloxacin	0.125 (0.125)	32 (0.25)	1.01	Additive
Fosfomycin	16 (8)	32 (8)	0.75	Additive
Trimethoprim	128 (16)	32 (16)	0.62	Additive
Chloramphenicol	32 (4)	32 (16)	0.62	Additive
Novobiocin	512 (0.5)	32 (16)	0.50[a]	Additive
Vancomycin	256 (128)	32 (16)	1.00	Additive
Clindamycin	1024 (64)	32 (16)	0.56	Additive
Linezolid	1024 (0.25)	32 (32)	1.00	Additive
Pleuromutilin	512 (8)	32 (16)	0.51	Additive
Rifampicin	16 (8)	32 (8)	0.75	Additive

[a] = FIC index is 0.500977 therefore not synergistic

Appendix Table III-4 Evaluation for synergism of **4** and clinically-used antibiotics against *P. aeruginosa* PAO1.

Drug	MIC$_{Drug}$ (MIC$_{Drug}$ in combo)	MIC$_4$ (MIC$_4$ in combo)	FIC index	Interpretation
Ceftazidime	2 (0.0625)	16 (8)	0.53	Additive
Piperacillin	4 (4)	8 (0.25)	1.03	Additive
Aztreonam	4 (0.0625)	16 (8)	0.51	Additive
Meropenem	1 (0.5)	8 (4)	1.00	Additive
Doripenem	1 (0.0625)	16 (8)	0.56	Additive
Minocycline	16 (4)	8 (4)	0.75	Additive
Doxycycline	8 (4)	8 (4)	1.00	Additive
Tobramycin	1 (1)	16 (0.25)	1.01	Additive
Streptomycin	16 (16)	8 (0.25)	1.03	Additive
Gentamicin	2 (2)	8 (0.25)	1.03	Additive
Moxifloxacin	1 (1)	8 (4)	1.50	Additive
Ciprofloxacin	0.125 (0.125)	8 (0.25)	1.03	Additive
Fosfomycin	32 (8)	8 (4)	0.75	Additive
Trimethoprim	128 (0.25)	8 (8)	1.00	Additive
Chloramphenicol	32 (4)	8 (4)	0.62	Additive
Novobiocin	512 (2)	8 (4)	0.50	Additive
Vancomycin	256 (64)	8 (4)	0.75	Additive
Clindamycin	1024 (128)	8 (4)	0.62	Additive
Linezolid	1024 (0.25)	8 (8)	1.00	Additive
Pleuromutilin	512 (4)	8 (4)	0.51	Additive
Rifampicin	16 (0.25)	8 (4)	0.51	Additive

Appendix Table III-5 Evaluation for synergism of **5** and clinically-used antibiotics against *P. aeruginosa* PAO1.

Drug	MIC$_{Drug}$ (MIC$_{Drug}$ in combo)	MIC$_5$ (MIC$_5$ in combo)	FIC index	Interpretation
Ceftazidime	2 (0.25)	16 (8)	0.62	Additive
Piperacillin	4 (2)	16 (8)	1.00	Additive
Aztreonam	4 (0.5)	16 (8)	0.62	Additive
Meropenem	1 (0.5)	16 (8)	1.00	Additive
Doripenem	1 (0.5)	16 (8)	1.00	Additive
Minocycline	16 (2)	16 (8)	0.62	Additive
Doxycycline	8 (0.25)	16 (8)	0.53	Additive
Tobramycin	1 (1)	16 (0.25)	1.01	Additive
Streptomycin	16 (8)	16 (8)	1.00	Additive
Gentamicin	2 (4)	16 (0.25)	2.01	Additive
Moxifloxacin	1 (0.25)	16 (8)	0.75	Additive
Ciprofloxacin	0.25 (0.125)	16 (8)	1.00	Additive
Fosfomycin	16 (1)	16 (8)	0.56	Additive
Trimethoprim	128 (16)	16 (8)	0.62	Additive
Chloramphenicol	32 (8)	16 (4)	0.50	Synergy
Novobiocin	512 (128)	16 (4)	0.50	Synergy
Vancomycin	256 (2)	16 (8)	0.51	Additive
Clindamycin	1024 (32)	16 (8)	0.53	Additive
Linezolid	1024 (32)	16 (8)	0.53	Additive
Pleuromutilin	512 (2)	16 (8)	0.50[a]	Additive
Rifampicin	16 (1)	16 (4)	0.31	Synergy

[a] = FIC index is 0.503906 therefore not synergistic

III-2. Checkerboard studies of polymyxin B nonapeptide with clinically used antibiotics

Appendix Table III-6 Evaluation for synergism of polymyxin B nonapeptide (PMBN) and clinically-used antibiotics against *P. aeruginosa* PAO1.

Drug	MIC_{Drug} (MIC_{Drug} in combo)	MIC_{PMBN} (MIC_{PMBN} in combo)	FIC index	Interpretation
Ceftazidime	2 (0.25)	128 (8)	0.19	Synergy
Piperacillin	4 (1)	128 (8)	0.31	Synergy
Aztreonam	4 (0.5)	128 (4)	0.16	Synergy
Meropenem	0.5 (0.125)	128 (16)	0.37	Synergy
Doripenem	1 (0.25)	128 (8)	0.31	Synergy
Minocycline	16 (0.5)	128 (8)	0.09	Synergy
Doxycycline	16 (0.25)	128 (4)	0.05	Synergy
Tobramycin	1 (1)	128 (0.5)	1.00	Additive
Streptomycin	16 (8)	128 (0.5)	0.50[a]	Additive
Gentamicin	2 (2)	128 (64)	1.50	Additive
Moxifloxacin	1 (0.125)	128 (32)	0.37	Synergy
Ciprofloxacin	0.125 (0.0312)	128 (32)	0.50	Synergy
Fosfomycin	16 (2)	128 (32)	0.37	Synergy
Trimethoprim	128 (8)	128 (4)	0.09	Synergy
Chloramphenicol	32 (2)	128 (1)	0.07	Synergy
Novobiocin	512 (4)	128 (4)	0.04	Synergy
Vancomycin	256 (4)	128 (1)	0.02	Synergy
Clindamycin	1024 (32)	128 (0.5)	0.03	Synergy
Linezolid	1024 (32)	128 (4)	0.06	Synergy
Pleuromutilin	512 (16)	128 (0.5)	0.03	Synergy
Rifampicin	16 (0.0625)	128 (0.5)	0.01	Synergy

[a] = FIC index is 0.503906 therefore not synergistic

Appendix IV: Supporting information for Chapter 7

Additional data shown below are complimentary to Chapter 7 and are based on my publication:

Ronald Domalaon, Xuan Yang, Yinfeng Lyu, George G. Zhanel, Frank Schweizer. **2017**. Polymyxin B$_3$-tobramycin hybrids with *Pseudomonas aeruginosa*-selective antibacterial activity and strong potentiation of rifampicin, minocycline and vancomycin. ACS Infect Dis 3:941-954. doi: 10.1021/acsinfecdis.7b00145.

Reproduced with permission.

IV-1. Synthesis and characterization of intermediates

Boc protection of tobramycin and characterization of Tobramycin-Boc (**4**)

Following an established protocol[1], Tobramycin and Boc anhydride (10 mol. eq.) were dissolved in an ample amount of 2:1 methanol:water. Triethylamine (22 mol. eq.) was added followed by stirring at 55 °C until tobramycin starting material is not TLC-visible (more than 20 hours). The solvent was removed *in vacuo* followed by co-distillation with DCM and toluene, successively. The compound was left drying under high-vacuum for more than 24 hours to afford a white solid (**4**). Crude was used directly for the next step. R_f = 0.22 (Ethyl acetate).
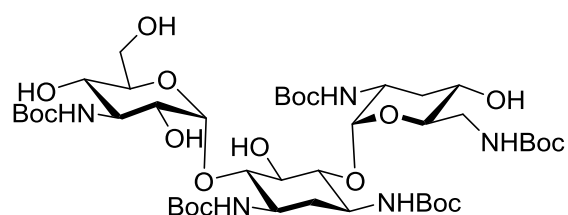

Tobramycin-Boc (4) ^{1}H NMR (500 MHz, Methanol-d_4) δ 5.17 – 4.98 (m, 2H), 3.96 – 3.89 (m, 1H), 3.82 – 3.75 (m, 1H), 3.75 – 3.65 (m, 2H), 3.65 – 3.55 (m, 3H), 3.55 – 3.31 (m, 10H), 2.16 – 1.95 (m, 2H), 1.69 – 1.58 (m, 1H), 1.50 – 1.40 (m, 45H). ^{13}C NMR (126 MHz, Methanol-d_4) δ

158.08, 157.99, 157.87, 156.52, 156.33, 98.22, 97.95, 82.17, 81.10, 79.28, 79.07, 79.00, 78.93, 78.73, 75.54, 73.29, 72.07, 70.67, 68.18, 65.04, 60.78, 55.76, 50.11, 49.69, 49.51, 40.55, 34.42, 32.81, 27.44, 27.39, 27.38, 27.35, 26.89, 26.79, 26.61. MALDI-TOF-MS m/z calcd for $C_{43}H_{77}N_5NaO_{19}$ (M+Na)$^+$ monoisotopic peak: 990.511, found: 990.520.

Selective TBDMS protection of **4** and characterization of Tobramycin-Boc-TBDMS (**5**)

Continuing with the previously followed protocol[1], compound **4** and *tert*-butyldimethylsilyl chloride (TBDMS-Cl) (11 mol. eq.) were dissolved in anhydrous DMF, followed by the addition of 1-imidazole (10 mol. eq.). The solution was stirred under N_2 atmosphere until the starting compound **4** is not TLC-visible (for more than 96 hours). Water was added followed by extraction using ethyl acetate (3x). The organic layer was washed with brine and dried over anhydrous sodium sulfate. The solvent was removed *in vacuo* followed by purification *via* flash chromatography using a mixture of solvent systems (eluent, hexanes and ethyl acetate at a 15:1, 10:1 and 8:1 ratio, successively) to afford **5** as a white solid (69% yield). R_f = 0.49 (hexanes/ethyl acetate = 4:1).

R: -OTBDMS
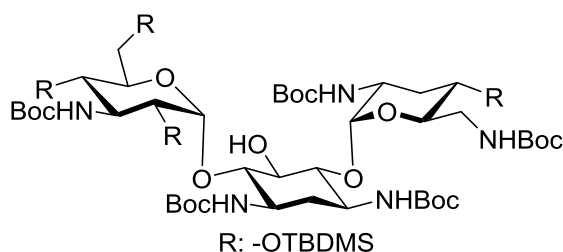
Tobramycin-Boc-TBDMS (5) ^{1}H NMR (500 MHz, Chloroform-*d*) δ 4.97 − 4.85 (m, 2H), 3.91 − 3.07 (m, 16H), 2.11 − 1.98 (m, 1H), 1.62 (q, *J* = 11.7 Hz, 1H), 1.57 − 1.50 (m, 1H), 1.47 − 1.36 (m, 45H), 0.94 − 0.82 (m, 36H), 0.08 (d, *J* = 28.8 Hz, 24H). ^{13}C NMR (126 MHz, Chloroform-*d*) δ 156.10, 155.86, 155.52, 155.10, 154.74, 99.37, 98.47, 83.24, 81.90, 79.88, 79.54, 79.43, 78.92, 78.74, 75.99, 75.25, 72.83, 71.30, 68.74, 67.43, 63.14, 56.56, 50.93, 50.40, 49.59, 41.41, 34.80,

34.67, 33.84, 28.70, 28.55, 28.42, 28.24, 28.01, 26.14, 26.06, 26.03, 25.95, 25.75, 18.47, 18.16, 18.09, 17.84, -3.77, -4.17, -4.20, -4.66, -4.73, -4.94, -4.99, -5.17. MALDI-TOF-MS *m/z* calcd for $C_{67}H_{133}N_5NaO_{19}Si_4$ (M+Na)$^+$ monoisotopic peak: 1446.857, found: 1446.881.

O-alkylation of *C*-5 Position and Characterization of Tobramycin-Boc-TBDMS-C_n-Br (**6a-e**)

Phase-transfer catalysis was utilized for the *C*-5 hydroxyl alkylation of compound **5** following published procedure[1]. Dibromoalkane (4 mol. eq.), where the carbon length were either 4, 6, 8, 10 or 12 carbons-long, was added to Tobramycin-Boc-TBDMS **5** dissolved in anhydrous toluene. Potassium hydroxide (2.5 mol. eq.) was added followed by the phase-transfer catalyst tetrabutylammonium hydrogen sulfate (TBAHS) (0.1 mol eq.). The mixture was then stirred rigorously under N_2 atmosphere for 19 hours. The solvent was removed *in vacuo* followed by purification *via* flash chromatography using a mixture of solvent systems (eluent, hexanes and ethyl acetate at a 20:1, 15:1, 10:1 and 8:1 ratio, successively) to afford **6a-e** as an opaque solid (53-62% yield). R_f = 0.56 (hexanes/ethyl acetate = 4:1).
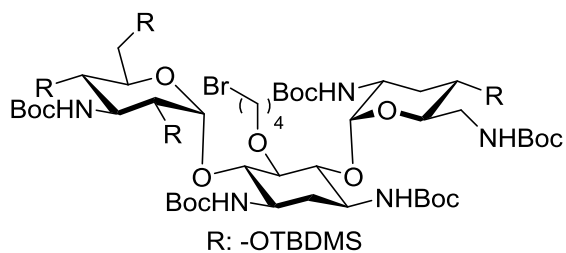
Tobramycin-Boc-TBDMS-C$_4$-Br (*6a*) ^{1}H NMR (500 MHz, Chloroform-*d*) δ 5.22 − 5.07 (m, 2H), 4.33 − 4.03 (m, 3H), 3.86 − 3.16 (m, 17H), 2.45 (d, *J* = 7.7 Hz, 1H), 2.03 − 1.97 (m, 1H), 1.94 − 1.84 (m, 2H), 1.65 − 1.57 (m, 2H), 1.56 − 1.50 (m, 1H), 1.48 − 1.29 (m, 45H), 1.08 − 0.98 (m, 1H), 0.96 − 0.82 (m, 36H), 0.22 − -0.06 (m, 24H). ^{13}C NMR (126 MHz, Chloroform-*d*) δ 155.69, 155.65, 155.47, 154.72, 154.59, 97.85, 96.49, 85.90, 79.95, 79.41, 79.27, 79.11, 78.78, 75.41, 72.67, 72.26, 71.57, 67.98, 67.05, 63.22, 57.14, 50.49,

48.82, 48.31, 41.61, 36.64, 36.03, 35.61, 34.62, 34.47, 33.72, 29.47, 29.22, 29.01, 28.60, 28.48, 28.41, 26.09, 25.97, 25.76, 25.24, 18.46, 18.28, 18.07, 17.89, -3.42, -3.76, -4.22, -4.91, -4.93, -5.06, -5.17, -5.20. MALDI-TOF-MS *m/z* calcd for $C_{71}H_{140}BrN_5NaO_{19}Si_4$ (M+Na)$^+$ monoisotopic peak: 1580.830, found: 1580.806.

Tobramycin-Boc-TBDMS-C$_6$-Br (6b) ^{1}H NMR (500 MHz, Chloroform-*d*) δ 5.22 − 5.06 (m, 2H), 4.27 − 3.98 (m, 3H), 3.81 − 3.09 (m, 17H), 2.48 − 2.37 (m, 1H), 1.99 − 1.91 (m, 1H), 1.89 − 1.74 (m, 2H), 1.53 (s, 1H), 1.51 − 1.22 (m, 51H), 1.06 − 0.95 (m, 1H), 0.93 − 0.77 (m, 36H), 0.16 − -0.03 (m, 24H). ^{13}C NMR (126 MHz, Chloroform-*d*) δ 155.76, 155.66, 155.46, 154.75, 154.58, 97.72, 96.42, 85.75, 79.89, 79.70, 79.37, 79.20, 78.78, 75.25, 73.17, 72.65, 71.56, 68.06, 67.00, 63.16, 57.25, 50.55, 48.90, 48.34, 41.68, 35.98, 35.72, 33.74, 33.52, 32.82, 32.59, 32.50, 30.42, 28.63, 28.50, 28.43, 27.27, 26.13, 26.00, 25.80, 25.33, 18.49, 18.32, 18.10, 17.92, -3.46, -3.77, -4.19, -4.87, -5.02, -5.15, -5.18, -5.28. MS (ESI) *m/z* calcd for $C_{73}H_{144}BrN_5NaO_{19}Si_4$ (M+Na)$^+$: 1611.2, found: 1611.6.

Tobramycin-Boc-TBDMS-C$_8$-Br (6c) ^{1}H NMR (500 MHz, Chloroform-*d*) δ 5.24 − 5.09 (m, 2H), 4.31 − 4.18 (m, 1H), 4.18 − 4.10 (m, 1H), 4.10 − 4.00 (m, 1H), 3.83 − 3.14 (m, 17H), 2.44 (d, *J* = 7.0 Hz, 1H), 2.02 − 1.95 (m, 1H), 1.86 − 1.78 (m, 2H), 1.56 − 1.51 (m, 1H), 1.40 (s, 45H), 1.38 − 1.18 (m, 10H), 1.07 − 0.98 (m, 1H), 0.96 − 0.80

(m, 36H), 0.18 – -0.03 (m, 24H). ^{13}C NMR (126 MHz, Chloroform-*d*) δ 155.69, 155.50, 154.72, 154.65, 154.55, 97.80, 96.42, 85.75, 79.90, 79.37, 79.21, 78.92, 78.84, 75.21, 73.26, 72.63, 71.55, 68.01, 66.88, 63.10, 57.25, 50.51, 48.88, 48.31, 41.65, 36.64, 35.91, 35.64, 33.88, 32.81, 30.56, 29.76, 28.72, 28.61, 28.48, 28.38, 28.14, 26.10, 26.03, 25.97, 25.76, 24.67, 23.46, 18.46, 18.30, 18.07, 17.89, -3.44, -3.81, -4.22, -4.90, -4.96, -5.09, -5.19, -5.24. MALDI-TOF-MS *m/z* calcd for C$_{75}$H$_{148}$BrN$_5$NaO$_{19}$Si$_4$ (M+Na)$^+$ monoisotopic peak: 1636.896, found: 1636.897.
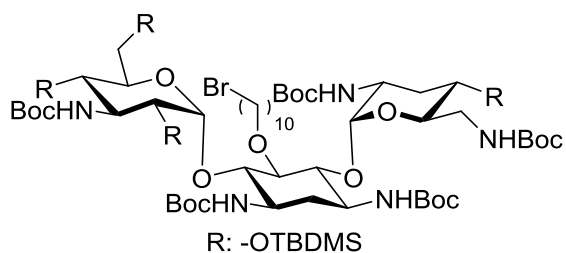
Tobramycin-Boc-TBDMS-C$_{10}$-Br (6d) ^{1}H NMR (300 MHz, Chloroform-*d*) δ 5.23 (d, *J* = 3.1 Hz, 1H), 5.19 – 5.13 (m, 1H), 4.33 – 4.22 (m, 1H), 4.18 (d, *J* = 10.2 Hz, 1H), 4.09 (d, *J* = 5.8 Hz, 1H), 3.87 – 3.10 (m, 17H), 2.48 (d, *J* = 11.4 Hz, 1H), 2.07 – 1.96 (m, 1H), 1.92 – 1.80 (m, 2H), 1.57 – 1.50 (m, 1H), 1.48 – 1.40 (m, 45H), 1.39 – 1.18 (m, 14H), 1.12 – 1.00 (m, 1H), 0.99 – 0.82 (m, 36H), 0.22 – -0.03 (m, 24H). ^{13}C NMR (75 MHz, Chloroform-*d*) δ 155.63, 155.55, 154.85, 154.77, 154.59, 97.87, 96.54, 85.78, 79.95, 79.63, 79.39, 79.24, 79.11, 77.45, 75.31, 73.37, 72.69, 71.56, 68.07, 66.88, 63.16, 63.13, 57.32, 50.57, 48.97, 48.38, 41.73, 36.66, 35.97, 35.90, 35.68, 33.99, 33.80, 32.88, 30.66, 30.43, 29.98, 29.72, 29.70, 29.65, 29.56, 29.47, 29.38, 28.80, 28.66, 28.53, 28.42, 28.20, 26.15, 26.02, 26.01, 25.80, 24.70, 23.45, 18.51, 18.35, 18.12, 17.93, -3.39, -3.77, -4.18, -4.86, -4.92, -5.06, -5.14, -5.20. MALDI-TOF-MS *m/z* calcd for C$_{77}$H$_{152}$BrN$_5$NaO$_{19}$Si$_4$ (M+Na)$^+$ monoisotopic peak: 1664.924, found: 1665.010.

R: -OTBDMS
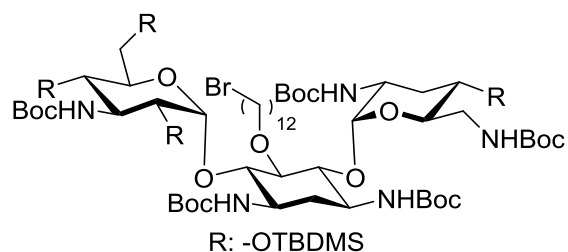
Tobramycin-Boc-TBDMS-C$_{12}$-Br (6e) ^{1}H NMR (500 MHz, Chloroform-*d*) δ 5.26 − 5.12 (m, 2H), 4.33 − 4.21 (m, 1H), 4.16 (d, *J* = 9.9 Hz, 1H), 4.12 − 4.02 (m, 1H), 3.82 − 3.17 (m, 17H), 2.46 (d, *J* = 7.7 Hz, 1H), 2.04 − 1.96 (m, 1H), 1.87 − 1.82 (m, 2H), 1.59 − 1.53 (m, 1H), 1.47 − 1.39 (m, 45H), 1.34 − 1.20 (m, 18H), 1.10 − 1.00 (m, 1H), 0.97 − 0.81 (m, 36H), 0.23 − -0.04 (m, 24H). ^{13}C NMR (126 MHz, Chloroform-*d*) δ 155.89, 155.67, 154.93, 154.88, 154.71, 97.94, 96.68, 85.87, 80.04, 79.99, 79.51, 79.35, 79.24, 75.45, 73.55, 72.85, 71.68, 68.16, 66.98, 63.49, 63.45, 63.25, 57.44, 50.67, 49.09, 48.52, 41.79, 36.79, 36.05, 35.79, 34.13, 33.97, 33.07, 33.01, 32.96, 30.77, 30.46, 30.17, 29.79, 29.70, 29.64, 29.58, 29.55, 29.53, 29.41, 29.30, 29.11, 28.94, 28.90, 28.87, 28.78, 28.66, 28.55, 28.34, 28.31, 28.29, 28.22, 26.31, 26.28, 26.16, 26.14, 25.93, 25.81, 24.83, 24.02, 23.57, 18.63, 18.48, 18.25, 18.06, -3.26, -3.65, -4.05, -4.73, -4.80, -4.93, -5.03, -5.08. MS (ESI) *m/z* calcd for C$_{79}$H$_{156}$BrN$_5$NaO$_{19}$Si$_4$ (M+Na)[+]: 1695.4, found: 1695.7.

Characterization of Tobramycin-Boc-TBDMS-C$_n$-azide (7a-e)

R: -OTBDMS
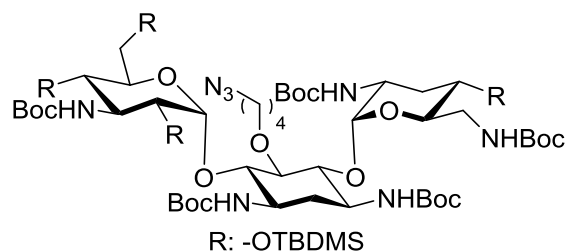
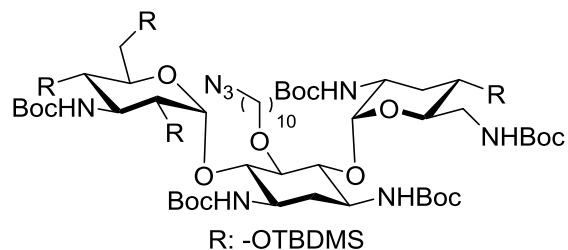***Tobramycin-Boc-TBDMS-C$_4$-N$_3$ (7a)*** ^{1}H NMR (500 MHz, Chloroform-*d*) δ 5.22 − 5.05 (m, 2H), 4.31 − 3.98 (m, 3H), 3.87 − 3.13 (m, 17H), 2.43 (d, *J* = 7.6 Hz, 1H), 2.01 − 1.93 (m, 1H), 1.66 − 1.57 (m, 2H), 1.56 − 1.51 (m, 2H), 1.51 − 1.47 (m, 1H), 1.47 − 1.27 (m, 45H), 1.08 − 0.97 (m, 1H), 0.95 − 0.75 (m, 36H), 0.17 − -0.04 (m, 24H). ^{13}C NMR (126 MHz, Chloroform-*d*) δ 155.65, 155.54, 155.44, 154.73, 154.58, 97.90, 96.40, 85.90,

79.93, 79.40, 79.36, 79.24, 79.10, 78.66, 75.38, 72.61, 72.45, 71.56, 67.98, 67.11, 63.22, 57.13, 51.39, 50.49, 48.83, 48.28, 41.61, 35.94, 35.62, 28.59, 28.46, 28.36, 27.57, 26.07, 25.94, 25.75, 25.41, 18.44, 18.26, 18.05, 17.88, -3.51, -3.79, -4.02, -4.24, -4.70, -4.92, -5.13, -5.23. MALDI-TOF-MS m/z calcd for $C_{71}H_{140}N_8NaO_{19}Si_4$ $(M+Na)^+$ monoisotopic peak: 1543.921, found: 1543.952.

R: -OTBDMS

Tobramycin-Boc-TBDMS-C_6-N_3 *(7b)* ^{1}H NMR (300 MHz, Chloroform-*d*) δ 5.21 (d, J = 3.0 Hz, 1H), 5.17 − 5.10 (m, 1H), 4.32 − 4.01 (m, 3H), 3.84 − 3.15 (m, 17H), 2.45 (d, J = 11.3 Hz, 1H), 2.05 − 1.93 (m, 1H), 1.66 − 1.56 (m, 2H), 1.55 − 1.51 (m, 1H), 1.49 − 1.37 (m, 45H), 1.36 − 1.21 (m, 6H), 1.10 − 1.00 (m, 1H), 0.98 − 0.79 (m, 36H), 0.18 − -0.05 (m, 24H). ^{13}C NMR (75 MHz, Chloroform-*d*) δ 155.83, 155.58, 154.93, 154.84, 154.71, 97.76, 96.53, 85.87, 80.04, 79.75, 79.50, 79.33, 78.95, 77.26, 75.35, 73.19, 72.82, 71.62, 68.15, 67.12, 63.28, 63.08, 57.41, 51.54, 50.64, 48.99, 48.42, 41.84, 36.07, 35.83, 32.73, 30.55, 29.77, 28.93, 28.89, 28.81, 28.73, 28.60, 28.51, 28.18, 27.11, 26.61, 26.46, 26.38, 26.22, 26.09, 25.88, 25.76, 25.62, 25.49, 18.58, 18.41, 18.19, 18.02, -3.37, -3.68, -4.11, -4.78, -4.96, -5.06, -5.10, -5.20. MALDI-TOF-MS m/z calcd for $C_{73}H_{144}N_8NaO_{19}Si_4$ $(M+Na)^+$ monoisotopic peak: 1571.952, found: 1571.956.

Tobramycin-Boc-TBDMS-C$_8$-N$_3$ (7c) ^{1}H NMR (500 MHz, Chloroform-*d*) δ 5.25 − 5.08 (m, 2H), 4.31 − 4.18 (m, 1H), 4.18 − 4.10 (m, 1H), 4.10 − 4.00 (m, 1H), 3.81 − 3.12 (m, 17H), 2.45 (d, *J* = 7.5 Hz, 1H), 2.02 − 1.94 (m, 1H), 1.59 − 1.54 (m, 2H), 1.52 − 1.49 (m, 1H), 1.39 (s, 45H), 1.36 − 1.18 (m, 10H), 1.10 − 0.98 (m, 1H), 1.02 (d, *J* = 30.5 Hz, 1H), 0.96 − 0.78 (m, 36H), 0.18 − -0.05 (m, 24H). ^{13}C NMR (126 MHz, Chloroform-*d*) δ 155.71, 155.64, 155.49, 154.69, 154.54, 97.86, 96.44, 85.74, 79.88, 79.34, 79.19, 79.04, 78.83, 75.25, 73.25, 72.63, 71.53, 67.99, 66.86, 63.10, 57.24, 51.40, 50.49, 48.87, 48.31, 41.64, 35.93, 35.64, 30.55, 29.78, 29.64, 29.08, 28.77, 28.60, 28.47, 28.37, 26.66, 26.09, 26.01, 25.95, 25.75, 18.45, 18.29, 18.06, 17.88, -3.46, -3.82, -4.24, -4.91, -4.97, -5.11, -5.21, -5.25. MALDI-TOF-MS *m/z* calcd for C$_{75}$H$_{148}$N$_8$NaO$_{19}$Si$_4$ (M+Na)$^+$ monoisotopic peak: 1599.984, found: 1600.001.

Tobramycin-Boc-TBDMS-C$_{10}$-N$_3$ (7d) ^{1}H NMR (300 MHz, Chloroform-*d*) δ 5.23 (d, *J* = 3.4 Hz, 1H), 5.19 − 5.11 (m, 1H), 4.34 − 4.23 (m, 1H), 4.17 (d, *J* = 10.4 Hz, 1H), 4.13 − 4.00 (m, 1H), 3.89 − 3.09 (m, 17H), 2.48 (d, *J* = 11.9 Hz, 1H), 2.07 − 1.97 (m, 1H), 1.66 − 1.57 (m, 2H), 1.57 − 1.52 (m, 1H), 1.50 − 1.39 (m, 45H), 1.37 − 1.20 (m, 14H), 1.12 − 1.01 (m, 1H), 0.98 − 0.82 (m, 36H), 0.20 − -0.00 (m, 24H). ^{13}C NMR (75 MHz, Chloroform-*d*) δ 155.73, 155.55, 154.80, 154.74, 154.59, 97.87, 96.57, 85.76, 79.95, 79.69, 79.39, 79.24, 79.12, 75.34, 73.37, 72.76, 71.57, 68.03, 66.88, 63.16, 57.32, 51.50, 50.53, 48.98, 48.39, 41.72, 36.66, 36.03, 35.96, 35.70, 30.66, 29.99, 29.70, 29.56, 29.52, 29.18, 28.97, 28.87, 28.66,

28.53, 28.42, 26.73, 26.16, 26.04, 26.01, 25.80, 18.51, 18.35, 18.12, 17.93, -3.39, -3.76, -4.18, -4.86, -4.92, -5.06, -5.15, -5.20. MS (ESI) m/z calcd for $C_{77}H_{152}N_8NaO_{19}Si_4$ (M+Na)$^+$: 1629.4, found: 1630.1.

R: -OTBDMS
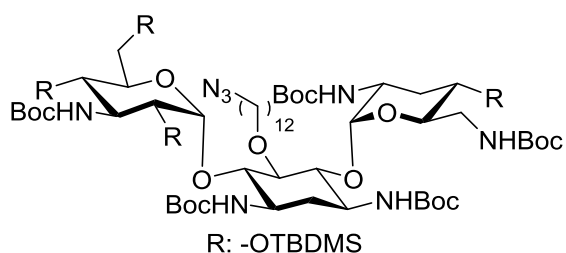
Tobramycin-Boc-TBDMS-C_{12}-N_3 (7e) ^{1}H NMR (500 MHz, Chloroform-d) δ 5.26 − 5.12 (m, 2H), 4.32 − 4.21 (m, 1H), 4.16 (d, J = 9.1 Hz, 1H), 4.11 − 4.03 (m, 1H), 3.81 − 3.18 (m, 17H), 2.46 (d, J = 9.4 Hz, 1H), 2.04 − 1.97 (m, 1H), 1.62 − 1.56 (m, 2H), 1.54 (d, J = 2.5 Hz, 0H), 1.53 (s, 0H), 1.51 (s, 0H), 1.52 − 1.49 (m, 1H), 1.54 − 1.47 (m, 1H), 1.45 − 1.34 (m, 45H), 1.31 − 1.20 (m, 18H), 1.08 − 0.99 (m, 1H), 0.96 − 0.81 (m, 36H), 0.19 − -0.01 (m, 24H). ^{13}C NMR (126 MHz, Chloroform-d) δ 155.65, 155.52, 154.74, 154.72, 154.55, 99.98, 96.52, 85.73, 79.88, 79.59, 79.36, 79.20, 79.04, 75.33, 73.37, 72.63, 71.54, 67.98, 66.83, 63.10, 57.30, 51.47, 50.50, 48.93, 48.37, 41.65, 35.95, 35.63, 32.91, 30.62, 30.01, 29.64, 29.54, 29.47, 29.43, 29.41, 29.17, 29.14, 29.10, 28.95, 28.83, 28.81, 28.62, 28.50, 28.39, 26.71, 26.68, 26.16, 26.12, 26.08, 26.00, 25.97, 25.91, 25.77, 25.65, 18.47, 18.32, 18.09, 17.90, -3.43, -3.81, -4.21, -4.89, -4.96, -5.09, -5.19, -5.25. MALDI-TOF-MS m/z calcd for $C_{79}H_{156}N_8NaO_{19}Si_4$ (M+Na)$^+$ monoisotopic peak: 1656.046, found: 1656.069.

IV-2. Synthesis and characterization of polymyxin B₃ (**PMB3**)
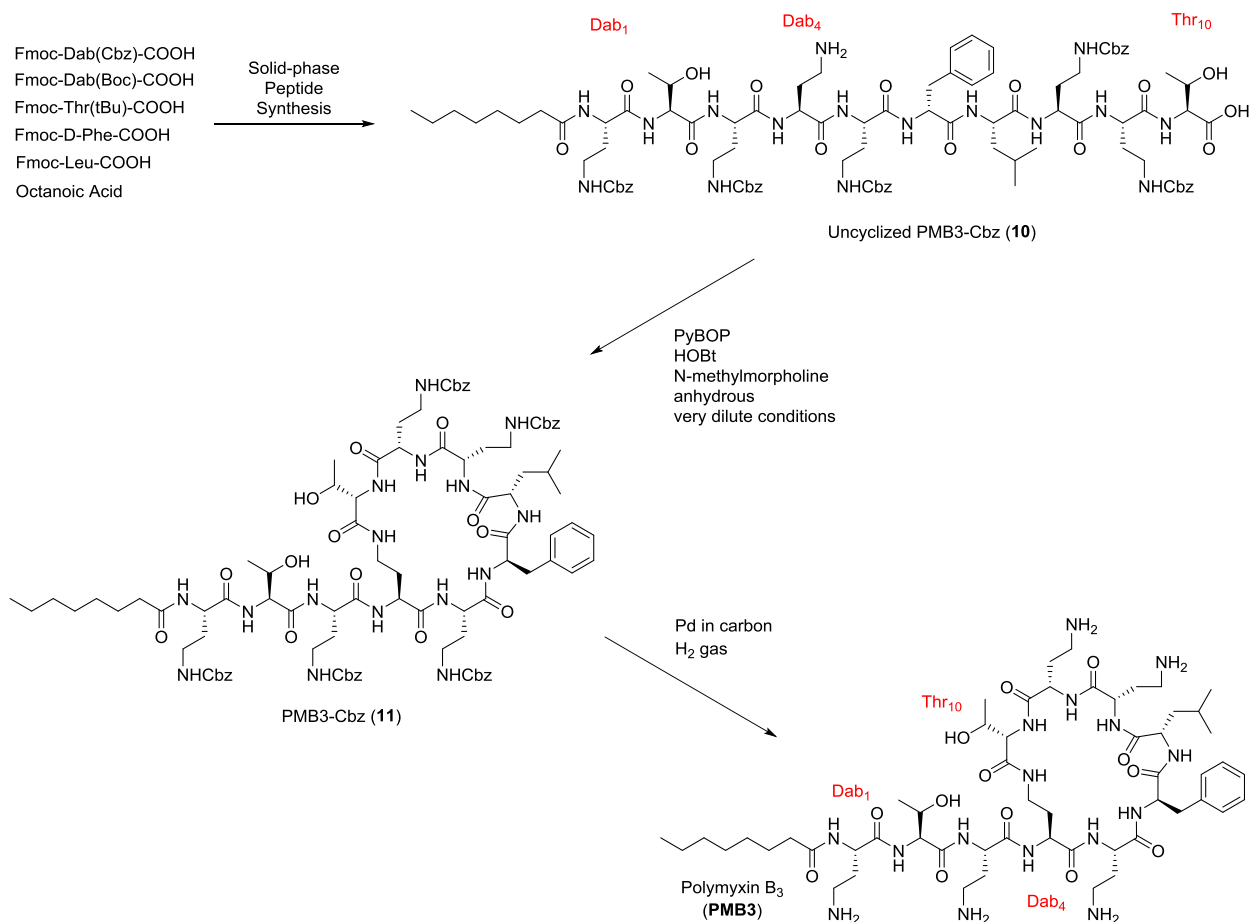
Appendix Scheme IV-1 Synthesis of polymyxin B₃ (**PMB3**) *via* standard solid-phase peptide synthesis followed by intramolecular cyclization (under very dilute conditions) and catalytic hydrogenolysis.

Solid-phase peptide synthesis of Uncyclized PMB3-Cbz (**10**)

Uncyclized polymyxin B₃ was prepared similar to **PMB3** intermediate **2**. The compound was synthesized in a solid-phase support (Wang resin) following a standard Fmoc protection strategy. A published protocol[2] was utilized with several modifications as follows. Amino acids with

protected functional groups were purchased and used to yield the uncyclized lipopeptide, having a carboxylic acid C-terminus of Thr_{10} and free amino side-chain of Dab_4. Therefore, all the Dab amino side-chain, with the exception of Dab_4 which was protected with Boc, were protected with Cbz protecting group. Fmoc removal was done by subjecting the resin to 4:1 DMF:piperidine solution. Coupling was achieved by the addition of a pre-activated coupling solution [Fmoc-amino acid or lipid tail (3 mol. eq.) was pre-mixed with the coupling reagent TBTU (3 mol. eq.) and *N*-methylmorpholine (8 mol. eq.) in DMF 5 minutes prior] to the immobilized peptide on solid support followed by gentle agitation using N_2 gas for 45 minutes. Both Fmoc removal and coupling steps were followed with thorough washing of the beads using DMF (3x), DCM (3x) and DMF (3x). A small amount of resin after the Fmoc removal and the coupling step were subjected to Kaiser test (5% chloranil in DMF) to qualitatively ensure that the reaction went to completion. Cleavage from the solid support was performed by the addition of 95:5 TFA:water solution followed by gentle stirring for 30 minutes. The solvent was removed *in vacuo* to obtain a dry crude. MALDI-TOF-MS was performed to check the presence of **10**.

Solution-phase synthesis of cyclized PMB3-Cbz (**11**)

The crude containing compound **10** was mixed with PyBOP (4 mol. eq.), HOBt (4 mol. eq.) and *N*-methymorpholine (10 mol. eq.) in DMF under very dilute and anhydrous conditions, followed by vigorous stirring for 2 hours, to afford the intramolecular cyclization *via* amide bond formation of Thr_{10} carboxyl end and Dab_4 amino side-chain. The solvent was removed *in vacuo* followed by co-distillation using DCM (2x), water and DCM (2x), successively. The product was precipitated from the crude by addition of cold water. The precipitate was filtered and obtained as a pale brown

solid. DCM was added to partially dissolve the product and was evaporated *in vacuo* to dryness. MALDI-TOF-MS was performed to confirm the product **11**.

Deprotection and characterization of **PMB3**

Catalytic hydrogenolysis using palladium was performed on **11** to remove all the Cbz protecting groups. The compound was dissolve in methanol (4 volume ratio) followed by the addition of acetic acid (5 volume ratio) and water (1 volume ratio). Palladium on carbon (Pd/C) was added and the compound was subjected to H_2 gas (balloon) with constant stirring until all the Cbz groups were removed. It was then filtered *via* Nylon filter followed by washing of ample amounts of methanol. The filtrate was evaporated to dryness *in vacuo*. The crude was then purified using reverse-phase flash chromatography having an eluent mixture of water and methanol (both spiked with 0.1% TFA), from 0% to 50% methanol in water ratio (25% step-wise), to afford an opaque solid **PMB3**.
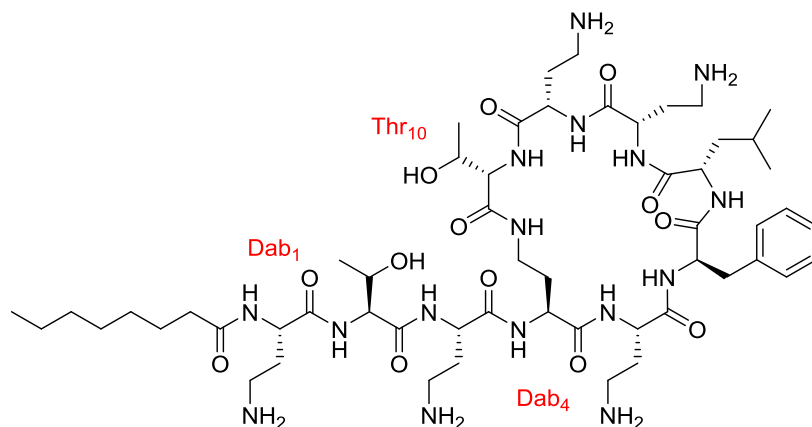
Polymyxin B₃ (PMB3) ^{1}H NMR (500 MHz, Methanol-d_4) δ 7.33 − 7.18 (m, 5H, D-Phe$_6$ aromatic), 4.53 (dd, J = 8.8, 4.5 Hz, 1H, Dab$_{5\alpha}$), 4.50 − 4.43 (m, 2H, Dab$_{1,8\alpha}$), 4.40 (dd, J = 10.0, 6.4 Hz, 1H, D-Phe$_{6\alpha}$), 4.38 − 4.24 (m, 5H, Dab$_{3,4,9\alpha}$ + Thr$_{2\alpha}$ + Thr$_{2\beta}$), 4.20 − 4.15 (m, 1H, Thr$_{10\beta}$), 4.14 − 4.09 (m, 1H, Leu$_{7\alpha}$), 4.04 (d, J = 5.0 Hz, 1H, Thr$_{10\alpha}$), 3.66 − 3.56 (m, 1H, Dab$_{4\gamma1}$), 3.17 − 2.87 (m, 13H, Dab$_{4\gamma2}$ + Dab$_{1,3,5,8,9\gamma}$ + D-Phe$_{6\beta}$), 2.50 − 2.37 (m, 1H, Dab$_{3\beta1}$), 2.29 (t, J = 7.6 Hz, 2H, PMB3 C$_8$'s -C$\underline{H}_2$CO-), 2.26 − 2.02 (m, 8H, Dab$_{3\beta2}$ + Dab$_{5\beta1}$ + Dab$_{1,8,9\beta}$), 2.02 − 1.90 (m, 3H, Dab$_{5\beta2}$ + Dab$_{4\beta}$), 1.67 − 1.58 (m, 2H, PMB3 C$_8$'s -C$\underline{H}_2$CH$_2$CO-), 1.54 − 1.46 (m, 1H, Leu$_{7\beta1}$), 1.38 − 1.26 (m, 9H, Leu$_{7\beta2}$ + PMB3 C$_8$'s -C$\underline{H}_2$-), 1.25 − 1.15 (m, 6H, Thr$_{2,10\gamma}$), 0.90 (t, J = 7.1 Hz, 3H, PMB3 C$_8$'s -C$\underline{H}_3$), 0.85 − 0.61 (m, 7H, Leu$_{7\gamma}$ + Leu$_{7\delta}$). ^{13}C NMR (126 MHz, Methanol-d_4) δ 175.89 (PMB3 C$_8$'s carbonyl), 173.94, 172.49, 172.39, 172.36, 172.30, 172.22, 171.53, 171.48, 171.40, 170.84, 135.80 (D-Phe$_6$ aromatic C without H), 128.86, 128.36, 126.73, 66.49 (Thr$_{2\beta}$), 65.81 (Thr$_{10\beta}$), 60.28 (Thr$_{10\alpha}$), 58.82 (Thr$_{2\alpha}$), 56.51 (D-Phe$_{6\alpha}$), 51.93, 51.62, 51.57, 51.46, 51.33, 50.93, 49.92 (Dab$_{5\alpha}$), 39.31(Leu$_{7\beta}$), 36.60, 36.44, 36.35, 36.26, 35.94, 35.36 (PMB3 C$_8$'s -C$\underline{H}_2$CO-), 35.08 (Dab$_{4\gamma}$), 31.44, 30.31, 30.25, 29.12, 28.95, 28.82, 28.70, 28.40, 25.52 (PMB3 C$_8$'s -C$\underline{H}_2$CH$_2$CO-), 23.48, 22.24, 22.17, 19.99, 19.18, 18.57, 12.96 (PMB3 C$_8$'s -C$\underline{H}_3$). MALDI-TOF-MS m/z calcd for C$_{55}$H$_{97}$N$_{16}$O$_{13}$ (M+H)$^+$: 1188.734, found: 1189.760.

IV-3. Molecular weight of PMB3-tobramycin hybrids, **PMB3** and **TOB** in salt form

Appendix Table IV-1 Molecular weight of the purified PMB3-tobramycin hybrids as a trifluoroacetate (TFA) salt form.

Compound	Abbre*via*tion	Molecular weight (g/mol)
Polymyxin B_3-triazole-C_4-tobramycin $\times$ 9 TFA	**1a**	2775.30
Polymyxin B_3-triazole-C_6-tobramycin $\times$ 9 TFA	**1b**	2803.36
Polymyxin B_3-triazole-C_8-tobramycin $\times$ 9 TFA	**1c**	2831.41
Polymyxin B_3-triazole-C_{10}-tobramycin $\times$ 9 TFA	**1d**	2859.46
Polymyxin B_3-triazole-C_{12}-tobramycin $\times$ 9 TFA	**1e**	2887.52
Polymyxin $B_3 \times$ 5 TFA	**PMB3**	1759.59
Tobramycin sulfate[a]	**TOB**	565.59
Tobramycin-C12 $\times$ 5 HCl	**TOB-C12**	818.13

[a] = data provided by the supplier, AK Scientific (USA)

IV-4. HPLC analysis of PMB3-tobramycin hybrids

Methodology

Equipment: Waters Breeze HPLC

Detector: 2998 PDA detector (1.2 nm resolution)

Column: Phenomenex Synergi Polar (50 x 2.0 mm) 4 micron reverse-phase column with phenyl ether-linked stationary phase

Flow rate: 0.5 mL/min

Wavelength: 215.0 nm

Eluent A: water spiked with 0.1% TFA

Eluent B: acetonitrile spiked with 0.1 % TFA

Note: all hybrids were dissolved in methanol spiked with ~1% DMSO

Appendix Table IV-2 HPLC gradient used

Time	% Eluent A	% Eluent B
0	100	0
4.5	84	16
5	68	32
16	68	32
17.5	84	16
20	100	0

Appendix Table IV-3 Purity of hybrids

Compound	1a	1b	1c	1d	1e
Purity (%)	98.6	99.8	99.8	98.8	98.8

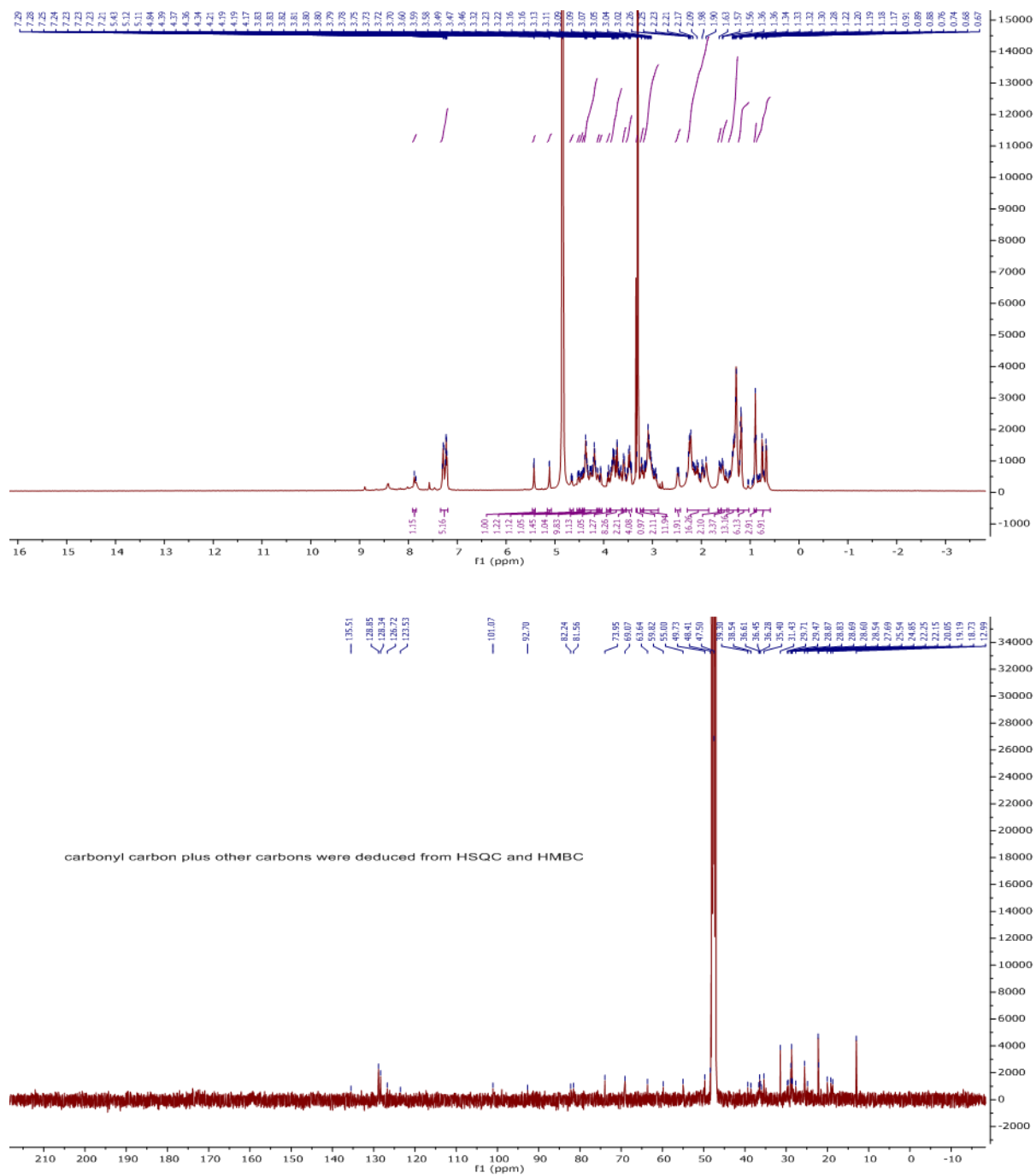# IV-5. HPLC chromatogram and NMR spectra of PMB3-tobramycin hybrids

PMB3-triazole-C$_4$-tobramycin (**1a**)
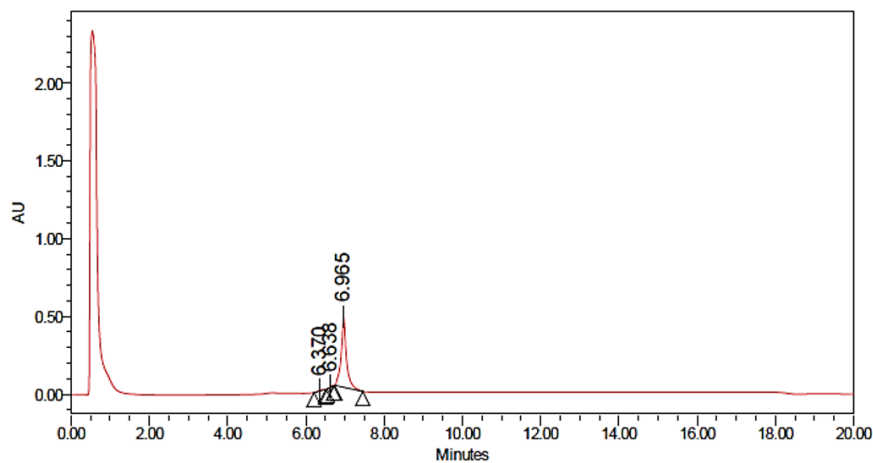
Processed Channel: PDA 215.0 nm

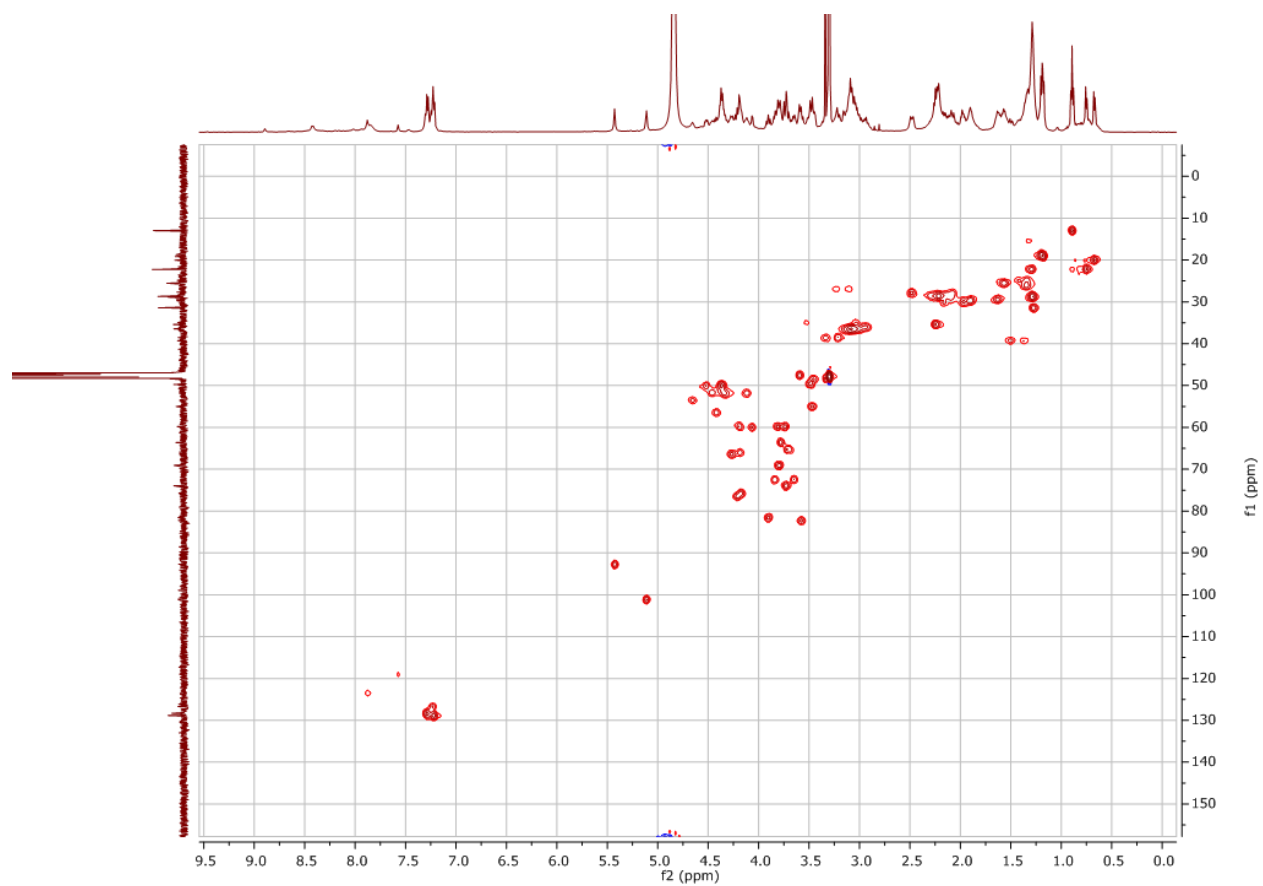|	Processed Channel	Retention Time (min)	Area	% Area	Height
1	PDA 215.0 nm	6.370	36565	0.85	5092
2	PDA 215.0 nm	6.638	25736	0.60	5991
3	PDA 215.0 nm	6.965	4240062	98.55	454505

*peak at 0.5 mins denotes for DMSO
(see Supporting information Figure 26)
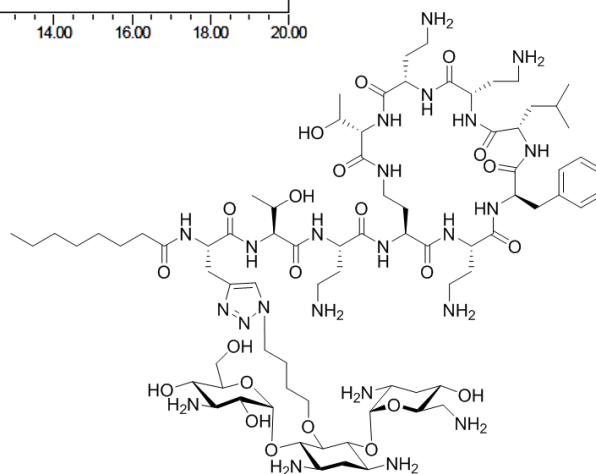
Appendix Figure IV-1 HPLC analysis chromatogram for hybrid **1a**.

Appendix Figure IV-2 ^{1}H (above) and ^{13}C (below) NMR spectra of hybrid **1a**.
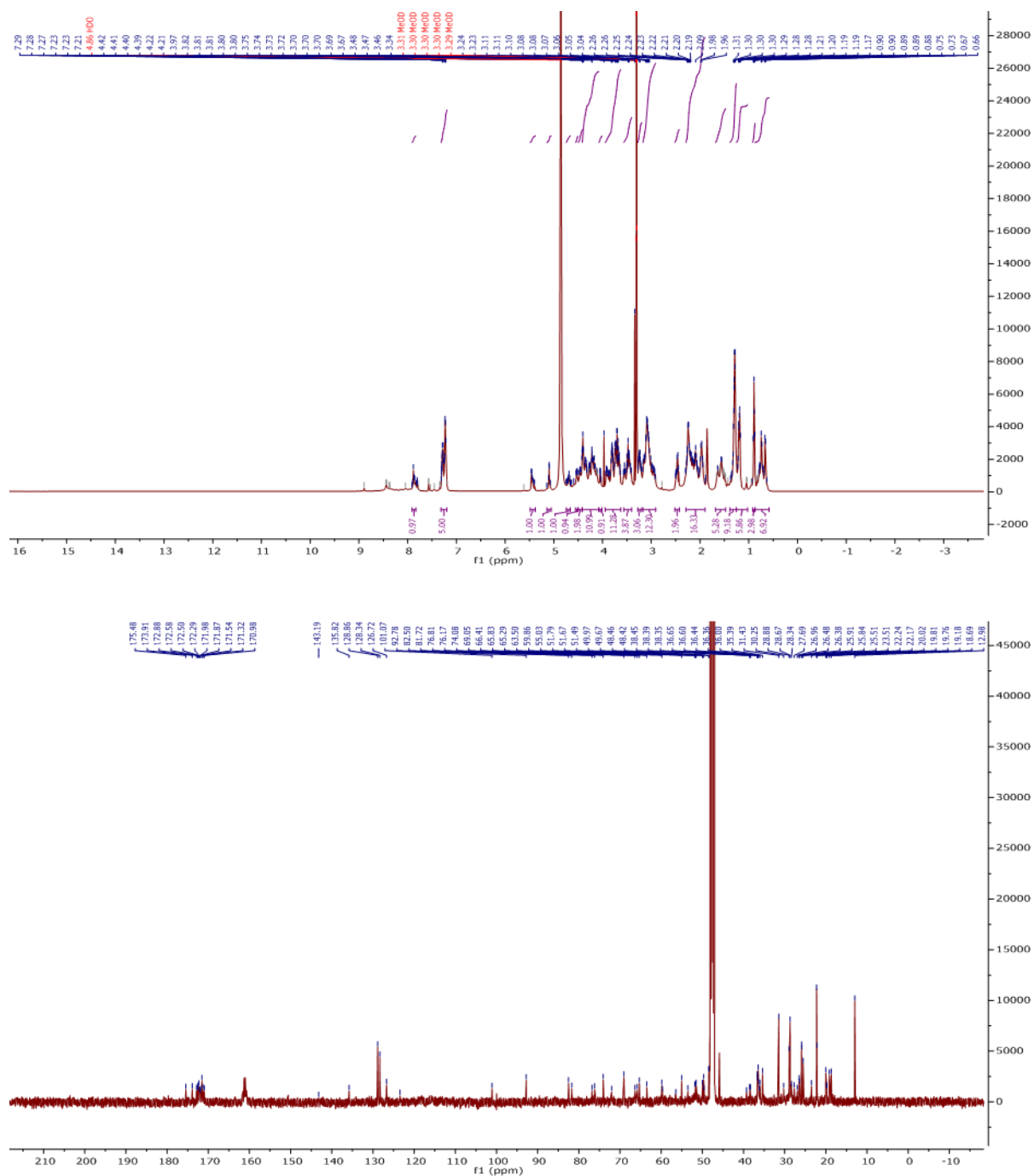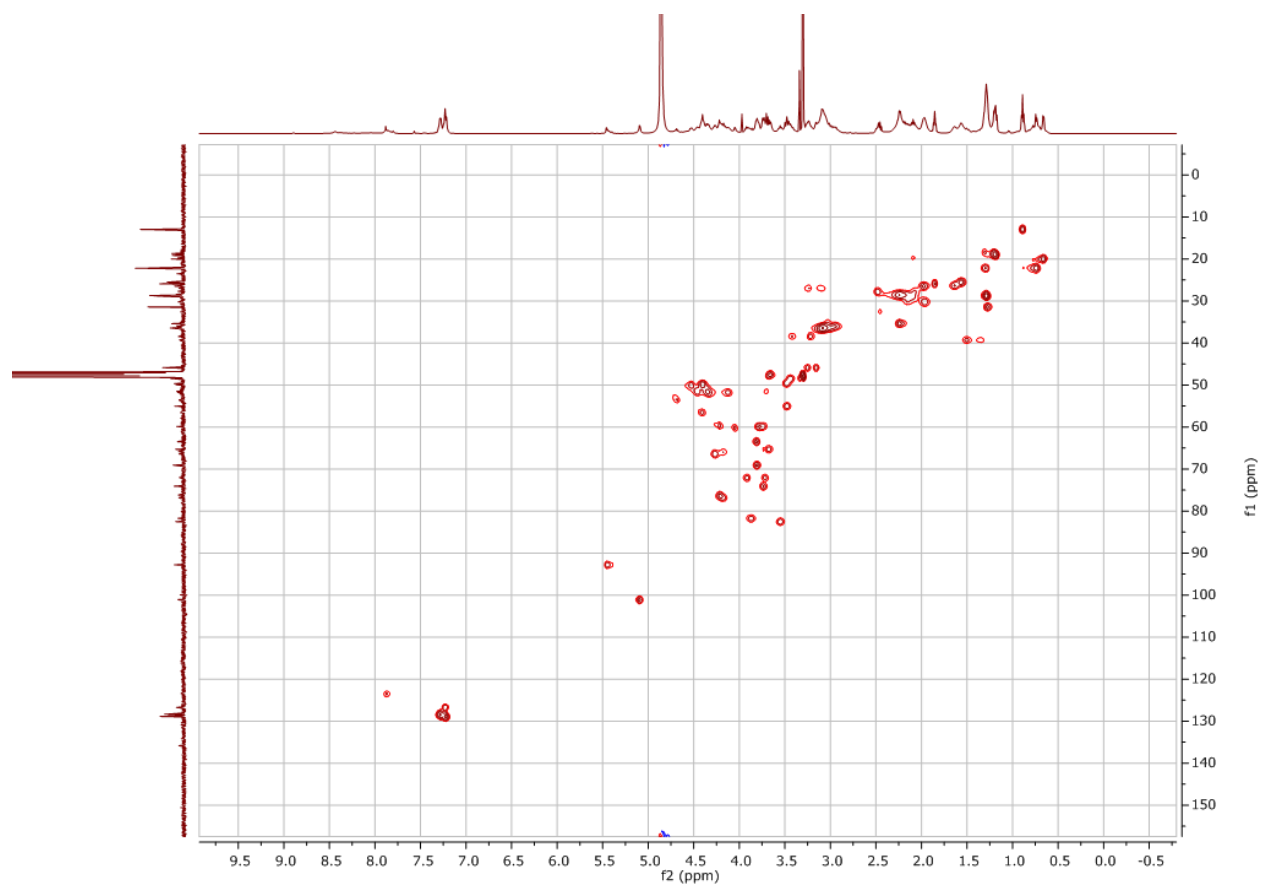
Appendix Figure IV-3 HSQC spectrum of hybrid **1a**.
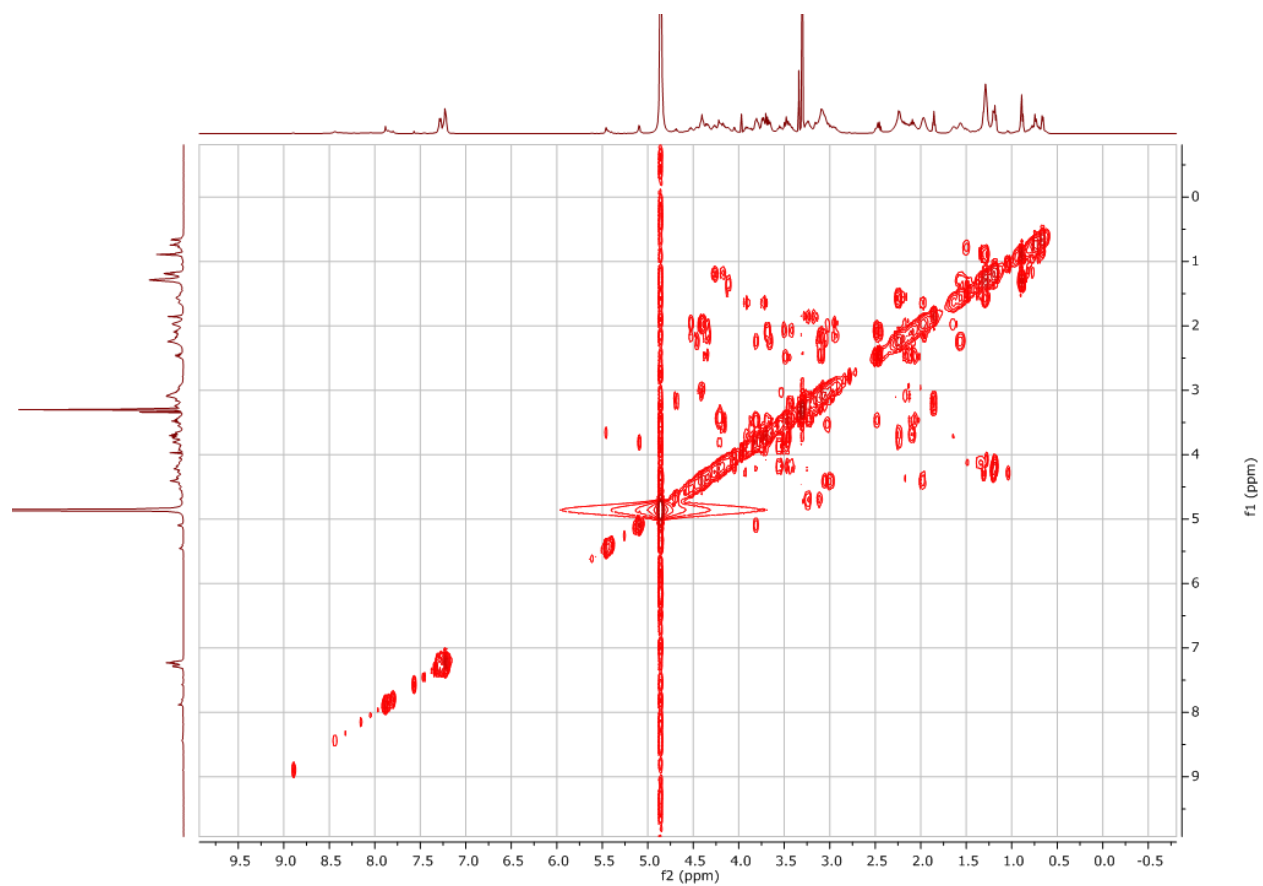
Appendix Figure IV-4 COSY spectrum of hybrid **1a**.
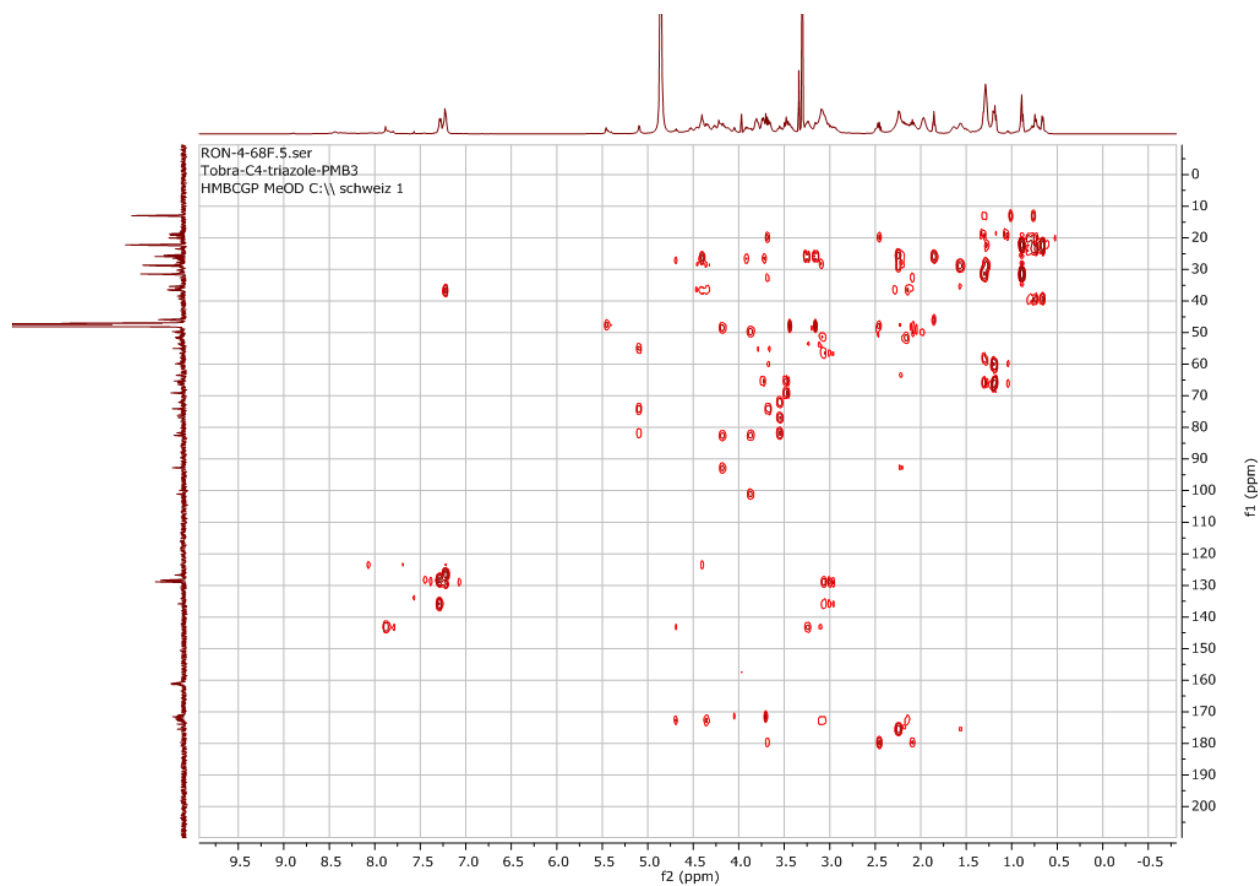
Appendix Figure IV-5 HMBC spectrum of hybrid **1a**.

Processed Channel: PDA 215.0 nm
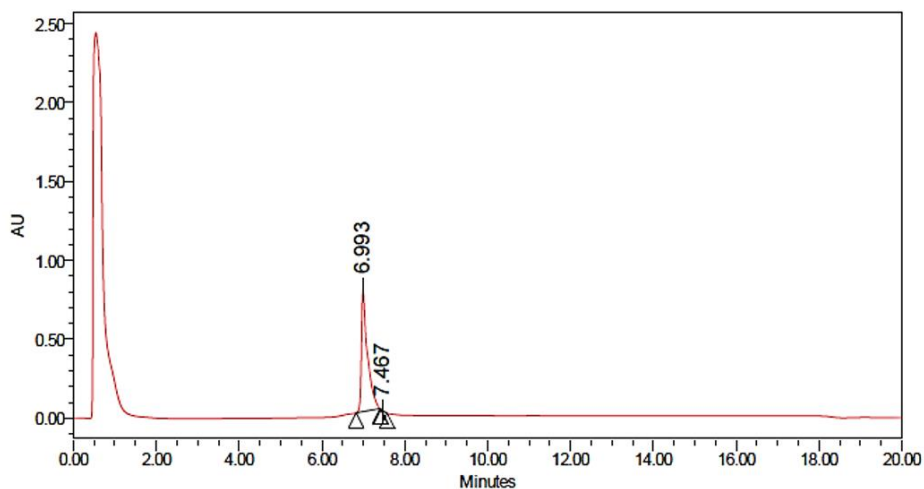
	Processed Channel	Retention Time (min)	Area	% Area	Height
1	PDA 215.0 nm	6.993	7749942	99.77	775639
2	PDA 215.0 nm	7.467	17656	0.23	-2957

*peak at 0.5 mins denotes for DMSO
(see Supporting information Figure 26)
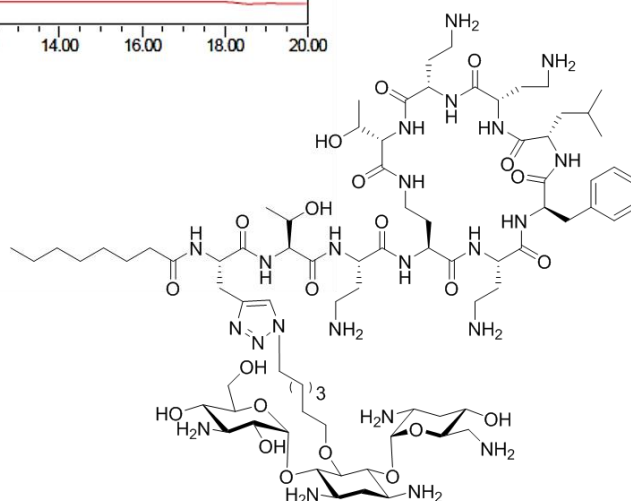
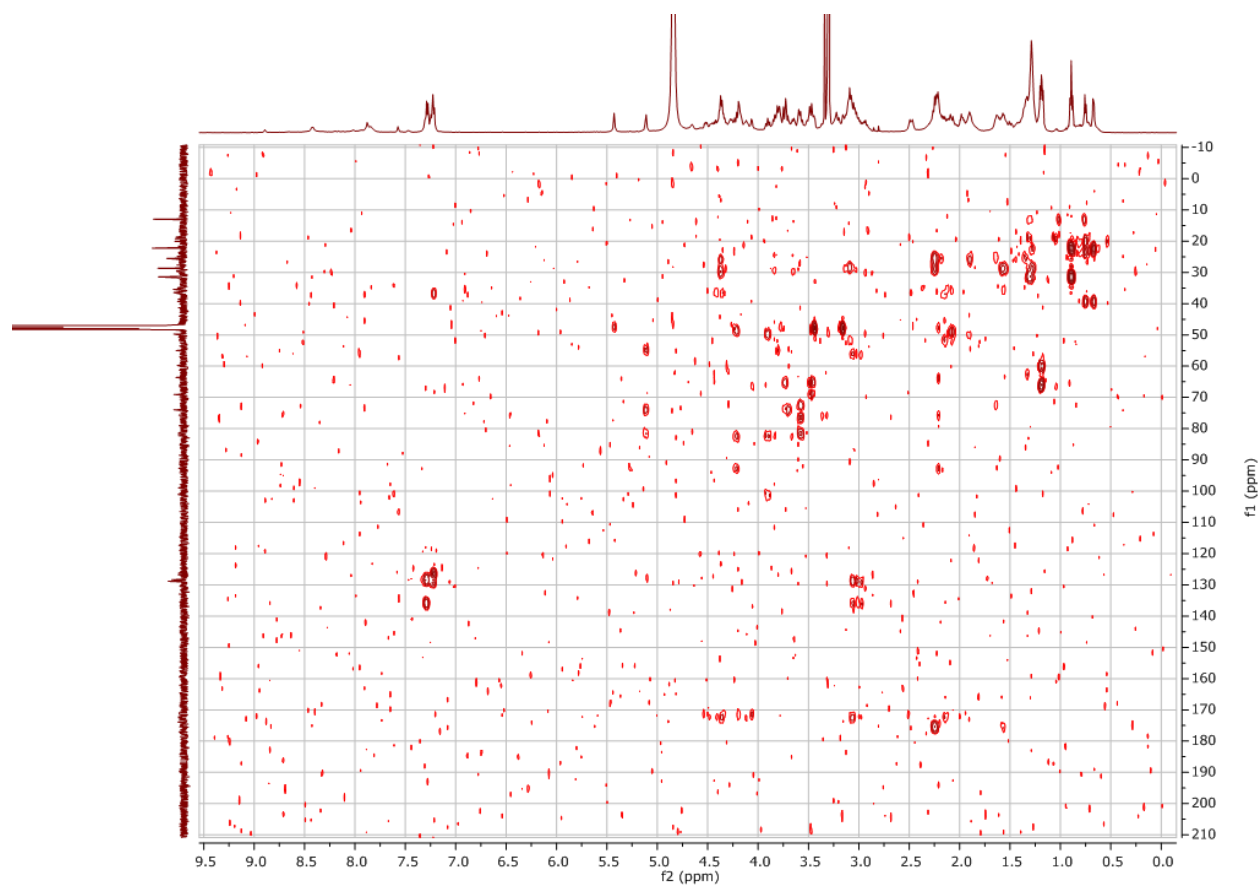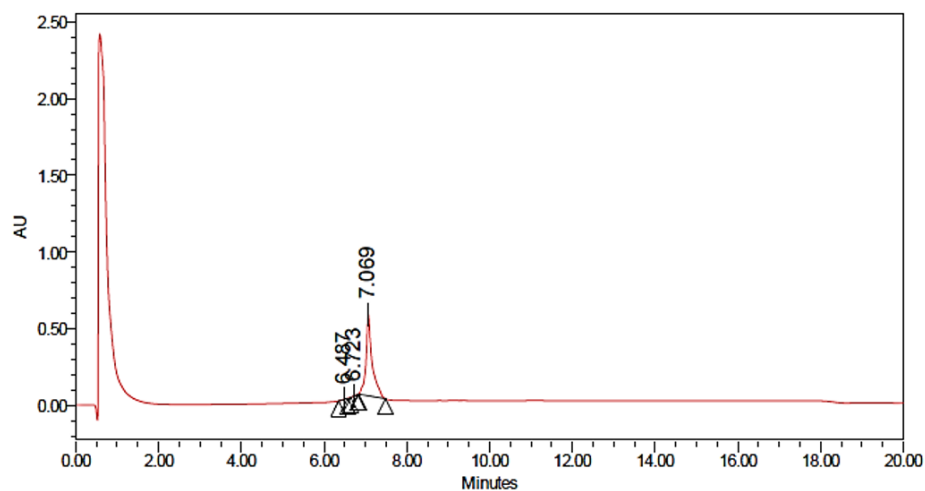**Appendix Figure IV-6** HPLC analysis chromatogram for hybrid **1b**.

Appendix Figure IV-7 ¹H (above) and ¹³C (below) NMR spectra of hybrid **1b**.

carbonyl carbon plus other carbons were deduced from HSQC and HMBC

Appendix Figure IV-8 HSQC spectrum of hybrid **1b**.
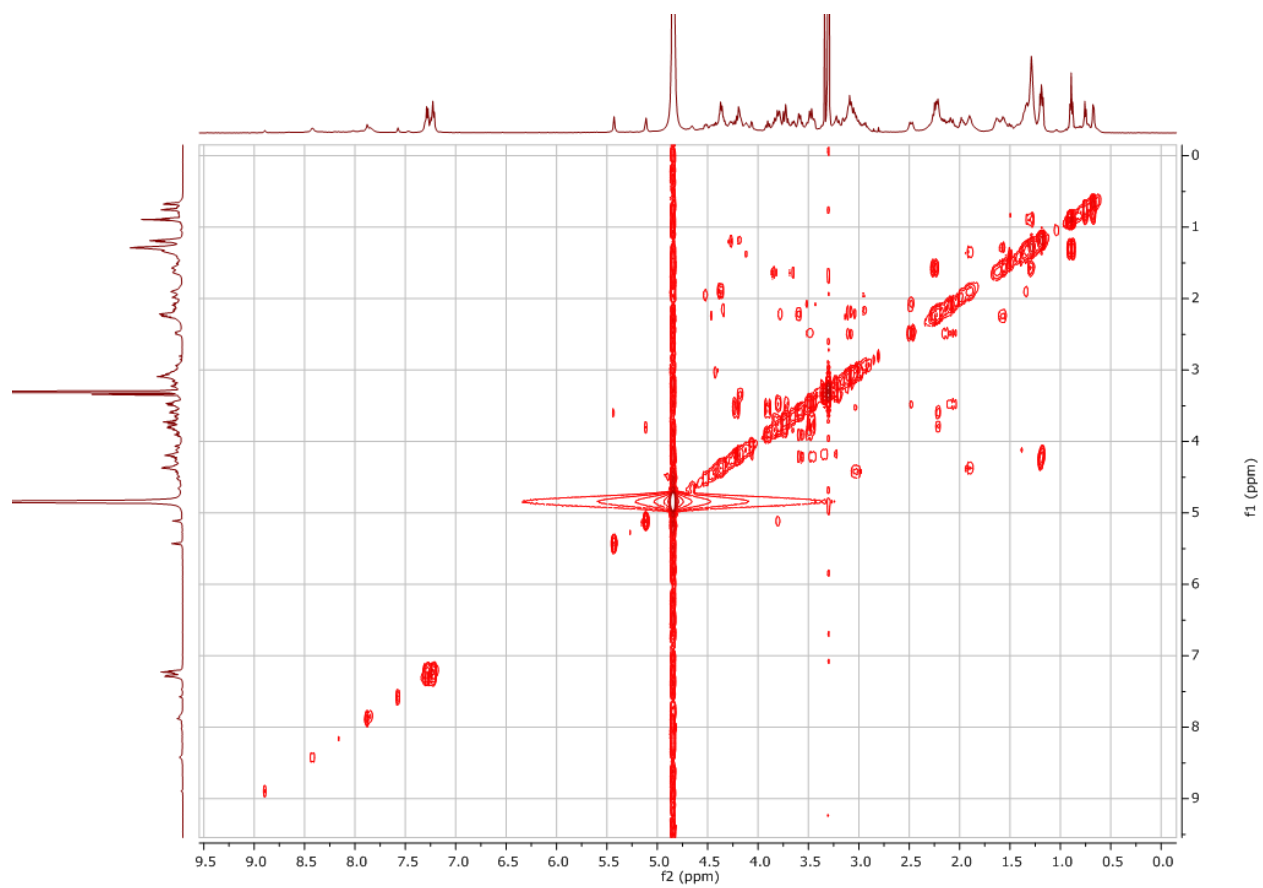
Appendix Figure IV-9 COSY spectrum of hybrid **1b**.
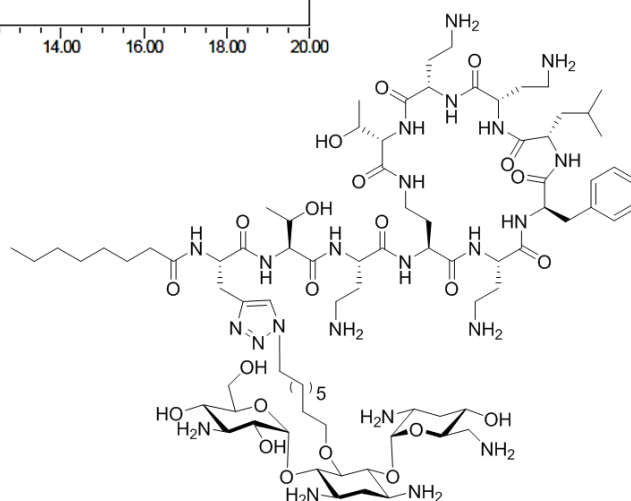
Appendix Figure IV-10 HMBC spectrum of hybrid **1b**.

Processed Channel: PDA 215.0 nm

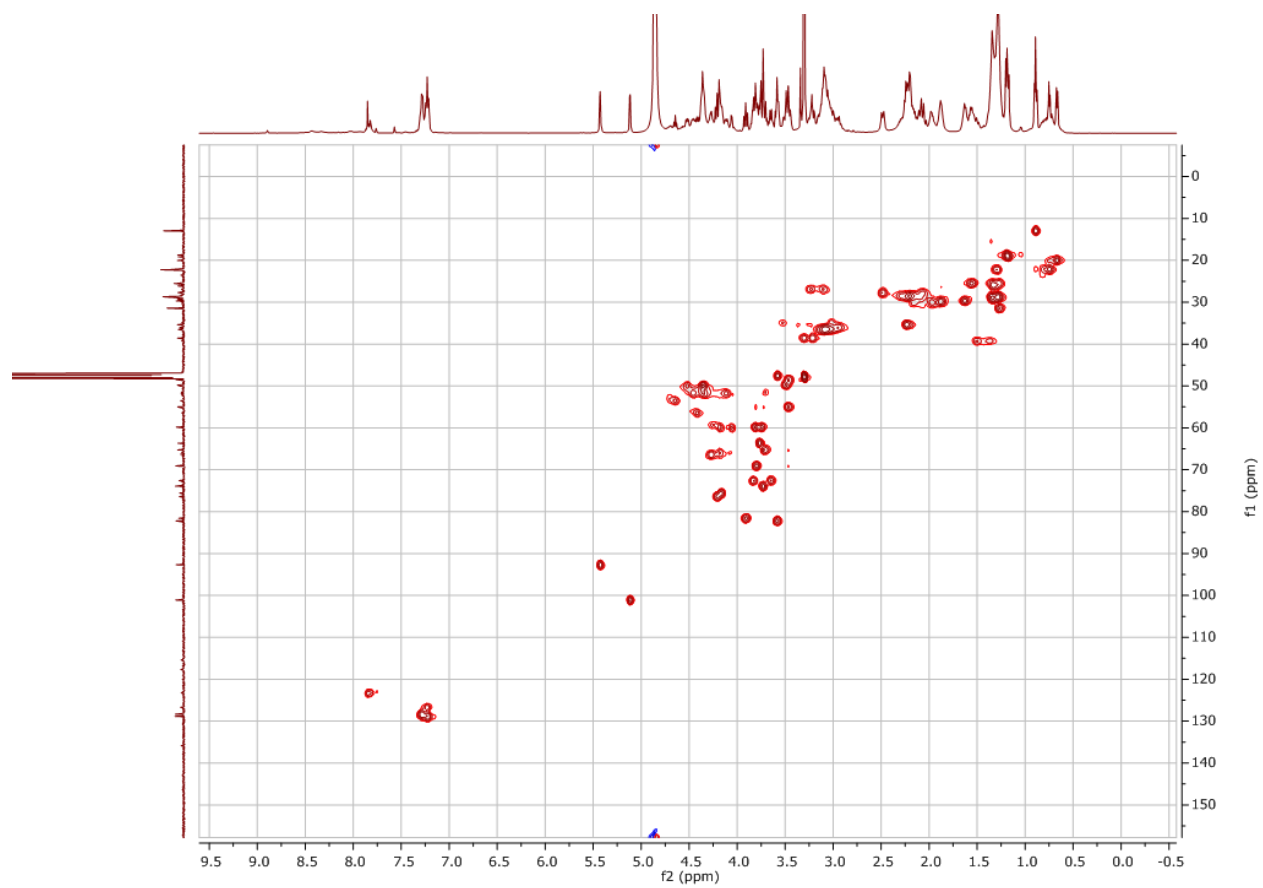|	Processed Channel	Retention Time (min)	Area	% Area	Height
1	PDA 215.0 nm	6.487	7497	0.14	1352
2	PDA 215.0 nm	6.723	2257	0.04	618
3	PDA 215.0 nm	7.069	5465876	99.82	531879

*peak at 0.5 mins denotes for DMSO
(see Supporting information Figure 26)

Appendix Figure IV-11 HPLC analysis chromatogram for hybrid **1c**.
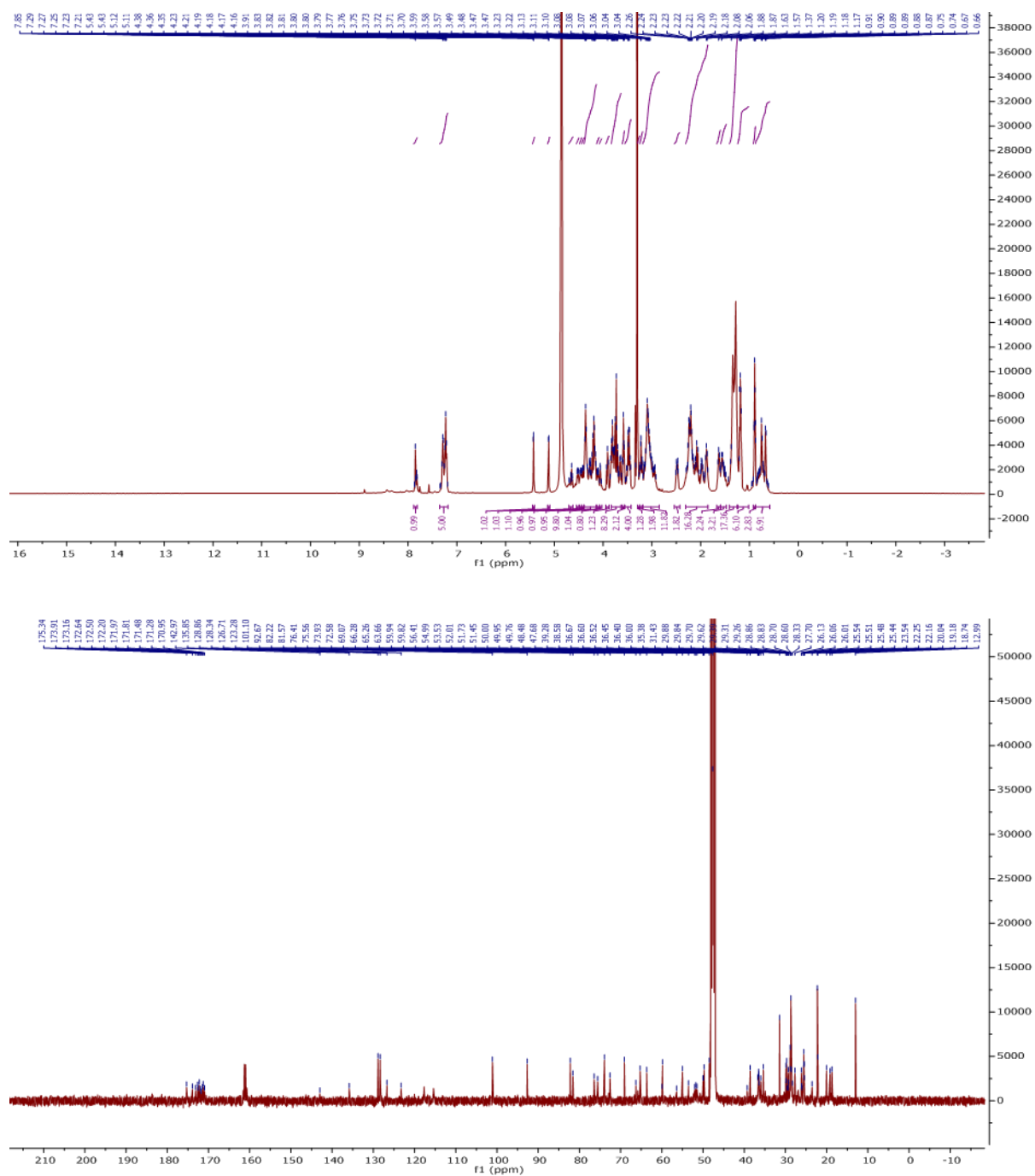
Appendix Figure IV-12 ^{1}H (above) and ^{13}C (below) NMR spectra of hybrid **1c**.

Appendix Figure IV-13 HSQC spectrum of hybrid **1c**.

Appendix Figure IV-14 COSY spectrum of hybrid **1c**.

Appendix Figure IV-15 HMBC spectrum of hybrid **1c**.

	Processed Channel	Retention Time (min)	Area	% Area	Height
1	PDA 215.0 nm	6.604	69459	0.94	4035
2	PDA 215.0 nm	7.207	7311735	98.82	695765
3	PDA 215.0 nm	7.778	17671	0.24	4398

*peak at 0.5 mins denotes for DMSO
(see Supporting information Figure 26)

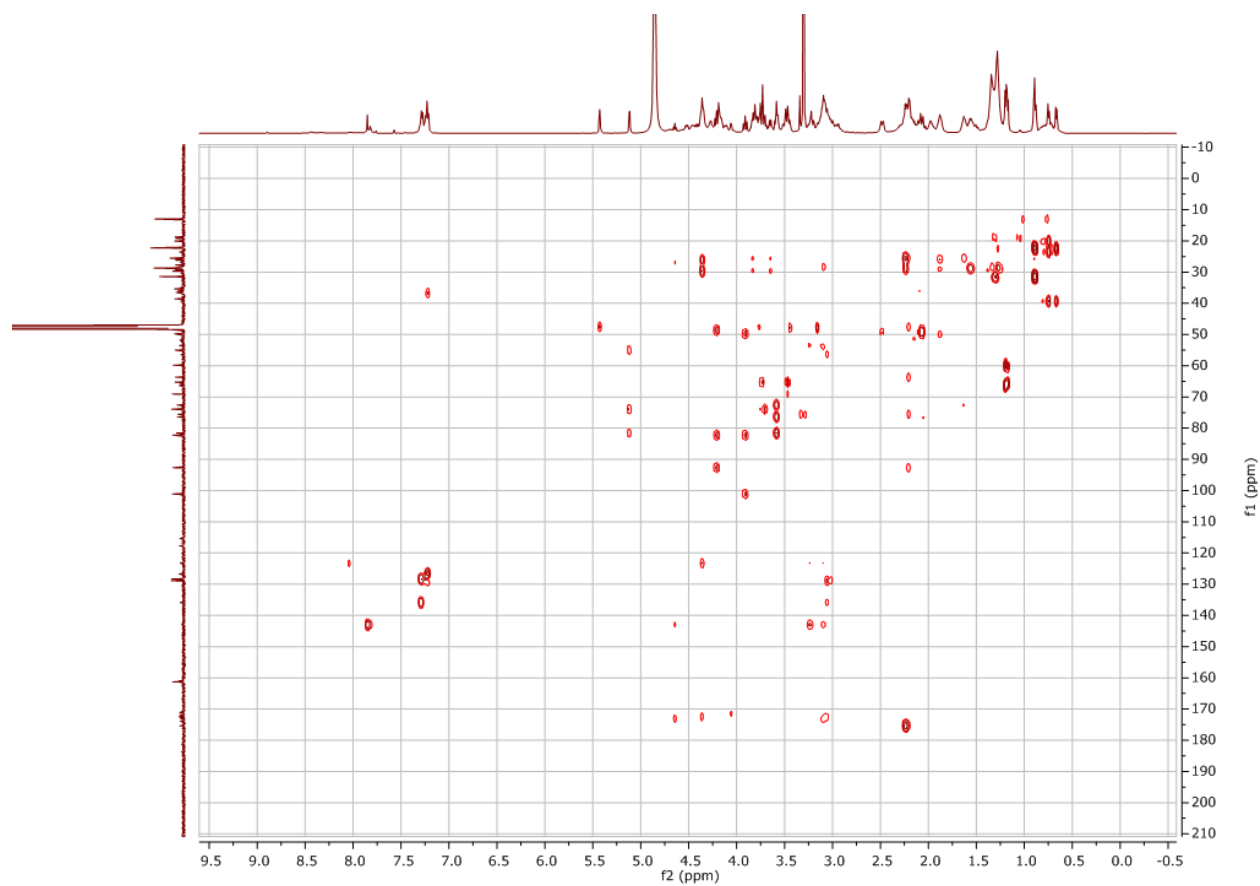**Appendix Figure IV-16** HPLC analysis chromatogram for hybrid **1d**.

Appendix Figure IV-17 ^{1}H (above) and ^{13}C (below) NMR spectra of hybrid **1d**.

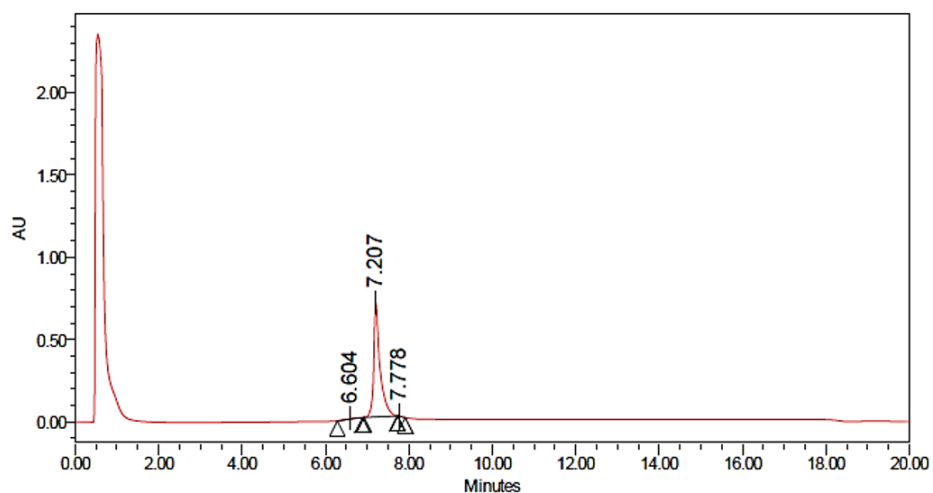**Appendix Figure IV-18** HSQC spectrum of hybrid **1d**.
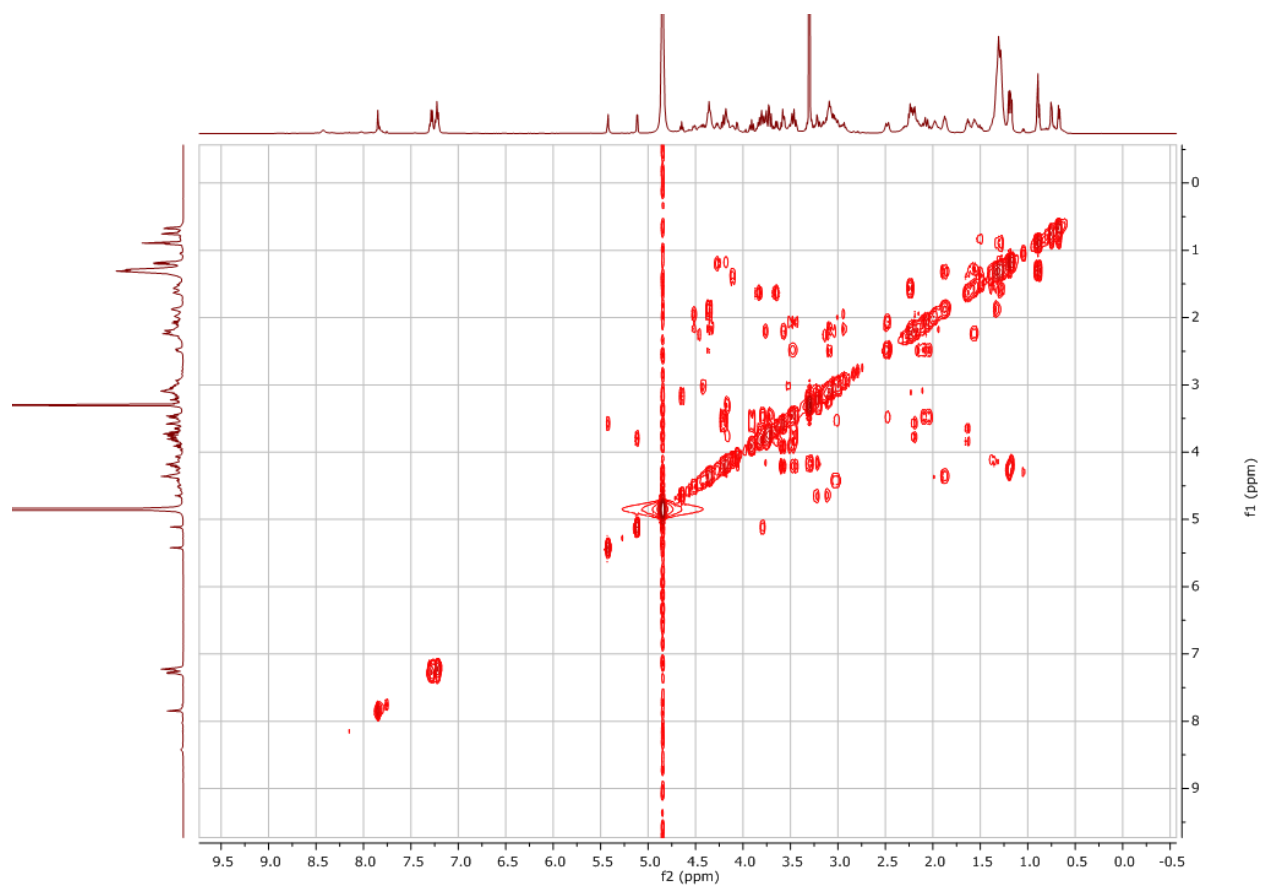
Appendix Figure IV-19 COSY spectrum of hybrid **1d**.
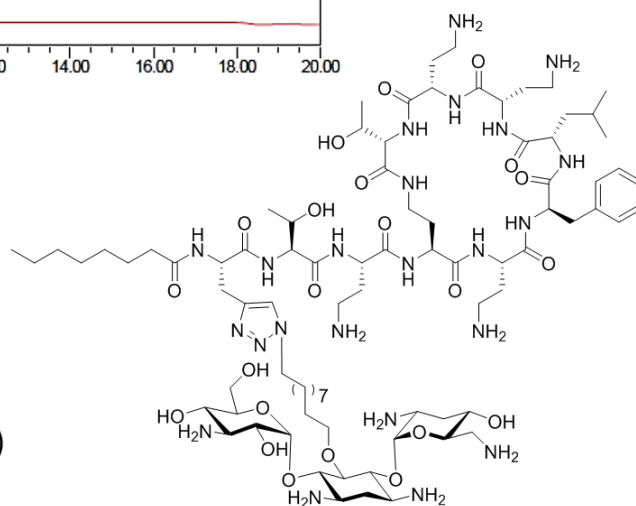
Appendix Figure IV-20 HMBC spectrum of hybrid **1d**.
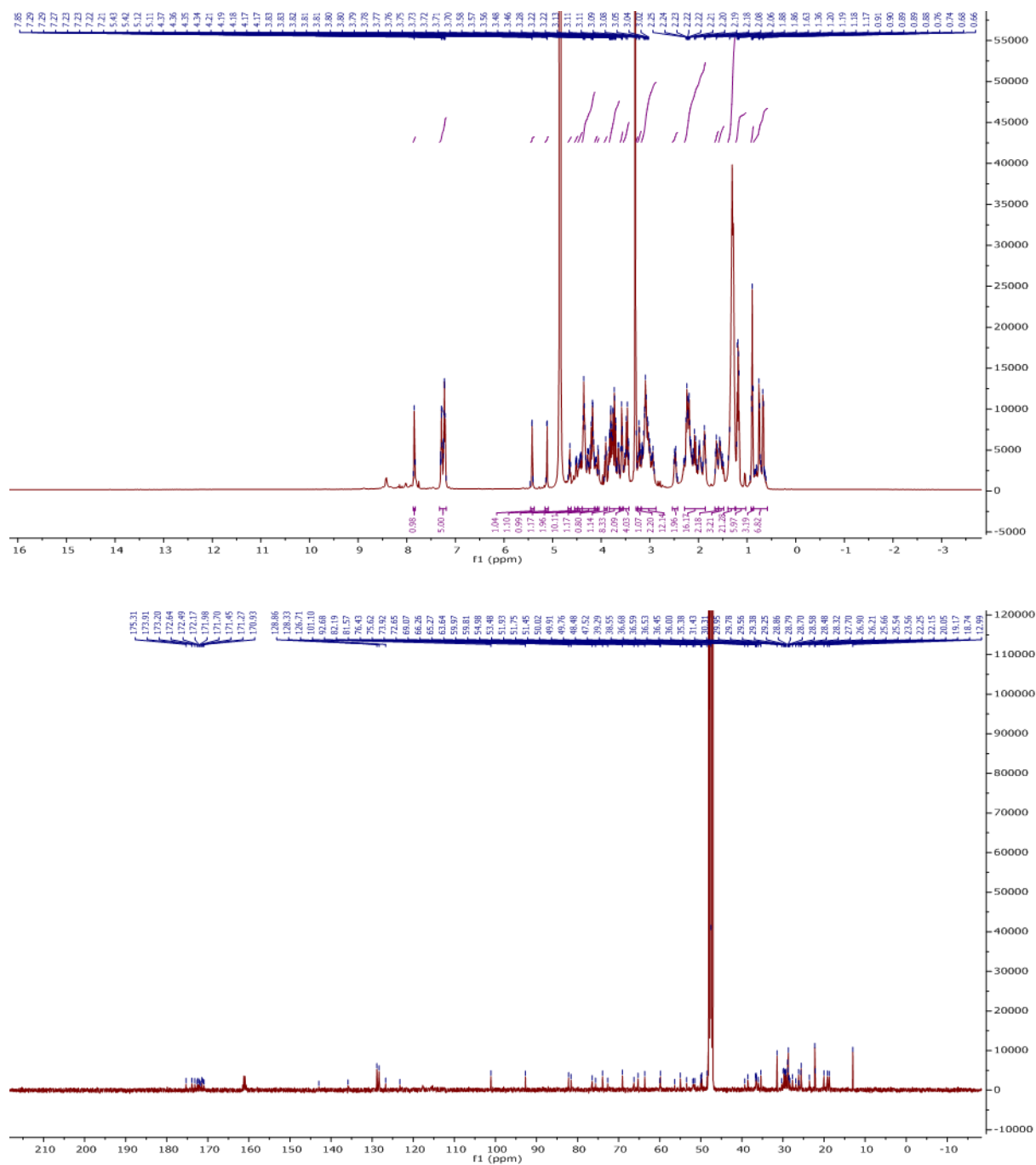
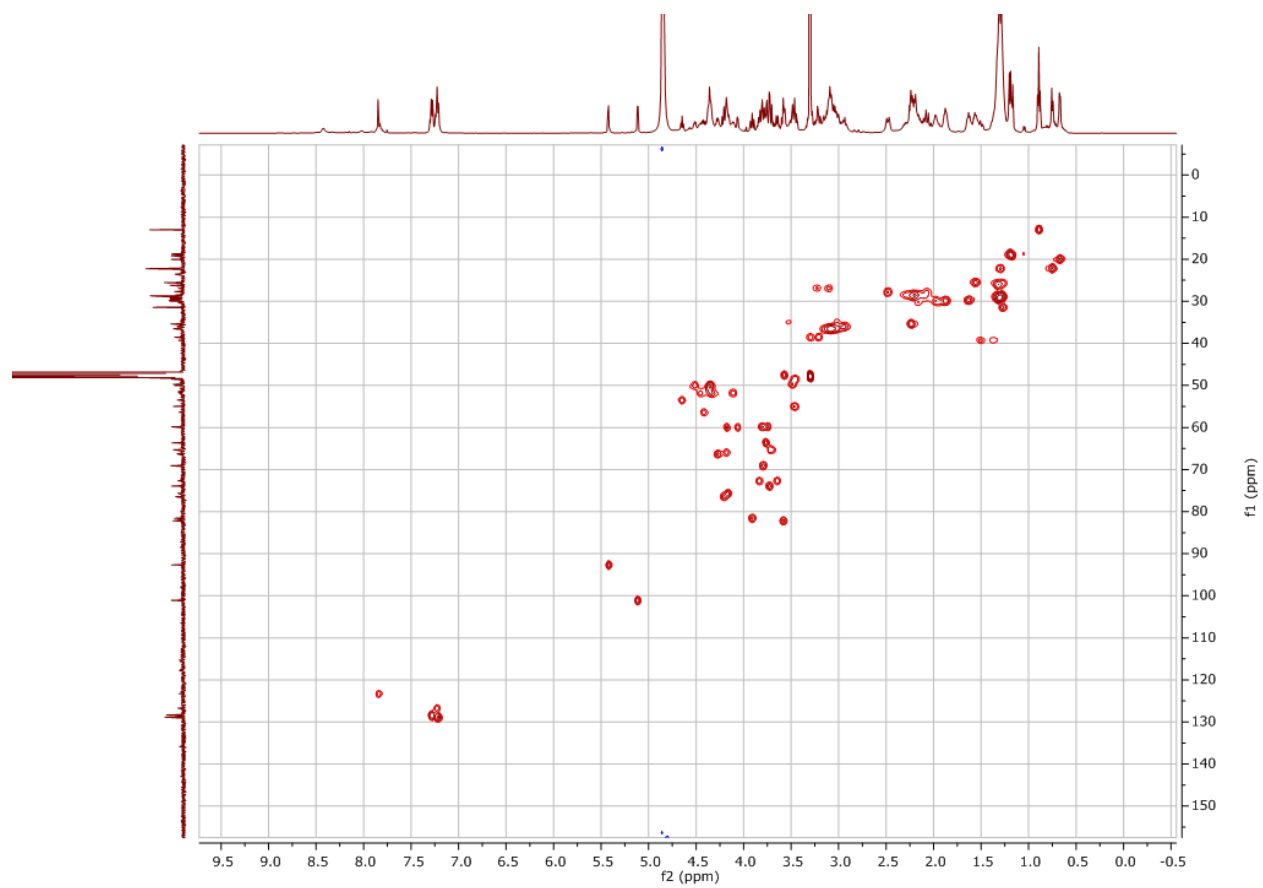PMB3-triazole-C$_{12}$-tobramycin (**1e**)
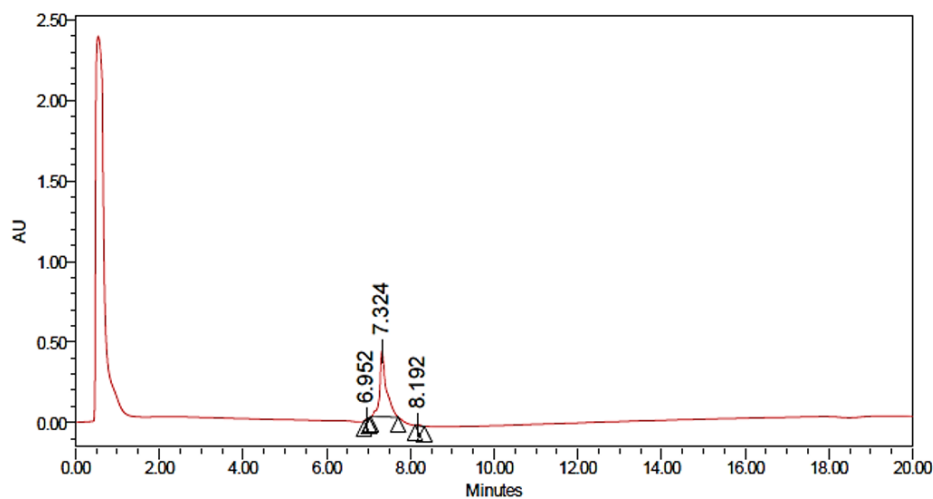
	Processed Channel	Retention Time (min)	Area	% Area	Height
1	PDA 215.0 nm	6.952	13407	0.29	4395
2	PDA 215.0 nm	7.324	4504559	98.84	410395
3	PDA 215.0 nm	8.192	39688	0.87	7656

*peak at 0.5 mins denotes for DMSO
(see Supporting information Figure 26)
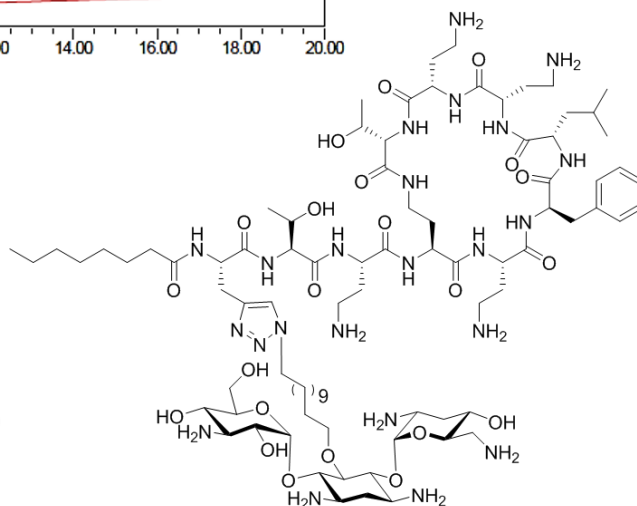
Appendix Figure IV-21 HPLC analysis chromatogram for hybrid **1e**.
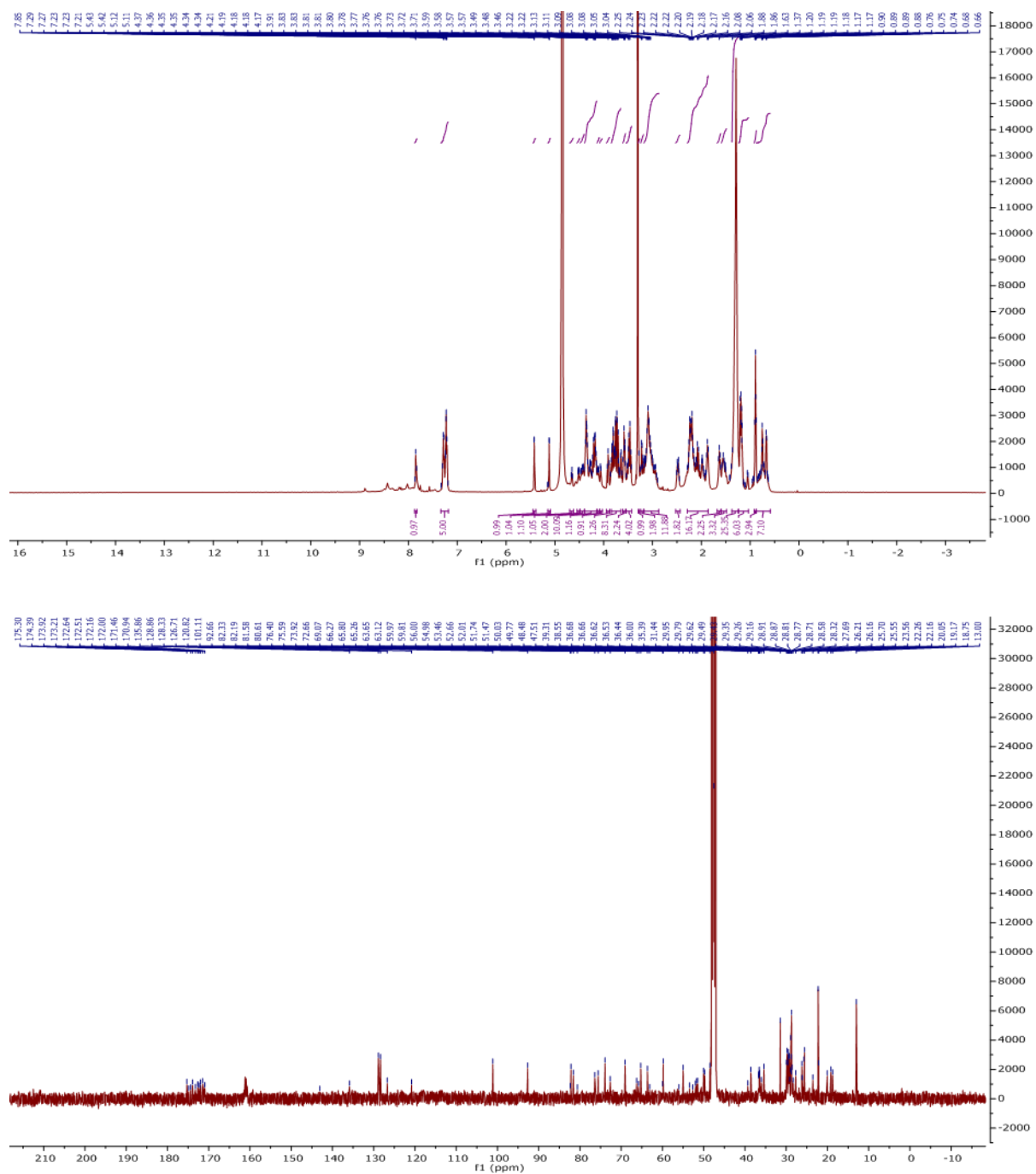
Appendix Figure IV-22 ^{1}H (above) and ^{13}C (below) NMR spectra of hybrid **1e**.
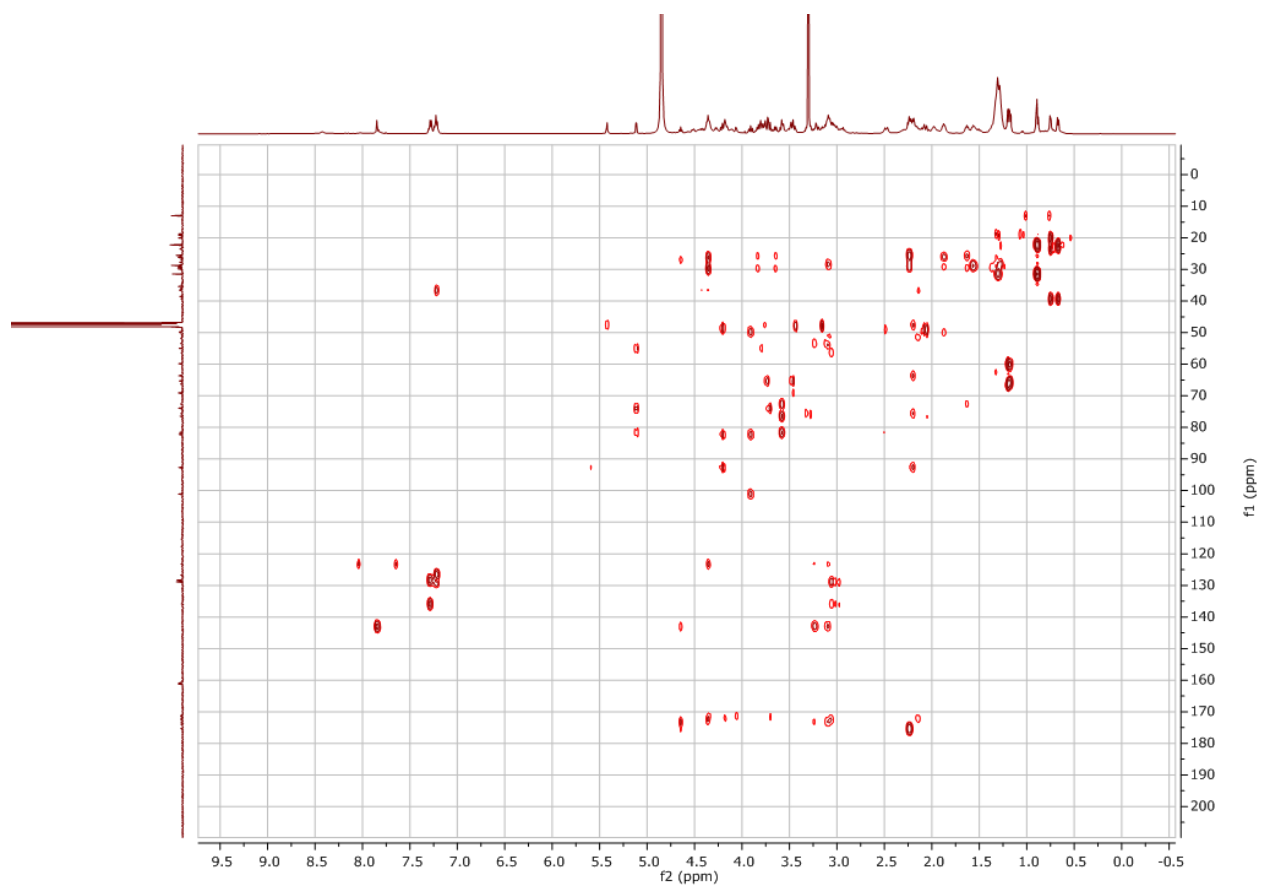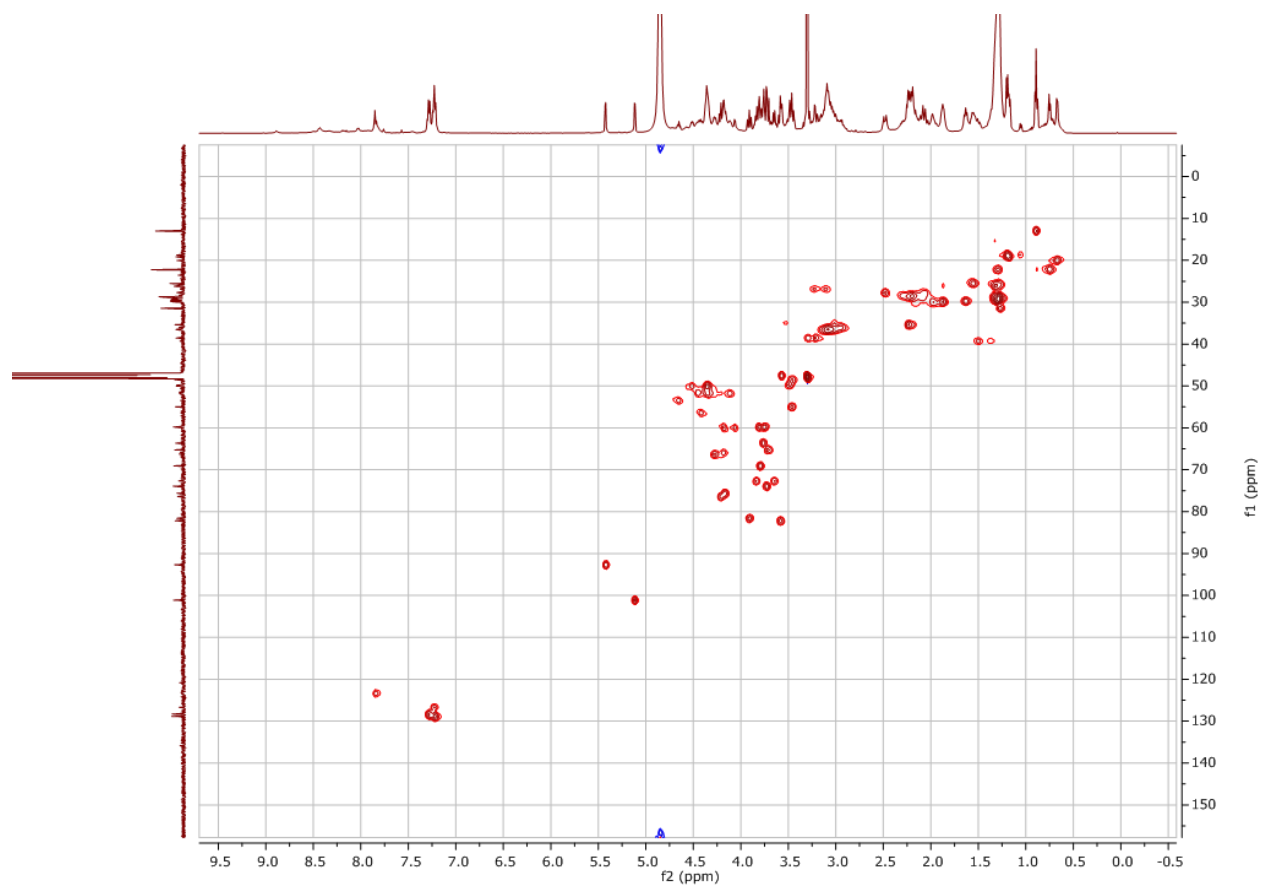
Appendix Figure IV-23 HSQC spectrum of hybrid **1e**.
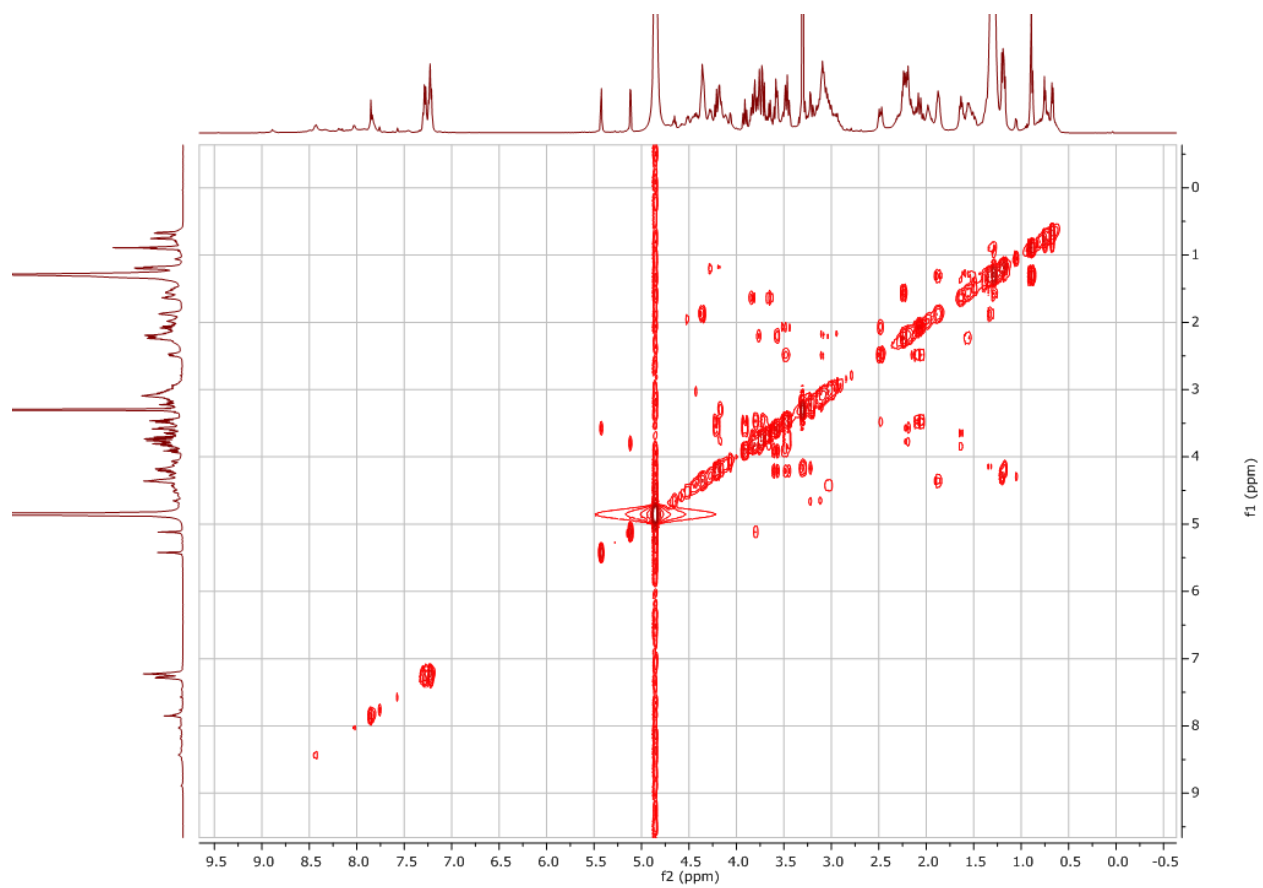
Appendix Figure IV-24 COSY spectrum of hybrid **1e**.
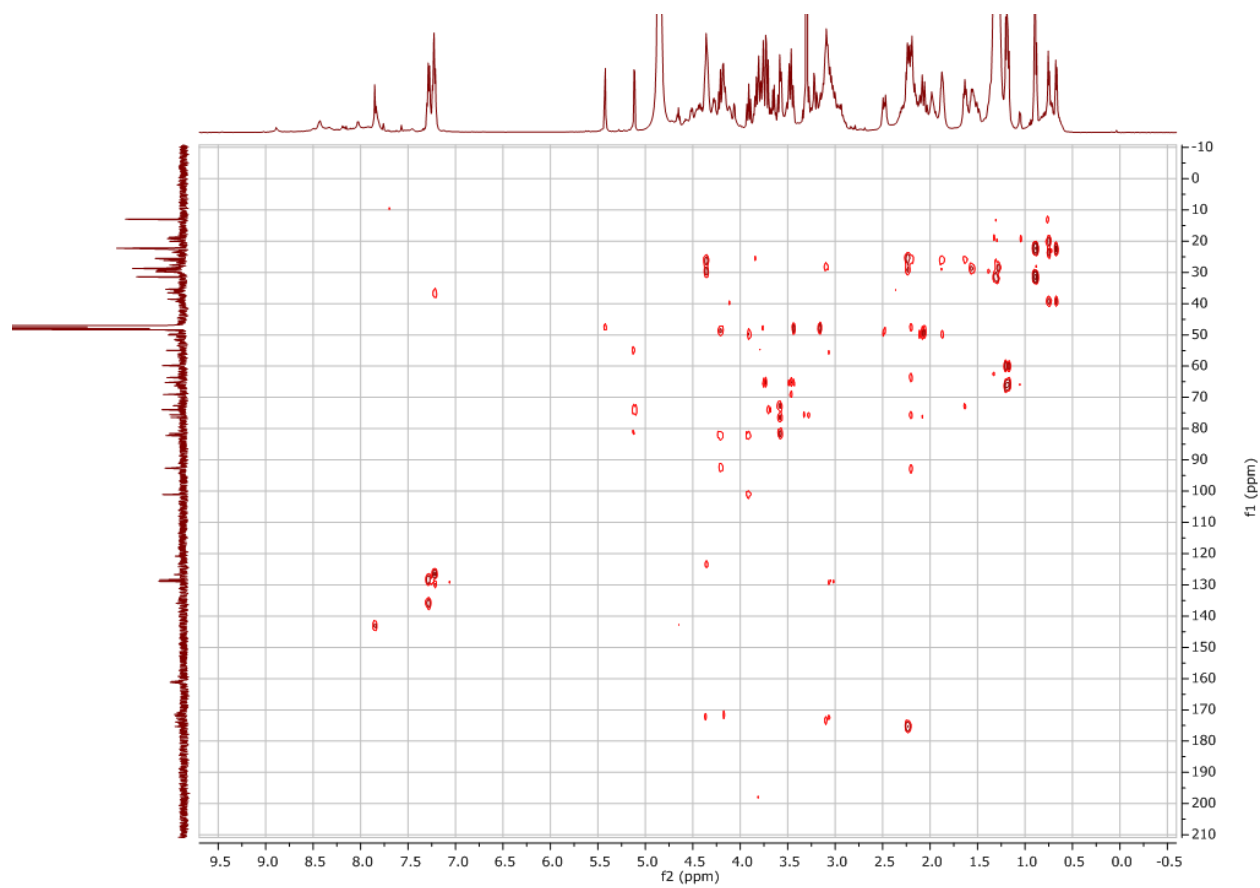
Appendix Figure IV-25 HMBC spectrum of hybrid **1e**.
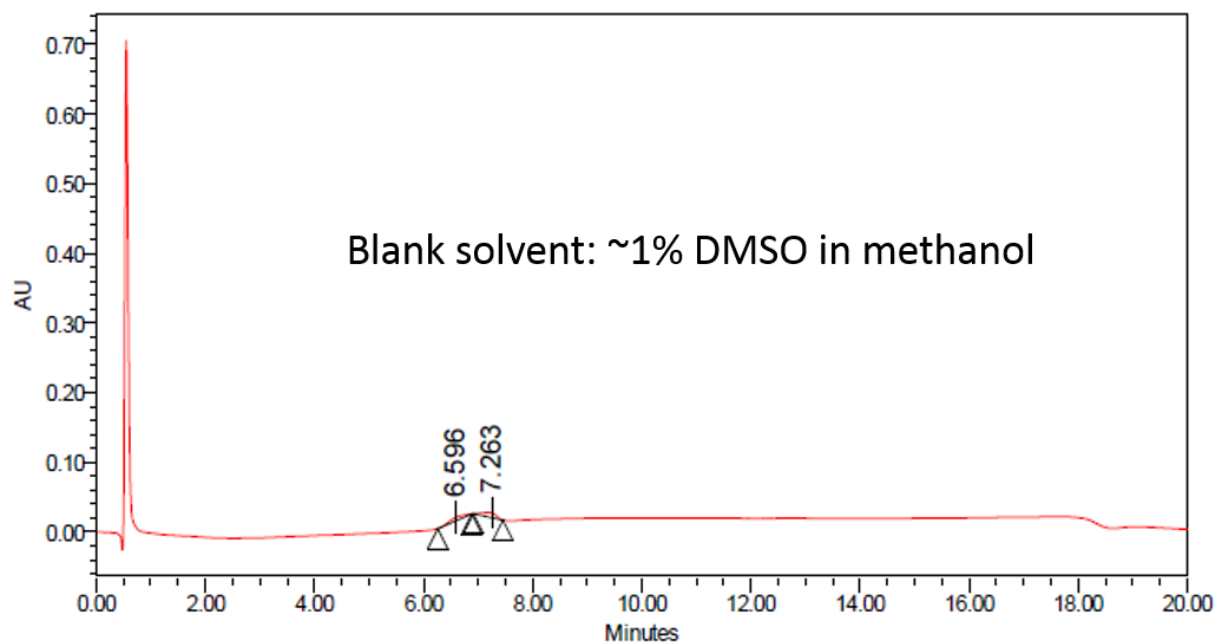
Processed Channel: PDA 215.0 nm

	Processed Channel	Retention Time (min)	Area	% Area	Height
1	PDA 215.0 nm	6.596	96003	44.32	4993
2	PDA 215.0 nm	7.263	120625	55.68	6886

Appendix Figure IV-26 Chromatogram for blank solvent (1% DMSO in methanol) used to dissolve hybrids for HPLC analysis.

IV-6. Evaluation of PMB3-triazole-C_{10}-tobramycin hybrid **1d** in combination with clinically-used antibiotics

Checkerboard assay with hybrid **1d**, **PMB3**, or **TOB** and antibiotics against wild-type *Pseudomonas aeruginosa* PAO1

Appendix Table IV-4 Assessment of potential synergism between hybrid **1d** and various clinically-used antibiotics in wild-type *P. aeruginosa* PAO1.

Antibiotic	$MIC_{Antibiotic}$, µg/mL	$MIC_{Antibiotic}$ in combination, µg/mL	MIC_{1d}, µg/mL	$MIC_{1d\ in}$ combination, µg/mL	FIC index	Interpretation
Erythromycin	256	64	2	1	0.75	Additive
Streptomycin	16	8	4	2	1.00	Additive
Amikacin	1	2	4	0.0625	2.01	Additive
Gentamicin	1	0.015625	4	2	0.51	Additive
Tobramycin	0.5	0.5	4	0.125	1.03	Additive
Minocycline	8	2	4	0.5	0.37	Synergistic
Doxycycline	16	1	2	0.25	0.19	Synergistic
Tigecycline	8	2	4	0.5	0.37	Synergistic
Moxifloxacin	1	1	2	0.0625	1.03	Additive
Ciprofloxacin	0.125	0.25	4	0.0625	2.01	Additive
Levofloxacin	0.25	0.125	4	2	1.00	Additive
Rifampicin	16	1	4	0.5	0.19	Synergistic
Vancomycin	1024	128	4	1	0.37	Synergistic
Meropenem	1	0.25	4	2	0.75	Additive
Doripenem	0.5	0.125	4	2	0.75	Additive
Novobiocin	512	16	4	1	0.28	Synergistic
Trimethoprim	128	8	4	1	0.31	Synergistic
Polymyxin B_3	1	0.5	4	2	1.00	Additive
Chloramphenicol	64	8	4	0.25	0.19	Synergistic
Ceftazidime	2	0.5	4	2	0.75	Additive
Cefotaxime	8	0.015625	2	2	1.00	Additive
Aztreonam	4	2	2	1	1.00	Additive
Clindamycin	1024	16	4	0.5	0.14	Synergistic
Linezolid	1024	32	4	1	0.28	Synergistic
Fosfomycin	16	2	4	2	0.62	Additive
Nitrofurantoin	512	128	4	4	1.25	Additive

Appendix Table IV-5 Assessment of potential synergism between **PMB3** and various clinically-used antibiotics in wild-type *P. aeruginosa* PAO1.

Antibiotic	MIC$_{Antibiotic}$, µg/mL	MIC$_{Antibiotic}$ in combination, µg/mL	MIC$_{PMB3}$, µg/mL	MIC$_{PMB3}$ in combination, µg/mL	FIC index	Interpretation
Tobramycin	0.5	0.001953	0.5	0.5	1.00	Additive
Minocycline	8	1	1	0.25	0.37	Synergistic
Doxycycline	8	0.25	0.5	0.125	0.28	Synergistic
Tigecycline	4	2	1	0.25	0.75	Additive
Rifampicin	16	0.0625	0.5	0.125	0.25	Synergistic
Vancomycin	1024	128	1	0.25	0.37	Synergistic
Novobiocin	256	1	1	0.5	0.50[a]	Additive
Trimethoprim	128	0.5	1	0.5	0.50[a]	Additive
Chloramphenicol	64	8	0.5	0.25	0.62	Additive
Clindamycin	2048	128	0.5	0.125	0.31	Synergistic
Linezolid	1024	32	1	0.25	0.28	Synergistic

[a] = exact FIC index value is 0.503906 and therefore not synergistic

Appendix Table IV-6 Assessment of potential synergism between **TOB** and various clinically-used antibiotics in wild-type *P. aeruginosa* PAO1.

Antibiotic	MIC$_{Antibiotic}$, µg/mL	MIC$_{Antibiotic}$ in combination, µg/mL	MIC$_{TOB}$, µg/mL	MIC$_{TOB}$ in combination, µg/mL	FIC index	Interpretation
Minocycline	8	4	1	0.5	1.00	Additive
Doxycycline	8	4	1	0.5	1.00	Additive
Tigecycline	4	0.03125	1	1	1.01	Additive
Rifampicin	16	8	0.5	0.25	1.00	Additive
Vancomycin	1024	128	1	0.25	0.37	Synergistic
Novobiocin	512	64	0.5	0.25	0.62	Additive
Trimethoprim	256	64	0.5	0.125	0.50	Synergistic
Chloramphenicol	128	0.25	0.5	0.5	1.00	Additive
Clindamycin	1024	1024	0.5	0.25	1.50	Additive
Linezolid	1024	0.25	1	1	1.00	Additive

Checkerboard assay with hybrid **1d**, **PMB3**, or **TOB** and antibiotics against multidrug-resistant (MDR) *P. aeruginosa* PA259-96918

Appendix Table IV-7 Assessment of potential synergism between **1d** and various clinically-used antibiotics in MDR *P. aeruginosa* PA259-96918

Antibiotic	$MIC_{Antibiotic}$, µg/mL	$MIC_{Antibiotic}$ in combination, µg/mL	MIC_{1d}, µg/mL	MIC_{1d} in combination, µg/mL	FIC index	Interpretation
Minocycline	32	0.125	8	1	0.13	Synergistic
Doxycycline	32	0.5	8	1	0.14	Synergistic
Tigecycline	8	1	4	0.5	0.25	Synergistic
Rifampicin	16	0.0625	8	1	0.13	Synergistic
Vancomycin	1024	8	4	0.5	0.13	Synergistic
Novobiocin	256	1	8	2	0.25	Synergistic
Trimethoprim	512	32	8	1	0.19	Synergistic
Chloramphenicol	1024	32	8	1	0.16	Synergistic
Clindamycin	>2048	16	4	1	0.25<x<0.26	Synergistic
Linezolid	1024	128	4	0.5	0.25	Synergistic

Appendix Table IV-8 Assessment of potential synergism between **PMB3** and various clinically-used antibiotics in MDR *P. aeruginosa* PA259-96918.

Antibiotic	$MIC_{Antibiotic}$, µg/mL	$MIC_{Antibiotic}$ in combination, µg/mL	MIC_{PMB3}, µg/mL	MIC_{PMB3} in combination, µg/mL	FIC index	Interpretation
Tobramycin	256	1	0.5	0.5	1.00	Additive
Minocycline	32	8	0.5	0.125	0.50	Synergistic
Doxycycline	32	8	0.5	0.125	0.50	Synergistic
Tigecycline	8	2	0.5	0.125	0.50	Synergistic
Rifampicin	16	8	0.25	0.125	1.00	Additive
Vancomycin	1024	128	0.25	0.0625	0.38	Synergistic
Novobiocin	256	1	0.5	0.25	0.50[a]	Additive
Trimethoprim	512	64	0.5	0.25	0.63	Additive
Chloramphenicol	1024	256	0.5	0.25	0.75	Additive
Clindamycin	>2048	256	0.5	0.0625	0.13<x<0.25	Synergistic
Linezolid	1024	16	0.25	0.125	0.52	Additive

[a] = exact FIC index value is 0.503906 and therefore not synergistic

318

Appendix Table IV-9 Assessment of potential synergism between **TOB** and various clinically-used antibiotics in MDR *P. aeruginosa* PA259-96918.

Antibiotic	MIC$_{Antibiotic}$, µg/mL	MIC$_{Antibiotic}$ in combination, µg/mL	MIC$_{TOB}$, µg/mL	MIC$_{TOB}$ in combination, µg/mL	FIC index	Interpretation
Minocycline	64	0.0625	256	128	0.50[a]	Additive
Doxycycline	64	32	128	64	1.00	Additive
Tigecycline	8	4	256	32	0.63	Additive
Rifampicin	32	8	256	16	0.31	Synergistic
Vancomycin	1024	64	256	32	0.19	Synergistic
Novobiocin	256	128	128	64	1.00	Additive
Trimethoprim	1024	256	128	64	0.75	Additive
Chloramphenicol	1024	512	256	64	0.75	Additive
Clindamycin	>4096	1024	256	128	0.50<x<0.75	Additive
Linezolid	1024	256	256	128	0.75	Additive

[a] = exact FIC index value is 0.500977 and therefore not synergistic

6.3. Checkerboard assay with **PMB3** or **TOB** and either minocycline, rifampicin, or vancomycin against MDR/extensively drug-resistant (XDR) *P. aeruginosa* clinical isolates

Appendix Table IV-10 Adjuvant potency of **PMB3** in combination with minocycline against wild-type and MDR/XDR *P. aeruginosa*.

P. aeruginosa strain	MIC$_{Minocycline}$, µg/mL	MIC$_{PMB3}$, µg/mL	FIC index	Absolute MIC$_{Minocycline}$,[a] µg/mL	Potentiation[b]
PAO1	8	1	0.38	1	8-fold
259-96918	32	0.5	0.50	8	4-fold
260-97103	16	0.25	0.50	4	4-fold
262-101856	64	4	0.08	1	64-fold
264-104354	16	1	0.28	0.5	32-fold
100036	16	2	0.16	0.5	32-fold
101243[c]	2	128	0.25	0.5	4-fold
101885	16	0.5	0.38	2	8-fold

[a] = MIC of minocycline in the presence of ≤¼ × MIC$_{PMB3}$ (≤ 4 µg/mL) of **PMB3**. [b] = degree of antibiotic potentiation in the presence of ≤¼ × MIC$_{PMB3}$ (≤ 4 µg/mL) of **PMB3**. [c] = colistin- and tobramycin-resistant.

Appendix Table IV-11 Adjuvant potency of **PMB3** in combination with rifampicin against wild-type and MDR/XDR *P. aeruginosa*.

P. aeruginosa strain	MIC$_{Rifampicin}$, µg/mL	MIC$_{PMB3}$, µg/mL	FIC index	Absolute MIC$_{Rifampicin}$,[a] µg/mL	Potentiation[b]
PAO1	16	0.5	0.25	≤0.0625	≥256-fold
259-96918	16	0.25	1.00	16	none
260-97103	8	0.25	0.37	1	8-fold
262-101856	512	8	0.05	0.5	1024-fold
264-104354	8	0.5	0.31	0.5	16-fold
100036	16	2	0.125<x<0.126	≤0.015625	≥1024-fold
101243[c]	4	128	0.01	≤0.007813	≥512-fold
101885	16	1	0.125<x<0.127	≤0.03125	≥512-fold

[a] = MIC of rifampicin in the presence of ≤¼ × MIC$_{PMB3}$ (≤ 4 µg/mL) of **PMB3**. [b] = degree of antibiotic potentiation in the presence of ≤¼ × MIC$_{PMB3}$ (≤ 4 µg/mL) of **PMB3**. [c] = colistin- and tobramycin-resistant.

Appendix Table IV-12 Adjuvant potency of **PMB3** in combination with vancomycin against wild-type and MDR/XDR *P. aeruginosa*.

P. aeruginosa strain	MIC$_{Vancomycin}$, µg/mL	MIC$_{PMB3}$, µg/mL	FIC index	Absolute MIC$_{Vancomycin}$,[a] µg/mL	Potentiation[b]
PAO1	1024	1	0.38	128	8-fold
259-96918	1024	0.25	0.38	128	8-fold
260-97103	512	0.25	0.63	256	2-fold
262-101856	1024	4	0.16	2	512-fold
264-104354	512	1	0.31	32	16-fold
100036	512	2	0.19	2	256-fold
101243[c]	128	128	0.50[d]	64	2-fold
101885	512	0.5	0.28	16	32-fold

[a] = MIC of vancomycin in the presence of ≤¼ × MIC$_{PMB3}$ (≤ 4 µg/mL) of **PMB3**. [b] = degree of antibiotic potentiation in the presence of ≤¼ × MIC$_{PMB3}$ (≤ 4 µg/mL) of **PMB3**. [c] = colistin- and tobramycin-resistant. [d] = exact FIC index value is 0.500488 and therefore not synergistic

Appendix Table IV-13 Adjuvant potency of **TOB** in combination with minocycline against wild-type and MDR/XDR *P. aeruginosa*.

P. aeruginosa strain	MIC$_{Minocycline}$, µg/mL	MIC$_{TOB}$, µg/mL	FIC index	Absolute MIC$_{Minocycline}$,[a] µg/mL	Potentiation[b]
PAO1	8	1	1.00	8	none
259-96918	64	256	0.50[d]	64	none
260-97103	16	64	1.03	16	none
262-101856	128	1024	0.52	128	none
264-104354	32	256	1.03	32	none
100036	32	128	1.00	32	none
101243[c]	2	256	0.51	2	none
101885	16	0.5	1.00	16	none

[a] = MIC of minocycline in the presence of ≤¼ × MIC$_{TOB}$ (≤ 4 µg/mL) of **TOB**. [b] = degree of antibiotic potentiation in the presence of ≤¼ × MIC$_{TOB}$ (≤ 4 µg/mL) of **TOB**. [c] = colistin- and tobramycin-resistant. [d] = exact FIC index value is 0.500977 and therefore not synergistic

Appendix Table IV-14 Adjuvant potency of **TOB** in combination with rifampicin against wild-type and MDR/XDR *P. aeruginosa*.

P. aeruginosa strain	MIC$_{Rifampicin}$, µg/mL	MIC$_{TOB}$, µg/mL	FIC index	Absolute MIC$_{Rifampicin}$,[a] µg/mL	Potentiation[b]
PAO1	16	0.5	1.00	16	none
259-96918	32	256	0.31	32	none
260-97103	16	64	0.37	8	2-fold
262-101856	512	512	0.75	512	none
264-104354	8	256	0.50	8	none
100036	16	128	0.28	4	4-fold
101243[c]	8	256	0.56	4	2-fold
101885	16	0.5	0.75	8	2-fold

[a] = MIC of rifampicin in the presence of ≤¼ × MIC$_{TOB}$ (≤ 4 µg/mL) of **TOB**. [b] = degree of antibiotic potentiation in the presence of ≤¼ × MIC$_{TOB}$ (≤ 4 µg/mL) of **TOB**. [c] = colistin- and tobramycin-resistant.

Appendix Table IV-15 Adjuvant potency of **TOB** in combination with vancomycin against wild-type and MDR/XDR *P. aeruginosa*.

P. aeruginosa strain	MIC$_{Vancomycin}$, µg/mL	MIC$_{TOB}$, µg/mL	FIC index	Absolute MIC$_{Vancomycin,}$[a] µg/mL	Potentiation[b]
PAO1	1024	1	0.38	128	8-fold
259-96918	1024	256	0.19	1024	none
260-97103	512	64	0.53	512	none
262-101856	1024	512	0.50[d]	1024	none
264-104354	512	256	0.625	512	none
100036	512	64	0.50	512	none
101243[c]	128	128	1.06	128	none
101885	512	0.5	0.75	512	none

[a] = MIC of vancomycin in the presence of $\leq \frac{1}{4} \times$ MIC$_{TOB}$ ($\leq$ 4 µg/mL) of **TOB**. [b] = degree of antibiotic potentiation in the presence of $\leq \frac{1}{4} \times$ MIC$_{TOB}$ ($\leq$ 4 µg/mL) of **TOB**. [c] = colistin- and tobramycin-resistant. [d] = exact FIC index value is 0.500244 and therefore not synergistic

IV-7. References

(1)   Yang, X.; Goswami, S.; Gorityala, B. K.; Domalaon, R.; Lyu, Y.; Kumar, A.; Zhanel, G. G.; Schweizer, F. A Tobramycin Vector Enhances Synergy and Efficacy of Efflux Pump Inhibitors against Multidrug-Resistant Gram-Negative Bacteria. *J. Med. Chem.* **2017**, *60* (9), 3913–3932.

(2)   Tsubery, H.; Ofek, I.; Cohen, S.; Fridkin, M. Structure-Function Studies of Polymyxin B Nonapeptide: Implications to Sensitization of Gram-Negative Bacteria. *J. Med. Chem.* **2000**, *43* (16), 3085–3092.

Appendix V: Copyrighted works used with permission

This appendix was meant to reaffirm that all materials in all Chapters of this thesis that were part of a published article were used with permission from the copyright owner and the publication house/journal.

V-1. Copyright permission

Chapter 1

Based on my publication:

Ronald Domalaon, George G. Zhanel, Frank Schweizer. **2016**. Short antimicrobial peptides and peptide scaffolds as promising antibacterial agents. Curr Top Med Chem 16:1217-1230. doi: 10.2174/1568026615666150915112459

Copyright © Bentham Science, Current Topics in Medicinal Chemistry

Chapter 2

Based on my publication:

Ronald Domalaon, Temilolu Idowu, George G. Zhanel, Frank Schweizer. **2018**. Antibiotic Hybrids: the Next Generation of Agents and Adjuvants against Gram-Negative Pathogens?. Clin Microbiol Rev 31:e00077-17. doi: 10.1128/CMR.00077-17

Copyright © American Society for Microbiology, Clinical Microbiology Reviews

Chapter 4

Based on my publication:

Ronald Domalaon, Yaroslav Sanchak, Linet Cherono Koskei, Yinfeng Lyu, George G. Zhanel, Gilbert Arthur, Frank Schweizer. **2018**. Short proline-rich lipopeptide potentiates minocycline and rifampin against multidrug- and extensively drug-resistant *Pseudomonas aeruginosa*. Antimicrob Agents Chemother 62:e02374-17. doi: 10.1128/AAC.02374-17.

Chapter 5

Based on my publication:

Ronald Domalaon, Marc Brizuela, Benjamin Eisner, Brandon Findlay, George G. Zhanel, Frank Schweizer. **2018**. Dilipid ultrashort cationic lipopeptides as adjuvants for chloramphenicol and other conventional antibiotics against Gram-negative bacteria. Amino Acids (Epub ahead of print). doi: 10.1007/s00726-018-2673-9.

Chapter 6

Based on my publication:

Ronald Domalaon, Liam Berry, Quinn Tays, George G. Zhanel, Frank Schweizer. **2018**. Development of dilipid polymyxins: investigation on the effect of hydrophobicity through its fatty acyl component. Bioorg Chem 80:639-648. doi: 10.1016/j.bioorg.2018.07.018.

Chapter 7

Based on my publication:

Ronald Domalaon, Xuan Yang, Yinfeng Lyu, George G. Zhanel, Frank Schweizer. **2017**. Polymyxin B$_3$-tobramycin hybrids with *Pseudomonas aeruginosa*-selective antibacterial activity and strong potentiation of rifampicin, minocycline and vancomycin. ACS Infect Dis 3:941-954. doi: 10.1021/acsinfecdis.7b00145.

Appendix I

Based on my publication:

Ronald Domalaon, Yaroslav Sanchak, Linet Cherono Koskei, Yinfeng Lyu, George G. Zhanel, Gilbert Arthur, Frank Schweizer. **2018**. Short proline-rich lipopeptide potentiates minocycline and rifampin against multidrug- and extensively drug-resistant *Pseudomonas aeruginosa*. Antimicrob Agents Chemother 62:e02374-17. doi: 10.1128/AAC.02374-17.

Appendix II

Based on my publication:

Ronald Domalaon, Marc Brizuela, Benjamin Eisner, Brandon Findlay, George G. Zhanel, Frank Schweizer. **2018**. Dilipid ultrashort cationic lipopeptides as adjuvants for chloramphenicol and other conventional antibiotics against Gram-negative bacteria. Amino Acids (Epub ahead of print). doi: 10.1007/s00726-018-2673-9.

Appendix III

Based on my publication:

Ronald Domalaon, Liam Berry, Quinn Tays, George G. Zhanel, Frank Schweizer. **2018**. Development of dilipid polymyxins: investigation on the effect of hydrophobicity through its fatty acyl component. Bioorg Chem 80:639-648. doi: 10.1016/j.bioorg.2018.07.018.

Appendix IV

Based on my publication:

Ronald Domalaon, Xuan Yang, Yinfeng Lyu, George G. Zhanel, Frank Schweizer. **2017**. Polymyxin B$_3$-tobramycin hybrids with *Pseudomonas aeruginosa*-selective antibacterial activity

and strong potentiation of rifampicin, minocycline and vancomycin. ACS Infect Dis 3:941-954.

doi: 10.1021/acsinfecdis.7b00145.